CURRENT ADVANCES IN NEURODEVELOPMENTAL DISORDERS: PIECING TOGETHER THE CANDIDATE PATH THAT GUIDES THE TRANSLATION FROM ETIOLOGY TO TREATMENT

EDITED BY: Li Yang, Stephen V. Faraone, Dong Liu, Li Sun and Xiaoyan Ke

PUBLISHED IN: Frontiers in Neuroscience

frontiers Research Topics

frontiers

ISSN 1664-8714
ISBN 978-2-88976-386-3
DOI 10.3389/978-2-88976-386-3

About Frontiers

Frontiers is more than just an open-access publisher of scholarly articles: it is a pioneering approach to the world of academia, radically improving the way scholarly research is managed. The grand vision of Frontiers is a world where all people have an equal opportunity to seek, share and generate knowledge. Frontiers provides immediate and permanent online open access to all its publications, but this alone is not enough to realize our grand goals.

Frontiers Journal Series

The Frontiers Journal Series is a multi-tier and interdisciplinary set of open-access, online journals, promising a paradigm shift from the current review, selection and dissemination processes in academic publishing. All Frontiers journals are driven by researchers for researchers; therefore, they constitute a service to the scholarly community. At the same time, the Frontiers Journal Series operates on a revolutionary invention, the tiered publishing system, initially addressing specific communities of scholars, and gradually climbing up to broader public understanding, thus serving the interests of the lay society, too.

Dedication to Quality

Each Frontiers article is a landmark of the highest quality, thanks to genuinely collaborative interactions between authors and review editors, who include some of the world's best academicians. Research must be certified by peers before entering a stream of knowledge that may eventually reach the public - and shape society; therefore, Frontiers only applies the most rigorous and unbiased reviews.
Frontiers revolutionizes research publishing by freely delivering the most outstanding research, evaluated with no bias from both the academic and social point of view. By applying the most advanced information technologies, Frontiers is catapulting scholarly publishing into a new generation.

What are Frontiers Research Topics?

Frontiers Research Topics are very popular trademarks of the Frontiers Journals Series: they are collections of at least ten articles, all centered on a particular subject. With their unique mix of varied contributions from Original Research to Review Articles, Frontiers Research Topics unify the most influential researchers, the latest key findings and historical advances in a hot research area! Find out more on how to host your own Frontiers Research Topic or contribute to one as an author by contacting the Frontiers Editorial Office: frontiersin.org/about/contact

CURRENT ADVANCES IN NEURODEVELOPMENTAL DISORDERS: PIECING TOGETHER THE CANDIDATE PATH THAT GUIDES THE TRANSLATION FROM ETIOLOGY TO TREATMENT

Topic Editors:
Li Yang, Peking University Sixth Hospital, China
Stephen V. Faraone, Upstate Medical University, United States
Dong Liu, Southern University of Science and Technology, China
Li Sun, Peking University Sixth Hospital, China
Xiaoyan Ke, Nanjing Brain Hospital Affiliated to Nanjing Medical University, China

Citation: Yang, L., Faraone, S. V., Liu, D., Sun, L., Ke, X., eds. (2022). Current Advances in Neurodevelopmental Disorders: Piecing Together the Candidate Path That Guides the Translation From Etiology to Treatment.
Lausanne: Frontiers Media SA. doi: 10.3389/978-2-88976-386-3

Table of Contents

frontiers in Neuroscience

ORIGINAL RESEARCH
published: 11 June 2021
doi: 10.3389/fnins.2021.664363

Shared and Distinct Topologically Structural Connectivity Patterns in Autism Spectrum Disorder and Attention-Deficit/Hyperactivity Disorder

*Lu Qian[1,2], Yun Li[1], Yao Wang[1], Yue Wang[1], Xin Cheng[1], Chunyan Li[1], Xiwen Cui[1], Gongkai Jiao[1] and Xiaoyan Ke[1]**

[1] Child Mental Health Research Center, Nanjing Brain Hospital Affiliated of Nanjing Medical University, Nanjing, China,
[2] Department of Psychiatry, Wuxi Mental Health Center, Nanjing Medical University, Wuxi, China

Background: Previous neuroimaging studies have described shared and distinct neurobiological mechanisms between autism spectrum disorders (ASDs) and attention-deficit/hyperactivity disorder (ADHD). However, little is known about the similarities and differences in topologically structural connectivity patterns between the two disorders.

Methods: Diffusion tensor imaging (DTI) and deterministic tractography were used to construct the brain white matter (WM) structural networks of children and adolescents (age range, 6–16 years); 31 had ASD, 34 had ADHD, and 30 were age- and sex-matched typically developing (TD) individuals. Then, graph theoretical analysis was performed to investigate the alterations in the global and node-based properties of the WM structural networks in these groups. Next, measures of ASD traits [Social Responsiveness Scale (SRS)] and ADHD traits (Swanson, Nolan, and Pelham, version IV scale, SNAP-IV) were correlated with the alterations to determine the functional significance of such changes.

Results: First, there were no significant differences in the global network properties among the three groups; moreover, compared with that of the TD group, nodal degree (*Ki*) of the right amygdala (AMYG.R) and right parahippocampal gyrus (PHG.R) were found in both the ASD and ADHD groups. Also, the ASD and ADHD groups shared four additional hubs, including the left middle temporal gyrus (MTG.L), left superior temporal gyrus (STG.L), left postcentral gyrus (PoCG.L), and right middle frontal gyrus (MFG.R) compared with the TD group. Moreover, the ASD and ADHD groups exhibited no significant differences regarding regional connectivity characteristics. Second, the ADHD group showed significantly increased nodal betweenness centrality (*Bi*) of the left hippocampus (HIP.L) compared with the ASD group; also, compared with the ADHD group, the ASD group lacked the left anterior cingulate gyrus (ACG.L) as a hub. Last, decreased nodal efficiency (*Enodal*) of the AMYG.R, *Ki* of the AMYG.R, and *Ki* of the PHG.R were associated with higher SRS scores in the ASD group. Decreased *Ki* of the PHG.R was associated with higher SRS scores in the full sample, whereas decreased *Bi* of the PHG.R was associated with lower oppositional defiance subscale scores of the

OPEN ACCESS

Edited by:
Li Yang,
Peking University Sixth Hospital, China

Reviewed by:
Fengmei Lu,
University of Macau, China
Cao Qingjiu,
Peking University, China

***Correspondence:**
Xiaoyan Ke
kexiaoyan@njmu.edu.cn

Specialty section:
This article was submitted to Neurodevelopment, a section of the journal Frontiers in Neuroscience

Received: *05 February 2021*
Accepted: *10 May 2021*
Published: *11 June 2021*

Citation:
Qian L, Li Y, Wang Y, Wang Y, Cheng X, Li C, Cui X, Jiao G and Ke X (2021) Shared and Distinct Topologically Structural Connectivity Patterns in Autism Spectrum Disorder and Attention-Deficit/Hyperactivity Disorder. Front. Neurosci. 15:664363. doi: 10.3389/fnins.2021.664363

SNAP-IV in the ADHD group, and decreased *Bi* of the HIP.L was associated with lower inattention subscale scores of the SNAP-IV in the full sample.

Conclusion: From the perspective of the topological properties of brain WM structural networks, ADHD and ASD have both shared and distinct features. More interestingly, some shared and distinct topological properties of WM structures are related to the core symptoms of these disorders.

Keywords: Autism spectrum disorder, attention-deficit/hyperactivity disorder, diffusion tensor imaging, white matter structural networks, topological properties

INTRODUCTION

Autism spectrum disorder (ASD) and attention-deficit/hyperactivity disorder (ADHD) are both neurodevelopmental disorders that manifest early in life. ASD is defined by core symptoms of persistent and pervasive deficits in social communication and interaction along with repetitive behavioral patterns and restricted interests or activities. ADHD is characterized by developmentally inappropriate levels of inattention, impulsivity, and hyperactivity (American Psychiatric Association, 2013).

Aside from distinctive features, overlaps in the clinical symptoms and the genetic traits of ASD and ADHD are well documented. First, in terms of clinical phenotypes, 30 to 80% of all ASD children met the diagnostic criteria for ADHD, and 20 to 50% of children diagnosed with ADHD also met the diagnostic criteria for ASD (Van der Meer et al., 2012). Second, from a genetic point of view, genome-wide association studies and linkage or candidate gene studies also identified a number of genetic risk variants common to both disorders (Rommelse et al., 2010; Stergiakouli et al., 2017; Gudmundsson et al., 2019).

Brain phenotypes serve as a bridge to understand the clinical symptoms and biological mechanisms of disorders. Although previous studies have endeavored to verify whether there are similarities and differences in brain phenotypes between ASD and ADHD, the results have been inconsistent. A newly published study from 151 cohorts worldwide using structural T1-weighted whole-brain magnetic resonance imaging (MRI) data revealed ASD-specific cortical thickness differences in the frontal cortex of adult patients and ADHD-specific subcortical differences in children and adolescents; notably, the researchers did not find shared differences across the two disorders (Boedhoe et al., 2020). A diffusion tensor imaging (DTI) study applied tract-based spatial statistics to a larger sample (n = 200) of school-aged children with ASD and ADHD compared with typically developing (TD) controls and found that decreased fractional anisotropy (FA) within the splenium of the corpus callosum was common among the three groups (Ameis et al., 2016). Evidence from an functional MRI (fMRI) study (n = 1,305) measuring functional connectivity of the brain network also confirmed shared dysfunctional connectivity in the default mode network, dorsal attention network, and salience network of both ASD and ADHD patients between 7 and 21 years of age (Kernbach et al., 2018). Interestingly, another fMRI study of 56 children with ASD, 45 children with ADHD, and 50 TD children exhibited shared and distinct intrinsic functional network centrality between children with ASD and children with ADHD. Some affected areas were common to both groups, such as the precuneus; other affected areas were disorder-specific and included ADHD-related increases in degree centrality in the right striatum/pallidum, in contrast to ASD-related increases in bilateral temporolimbic areas specifically (Di Martino et al., 2013). Inconsistencies between previous findings might be due to participant heterogeneity, statistical power, or methods used.

Independent studies of ADHD and ASD have increasingly emphasized the role of dysconnectivity in large-scale networks in both disorders (Konrad and Eickhoff, 2010; Travers et al., 2012). As the brain is a complex network of structurally and functionally interconnected regions (Bullmore and Sporns, 2009), evaluating the brain as a whole and studying its networks can help us fully delineate the organizational patterns of internal connectivity in the human brain (Bullmore and Sporns, 2012).

Previous network studies have mainly focused on functional networks, while functional connectivity opens the door to the analysis of brain networks. We should not ignore that functional connections need structural support to make sense. DTI can help us map the structural connectivity between gray matter (GM) regions using white matter (WM) tractography, providing an avenue to probe structurally interconnected brain networks (Hagmann et al., 2008).

Accordingly, in the present study, we analyzed DTI data from 95 children and adolescents aged 6 to 16 years with ASD, with ADHD, and who were TD to map their WM structural networks. First, we investigated the alterations in the global and regional properties of the WM structural networks in these groups. Second, we examined the relationship between the alterations and measures of ASD traits, as well as ADHD traits, to determine the functional significance of such changes. To our knowledge, no previous studies have directly contrasted the global and regional properties of WM structural networks in individuals with ASD, individuals with ADHD, and TD controls. Our work might be an important supplement to previous studies.

MATERIALS AND METHODS

Participants and Assessments

Patients were recruited via the Nanjing Brain Hospital affiliated with Nanjing Medical University, and controls were volunteers

recruited through advertising on the hospital website and WeChat official account. In total, 95 participants aged 6 to 16 years were enrolled in our study, including 31 with ASD, 34 with ADHD, and 30 TD controls. Written informed consent was obtained from all legal guardians. All participants were age and sex matched. The intelligence quotient (IQ) scores of all participants were evaluated using the Wechsler Intelligence Scale for Children-IV (Feis, 2010), and those who scored less than 80 on the estimated full-scale IQ were excluded. The diagnoses for ASD and ADHD were based on the *Diagnostic and Statistical Manual of Mental Disorders, Fourth Text Revision* (*DSM-IV-TR*) diagnostic criteria supported by parent interviews, direct observations, available teacher forms, and prior records. ASD diagnosis was supported by standardized clinical assessments, including the Autism Diagnostic Observation Scale (Lord et al., 1989) and Autism Diagnostic Inventory – Revised (Lord et al., 1994). TD controls had no developmental disorders and no first-degree family history of such disorders. All participants with any systemic diseases, with a family history of head injury, with genetic syndromes, currently using antipsychotics, or with neurological disorders or psychiatric illness were excluded from the study. To discern brain–behavior relationships, we used parent ratings of ASD traits indexed by the Social Responsiveness Scale (SRS) (Constantino, 2013), which is a 65-item questionnaire covering each of the three *DSM-IV* criterion domains (social; language; and repetitive, stereotypic behaviors/restricted range of interest). ADHD traits were indexed by Swanson, Nolan, and Pelham-IV (SNAP-IV) (Gau et al., 2008), which is a widely used scale that measures the core symptoms of ADHD.

Image Acquisition and Preprocessing

MRI data were acquired using the 3.0-T Verio MRI system (Siemens Medical Systems, Germany) with a birdcage gradient head coil. The head of each participant was gently restrained with foam cushions to avoid the generation of motion artifacts during the scan. High-resolution T1-weighted images were obtained using a three-dimensional spoiled gradient recalled pulse sequence with the following scanning parameters: repetition time (TR) = 2,530 ms, echo time (TE) = 3.34 ms, flip angle = 7°, inversion time = 1,100 ms, field of view (FOV) = 256 × 256 mm, matrix = 256 × 159, slice thickness = 1.33 mm, and total scanning time = 8.7 min. Each participant's head was positioned parallel to the anterior commissure–posterior commissure plane. DTI was performed with single-shot echo planar imaging sequences with diffusion gradients applied in 30 non-collinear directions and b = 1,000 s/mm^2. The thickness of each slice was 2.5 mm without a gap. The sequence parameters for the DTI were as follows: TE = 104 ms, TR = 9,000 ms, FOV = 230 × 230 mm^2, and acquisition matrix = 128 × 128. The total DTI scanning time was 5.1 min. Before preprocessing, all the structural images were checked for artifacts. DWI image data were screened for subject motion and common artifacts related to diffusion sequences using PANDA (Cui et al., 2013), a pipeline toolbox for analyzing brain diffusion images. In brief, the overall preprocessing pipeline comprised the following steps: converting DICOM files into NIfTI images, estimating the brain mask (the b0 image without diffusion weighting was used for the estimation), cropping the raw images, correcting for the eddy-current effect, and averaging multiple acquisitions, which are detailed in PANDA (Cui et al., 2013).

Network Construction

Network Node Definition

Node definition is an important step in brain network construction as the node is a vital element of a network (Sporns et al., 2005). Typically, the entire brain is divided into multiple regions using a prior GM atlas, where each region represents a network node (Bullmore and Sporns, 2009). In the present study, we used the automated anatomical labeling (AAL) atlas (Tzourio-Mazoyer et al., 2002) to parcellate the cerebral cortex into 90 regions (45 for each hemisphere, see **Table 1** for details), and each region represents a node of the cortical network. As the parcellation process was conducted in the DTI native space for each subject, the individual FA image in native space was coregistered to its corresponding T1-weighted image using an affine transformation, and the individual resultant T1-weighted image was then non-linearly registered to the ICBM152 template in MNI space. Then, a prior atlas in standard space could be inversely warped back to the individual native space by applying the inverse warping transformation.

Network Edge Definition

Deterministic tractography was used to define the network edges of the 90 regions. FA thresholding was set as 0.1–1, with an interval of 0.1, and the turning angle threshold was set at 35. In this study, we selected a threshold value of 3 (T = 3) for the number of fiber bundles, meaning two regions were considered structurally connected if at least three fibers with two endpoints were located in these two regions. Such a threshold selection was reported to reduce the risk of false-positive connections due to noise or limitations in deterministic tractography (Shu et al., 2011). After defining the network edges, PANDA was used to calculate the fiber number (FN)–weighted WM network for each participant, which was represented by a symmetric 90 × 90 matrix.

Network Analysis

We investigated the topological properties of the WM structural networks at the global and nodal levels. Characteristic path length (*Lp*), clustering coefficient (*Cp*), normalized shortest path length (λ), normalized clustering coefficient (γ), small-worldness σ (σ = λ/γ), local efficiency (*Eloc*), and global efficiency (*Eglob*) of the whole brain network were calculated to quantify the global network architecture. Also, we computed the local efficiency of node i (*Enodal*), nodal degree of node i (*Ki*), and betweenness centrality of node i (*Bi*) to determine the nodal (regional) characteristics of the networks. In addition, the normalized betweenness (*bi*) was used to identify the most central nodes (hubs) of the networks. These measures are detailed in the article by Rubinov and Sporns (2010). Briefly, *Lp* is the average shortest path length between the nodes that quantifies the ability of a network to propagate

TABLE 1 | The regions are listed in terms of a prior template of the automated anatomical labeling atlas.

Index	Regions	Abbreviation	Index	Regions	Abbreviation
(1,2)	Precental gyrus	PreCG	(47,48)	Lingual gyrus	LING
(3,4)	Superior frontal gyrus, dorsolateral	SFGdor	(49,50)	Superior occipital gyrus	SOG
(5,6)	Superior frontal gyrus, orbital part	ORBsup	(51,52)	Middle occipital gyrus	MOG
(7,8)	Middle frontal gyrus	MFG	(53,54)	Inferior occipital gyrus	IOG
(9,10)	Middle frontal gyrus, orbital part	ORBmid	(55,56)	Fusiform gyrus	FFG
(11,12)	Inferior frontal gyrus, opercular part	IFGoperc	(57,58)	Postcentral gyrus	PoCG
(13,14)	Inferior frontal gyrus, triangular part	IFGtriang	(59,60)	Superior parietal gyrus	SPG
(15,16)	Inferior frontal gyrus, orbital part	ORBinf	(61,62)	Inferior parietal, but supramarginal and angular gyri	IPL
(17,18)	Rolandic operculum	ROL	(63,64)	Supramarginal gyrus	SMG
(19,20)	Supplementary motor area	SMA	(65,66)	Angular gyrus	ANG
(21,22)	Olfactory cortex	OLF	(67,68)	Precuneus	PCUN
(23,24)	Superior frontal gyrus, media	SFGmed	(69,70)	Paracentral lobule	PCL
(25,26)	Superior frontal gyrus, medial orbital	ORBsupmed	(71,72)	Caudate nucleus	CAU
(27,28)	Gyrus rectus	REC	(73,74)	Lenticular nucleus, putamen	PUT
(29,30)	Insula	INS	(75,76)	Lenticular nucleus, pallidum	PAL
(31,32)	Anterior cingulate and paracingulate gyri	ACG	(77,78)	Thalamus	THA
(33,34)	Median cingulate and paracingulate gyri	DCG	(79,80)	Heschl gyrus	HES
(35,36)	Posterior cingulate gyrus	PCG	(81,82)	Superior temporal gyrus	STG
(37,38)	Hippocampus	HIP	(83,84)	Temporal pole: superior temporal gyrus	TPOsup
(39,40)	Parahippocampal gyrus	PHG	(85,86)	Middle temporal gyrus	MTG
(41,42)	Amygdala	AMYG	(87,88)	Temporal pole: middle temporal gyrus	TPOmid
(43,44)	Calcarine fissure and surrounding cortex	CAL	(89,90)	Inferior temporal gyrus	ITG

The regions are listed in terms of a prior template of an automated anatomical labeling atlas (Tzourio-Mazoyer et al., 2002).

parallel information, and *Cp* represents the fraction of the node's neighbors that are also neighbors of each other, $\lambda = Lp^{real}/Lp^{rand}$, $\gamma = Cp^{real}/Cp^{rand}$, where Lp^{rand} and Cp^{rand} are the mean shortest path length and the mean clustering coefficient of 100 matched random networks, respectively. *Eloc* is the mean of the local efficiency of all the nodes in the graph. *Eglob* is the average inverse shortest path length and can be used to estimate the efficiency with which brain regions communicate. *Enodal* represents the regional efficiency of a node. The degree *Ki* is defined as the number of connections to that node, and highly connected nodes have a large degree. *Bi* is defined as the fraction of all the shortest paths in the network that pass through a given node.

Statistical Analysis

The statistics of demographic and clinical characteristics were conducted using Statistical Product and Service Solutions (SPSS, version 22.0). Normality of the distributions was assessed by the Shapiro–Wilk test. Categorical variables (sex) were investigated with χ^2 tests, whereas continuous variables, such as age, IQ, clinical scale scores, and network properties, were investigated with one-way analysis of variance (ANOVA), followed by Bonferroni *post hoc* analysis. Effect size η_p^2 is reported for one-way ANOVA tests, with 0.01, 0.06, and 0.14 representing small, medium, and large effects, respectively.

To identify the hub regions of the networks between groups, we first calculated the *bi* of all 90 regions for each subject and then calculated the mean value of the *bi* for each region according to the groups. If *bi* was greater than 1.5 times the average betweenness (the mean value of *bi* for all 90 regions) of the network, the nodes were considered to be pivotal nodes (i.e., hubs).

Network-based statistics (NBS) (Zalesky et al., 2010) is a non-parametric method based on the principles of traditional cluster-based thresholding of statistical parametric maps to control the familywise error rate; hence, it can be used to identify subnetworks of topologically connected suprathreshold connections. We conducted an independent *F* test on every connectivity value to compare the structural connectivity differences between the ASD, ADHD, and TD groups. We set the primary threshold at $p = 0.001$ for the resulting *F* statistic matrix (based on a height threshold of $F = 3.2$ to stringently control for type I errors). Next, the data across groups were randomized 5,000 times to obtain the reference cluster distribution. We used the maximum number of connections across all clusters to form the reference distribution for each randomization; cluster scores exceeding the 95th percentile were considered significant ($p < 0.05$). For *post hoc* paired comparisons (e.g., the ASD group vs. the ADHD group), the procedure was similar.

Additionally, Pearson correlation analysis, performed in SPSS, was used to examine correlations in the full sample, and *post hoc* analyses examined Pearson correlations in the patient groups to reveal the relationships between altered regional properties and ASD traits, as well as between altered regional properties and ADHD traits.

RESULTS

Demographic and Clinical Characteristics

One-way ANOVAs indicated that the three groups were matched for age and sex but not matched for IQ ($F = 4.979$, $p = 0.009$, $\eta_p^2 = 0.098$) (it should be noted that the IQ effect was removed in all of the following network analyses). The ANOVAs showed significant group effects on SRS total scores ($F = 13.236$, $p = 0.000$, $\eta_p^2 = 0.223$) and SNAP-IV subscale scores, including inattention ($F = 65.038$, $p = 0.000$, $\eta_p^2 = 0.591$), hyperactivity ($F = 40.230$, $p = 0.000$, $\eta_p^2 = 0.472$), and oppositional defiance ($F = 10.626$, $p = 0.000$, $\eta_p^2 = 0.191$). Specifically, for pairwise comparisons, the ASD group showed greater social deficits than the ADHD and TD groups; moreover, the ADHD group showed more severe ADHD symptoms than the ASD and TD groups (see **Table 2** for details).

Global Topological Properties of the WM Structural Networks

Based on the constructed networks, we calculated the topological properties (i.e., *Lp*, *Cp*, λ, γ, σ, *Eloc*, and *Eglob*) of the global network for each participant and showed the mean values of these properties of the three groups. Analyses of covariance (ANCOVAs) on the global network properties showed no significant group effects of all the global topological properties (*Lp*: $F = 1.625$, $p = 0.202$, $\eta_p^2 = 0.034$; *Cp*: $F = 0.666$, $p = 0.516$, $\eta_p^2 = 0.014$; λ: $F = 0.583$, $p = 0.560$, $\eta_p^2 = 0.013$; γ: $F = 1.253$, $p = 0.290$, $\eta_p^2 = 0.027$; σ: $F = 2.343$, $p = 0.078$, $\eta_p^2 = 0.072$; *Eloc*: $F = 1.195$, $p = 0.308$, $\eta_p^2 = 0.025$; and *Eglob*: $F = 2.535$, $p = 0.085$, $\eta_p^2 = 0.052$) among the three groups.

Node-Based Analysis of the WM Structural Networks

Identification of Regional Property Differences

Enodal, *Ki*, and *Bi* were calculated to identify the differences in nodal properties in the participants. Among the three groups, ANCOVAs showed that the regions with significant group effects were distributed in the temporal [the left amygdala (AMYG.L), right amygdala (AMYG.R), left hippocampus (HIP.L), and right parahippocampal gyrus (PHG.R)], and subcortical [the right insula (INS.R)] cortices (see **Table 3** for details). *Post hoc* tests showed that the *Ki* values of the AMYG.R and PHG.R were significantly decreased in both the ASD and ADHD groups compared with the TD controls (i.e., ASD and ADHD shared deficits). Only one region (i.e., the HIP.L) showed significant group differences, with a higher *Bi* observed in the ADHD group than in the ASD and TD groups (i.e., ADHD-specific deficits) (**Figure 1**).

Identification of Hub Distributions

To identify the hub regions, we examined the *Bi* of each node in all networks. In total, 23 hub regions were the same for all of the groups, including 10 regions of the association cortex [the left precuneus (PCUN.L), right precuneus (PCUN.R), left fusiform gyrus (FFG.L), right fusiform gyrus (FFG.R), left lingual gyrus (LING.L), right lingual gyrus (LING.R), left dorsolateral superior frontal gyrus (SFGdor.L), right dorsolateral superior frontal gyrus (SFGdor.R), left middle frontal gyrus (MFG.L), and right rolandic operculum (ROL.R)], four regions of subcortical structures [the left putamen (PUT.L), right putamen (PUT.R), left caudate nucleus (CAU.L), and right caudate nucleus (CAU.R)], four paralimbic regions [the left median cingulate gyrus (DCG.L), right median cingulate gyrus (DCG.R), left insula (INS.L), and INS.R], and five primary regions [the left calcarine fissure (CAL.L), right calcarine fissure (CAL.R), left precental gyrus (PreCG.L), right precental gyrus (PreCG.R), and right postcentral gyrus (PoCG.R)]. The common hubs identified for all of the groups were predominantly distributed in the association cortices. Specially, the left anterior cingulate gyrus (ACG.L) was identified as a hub in the ADHD and TD groups but not in the ASD group, and both the ASD and ADHD groups exhibited four additional hubs [the left middle temporal gyrus (MTG.L), left superior temporal gyrus (STG.L), left postcentral gyrus (PoCG.L), and right middle frontal gyrus (MFG.R)] compared with TD controls (**Table 4** and **Figure 2**).

Connectivity-Based Analysis

We used the NBS method to identify the disrupted connected components among the three groups, and we found that a connected network with nine nodes and eight edges was altered ($p = 0.001$, corrected). The involved nodal regions were the PreCG.L, left middle frontal gyrus (MFG.L), SFGdor.L, left inferior frontal gyrus, opercular part (IFGoperc.L), left rolandic operculum (ROL.L), left middle occipital gyrus (MOG.L), left paracentral lobule (PCL.L), PUT.L, and CAU.L. However, no significant differences were found with respect to connected components between the ASD and ADHD groups (**Figure 3**).

Correlation of Altered Regional Properties With ASD and ADHD Traits

Correlation analysis between altered regional properties and ASD traits and that between altered regional properties and ADHD traits were examined in the full sample and in the patient groups. For regional properties, we examined the nodes with significant group effects that are listed in **Table 3**. In the full sample, *Bi* of the PHG.R was significantly correlated with SRS scores ($r = -0.242$, $p = 0.018$, $r^2 = 0.059$), and *Bi* of the HIP.L was significantly correlated with inattention subscale scores of the SNAP-IV ($r = 0.220$, $p = 0.034$, $r^2 = 0.048$). In the ASD group, *Enodal* of the AMYG.R was significantly correlated with SRS scores ($r = -0.512$, $p = 0.003$, $r^2 = 0.262$; also, *Ki* of the AMYG.R was significantly correlated with SRS scores ($r = -0.359$, $p = 0.005$, $r^2 = 0.128$), and *Ki* of the PHG.R was significantly correlated with SRS scores ($r = -0.368$, $p = 0.004$, $r^2 = 0.135$). In the ADHD group, *Bi* of the PHG.R was significantly correlated with oppositional defiance subscale scores of the SNAP-IV ($r = 0.374$, $p = 0.032$, $r^2 = 0.140$) (**Figure 4**).

TABLE 2 | The demographic and clinical characteristics of all participants.

	ASD (n = 31)	ADHD (n = 34)	TD (n = 30)	p value[a]	Pairwise[b]
Gender: male/female	27/4	32/2	22/8	0.051	–
Age (std)	9.00 (1.92)	9.44 (1.67)	9.67 (2.88)	0.483	–
IQ (std)	102.26 (19.70)	104.09 (15.56)	107.07 (18.43)	0.009*	ASD vs. ADHD, n.s. ASD vs. TD, p = 0.014 ADHD vs. TD, p = 0.036
SRS-total[c] (std)	64.65 (15.77)	51.71 (13.60)	46.43 (8.54)	0.000*	ASD vs. ADHD, p = 0.000* ASD vs. TD, p = 0.000* ADHD vs. TD, n.s.
SNAP-IV[d] subscales					
Inattention (std)	9.35 (2.24)	17.06 (3.82)	7.24 (4.44)	0.000*	ASD vs. ADHD, p = 0.000* ASD vs. TD, n.s. ADHD vs. TD, p = 0.000*
Hyperactivity (std)	6.97 (2.52)	12.58 (5.21)	3.79 (3.36)	0.000*	ASD vs. ADHD, p = 0.000* ASD vs. TD, p = 0.007* ADHD vs. TD, p = 0.000*
Oppositional defiant (std)	4.13 (2.99)	8.55 (5.22)	5.31 (3.18)	0.000*	ASD vs. ADHD, p = 0.000* ASD vs. TD, n.s. ADHD vs. TD, p = 0.006*

*$p < 0.05$. std: standard deviation; n.s.: no significance.
[a] p value for sex using the χ^2 test; other p values for the comparisons based on one-way ANOVA.
[b] Post hoc pairwise comparisons were then performed using the t test.
[c] Total scores based on the Social Responsiveness Scale.
[d] Swanson, Nolan, and Pelham, version IV scale.

TABLE 3 | Regions showing significant differences in the nodal topological properties among the ASD, ADHD, and TD groups.

Nodal metrics	ASD		ADHD		TD		F	p value[a]	η_p^{2b}
	Mean	std	Mean	std	Mean	std			
*Enodal*_AMYG.R	10.31	1.98	10.44	2.01	11.73	2.44	3.266	0.025*	0.097
*Ki*_ PHG.R	326.5	50.39	331.6	71.76	373.2	75.50	3.684	0.015*	0.108
*Ki*_ AMYG.L	105.7	31.90	103.7	27.19	124.4	35.62	2.946	0.037*	0.089
*Ki*_ AMYG.R	99.71	34.90	98.26	31.62	124.3	41.42	5.278	0.002*	0.148
*Bi*_INS.R	611.20	206.30	528.80	228.40	482.50	157.90	2.914	0.039*	0.088
*Bi*_HIP.L	120.20	73.08	171.70	78.97	135.40	94.14	2.714	0.049*	0.082
*Bi*_PHG.R	134.60	59.08	143.50	98.06	196.30	113.20	2.890	0.040*	0.087

*$p < 0.05$. std: standard deviation; for the definitions of the abbreviations, see ***Table 1***.
[a] p value for using one-way ANCOVA tests.
[b] η_p^2: effect size for one-way ANCOVA tests.

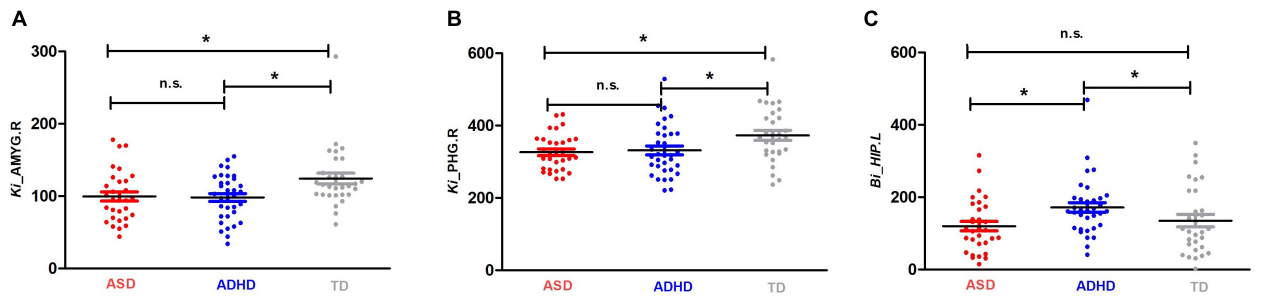

FIGURE 1 | Shared and specific nodal topological properties in diagnostic groups. **(A,B)** represent the regions with shared deficits in ASD and ADHD topological properties compared with the properties of TD controls, and **(C)** represents the region in which ADHD topological properties differ from both TD controls and individuals with ASD by Bonferroni *post hoc* analysis; for the definitions of the abbreviations, see **Table 1**. For each node, the bar and error bar represent the mean value and SD, respectively; a single asterisk (*) represents a significant group difference at $p < 0.05$; n.s. represents no significance.

DISCUSSION

The present study compared the global and regional properties of the WM structural networks in children and adolescents with ASD, ADHD, and TD controls; the findings suggest shared and distinct features underlying neurobiological mechanisms in ASD and ADHD children and adolescents from a network perspective.

The human brain is a complex system with an optimal balance between local specialization and global integration (Shu et al., 2011). In this study, we identified the global topological properties of the WM networks in ASD and ADHD patients and TD controls, exhibiting no significant differences among the three groups. Our results are supported by a network study that showed measures of structural *Cp* and *Lp* did not significantly differ between children and adolescents with ASD and TD

TABLE 4 | Hub distributions of the WM structural networks among the ASD, ADHD, and TD groups.

ASD		ADHD		TD	
Regions	**Class[a]**	**Regions**	**Class[a]**	**Regions**	**Class[a]**
PCUN.R	Association	PCUN.R	Association	PCUN.R	Association
DCG.L	Paralimbic	PCUN.L	Association	PCUN.L	Association
PCUN.L	Association	DCG.L	Paralimbic	DCG.L	Paralimbic
DCG.R	Paralimbic	INS.R	Paralimbic	DCG.R	Paralimbic
INS.R	Paralimbic	DCG.R	Paralimbic	CAL.R	Primary
INS.L	Paralimbic	INS.L	Paralimbic	INS.L	Paralimbic
PoCG.R	Primary	PoCG.R	Primary	INS.R	Paralimbic
PreCG.R	Primary	CAL.R	Primary	FFG.L	Association
CAL.R	Paralimbic	CAL.L	Primary	CAL.L	Primary
FFG.L	Association	CAU.L	Subcortical	FFG.R	Association
PUT.R	Paralimbic	ROL.R	Association	PUT.R	Subcortical
FFG.R	Association	MFG.L	Association	LING.L	Association
CAL.L	Primary	PUT.R	Subcortical	PreCG.L	Primary
CAU.R	Primary	PreCG.L	Primary	MFG.L	Association
MFG.L	Association	SFGdor.L	Association	PoCG.R	Primary
ROL.R	Association	FFG.L	Association	SFGdor.L	Association
SFGdor.L	Association	CAU.R	Subcortical	LING.R	Association
CAU.L	Paralimbic	FFG.R	Association	PreCG.R	Primary
LING.R	Association	PUT.L	Subcortical	CAU.L	Subcortical
PUT.L	Paralimbic	SFGdor.R	Association	PUT.L	Subcortical
SFGdor.R	Association	MFG.R	Association	SFGdor.R	Association
MTG.L	Association	LING.L	Association	CAU.R	Subcortical
PreCG.L	Primary	ACG.L	Paralimbic	ROL.R	Association
STG.L	Association	LING.R	Association	ACG.L	Paralimbic
MFG.R	Association	PreCG.R	Primary		
LING.L	Association	MTG.L	Association		
PoCG.L	Primary	STG.L	Association		
		PoCG.L	Primary		

For the definitions of the abbreviations, see ***Table 1****.*

[a] *The cortical regions are classified as primary, association, subcortical, limbic, and paralimbic (Supekar et al., 2009).*

controls (Rudie et al., 2013). However, a recent work exploring the topologic architecture of WM connectivity networks in preschool-aged children demonstrated that children with ASD had shortened *Lp* and increased *Eglob* and *Cp* compared with the TD children (Li et al., 2018). Another study focused on wiring of the connectome in adults with high-functioning ASD showed that *Eglob* was significantly decreased, and *Lp* was significantly increased in subjects with ASD (Roine et al., 2015). In addition, consistent with our results, Justina et al., in an investigation of the organization of structural brain networks in adults with ADHD and unaffected controls, also showed no significant differences in global network metrics, including σ, *Eglob*, and *Cp* (Sidlauskaite et al., 2015). However, Chen et al. (2019) demonstrated altered topological characteristics of lower *Eglob*, lower *Eloc*, and longer *Lp* of brain functional networks in drug-naive children with ADHD, whereas in the other two studies using drug-treated samples, no significant changes in *Eglob* in ADHD subjects were found (Wang et al., 2009; Xia et al., 2014). Therefore, age range and medication effects might contribute to the differences in findings regarding the global topological properties of brain networks in patients with ASD and those with ADHD.

Shared deficits of regional alterations were associated with a tendency of decreased *Ki* of the AMYG.R and PHG.R in the ASD and ADHD groups. Converging neuroscientific evidence has suggested that the neuropathology of ASD is widely distributed, involving impaired connectivity throughout the brain (Just et al., 2004; Ameis and Catani, 2015). One region consistently highlighted by structural MRI (Gibbard et al., 2017) and fMRI (Guo et al., 2016; Odriozola et al., 2018; Iidaka et al., 2019) studies is the amygdala. Abnormal amygdala structure and function are correlated with alterations in the social–emotional functions of ASD in rodents (Schoch et al., 2016) and in humans (Gotts et al., 2012; Mundy, 2017). The commonality of amygdala abnormalities has also been identified in ADHD (Posner et al., 2011; Hulvershorn et al., 2014), and altered amygdala activation and connectivity have been suggested to be related to dysfunction of emotion regulation in ADHD (Christiansen et al., 2019, such as facial and contextual emotion processing (Fonseca et al., 2009; Miller et al., 2011). A recent structural neuroimaging study directly comparing amygdala volumes and correlates of social deficits showed that larger amygdala volumes were associated with fewer social deficits in both ASD and ADHD children, supporting a common underlying biology between these disorders (Baribeau et al., 2019). Additionally, the PHG is thought to be a structure of the default mode network (Fox et al., 2005) known to be particularly active when participants are at rest, and it has been identified as a key anatomical region in the mesial temporal lobe associated with memory (Aggleton et al., 2010; Catani et al., 2013). One study reported that the PHG was involved in the involuntary reactivation of contextual fear memory that results in avoidance (Paquette et al., 2003). Moreover, it is a part of the limbic system, which was mentioned as a socially related area of the brain (Pagani et al., 2012; Catani et al., 2013). Several ASD (Monk et al., 2009; Weng et al., 2010; Lee et al., 2016) and ADHD (Anderson et al., 2014) studies have revealed altered functional connectivity between the PHG and other brain regions compared with the functional connectivity of TD controls. Our work suggests shared deficits of *Ki* in the PHG.R in the ASD and ADHD groups.

A novel finding in this study was the identification of an increased tendency of *Bi* of the HIP.L in the ADHD group compared with the ASD and TD groups. Studies from animal models of ADHD have suggested abnormalities in neuronal signaling systems within the hippocampus (Medin et al., 2013; Sterley et al., 2013). A multimodal MRI study in children with ADHD showed that hippocampal volumes were reduced in children with ADHD and that hippocampal–orbitofrontal cortex connectivity was also reduced in children with ADHD (Posner et al., 2014). Another study also confirmed reduced hippocampal volume in children with ADHD (Hoogman et al., 2017). Furthermore, a study showed that synaptic plasticity of neurons in the hippocampus may contribute to learning and memory processes (Filippo et al., 2009), and dysfunction of the hippocampus could affect learning processes and further result in ADHD symptoms. However, in terms of ASD, Groen et al. (2010) showed that the HIP.L was significantly enlarged in

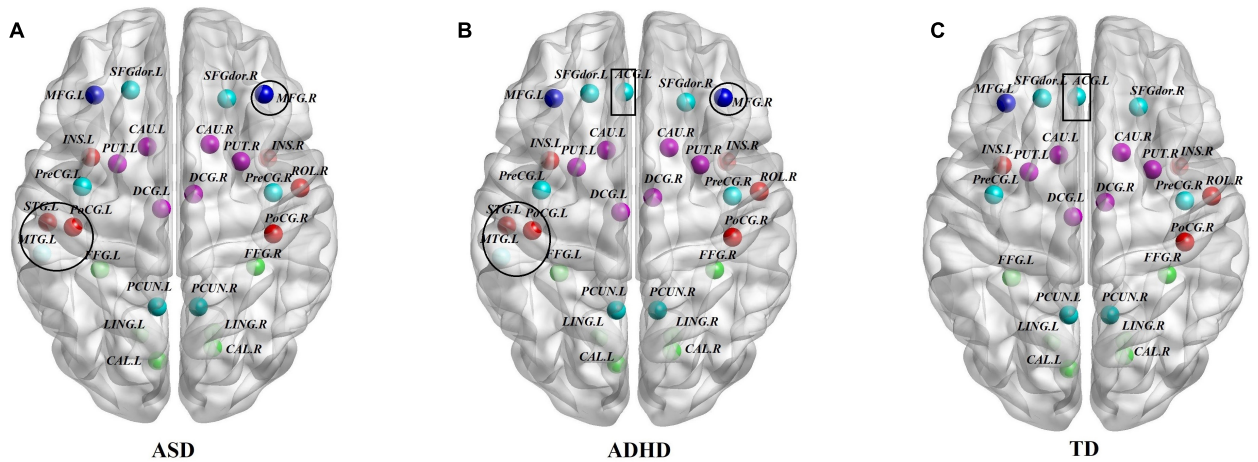

FIGURE 2 | Comparisons of hub distributions among the ASD, ADHD, and TD groups. **(A)** ASD hub distributions, **(B)** ADHD hub distributions, **(C)** TD hub distributions; for the definitions of the abbreviations, see **Table 1**; regions in the black circle including the MTG.L, STG.L, PoCG.L, and MFG.R were additional hubs of both the ASD and ADHD groups compared with the TD controls. In addition, the ACG.L in the black rectangle was identified as a hub in the ADHD and TD groups but not in the ASD group. The regions were mapped onto the cortical surfaces using BrainNet viewer software (www.nitrc.org/projects/bnv/). Note that the FN-weighted WM network for each participant was constructed using the AAL template.

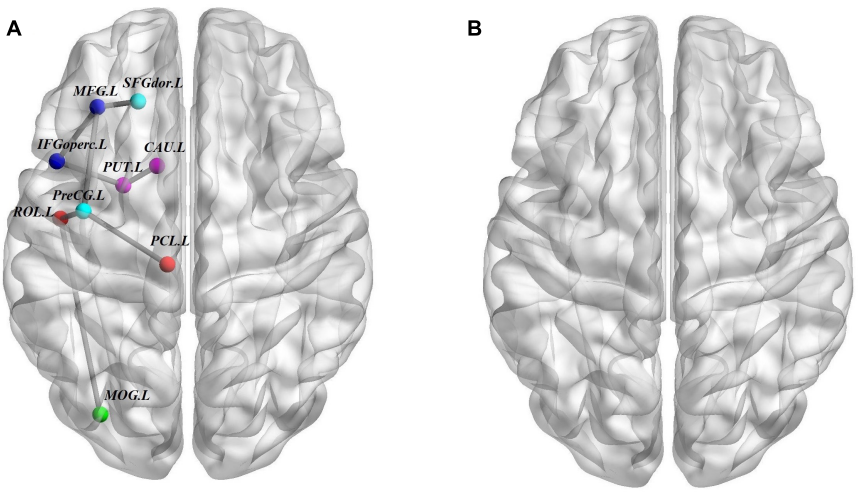

FIGURE 3 | Structural connectivity (SC) differences. **(A)** The structural connectome network differences among ASD, ADHD, and TD groups identified by NBS; these connections formed a single connected network with nine nodes and eight connections ($p = 0.001$, corrected). **(B)** Similar to A but between ASD and ADHD groups, no connected components with significant differences were found. For the definitions of the abbreviations, see **Table 1**. The nodes and connections were mapped onto the cortical surfaces using BrainNet viewer software (www.nitrc.org/projects/bnv/). Note that the FN-weighted WM network for each participant was constructed using the AAL template.

adolescents with autism compared with that of the control group. Schumann et al. (2004) also revealed enlarged hippocampi, especially in a high-functioning autism group of 7.5- to 12.5-year-olds. In agreement with previous studies showing structural differences of the hippocampus between ADHD and ASD patients, our findings suggest that regional characteristics of the hippocampus might be a valuable brain network marker for distinguishing ADHD from ASD.

In terms of hubs, we used the index of *Bi* to identify the hub regions of the WM networks in the present study. Surprisingly, the distributions of hubs in the ASD and ADHD groups were almost the same. We found that most of the hubs were located in the association cortex, which plays a central role in receiving convergent inputs from multiple cortical regions (Mesulam, 1998). These findings are in accordance with several previous studies of ASD (Takashi et al., 2014; Qian et al., 2018) and ADHD (Sidlauskaite et al., 2015), which identified the association cortex a critical node in both structural and functional brain networks. Moreover, compared with the TD control group, both the ASD and ADHD groups exhibited common alterations

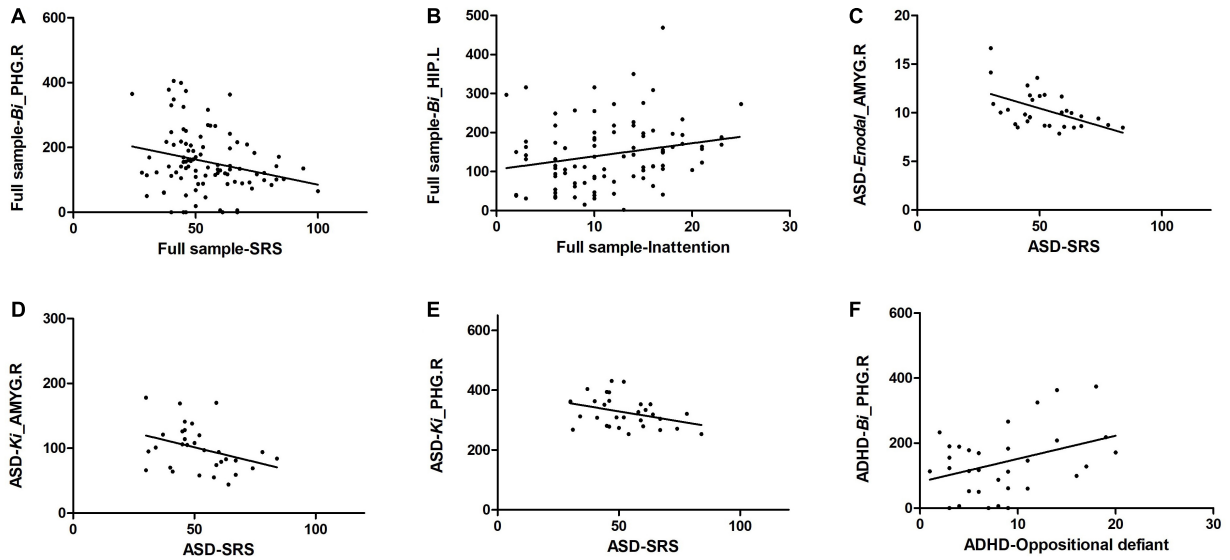

FIGURE 4 | Significant correlation of altered regional properties with ASD and ADHD traits. **(A)** *Bi* of the PHG.R was significantly correlated with SRS scores in the full sample; **(B)** *Bi* of the HIP.L was significantly correlated with inattention subscale scores of the SNAP-IV in the full sample; **(C)** *Enodal* of the AMYG.R was significantly correlated with SRS scores in the ASD group; **(D)** *Ki* of the AMYG.R was significantly correlated with SRS scores in the ASD group; **(E)** *Ki* of the PHG.R was significantly correlated with SRS scores in the ASD group, and **(F)** *Bi* of the PHG.R was significantly correlated with oppositional defiance subscale scores of the SNAP-IV in the ADHD group.

in hub distributions with four additional regions, including the MTG.L, STG.L, PoCG.L, and MFG.R. ASD subjects were found to have similar hub alterations comparable with ADHD subjects, particularly in the frontal and temporal regions, which is in accordance with the results of previous meta-analyses and mega-analyses (Van Rooij et al., 2018; Hoogman et al., 2019). According to the hub results, we found that the ASD group lacked one hub region of the ACG.L compared with the ADHD and TD groups. As hub regions are believed to handle multimodal or integrative functions, damage to these regions could dramatically affect the stability and efficiency of the network (Achard et al., 2006). A 4-year longitudinal study in healthy control participants reported that greater age-related thinning of the left anterior cingulate cortex was associated with less reduction in effortful control and in turn is associated with improvements in socioemotional functioning (Vijayakumar et al., 2014). Moreover, many studies performed in both humans and rodents have shown that the ACG is anatomically and functionally connected to a broad set of regions engaged in social information processing (Chang et al., 2012; Apps et al., 2016) and therefore is likely to represent an information hub for the social network (Guo et al., 2019). In addition, the ACG is part of the default mode network and is a primary node of the salience network; both networks are strongly implicated in autism (Zielinski et al., 2012). Although the exact etiopathogenesis of ASD remains unclear, a consistent biomarker could estimate patient impairment and guide tailored rehabilitation. Our study reveals that the hubness of the ACG might be a potential biomarker for the diagnosis of ASD, distinguishing it from ADHD and neurotypical development. Moreover, despite shared regional characteristics, we found common structural connectivity patterns of both the ASD and ADHD groups by NBS. We assumed that this might be partly related to the common distribution of hubs between the two groups. Evidence from Kernbach et al. (2018) also showed shared dysfunctional connectivity in the default mode network, dorsal attention network, and salience network in ASD and ADHD subjects, which is consistent with our work.

Numerous prior studies have addressed the relationship between the amygdala and autistic symptoms in ASD patients (Gotts et al., 2012; Mundy, 2017). Our correlation results were in accordance with previous studies revealing decreased *Ki* and *Enodal* of the AMYG.R that was associated with severe autistic symptoms in the ASD group. However, our correlation results failed to exhibit a significant association between the regional properties of the AMYG.R and SRS scores in the ADHD group. This outcome might be because ADHD subjects in our study showed no deficits that are considered ASD traits measured by the SRS. Moreover, our correlation results showed a decreased *Bi* of the PHG.R and *Ki* of the PHG.R; these values were also significantly correlated with severe autistic symptoms in the full sample and the ASD group, respectively. This common tendency is consistent with the findings of a previous study, which showed that the greater the degree of social impairment, the weaker the connectivity between the PHG and other brain regions (Weng et al., 2010). Notably, decreased *Bi* of the PHG.R was associated with better performance on the oppositional defiance subscale in the ADHD group, which might be an important complement to previous studies. Notably, our results revealed that abnormal *Bi* of the HIP.L was an ADHD-specific region in the brain network, and our correlation analysis further showed the relationship between altered *Bi* of the HIP.L and ADHD core symptoms

(i.e., inattention) in the full sample; these findings suggest the unique role of the HIP.L in the pathogenesis of ADHD.

In conclusion, our findings demonstrate that *Bi* of the HIP.L and hubness of the ACG.L might be valuable markers for distinguishing ASD from ADHD. While disorder-specific abnormalities are present, overlapping results are consistent with the growing clinical, molecular, and neuroimaging evidence of commonalities (Rommelse et al., 2011). In the present study, we found shared *Ki* alterations of the AMYG.R and PHG.R, as well as shared global network properties, hub distributions, and regional connectivity in the ASD and ADHD groups. In addition, altered *Enodal* of the AMYG.R, *Ki* of the AMYG.R, *Bi* of the PHG.R, and *Ki* of the PHG.R were associated with autistic symptoms, and altered *Bi* of the PHG.R and *Bi* of the HIP.L were associated with ADHD symptoms. Several aspects of our study are intriguing. First, no previous studies have concentrated on comparing topological properties of WM structural networks in individuals with ASD, individuals with ADHD, and TD controls concurrently. Our study is an important complement to previous studies. Second, our study analyzed different domains of topological properties, including global-based and node-based (e.g., regional properties, hub distributions, and regional connectivity) properties, providing comprehensive evidence for both shared and distinct underlying mechanisms in ASD and ADHD children and adolescents. Third, identifying and validating the similarities and differences of brain-based endophenotypes in the two disorders may be beneficial for personalized medicine (Collins and Varmus, 2015).

LIMITATIONS

There are several limitations that should be addressed. First, as mentioned previously, ASD and ADHD are neurodevelopmental disorders with overlapping clinical presentations (Van der Meer et al., 2012), while individuals without comorbid ADHD symptoms were included as ASD subjects in our study. Future analyses are required to explore the extent to which ADHD-like comorbidities in ASD share common neural correlates with ADHD. Second, this study used a deterministic tractography tracking procedure that produces more image noise and is of low resolution, making fiber tracking more error-prone because of the "fiber crossing" problem (Mori and van Zijl, 2002). The use of probabilistic tractography to define network edges could be helpful in addressing this issue (Iturria-Medina et al., 2008). Third, although the three groups did not differ significantly in sex distribution, most participants were male, reflecting the higher prevalence of boys with ASD and ADHD. Thus, our results may not generalize to girls, and future studies can enroll more female participants to further reveal sex differences in WM topological properties. Finally, the present participants were not matched for IQ; although the IQ effect was removed in all of the network analyses, these data should be interpreted with caution.

DATA AVAILABILITY STATEMENT

The raw data supporting the conclusions of this article will be made available by the authors, without undue reservation.

ETHICS STATEMENT

The studies involving human participants were reviewed and approved by the Medical Ethics Committees of the Nanjing Brain Hospital Affiliated to Nanjing Medical University. Written informed consent to participate in this study was provided by the participants' legal guardian/next of kin.

AUTHOR CONTRIBUTIONS

XK designed the study and revised the draft. LQ, YL, YaW, YuW, XC, CL, XC, and GJ collected and analyzed the data. LQ wrote the first draft of the manuscript. All authors contributed to and approved the final manuscript.

FUNDING

This work was supported the National Key Research and Development Program of China (2016YFC1306200), the National Natural Science Foundation of China (81771478), and the "Special disease cohort" Research Project of Nanjing Medical University (NMUC2018010A).

ACKNOWLEDGMENTS

We are thankful for the support of the funding mentioned above and acknowledge the patients and their families for their support and participation, as they made this study possible.

REFERENCES

Achard, S., Salvador, R., Whitcher, B., Suckling, J., and Bullmore, E. D. (2006). A resilient, low-frequency, small-world human brain functional network with highly connected association cortical hubs. *J. Neurosci.* 26, 63–72. doi: 10.1523/JNEUROSCI.3874-05.2006

Aggleton, J. P., O'Mara, S. M., Vann, S. D., Wright, N. F., Tsanov, M., and Erichsen, J. T. (2010). Hippocampal-anterior thalamic pathways for memory: uncovering a network of direct and indirect actions. *Eur. J. Neurosci.* 31, 2292–2307. doi: 10.1111/j.1460-9568.2010.07251.x

Ameis, S. H., and Catani, M. (2015). Altered white matter connectivity as a neural substrate for social impairment in autism spectrum disorder. *Cortex* 62, 158–181. doi: 10.1016/j.cortex.2014.10.014

Ameis, S. H., Lerch, J. P., Taylor, M. J., Lee, W., Viviano, J. D., Pipitone, J., et al. (2016). A diffusion tensor imaging study in children with ADHD, autism spectrum disorder, OCD, and matched controls distinct and non-distinct white matter disruption and dimensional brain-behavior relationships. *Am. J. Psychiatry* 173, 1213–1222. doi: 10.1176/appi.ajp.2016.15111435

American Psychiatric Association (2013). *Diagnostic and Statistical Manual of Mental Disorders*, 5th Edn, Arlington, VA: American Psychiatric Association.

Anderson, A., Douglas, P. K., Kerr, W. T., Haynes, V. S., Yuille, A. L., Xie, J., et al. (2014). Non-negative matrix factorization of multimodal MRI, fMRI and phenotypic data reveals differential changes in default mode subnetworks in ADHD. *Neuroimage* 102, 207–219. doi: 10.1016/j.neuroimage.2013.12.015

Apps, M. A., Rushworth, M. F., and Chang, S. W. (2016). The anterior cingulate gyrus and social cognition: tracking the motivation of others. *Neuron* 90, 692–707. doi: 10.1016/j.neuron.2016.04.018

Baribeau, D. A., Dupuis, A., Paton, T. A., Hammill, C., Scherer, S. W., Schachar, R. J., et al. (2019). Structural neuroimaging correlates of social deficits are similar in autism spectrum disorder and attention-deficit/hyperactivity disorder: analysis from the pond network. *Transl. Psychiat.* 9:72. doi: 10.1038/s41398-019-0382-0

Boedhoe, P. S. W., van Rooij, D., Hoogman, M., Twisk, J. W. R., Schmaal, L., Abe, Y., et al. (2020). Subcortical brain volume, regional cortical thickness, and cortical surface area across disorders: findings from the ENIGMA ADHD, ASD, and OCD working groups. *Am. J. Psychiatry* 177, 834–843. doi: 10.1176/appi.ajp.2020.19030331

Bullmore, E., and Sporns, O. (2009). Complex brain networks: graph theoretical analysis of structural and functional systems. *Nat. Rev. Neurosci.* 10:312. doi: 10.1038/nrn2618

Bullmore, E., and Sporns, O. (2012). The economy of brain network organization. *Nat. Rev. Neurosci.* 13, 336–349. doi: 10.1038/nrn3214

Catani, M., Dell'Acqua, F., and Thiebaut, D. S. M. (2013). A revised limbic system model for memory, emotion and behaviour. *Neurosci. Biobehav. Rev.* 37, 1724–1737. doi: 10.1016/j.neubiorev.2013.07.001

Chang, S. W. C., Gariépy, J., and Platt, M. L. (2012). Neuronal reference frames for social decisions in primate frontal cortex. *Nat. Neurosci.* 16, 243–250. doi: 10.1038/nn.3287

Chen, Y., Huang, X., Wu, M., Li, K., Hu, X., Jiang, P., et al. (2019). Disrupted brain functional networks in drug-nave children with attention deficit hyperactivity disorder assessed using graph theory analysis. *Hum. Brain Mapp.* 40, 4877–4887. doi: 10.1002/hbm.24743

Christiansen, H., Hirsch, O., Albrecht, B., and Chavanon, M. L. (2019). Attention-deficit/hyperactivity disorder (ADHD) and emotion regulation over the life span. *Curr. Psychiat. Rep.* 21:17. doi: 10.1007/s11920-019-1003-6

Collins, F. S., and Varmus, H. (2015). A new initiative on precision medicine. *New Engl. J. Med.* 372, 793–795. doi: 10.1056/NEJMp1500523

Constantino, J. N. (2013). *Social Responsiveness Scale: Encyclopedia of Autism Spectrum Disorders*. New York, NY: Springer.

Cui, Z., Zhong, S., Xu, P., He, Y., and Gong, G. (2013). PANDA: a pipeline toolbox for analyzing brain diffusion images. *Front. Hum. Neurosci.* 7:42. doi: 10.3389/fnhum.2013.00042

Di Martino, A., Zuo, X. N., Kelly, C., Grzadzinski, R., Mennes, M., Schvarcz, A., et al. (2013). Shared and distinct intrinsic functional network centrality in autism and attention-deficit/hyperactivity disorder. *Biol. Psychiat.* 74, 623–632. doi: 10.1016/j.biopsych.2013.02.011

Feis, Y. F. (2010). "Wechsler intelligence scale for children-IV (WISC-IV)," in *Encyclopedia of Cross-Cultural School Psychology*, ed. C. S. Clauss-Ehlers (Boston, MA: Springer), 1030–1032. doi: 10.1007/978-0-387-71799-9_446

Filippo, M. D., Picconi, B., Tantucci, M., Ghiglieri, V., Bagetta, V., Sgobio, C., et al. (2009). Short-term and long-term plasticity at corticostriatal synapses: implications for learning and memory. *Behav. Brain Res.* 199, 108–118. doi: 10.1016/j.bbr.2008.09.025

Fonseca, D. D., Seguier, V., Santos, A., Poinso, F., and Deruelle, C. (2009). Emotion understanding in children with ADHD. *Child Psychiat. Hum. Dev.* 40, 111–121. doi: 10.1007/s10578-008-0114-9

Fox, M. D., Snyder, A. Z., Vincent, J. L., Corbetta, M., Van Essen, D. C., and Raichle, M. E. (2005). From the Cover: the human brain is intrinsically organized into dynamic, anticorrelated functional networks. *Proc. Natl. Acad. Sci. U.S.A.* 102, 9673–9678. doi: 10.1073/pnas.0504136102

Gau, S. F., Shang, C. Y., Liu, S. K., Lin, C. H., Swanson, J. M., Liu, Y.-C., et al. (2008). Psychometric properties of the Chinese version of the Swanson, Nolan, and Pelham, version IV scale - parent form. *Int. J. Method Psychiatr. Res.* 17, 35–44. doi: 10.1002/mpr.237

Gibbard, C. R., Ren, J. J., Skuse, D. H., Clayden, J. D., and Clark, C. A. (2017). Structural connectivity of the amygdala in young adults with autism spectrum disorder. *Hum. Brain Mapp.* 39, 1270–1282. doi: 10.1002/hbm.23915

Gotts, S. J., Kyle, S. W., Milbury, L. A., Wallace, G. L., Cox, R. W., and Alex, M. (2012). Fractionation of social brain circuits in autism spectrum disorders. *Brain* 135, 2711–2725. doi: 10.1093/brain/aws160

Groen, W., Teluij, M., Buitelaar, J., and Tendolkar, I. (2010). Amygdala and hippocampus enlargement during adolescence in autism. *J. Am. Acad. Child Psychiatry* 49, 552–560. doi: 10.1016/j.jaac.2009.12.023

Gudmundsson, O. O., Walters, G. B., Ingason, A., Johansson, S., Zayats, T., Athanasiu, L., et al. (2019). Attention-deficit hyperactivity disorder shares copy number variant risk with schizophrenia and autism spectrum disorder. *Transl. Psychiatry* 9:258. doi: 10.1038/s41398-019-0599-y

Guo, B., Chen, J., Chen, Q., Ren, K., Feng, D., Mao, H., et al. (2019). Anterior cingulate cortex dysfunction underlies social deficits in shank3 mutant mice. *Nat. Neurosci.* 22, 1223–1234. doi: 10.1038/s41593-019-0445-9

Guo, X. N., Duan, X. J., Long, Z. L., Chen, H., Wang, Y. F., Zheng, J. J., et al. (2016). Decreased amygdala functional connectivity in adolescents with autism: a resting-state fMRI study. *Psychiat. Res. Neuroimage* 257, 47–56. doi: 10.1016/j.pscychresns.2016.10.005

Hagmann, P., Cammoun, L., Gigandet, X., Meuli, R., Honey, C. J., Wedeen, V. J., et al. (2008). Mapping the structural core of Human Cereb. *Cortex PLoS Biol.* 6:e159. doi: 10.1371/journal.pbio.0060159

Hoogman, M., Bralten, J., Hibar, D. P., Mennes, M., Zwiers, M. P., Schweren, L. S. J., et al. (2017). Subcortical brain volume differences in participants with attention deficit hyperactivity disorder in children and adults: a cross-sectional mega-analysis. *Lancet Psychiatry* 4, 310–319. doi: 10.1016/S2215-0366(17)30049-4

Hoogman, M., Muetzel, R., Guimaraes, J. P., Shumskaya, E., Mennes, M., Zwiers, M. P., et al. (2019). Brain imaging of the cortex in ADHD: a coordinated analysis of large-scale clinical and population-based samples. *Am. J. Psychiatry* 176, 531–542. doi: 10.1176/appi.ajp.2019.18091033

Hulvershorn, L. A., Mennes, M., Castellanos, F. X., Di Martino, A., Milham, M. P., Hummer, T. A., et al. (2014). Abnormal Amygdala functional connectivity associated with emotional lability in children with attention-deficit/hyperactivity disorder. *J. Am. Acad. Child Psychiatry* 53, 351–361.e1. doi: 10.1016/j.jaac.2013.11.012

Iidaka, T., Kogata, T., Mano, Y., and Komeda, H. (2019). Thalamocortical hyperconnectivity and amygdala-cortical hypoconnectivity in male patients with autism spectrum disorder. *Front. Psychiatry* 10:252. doi: 10.3389/fpsyt.2019.00252

Iturria-Medina, Y., Sotero, R. C., Canales-Rodríguez, E. J., Alema'n-Go'mez, Y., and Melie-García, L. (2008). Studying the human brain anatomical network via diffusion-weighted MRI and graph theory. *Neuroimage* 40, 1064–1076. doi: 10.1016/j.neuroimage.2007.10.060

Just, M. A., Cherkassky, V. L., Keller, T. A., and Minshew, N. J. (2004). Cortical activation and synchronization during sentence comprehension in high-functioning autism: evidence of underconnectivity. *Brain* 127(Pt 8), 1811–1821. doi: 10.1093/brain/awh199

Kernbach, J. M., Satterthwaite, T. D., Bassett, D. S., Jonathan, S., Daniel, M., Sarah, K., et al. (2018). Shared endo-phenotypes of default mode dysfunction in attention deficit/hyperactivity disorder and autism spectrum disorder. *Transl. Psychiatry* 8:133. doi: 10.1038/s41398-018-0179-6

Konrad, K., and Eickhoff, S. B. (2010). Is the ADHD brain wired differently? A review on structural and functional connectivity in attention deficit hyperactivity disorder. *Hum. Brain Mapp.* 31, 904–916. doi: 10.1002/hbm.21058

Lee, J. M., Kyeong, S., Kim, E., and Cheon, K. (2016). Abnormalities of Inter- and Intra-hemispheric functional connectivity in autism spectrum disorders: a study using the autism brain imaging data exchange database. *Front. Neurosci.* 10:191. doi: 10.3389/fnins.2016.00191

Li, S. J., Wang, Y., Qian, L., Liu, G., Liu, S. F., Zou, L. P., et al. (2018). Alterations of white matter connectivity in preschool children with autism spectrum disorder. *Radiology* 288:170059. doi: 10.1148/radiol.2018170059

Lord, C., Rutter, M., and Couteur, L. A. (1994). Autism diagnostic interview-revised: a revised version of a diagnostic interview for caregivers of individuals with possible pervasive developmental disorders. *J. Autism Dev. Disord.* 24, 659–685. doi: 10.1007/BF02172145

Lord, C., Rutter, M., Goode, S., Heemsbergen, J., Jordan, H., Mawhood, L., et al. (1989). Autism diagnostic observation schedule: a standardized observation of communicative and social behavior. *J. Autism Dev. Disord.* 19, 185–212. doi: 10.1007/bf02211841

Medin, T., Rinholm, J. E., Owe, S. G., Sagvolden, T., Gjedde, A., Storm-Mathisen, J., et al. (2013). Low dopamine D5 receptor density in hippocampus in an animal model of attention-deficit/hyperactivity disorder (ADHD). *Neuroscience* 242, 11–20. doi: 10.1016/j.neuroscience.2013.03.036

Mesulam, M. M. (1998). From sensation to cognition. *Brain* 121(Pt 6), 1013–1052. doi: 10.1093/brain/121.6.1013

Miller, M., Hanford, R. B., Fassbender, C., Duke, M., and Schweitzer, J. B. (2011). Affect recognition in adults with ADHD. *J. Attention Disord.* 15, 452–460. doi: 10.1177/1087054710368636

Monk, C. S., Peltier, S. J., Wiggins, J. L., Weng, S. J., Carrasco, M., Risi, S., et al. (2009). Abnormalities of intrinsic functional connectivity in autism spectrum disorders. *Neuroimage* 47, 764–772. doi: 10.1016/j.neuroimage.2009.04.069

Mori, S., and van Zijl, P. C. M. (2002). Fiber tracking: principles and strategies - a technical review. *NMR Biomed.* 15, 468–480. doi: 10.1002/nbm.781

Mundy, P. (2017). A review of joint attention and social-cognitive brain systems in typical development and autism spectrum disorder. *Eur. J. Neurosci.* 47, 497–514. doi: 10.1111/ejn.13720

Odriozola, P., Dajani, D. R., Burrows, C. A., Gabard-Durnam, L. J., Goodman, E., Baez, A. C., et al. (2018). Atypical frontoamygdala functional connectivity in youth with autism. *Dev. Cogn. Neurosci.* 37:100603. doi: 10.1016/j.dcn.2018.12.001

Pagani, M., Manouilenko, I., Stone-Elander, S., Odh, R., Salmaso, D., Hatherly, R., et al. (2012). Brief report: alterations in cerebral blood flow as assessed by PET/CT in adults with autism spectrum disorder with normal IQ. *J. Autism Dev. Disord.* 42, 313–318. doi: 10.1007/s10803-011-1240-y

Paquette, V., Lévesque, J., Mensour, B., Leroux, J. M., Beaudoin, G., Bourgouin, P., et al. (2003). "Change the mind and you change the brain": effects of cognitive-behavioral therapy on the neural correlates of spider phobia. *Neuroimage* 18, 401–409. doi: 10.1016/s1053-8119(02)00030-7

Posner, J., Nagel, B. J., Maia, T. V., Mechling, A., Oh, M., Wang, Z., et al. (2011). Abnormal amygdalar activation and connectivity in adolescents with attention-deficit/hyperactivity disorder. *J. Am. Acad. Child Psychiatry* 50, 828–837.e3. doi: 10.1016/j.jaac.2011.05.010

Posner, J., Siciliano, F., Wang, Z., Liu, J., Sonuga-Barke, E., and Greenhill, L. (2014). A multimodal MRI study of the hippocampus in medication-naive children with ADHD: what connects ADHD and depression? *Psychiat. Res. Neuroimage* 224, 112–118. doi: 10.1016/j.pscychresns.2014.08.006

Qian, L., Wang, Y., Chu, K., Li, Y., Xiao, C., Xiao, T., et al. (2018). Alterations in hub organization in the white matter structural network in toddlers with autism spectrum disorder: a 2-year follow-up study. *Autism Res.* 11, 1218–1228. doi: 10.1002/aur.1983

Roine, U., Roine, T., Salmi, J., Taina, N. W., Tani, P., Leppämäki, S., et al. (2015). Abnormal wiring of the connectome in adults with high-functioning autism spectrum disorder. *Mol. Autism.* 6:65. doi: 10.1186/s13229-015-0058-4

Rommelse, N. N. J., Franke, B., Geurts, H. M., Hartman, C. A., and Buitelaar, J. K. (2010). Shared heritability of attention-deficit/hyperactivity disorder and autism spectrum disorder. *Eur. Child Adoles. Psychiatry* 19, 281–295. doi: 10.1007/s00787-010-0092-x

Rommelse, N. N. J., Geurts, H. M., Franke, B., Buitelaar, J. K., and Hartman, C. A. (2011). A review on cognitive and brain endophenotypes that may be common in autism spectrum disorder and attention-deficit/hyperactivity disorder and facilitate the search for pleiotropic genes. *Neurosci. Biobehav. Rev.* 35, 1363–1396. doi: 10.1016/j.neubiorev.2011.02.015

Rubinov, M., and Sporns, O. (2010). Complex network measures of brain connectivity: uses and interpretations. *Neuroimage* 52, 1059–1069. doi: 10.1016/j.neuroimage.2009.10.003

Rudie, J. D., Brown, J. A., Beck-Pancer, D., Hernandez, L. M., Dennis, E. L., Thompson, P. M., et al. (2013). Altered functional and structural brain network organization in autism. *Neuroimage Clin.* 2, 79–94. doi: 10.1016/j.nicl.2012.11.006

Schoch, H., Kreibich, A. S., Ferri, S. L., White, R. S., Bohorquez, D., Banerjee, A., et al. (2016). Sociability deficits and altered amygdala circuits in mice lacking Pcdh10. *Ann. Autism Assoc. Gene Biol. Psychiatry* 81, 193–202. doi: 10.1016/j.biopsych.2016.06.008

Schumann, C. M., Hamstra, J., Goodlin-Jones, B. L., Lotspeich, L. J., and Amaral, D. G. (2004). The amygdala is enlarged in children but not adolescents with autism; the hippocampus is enlarged at all ages. *J. Neurosci.* 24:6392. doi: 10.1523/JNEUROSCI.1297-04.2004

Shu, N., Liu, Y., Li, K., Duan, Y., Wang, J., Yu, C., et al. (2011). Diffusion tensor tractography reveals disrupted topological efficiency in white matter structural networks in multiple sclerosis. *Cereb. Cortex* 21, 2565–2577. doi: 10.1093/cercor/bhr039

Sidlauskaite, J., Caeyenberghs, K., Sonuga-Barke, E., Roeyers, H., and Wiersema, J. R. (2015). Whole-brain structural topology in adult attention-deficit/hyperactivity disorder: preserved global - disturbed local network organization. *Neuroimage Clin.* 9, 506–512. doi: 10.1016/j.nicl.2015.10.001

Sporns, O., Tononi, G., and Kotter, R. (2005). The human connectome: a structural description of the human brain. *PLoS Comput. Biol.* 1:e42. doi: 10.1371/journal.pcbi.0010042

Stergiakouli, E., Smith, G. D., Martin, J., Skuse, D. H., Viechtbauer, W., Ring, S. M., et al. (2017). Shared genetic influences between dimensional ASD and ADHD symptoms during child and adolescent development. *Mol. Autism.* 8:18. doi: 10.1186/s13229-017-0131-2

Sterley, T. L., Howells, F. M., and Russell, V. A. (2013). Evidence for reduced tonic levels of GABA in the hippocampus of an animal model of ADHD, the spontaneously hypertensive rat. *Brain Res.* 1541, 52–60. doi: 10.1016/j.brainres.2013.10.023

Supekar, K., Musen, M., and Menon, V. (2009). Development of large-scale functional brain networks in children. *PLoS Biol.* 7:e1000157. doi: 10.1371/journal.pbio.1000157

Takashi, I., Takashi, Y., Hiromi, W., Motoaki, N., Daiki, J., Seiji, S., et al. (2014). Altered network topologies and hub organization in adults with autism: a resting-state fMRI study. *PLoS One* 9:e94115. doi: 10.1371/journal.pone.0094115

Travers, B. G., Adluru, N., Ennis, C., Tromp do, P. M., Destiche, D., Doran, S., et al. (2012). Diffusion tensor imaging in autism spectrum disorder: a review. *Autism Res.* 5, 289–313. doi: 10.1002/aur.1243

Tzourio-Mazoyer, N., Landeau, B., Papathanassiou, D., Crivello, F., Etard, O., Delcroix, N., et al. (2002). Automated anatomical labeling of activations in SPM using a macroscopic anatomical parcellation of the MNI MRI single-subject brain. *Neuroimage* 15, 273–289. doi: 10.1006/nimg.2001.0978

Van der Meer, J. M. J., Oerlemans, A. M., van Steijn, D. J., Lappenschaar, M. G. A., de Sonneville, L. M. J., Buitelaar, J. K., et al. (2012). Are autism spectrum disorder and attention-deficit/hyperactivity disorder different manifestations of one overarching disorder? cognitive and symptom evidence from a clinical and population-based sample. *J. Am. Acad. Child Psychiatry* 51, 1160–1172.e3. doi: 10.1016/j.jaac.2012.08.024

Van Rooij, D., Anagnostou, E., Arango, C., Auzias, G., Behrmann, M., Busatto, G. F., et al. (2018). Cortical and subcortical brain morphometry differences between patients with autism spectrum disorder and healthy individuals across the lifespan: results from the ENIGMA ASD working group. *Am. J. Psychiatry* 175, 359–369. doi: 10.1176/appi.ajp.2017.17010100

Vijayakumar, N., Whittle, S., Dennison, M., Yücel, M., Simmons, J., and Allen, N. B. (2014). Development of temperamental effortful control mediates the relationship between maturation of the prefrontal cortex and psychopathology during adolescence: a 4-year longitudinal study. *Dev. Cogn. Neurosci.* 9, 30–43. doi: 10.1016/j.dcn.2013.12.002

Wang, L., Zhu, C., He, Y., Zang, Y., Zang, Y., Cao, Q., et al. (2009). Altered small-world brain functional networks in children with attention deficit/hyperactivity disorder. *Hum. Brain Mapp.* 30, 638–649. doi: 10.1002/hbm.20530

Weng, S. J., Wiggins, J. L., Peltier, S. J., Carrasco, M., Risi, S., Lord, C., et al. (2010). Alterations of resting state functional connectivity in the default network in adolescents with autism spectrum disorders. *Brain Res.* 1313, 202–214. doi: 10.1016/j.brainres.2009.11.057

Xia, S., Foxe, J. J., Sroubek, A. E., Branch, C., and Li, X. (2014). Topological organization of the "small-world" visual attention network in children with attention deficit/hyperactivity disorder (ADHD). *Front. Hum. Neurosci.* 8:162. doi: 10.3389/fnhum.2014.00162

Zalesky, A., Fornito, A., and Bullmore, E. T. (2010). Network-based statistic: identifying differences in brain networks. *Neuroimage* 53, 1197–1207. doi: 10.1016/j.neuroimage.2010.06.041

Zielinski, B. A., Anderson, J. S., Froehlich, A. L., Prigge, M. B. D., Nielsen, J. A., Cooperrider, J. R., et al. (2012). scMRI reveals large-scale brain network abnormalities in autism. *PLoS One* 7:e49172. doi: 10.1371/journal.pone.0049172

Conflict of Interest: The authors declare that the research was conducted in the absence of any commercial or financial relationships that could be construed as a potential conflict of interest.

frontiers in Neuroscience

REVIEW
published: 25 August 2021
doi: 10.3389/fnins.2021.698812

Pre-clinical Investigation of Rett Syndrome Using Human Stem Cell-Based Disease Models

*Florencia D. Haase[1,2,3], Bronte Coorey[1,2,3], Lisa Riley[4], Laurence C. Cantrill[1,5], Patrick P. L. Tam[6,7] and Wendy A. Gold[2,3,4]**

[1] Faculty of Medicine and Health, The University of Sydney, Sydney, NSW, Australia, [2] Kids Neuroscience Centre, Kids Research, Children's Hospital at Westmead, Westmead, NSW, Australia, [3] Molecular Neurobiology Research Laboratory, Kids Research, Children's Hospital at Westmead, and Children's Medical Research Institute, Westmead, NSW, Australia, [4] Rare Diseases Functional Genomics Laboratory, Kids Research, Children's Hospital at Westmead, and Children's Medical Research Institute, Westmead, NSW, Australia, [5] Kids Research, Children's Hospital at Westmead, Westmead, NSW, Australia, [6] Embryology Research Unit, Children's Medical Research Institute, The University of Sydney, Sydney, NSW, Australia, [7] School of Medical Sciences, Faculty of Medicine and Health, The University of Sydney, Sydney, NSW, Australia

Rett syndrome (RTT) is an X-linked neurodevelopmental disorder, mostly caused by mutations in *MECP2*. The disorder mainly affects girls and it is associated with severe cognitive and physical disabilities. Modeling RTT in neural and glial cell cultures and brain organoids derived from patient- or mutation-specific human induced pluripotent stem cells (iPSCs) has advanced our understanding of the pathogenesis of RTT, such as disease-causing mechanisms, disease progression, and cellular and molecular pathology enabling the identification of actionable therapeutic targets. Brain organoid models that recapitulate much of the tissue architecture and the complexity of cell types in the developing brain, offer further unprecedented opportunity for elucidating human neural development, without resorting to conventional animal models and the limited resource of human neural tissues. This review focuses on the new knowledge of RTT that has been gleaned from the iPSC-based models as well as limitations of the models and strategies to refine organoid technology in the quest for clinically relevant disease models for RTT and the broader spectrum of neurodevelopmental disorders.

Keywords: Rett syndrome, neurodevelopmental disorders, iPSCs (induced pluripotent stem cells), brain organoids, disease modeling

OPEN ACCESS

Edited by:
Li Yang,
Peking University Sixth Hospital, China

Reviewed by:
In-Hyun Park,
Yale University, United States
Madeline Andrews,
University of California, San Francisco, United States

***Correspondence:**
Wendy A. Gold
Wendy.gold@sydney.edu.au

Specialty section:
This article was submitted to Neurodevelopment, a section of the journal Frontiers in Neuroscience

Received: *22 April 2021*
Accepted: *19 July 2021*
Published: *25 August 2021*

Citation:
Haase FD, Coorey B, Riley L, Cantrill LC, Tam PPL and Gold WA (2021) Pre-clinical Investigation of Rett Syndrome Using Human Stem Cell-Based Disease Models. Front. Neurosci. 15:698812. doi: 10.3389/fnins.2021.698812

INTRODUCTION

Since the discovery that mutations in the MECP2 gene were the underlying cause of RTT, a great amount of work has been undertaken to understand the molecular function of MeCP2 (Amir et al., 1999; **Figure 1**). MeCP2 was initially identified as a transcriptional repressor located in the nucleus that bound to methylated DNA (Lewis et al., 1992). However, subsequently, it was described as a pluripotent transcriptional regulator, with the capacity to activate or repress target genes depending on the molecular context (Chahrour et al., 2008). More recently, the roles of MeCP2 have expanded to include alternative splicing, chromatin remodeling and miRNA processing (as reviewed in Tillotson and Bird, 2020). Patients with RTT, generally, present reduced brain volume associated with an abnormal morphology of neurons, including small and densely packed structures

(Armstrong et al., 1995). It has also been observed that the dendrites of pyramidal neurons are significantly shorter than in wild type brains. Observations using MRI data have also shown reductions in the volume of the parietal and temporal lobes in RTT patients with conservation of the occipital cortex (Carter et al., 2008).

From a cellular point of view, it is known that MeCP2 loss affects different cell types in the brain. Region specific knockouts in mouse brains have shown several different phenotypes; for instance, removal of MeCP2 from dopaminergic and noradrenergic neurons induced motor incoordination (Samaco et al., 2009) and removal from the brainstem and spinal cord led to abnormal heart rate and breathing patters (Huang et al., 2016). Loss of MeCP2 in inhibitory neurons has also shown a prominent reproducibility of severe forms of RTT phenotypes, emphasizing the importance of E/I balance to MeCP2-mediated functions (Chao et al., 2010).

CLINICAL FEATURES OF RETT SYNDROME

Rett syndrome (RTT) is a rare neurodevelopmental disorder that manifests between 6 and 18 months of age after a period of apparently normal prenatal and postnatal development. Symptoms vary amongst individuals and include loss of fine and gross motor skills, abnormal social behavior, growth retardation, seizures, breathing dysregulation and stereotypic hand wringing movements (Neul et al., 2010). RTT has a worldwide prevalence of 1 in 10,000 individuals and predominantly affects females.

The majority of RTT cases are caused by *de novo* mutations in the X-linked methyl-CpG-binding protein 2 (*MECP2*) gene, which plays a critical role in normal brain development, specifically in the maturation of the central nervous system (CNS) and synapse development and function (Liyanage and Rastegar, 2014).

Substantial phenotypic variability is observed in girls with RTT, which is attributed to the type of mutation (missense, nonsense, etc.) and its location on *MECP2* as well as X chromosome inactivation (XCI). As the mutations observed in RTT girls are predominantly hemizygous, XCI renders a mosaic expression of the variant with some cell populations expressing the mutant *MECP2* allele and others, the wild type allele. While these two populations are normally present in nearly equal (1:1) proportion, the X inactivation pattern can be skewed, favoring the expression of one cell population over the other. In contrast, RTT males present with a homogenous population of mutant cells and are thus more severely affected.

Although *MECP2* is ubiquitously expressed, its expression is particularly high in post-mitotic neurons in the brain. Mutations that result in the dysregulation of *MECP2* cause a range of abnormalities at the anatomical, cellular, and molecular levels that is well characterized. There is an apparent reduction in brain volume in both humans and mouse models correlating with the severity of the phenotype (Carter et al., 2008), however, this reduction in brain size is not due to gross anatomical defects, but rather to small and densely packed neurons of reduced dendritic branching, soma size, spine density and synapse number (Belichenko et al., 2009).

Currently, treatment for RTT is purely symptomatic and requires a multidisciplinary approach for medical management. Furthermore, despite almost 60 observational and interventional clinical trials being conducted, it is still unknown whether all symptoms can be reversed. One of the most significant contributions to the field of RTT has been the phenotypic reversal of *Mecp2*-deficient transgenic mice to wild type upon the reinstatement of *Mecp2* expression, revealing the potential of gene therapy as a treatment (Guy et al., 2007). However, none of the recent gene transfer therapy studies in RTT mouse models have been able to entirely correct all RTT-associated symptoms (Gadalla et al., 2013, 2017; Garg et al., 2013; Sinnett et al., 2017; Tillotson et al., 2017; Luoni et al., 2020).

MODELING RETT SYNDROME USING iPSCs

The modeling of neurodevelopmental disorders is hampered by the inaccessibility and the limited source of live human brain tissue. Post-mortem tissue and immortalized cell lines have been adopted as the standard models for investigating the pathology of RTT predominately at the end-stage of the disease. Genetic mouse models of RTT that replicate salient features of the human neuropathology and cognitive deficits has further allowed the study of the pathophysiology and the natural history of disease progression. However, the inter-species differences in brain development and physiological function, and the inherent differentiation in cell composition between humans and mice at fetal and adult stages (Velasco et al., 2019; Eze et al., 2021) raise reservations about the fidelity of the animal study in modeling human neurodevelopmental disorders. Therefore, understanding of the disease causing mechanisms and pathophysiology of RTT with a view to developing effective therapies requires development of humanized disease models, which could be accomplished by using human pluripotent stem cells to generate cellular models and brain organoids.

The introduction of human embryonic stem cells (hESCs) and induced pluripotent stem cells (iPSCs) to the discipline of precision medicine and advanced therapeutics has revolutionized the pre-clinical research of neurodevelopmental disorders (NDDs) such as RTT. hESCs are derived from blastocyst-stage human embryos whereas iPSCs are derived from somatic cells such as fibroblasts, blood and exfoliated urinary epithelial cells by cell reprogramming through transgenesis or foot-print free genetic modulation (Martinez-Fernandez et al., 2010; Yamanaka, 2012; Hsu et al., 2020). Both types of stem cells can be subjected to genetic modification to generate specific disease variants for modeling NDDs, where mutation- or patient- specific stem cells cannot be obtained. Stem cells have been used to create cellular models for a variety of cell types such as cortical and ventral neurons and glial cells in a conventional tissue culture setting (Takahashi and Yamanaka, 2006; Marchetto et al., 2010), as well as three-dimensional (3-D) complex tissue spheroids, organoids and assembloids that recapitulate different brain parts

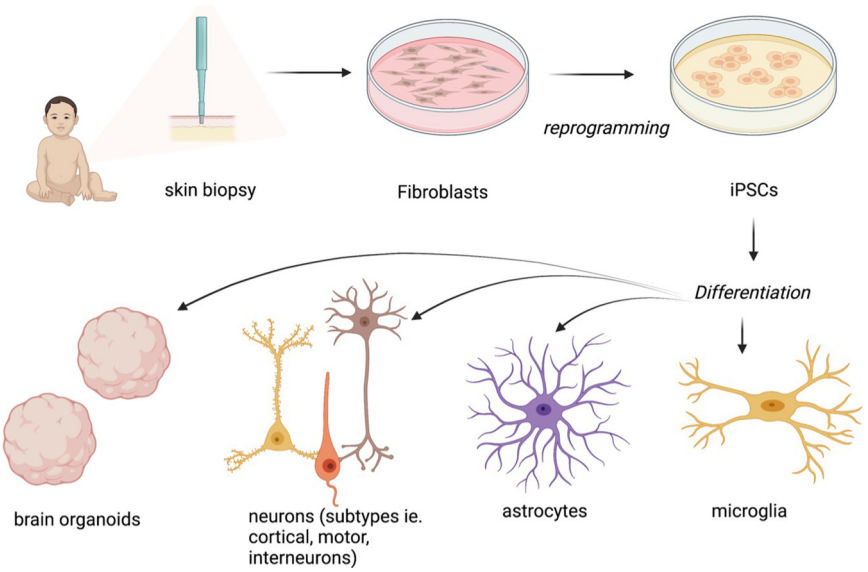

FIGURE 1 | Normal MeCP2 function as a transcriptional repressor and activator and consequences of abnormal MeCP2 function in the brain at a cellular level. "Created with BioRender.com."

(Lancaster et al., 2013; Marton and Paşca, 2020; **Figure 2**). In brief, spheroids are simple clusters of cells that do not require scaffolding to form three dimensional structures and hence are not as advanced as organoids, which in contrast are more complex clusters of organ specific cells such as different types of neural cells; assembloids are structures formed by the assembly of different tissue specific organoids.

The use of iPSCs has been particularly useful as a complementary approach to existing disease models, such as murine and post-mortem tissue, as they offer a more human-centered approach in which to test therapies given the inaccessibility to patient brain tissue. Encouragingly, disease modeling has been achieved for neurodegenerative disorders such as Alzheimer's, Parkinson's, and Huntington's disease, extending recently to neuropsychiatric, monogenetic, and chromosomal aberration disorders.

Resource of MECP2-Mutant iPSCs

There are over 500 pathogenic mutations in *MECP2,* with the majority lying in exons 3 and 4 in the methyl binding domain (MBD), transcriptional repressor domain (TRD) and the C-terminal functional domain (CTD) regions, disrupting the normal function of the MeCP2 protein (Wan et al., 1999; Gold et al., 2018). Several iPSC lines harboring a range of *MECP2* mutations, including point mutations, frameshift mutations, deletions, and nonsense mutations have been generated and used in RTT studies (**Supplementary Table 1**).

All RTT studies using iPSC models have used iPSCs reprogrammed from patient-derived fibroblast cells (**Table 1**). As RTT manifests mostly in girls, the majority of studies to date have used iPSC lines from female patients, with the exception of five studies that used male patient-specific iPSCs (Tang et al., 2016; Zhang et al., 2016; de Souza et al., 2017; Yoo et al., 2017; Kim et al., 2019; **Supplementary Table 1**). To take into consideration the impact of XCI and genetic background of individuals, female lines are usually compared to their isogenic controls, which are genetically corrected iPSCs from the same patient (Kim et al., 2011; Cheung et al., 2012; Andoh-Noda et al., 2015; Djuric et al., 2015; Chin et al., 2016; Landucci et al., 2018; Nguyen et al., 2018). In studies where male lines are used, the control cell lines have been derived from the unaffected father, acting as a surrogate isogenic control (Tang et al., 2016; de Souza et al., 2017; Yoo et al., 2017; Kim et al., 2019).

Modeling RTT Neuronal Cells

Rett syndrome is an archetypical genetic disease and was one of the first pediatric neurological disorders to be studied using stem cell-based models (Xie and Tang, 2016). The phenotypes of neuronal cells of mice and post-mortem human brains include smaller soma size and reduced dendritic branching, spine density and morphology, as well as axonal bouton arborization and synapse formation (Belichenko et al., 2009; Marchetto et al., 2010; Baj et al., 2014; **Figure 1**). These anatomical defects are accompanied by an imbalance of excitatory/inhibitory (E/I) activity, with more excitatory and less inhibitory synaptic activity in the hippocampus and cortex (Nelson et al., 2006; Chao et al., 2010). iPSCs from RTT patient fibroblasts have been successfully differentiated into neuronal progenitor cells (NPCs), neurons and glia and the modeling has recapitulated some of the cellular and physiological phenotypes of these cell types, including morphological and electrophysiological defects.

The distinct phenotype of post-mortem and murine RTT neurons, characterized by a smaller soma size and reduced dendritic branching, spine density and axonal arborization, is well documented (Belichenko et al., 2009; Marchetto et al., 2010; Baj et al., 2014). This robust phenotype has

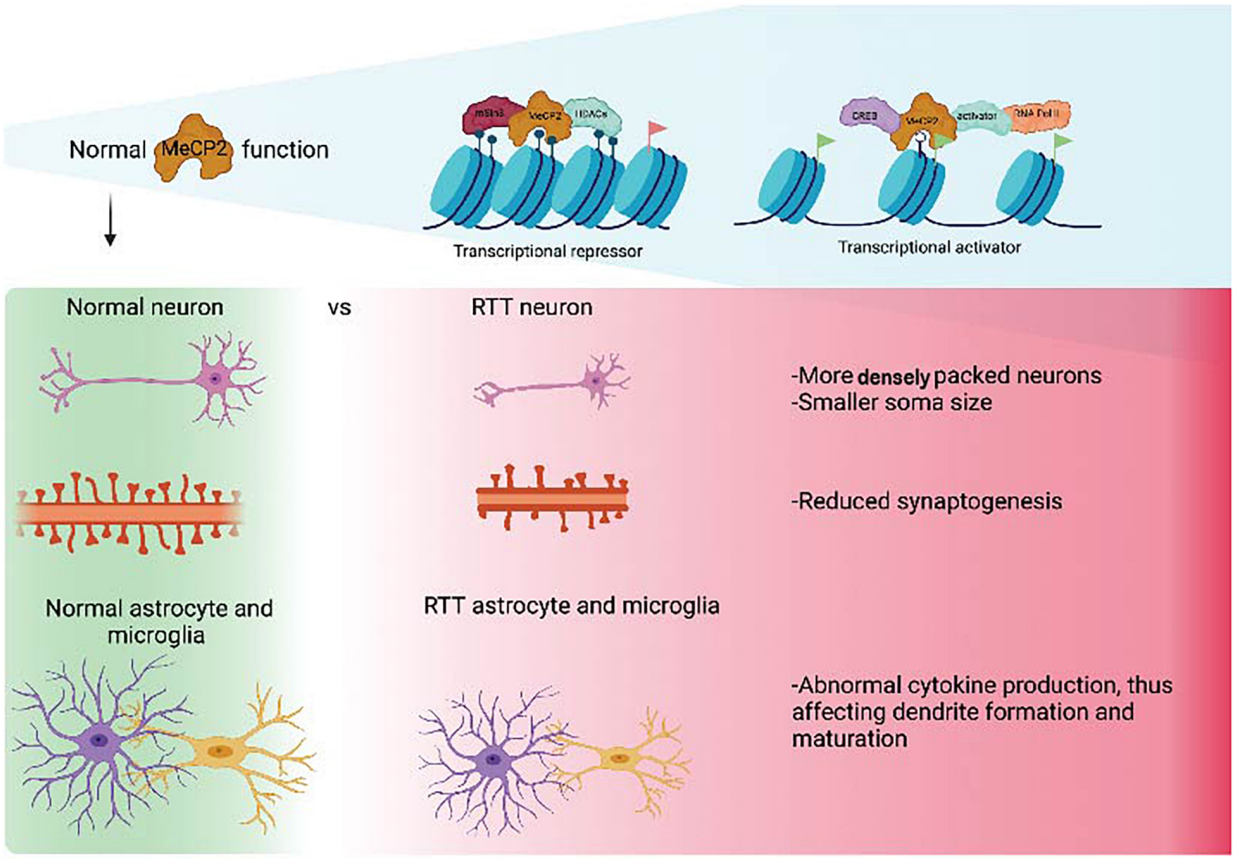

FIGURE 2 | Overview of different methodologies employed in the articles used in this review to model RTT using iPSCs. "Created with BioRender.com."

TABLE 1 | XCI status of different cell lines used.

Group	Fibroblasts reprogrammed	XCI status of iPSC clones
Cheung et al., 2011	MECP2: Δ3–4 (g.61340_67032delinsAGTTGTGCCAC and g.67072_67200del) – female, GM11270 (R306C) – female, GM17880 (T158M) – female	Retained Xi
Ananiev et al., 2011	MECP2: GM17880 (T158M) – female, GM07982 (V247*) – female, GM11270 (R306C) – female, RS0502 (R294*) – female	Retained Xi
Amenduni et al., 2011	CDKL5 (Q347*) – female CDKL5 (T288I) – male	Retained Xi
Pomp et al., 2011	MECP2: GM11272 (1155del32) – female, GM17880 (T158M) – female	Retained Xi
Marchetto et al., 2010	MECP2: GM11270 (R306C) – female, GM11272 (1155del32) – female, GM16548 (Q244*) – female, GM17880 (T158M) – female	Expressed Xi
Kim et al., 2011	MECP2: GM07982 (705delG) – female, GM11270 (R306C) – female, GM16548 (Q244*) – female, GM17567 (X487*) – female, GM17880 (T158M) -female	Expressed Xi

been recapitulated in a number of patient-derived iPSCs harboring pathogenetic mutations in *MECP2*. Several studies have demonstrated that neurons differentiated from RTT-iPSCs in 2D cultures have a distinctly smaller soma size compared to that of controls (Marchetto et al., 2010; Cheung et al., 2012; Djuric et al., 2015; Chin et al., 2016). The cell lines used in these studies harbored mutations at p.R306C (Cheung et al., 2011; Chin et al., 2016), p.L386R (Marchetto et al., 2010), and p.T158M (Cheung et al., 2011), and deletions at p.G16Efs*22, g.61340_67032delinsAGTTGTGCCAC (p.?) and g.67072_67200del (p.?) (Djuric et al., 2015). Consistent with post-mortem and animal studies, all RTT iPSC cell lines have

shown a significant decrease in cell soma size, with a 14.31-fold ± 4.38% decrease (Marchetto et al., 2010) and a 20–25% reduction (Chin et al., 2016) compared to controls. Post-mortem and mature murine neurons show fewer synapses and reduced dendritic branching (Belichenko et al., 2009; Marchetto et al., 2010; Baj et al., 2014), which has been corroborated by recent RTT-iPSC differentiated neuron studies in both female (Chapleau et al., 2009) and male (Yoo et al., 2017) cell lines. Both RTT-iPSC-derived neurons from a female cell line with a point mutation (p.*487Trpext*27) and a female cell line with a frameshift mutation that results in a truncated transcript (p.V247*) showed significantly reduced dendritic branching. Interestingly, a reduction in expression of the tumor suppressor protein p53 was also observed (Ohashi et al., 2018). p53 is known for its involvement in cellular senescence and activates downstream pathways of DNA repair and apoptosis. Ohashi et al. (2018) found that upon inhibition of p53, dendritic branching in RTT-iPSC neurons was restored, suggesting a role for p53 in dendritic branching. This finding is consistent with previous murine studies, where induced p53 expression led to defective dendritic branching in RTT (Ferrón et al., 2009).

Interestingly, neuronal morphological traits have been inconsistent amongst RTT iPSC studies. For instance, two male cell lines harboring mutations at p.Q83* and p.N126I showed no difference in NPC morphology compared to their respective paternal control (Kim et al., 2011). In contrast, another study reported that the average neurite length was significantly higher in controls than in mutants (Yoo et al., 2017). It was also suggested that there might be a link between the neuronal cell adhesion molecule L1 and MeCP2 activity (Muotri et al., 2010; Yoo et al., 2017). L1 plays crucial roles in multiple cellular functions, including neuronal migration, adhesion, differentiation and survival, as well as neurite outgrowth, axonal targeting, myelination, synapse formation and synaptic plasticity (Yoo et al., 2017) and thus may be a therapeutic target for RTT. Indeed, upon measuring L1 protein expression, a 2.6-fold decrease in expression was observed in RTT-NPCs compared to wild type-NPCs. Phenotypic rescue was observed when cells were transfected with an L1 plasmid construct, suggesting that L1 may be a key driver in cortical development (Yoo et al., 2017). Reduced maturation was also found in RTT-iPSC-derived neurons, this was shown by decreased expression of the mature neuronal markers Tuj (βIII tubulin) (Kim et al., 2011) and MAP2 (Ohashi et al., 2018) in RTT-iPSC neurons compared to controls.

Modeling the Synaptic and Electrophysiological Phenotype of RTT Cells

Rett syndrome is known to be a disorder of neuronal plasticity (Dani et al., 2005; Zhang et al., 2008; Maliszewska-Cyna et al., 2010) where aberrant expression of receptors and neurotransmitters suggest that MeCP2 is required to maintain synaptic excitation and inhibition that are fundamental to normal circuitry function (Blackman et al., 2012). This is supported by evidence that RTT patients display elevated glutamate levels and reduced GABA levels (Livide et al., 2015).

Synaptic function has been measured in neurons derived from RTT-iPSCs harboring different mutations. Comparison of the excitatory synapse number between RTT neurons (p.R306C, p.L386Rfs*, p.Q244X, p.T158M) and control iPSC-derived neurons has demonstrated a significant reduction in synapse number (measured according to VGLUT1 puncta), pointing to glutamate transport defects in RTT iPSC differentiated neurons (Marchetto et al., 2010). These electrophysiological defects have been validated in neurons from iPSCs with different mutations by Chin et al. (2016) and Djuric et al. (2015). Despite the use of different measurement techniques, synaptic transmission in female iPSC-derived neurons (p.R306C and p.L386Rfs) (Chin et al., 2016) and g.61340_ 67032delinsAGTTGTGCCAC (p.?) and g.67072_67200del (p.?) (Djuric et al., 2015) has shown significantly lower postsynaptic frequency in RTT-iPSCs compared to the controls, supporting a *MECP2*-dependent synaptic dysfunction phenotype.

Delayed GABA functional switching from excitatory to inhibitory, mediated by the membrane potassium chloride co-transporter KCC2, has been demonstrated in male RTT-iPSCs (p.Q83*) (Tang et al., 2016). In addition, RNA-seq profiling revealed a disruption of GABAergic circuits in RTT-iPSC-derived neurons harboring the p.T158M and p.R306C mutations (Landucci et al., 2018). Functional RTT studies using whole-cell patch clamping revealed reduced spontaneous GABAergic currents and amplitude as well as hyper-excitability in the RTT-iPSC neurons, which is in line with previous mouse model studies (Marchetto et al., 2010; Chin et al., 2016).

Synaptic function and plasticity have been studied in RTT derived iPSCs and controls using several methods including electrophysiology, gene expression and imaging. However, each method has its own challenges. Whole cell electrophysiological recordings provide high temporal and spatial localization, but the restriction of measurements to individual neuronal cells limits its efficacy in understanding complex network interactions (Glasgow et al., 2019). On the other hand, techniques including immunohistochemistry or transcriptomic analysis provide high neuroanatomical specificity and can allow for quantitative comparison, although they exhibit low temporal acuity. It is known that synaptic transmission is a complex phenomenon, but recent developments of more accurate techniques to measure plasticity, such as the use of optical tools alongside classical electrophysiological techniques, are providing new insights into the traditional interpretation of synaptic function. Moving forward, multiple experimental techniques should be used, when possible, to evaluate all possible sites of action.

Modeling Therapeutic Targets in RTT Cells

Currently, there are two major targets for therapy for RTT syndrome: therapeutic targets downstream of MeCP2 and gene therapy strategies. The iPSC model provides unique opportunities both for gene therapy and for drug screening, where variant-specific biochemical activities can be used as readouts of drug action. Given the reversibility of the RTT phenotype in mice (Guy et al., 2007), the possibility of rescuing the phenotype *in vitro* by treatment with candidate drugs has been an obvious area of exploration (Marchetto et al., 2010). The read-through drug gentamicin has been tested on iPSCs

harboring the nonsense p.Q244* mutation to determine whether a read-through of the premature stop codon could be elicited (Marchetto et al., 2010). Treatment with gentamicin resulted in increased MeCP2 protein levels and a concomitant number of glutamatergic synapses in iPSC-derived neurons in culture (Marchetto et al., 2010).

A deficiency in the expression of potassium chloride cotransporter 2 (KCC2) in RTT iPSC-derived neurons has been demonstrated to result in a delayed GABA functional switch from excitation to inhibition (Tang et al., 2016). MeCP2 regulates KCC2 through REST, hence controlling GABA functions in neurons. Recent studies have shown that inhibiting NKCC1 (chloride transporter with opposite functions to KCC2) can be used to treat autism and fragile X syndrome (Tang et al., 2016). Given the critical role of IGF1 in neurodevelopment and its capacity to rescue glutamatergic deficits, the effects of insulin like growth factor (IGF1) were tested in neuronally differentiated RTT-iPSCs. Although MeCP2 expression did not change, KCC2 was increased significantly, suggesting that IGF1 may upregulate KCC2 independently of MeCP2 activity (Tang et al., 2016). The effects of IGF1 treatment have been investigated by another group (de Souza et al., 2017) in RTT (p.Q83*) and control iPSCs (HUES6) by measuring the global gene expression profiles of RTT-iPSCs and control lines at different stages of differentiation. This *in vitro* study showed that the thyroid hormone receptor alpha 3 gene (TRalpha3), which encodes a hormone receptor critical for brain development, displayed a different expression profile in the mutant cells. It was demonstrated that treatment with IGF1, mediated by TRalpha3, was able to enhance neurite growth in MeCP2-deficient cells, suggesting IGF1 as a treatment option (de Souza et al., 2017, 2019).

Motor and cognitive impairments in RTT mouse models may be related to abnormalities in the cholinergic system (Nag and Berger-Sweeney, 2007) and thus RTT-iPSC-derived neurons have been used to test whether choline could rescue RTT-associated defects. From these studies, choline supplementation was shown to alleviate the synaptic defects in RTT-iPSC-derived neurons in culture (Chin et al., 2016). The action of histone deacetylase 6 (HDAC6) inhibitors has also been tested in RTT-iPSCs. HDAC6 is a cytoplasmic microtubule-associated deacetylase that catalyzes the deacetylation of alpha-tubulin. Disruptions in acetylated α-tubulin and over-expression of HDAC6 have been reported in murine models and RTT fibroblasts (Gold et al., 2015). Recently, the administration of multiple HDAC6 inhibitors (for instance, ACY-1215) was shown to induce a marked increase in acetylated α-tubulin in RTT iPSC-derived neurons (Landucci et al., 2018). These studies demonstrate the capability of iPSC models to recapitulate the molecular abnormalities of RTT and the utility of HDAC6 inhibitors for RTT therapy.

The development of therapeutic strategies like the ones listed in this review (**Table 2**) needs to take into account the cell type, time of dosing and target; iPSCs demonstrate to be a useful tool to do preliminary studies on treatment strategies. In addition, other therapeutic targets currently being tested include: BRD4 targeting (Xiang et al., 2020); reactivation of the inactive X chromosome [Reviewed in Good et al. (2021)]; and other histone deacetylase inhibitors (including HDAC3) (Nott et al., 2016).

Modeling RTT Glial Cells

Glia cells, including astrocytes and microglia, play a critical role in mediating dendritic growth, synapse formation, synaptic function and immune responses in the neuropathology of RTT (Lioy et al., 2011). Despite being expressed at lower levels in astrocytes than in neuronal cells, MeCP2 is critical for astrocyte differentiation and function where MeCP2-deficient astrocytes have abnormal BDNF regulation, cytokine production, and neuronal dendritic formation and maturation (Maezawa et al., 2009). Several RTT studies have demonstrated that astrocytes negatively impact neurons in a non-cell autonomous manner (Ballas et al., 2009; Maezawa et al., 2009; Lioy et al., 2011), revealing distinct roles for astrocytes and neurons in disease progression, where mutant neurons primarily initiate the disease state and mutant astrocytes influence disease progression. Early *in vitro* studies demonstrated that co-cultured mutant mouse astrocytes, and the supplementation of mutant astrocyte conditioned medium, failed to support normal dendritic morphology of wild type and mutant hippocampal neurons (Ballas et al., 2009). Further *in vivo* studies show that re-expression of MeCP2 in astrocytes reverted RTT-specific phenotypic behaviors. Re-expression also restored aberrant dendritic morphology and increased the levels of the excitatory glutamate transporter VGLUT1 in a non-cell autonomous manner (Lioy et al., 2011).

More recently, RTT patient-derived iPSCs have been successfully differentiated into glial cells including astrocytes and microglia in three different patient cell lines (p.V247*, p.R294*, and p.R306C) (Williams et al., 2014). To understand whether human MeCP2-deficient astrocytes have a non-cell-autonomous effect on mouse neurons, RTT patient iPSC-derived astrocytes differentiated from late-phase isogenic astroglia progenitors were co-cultured with either wild type or mutant murine P0 primary hippocampal neurons. In agreement with previous

TABLE 2 | Summary of therapeutic targets and outcomes.

Study	Therapeutic targets	Outcome
Marchetto et al., 2010	Gentamicin	Increased levels of MeCP2 and increased number of glutamatergic synapsis in neuron cultures.
de Souza et al., 2017	IGF1	Showed possible link between IGF1/IGF1R and TRalpha3, overexpression of IGF1R caused neurite improvement and RTT derived neurons
Tang et al., 2016	KCC2	Restoration of KCC2 levels rescues GABA functional deficits in RTT neurons
Chin et al., 2016	Choline	Choline supplementation was shown to alleviate the synaptic defects in RTT-iPSC-derived neurons in culture
Landucci et al., 2018	HDAC6 inhibitor	Increase in acetylated α-tubulin in RTT derived neurons, improving synaptic function.

studies, the mutant astrocytes adversely affected the morphology and function of the murine neurons in a non-cell-autonomous manner (Williams et al., 2014). Neuronal deficits caused by mutant RTT astrocytes were partially rescued by introduction of insulin-like growth factor 1 (IGF-1) and its truncated derivative glycine-proline-glutamate (GPE) (Williams et al., 2014). Short-term treatment with IGF-1 or GPE in co-culture combinations of mutant and wild type interneuron/astrocyte demonstrated an indirect effect of IGF-1 treatment on neurons with a direct impact on astrocytes (Williams et al., 2014).

Induced pluripotent stem cell studies generated from female monozygotic twins harboring a frameshift mutation (p.G269Afs*) in *MECP2* revealed abnormal growth patterns and gene expression in differentiated mutant astrocyte cells compared to their isogenic controls. In particular, the glial marker GFAP (glial fibrillary acidic protein) was shown to be dysregulated in MeCP2-deficient neural cells, suggesting that abnormal astrocytic differentiation is involved in the pathogenesis of disease and a likely therapeutic target for RTT (Andoh-Noda et al., 2015).

Astrocytes have also been generated from male RTT-iPSC lines harboring loss of function mutations (p.Q83*, p.N126I). In comparison to iPSC lines from unaffected fathers (WT83, WT126), mutant lines showed significantly reduced levels of expression of astrocytic markers (Kim et al., 2019), suggesting that RTT-NPCs can differentiate into GFAP-positive glia, albeit at a reduced capacity. In this study, proteomic analyses of molecular pathways identified abnormal upregulation of LIN28, a driver of neural differentiation essential for cell-fate regulation and developmental timing in *MECP2* mutant-expressing NPCs compared to controls. From these studies, LIN28 expression was found to be inversely correlated with GFAP-positive glia generation, indicating that high LIN28 expression in mutant NPCs hampers astrocytic differentiation by reducing neuronal synapse density (Kim et al., 2019). Knockdown of LIN28 allowed for a partial reversal of synaptic deficiencies in MECP2 mutant lines (Kim et al., 2019).

It has been shown that restoration of MeCP2 in neurons alone was not able to recover the phenotype in mouse brains, suggesting the involvement of other CNS cell types such as glia (Alvarez-Saavedra et al., 2007). The above-mentioned studies have successfully used iPSC-derived astrocytes and microglia to investigate the effects of these cell types in RTT pathophysiology, but the exploration of potential therapeutic candidates targeting glia remains largely unexplored and continued investigation is needed to understand the involvement of glia in RTT.

Modeling the Impact of X-Chromosome Inactivation

X-chromosome inactivation (XCI) is a phenomenon of female (XX) somatic cells, where one X chromosome undergoes inactivation in a stochastic manner such that genes of only one X-chromosome are expressed in each cell, thus balancing the dosage of X-linked genes with the male (XY) cells. This is critical to RTT as *MECP2* is located on the X chromosome and subjected to random silencing that can result in mosaic expression of *MECP2* with some cells expressing the mutant *MECP2* allele and others the wild type allele.

Female iPSCs have been shown to retain the inactive X-chromosome (Tchieu et al., 2010), in contrast to murine pluripotent stem cells, which can express both X-chromosomes (Maherali et al., 2007). However, it has been demonstrated that despite the X chromosome status at the iPSC stage, iPSCs that have two active X chromosomes will inactivate an X chromosome upon neuronal differentiation (Marchetto et al., 2010), thus regaining the XCI status found in somatic cells.

The activation status of the X chromosome is critical when using iPSCs as cellular models for RTT research and thus warrants careful investigation. The XCI status has been studied in RTT iPSCs by several groups (Marchetto et al., 2010; Amenduni et al., 2011; Ananiev et al., 2011; Cheung et al., 2011; Kim et al., 2011; Pomp et al., 2011). Interestingly, the XCI status of the different lines and clones has been inconsistent (**Table 1**). Some groups observed clones that reactivate the previously inactive X chromosome and in some cases up to 95% of the cells in the line (Marchetto et al., 2010). In contrast, a number of groups observed retention of the inactive X chromosome (Amenduni et al., 2011; Ananiev et al., 2011; Cheung et al., 2011; Pomp et al., 2011), reactivation of the inactive X (Marchetto et al., 2010) or combinations of both (Kim et al., 2011). These findings suggest that during reprogramming, some clones may erase the memory of the XCI status. This erosion of the inactive X chromosome characterized by loss of XIST coating or DNA methylation, has been observed in many X-linked iPSC studies (Luo et al., 2014; Geens et al., 2016; Vallot et al., 2017). Although this phenomenon is not completely understood, it is speculated to be an artifact of culture conditions. Derivation and cell culture conditions have been shown to have a significant impact on the XCI status, and include oxygen percentage and supplementation with small molecules like sodium butyrate and 3-deazaneplanocin A or antioxidants (Lengner et al., 2010). Obviously, the use of male iPSC would avoid the issue of XCI, however, as most Rett patients are female, this is not relevant for most cell lines. Clearly the optimization of culture methods is warranted in order to obtain the natural XCI state of the iPSC line.

There is much speculation regarding the cause of the differences in the XCI status of these iPSC cell lines. XCI status may be influenced by physiological stress, as in hESCs where changes in CO_2 levels result in the expression of both alleles of the X-linked gene (Lengner et al., 2010). However, iPSCs can maintain their XCI status through many culture passages and freeze-thaw events (Kim et al., 2011). Despite the origin of each cell line, the culturing conditions of the lines and the reprogramming methods used have been broadly similar, although subtle variations in reprogramming protocols cannot be completely ruled out. Indeed, while similar programming methods were used to generate the iPSCs (Ananiev et al., 2011; Cheung et al., 2011; Kim et al., 2011; Pomp et al., 2011), reactivation of the previously inactive X indicates that the stability of the XCI status is not always assured and other unknown factors may be at play. Thus, the programming methods may affect the XCI status of the iPSCs and should be carefully considered when using these cell lines. Regular assessment of the XCI status, in

particular the skewed pattern, should be undertaken during the differentiation process to validate the XCI status of the cell line.

As observed in RTT patients, skewed XCI has also been reported in neuronally differentiated iPSCs (p.R294*, p.T158M, and p.V247*) (Ananiev et al., 2011). A drastic skewing was found in iPSC-derived neurons harboring a p.L386R*fs** mutation (6:4 to 98:2), despite the originating fibroblasts showing equal expression of both alleles (55:45) (Marchetto et al., 2010). Extreme XCI skewing was also found in the Δ3–4 iPSC (96:4 to 99:1), p.T158M iPSC (91:9 to 99:1) and p.R306C iPSC (84:16 to 81:19) lines, with the originating fibroblasts exhibiting a balanced pattern of XCI. In addition, some clones from the Δ3–4 iPSC line were skewed toward the same parental X chromosome, and others toward the other parental X chromosome, whereas the skewed pattern in the p.T158M and p.R306C lines retained the inactive parental chromosome. This demonstrates that inactivation of the X chromosome in iPSCs derived from the fibroblasts of these patients seems to be non-random. Despite this, the XCI pattern of *MECP2* is retained during neuronal differentiation, allowing the generation of isogenic controls (expressing wild type *MECP2*) and experimental iPSC lines (expressing mutant *MECP2*). Recommendations to ensure that the iPSCs and derived cells retain the XCI status of the parental patient cell lines, whether they originate from fibroblasts, urine or blood, require validation by mRNA expression of which X chromosome is being expressed, and selection of iPSC clones that only express the same X chromosome and skewing as the parental line.

MODELING RTT USING BRAIN ORGANOIDS

Despite their simplicity and utility, 2D cell cultures do not completely recapitulate the complex functional interaction between different cell types and the 3D dimensional architecture of neural tissue in the brain. Capitalizing on the capacity of iPSC-derived neural cells to differentiate in response to mechanical and chemical stimuli, and the ability of stem-cell derivatives to self-organize into organotypic structures that resemble the brain, enables the production of 3D organoids *in vitro*. The discovery that neural rosettes (neural progenitors) can be generated from embryonic stem cells has powered the development of cerebral organoids (Lancaster et al., 2013; Lancaster and Knoblich, 2014). Subsequent culture methods facilitated "self-patterning" of cells (Lancaster et al., 2013) and "direct patterning" toward defined brain regions such as the cortex, forebrain (Qian et al., 2016) and midbrain (Paşca, 2019). Single-cell RNA-sequencing analysis has shown that whole-brain organoids generated by "self-patterning" display a high degree of variability and low reproducibility of cell types in comparison to "direct patterning" (Velasco et al., 2019). Direct patterning protocols use morphogenetic factors and inhibitors to drive the patterning of specific brain regions to allow complex assembly of different brain regions (the assembloid) as well as the inclusion of other cell types such as microglia, endothelial cells and even brain blood barrier-like structures. Brain organoid models have facilitated investigations into the intricate cellular interaction during neurodevelopment and the disease process, providing a human-like model for screening therapeutics and preclinical testing of potential therapies. Different human brain organoid culturing methods have been reviewed in more detail elsewhere (Wang, 2018).

Two recent studies using RTT patient iPSC-derived brain organoids have characterized the morphology and synaptic function of mutant neurons (Trujillo et al., 2018) and the dysregulation of signaling pathways (Mellios et al., 2018). Despite differences between the two methods, their impacts on the field have been significant. Trujillo et al. (2018) developed cortical brain organoids by culturing male patient-derived iPSCs (p.Q83* and p.N126I) and the paternal controls in the presence of dual SMAD inhibition and Y-27 (ROCK inhibitor) in a spinning orbital shaker. To enhance the growth of the organoids and initiate neuroepithelium differentiation, the culture was initially supplemented with fibroblast growth factor (FGF), epidermal growth factor (EGF) and then BDNF, GDNF, NT-3, L-ascorbic acid, and dibutyryl cAMP. Organoids were then matured in an orbital shaker for 10 months (Trujillo et al., 2018). In contrast, Mellios et al. (2018) generated spheroids from two female RTT patient cell lines carrying a missense mutation (p.R106W) and a frameshift deletion (p.E235fs), respectively, and the corresponding isogenic controls, and two wild type control lines (male GM08330 and female GM23279). Spheroids were made by generating embryo bodies in ultra-low attachment well plates with neural induction media, using iPSCs previously grown on mouse embryonic cells (MEFs). Spheroid differentiation occurred in B-27 supplemented media followed by dual SMAD inhibition (SB-431542 and LDN-193189) at the induction phase. The spheroids were embedded in Matrigel for maturation in a bioreactor for 5 weeks (Mellios et al., 2018).

Mellios et al. (2018) explored the role of miRNAs in neurogenesis by electroporating the organoids with a MeCP2 short hairpin RNA (shRNA) construct. Novel MeCP2-regulated miRNAs were identified, such as miR-199 and miR-214 that can differentially regulate the extracellular signal-regulated kinase (EKR/MAPK) and protein kinase B (PKB/AKT) signaling pathways. By inhibiting miR-199 and miR-214 expression at the neural progenitor stage, AKT and ERK activation was restored, leading to amelioration of the RTT-like phenotype (Mellios et al., 2018). Trujillo et al. (2018) used the organoid models to investigate the electrophysiological activity of RTT neurons. To deduce whether the organoids could recapitulate the synaptic function of the human brain, synaptic maturation was measured using microelectrode arrays (MEAs) and compared to electroencephalogram data of preterm infants by machine learning. Neurons in the *MECP2*-deficient organoids showed significant reductions in cell size, neural protrusions, spine-like density and synaptic puncta. In addition, reduced neural activity indicated an absence of network oscillations, which was not found in the isogenic controls at the same age *in vitro*. Not only were significant differences in neuronal morphology and function observed between RTT and wild type organoids, but this work also provides a cortical organoid model that recapitulates the synaptic function of the *in vivo* prenatal brain, the incremental

emergence of glial cells, and the formation of inhibitory neurons by 6 months in culture (Trujillo et al., 2018). As RTT post-mortem brain tissue is not easily accessible, 3D organoid models provide an exciting avenue to explore disease mechanisms and potential therapies.

Human brain organoids offer the opportunity to better understand neural circuits, enabling elucidation of the mechanisms that underlie the properties of human circuits. However, despite considerable progress in the field, there has been little evidence to demonstrate the establishment of reliable cortical circuits. One of the obvious obstacles is that brain organoids lack critical cell types of the human cortex, including endothelial cells, and microglia and oligodendrocytes. Recently, efforts have been made to implement vascular structure in human brain organoids by adjusting cultivation protocols, introducing microfluidic devices, and transplanting organoids into immunodeficient mice (Cakir et al., 2019; Shi et al., 2020). Another confounding factor is that even though organoids show some structural features of cortical layering and ventricular zones, more complex levels of cortical organization such as gyrification, radial glial scaffolds and neuronal connections are still to be established. Finally, an overriding issue regarding brain organoids as a model is their relative immaturity. Whether more complex structures can be developed that possess improved organization and model later stages of development, remains to be seen.

Limitations of the Brain Organoid Model

One caveat in the utility of iPSCs is related to their variability in lineage propensity and this has a confounding effect on the consistency and reproducibility of the cellular composition of the organoid. iPSC derivation and differentiation is a multi-step processes and experimental procedure variations can produce different outcomes (Popp et al., 2018). Often, the impact of variation can overpower any biological differences, especially where sample sizes are small (Ghaffari et al., 2018). Studies have also confirmed that the individual donor's genetic background and differences in differentiation protocols might significantly influence the methylation landscape, affecting pluripotency between iPSCs from different donors (de Boni et al., 2018). Analysis has shown that induction and differentiation can also introduce variation themselves (Schwartzentruber et al., 2018). Hence, measures need to be put in place to minimize variation while differentiating iPSCs, such as consistencies in passage number and differentiation protocols, including culture media and matrices.

Another known and reported limitation is the inadequate functionality of the tissue in the organoid such as the lack of vascularization. Vascularization supports efficient transport of oxygen and nutrients to the core of the brain organoids, which are critical for proper growth and differentiation, because non-vascularized organoids often display tissue necrosis. An appealing approach is the xenograft transplantation of brain organoids into mice, allowing the murine blood vessels to transport oxygen and nutrients to support the growth of the transplanted organoids (Mansour et al., 2018). Concurrently a variety of *in vitro* models for vascularization are also being devised including endothelial cells cultured on microfluidic channels made with degradable materials to resemble the blood vessels in tissues (Bhatia and Ingber, 2014; van Duinen et al., 2015).

The most critical limitation is related to the ability to mimic the normal development trajectory of the human brain. iPSC-derived patient neurons and brain organoids are imperfect in that they are highly heterogenous, only replicate a specific brain region, and are not connected to the peripheral nervous system, amongst other shortcomings. Directed patterned and self-patterned models have been developed to replicate the anatomically relevant spatial organization found *in vivo*. A single cell RNA sequencing study has shown that directed patterned organoids have a higher rate of reproducibility over self-patterned whole brain organoids (Velasco et al., 2019). However, the former approach only allows for specific regions of the brain to be generated including cerebral cortex, hippocampus (Sakaguchi et al., 2015) midbrain (Jo et al., 2016; Qian et al., 2016) forebrain (Velasco et al., 2019) and cerebellum (Muguruma et al., 2015) with no studies yet having combined these regions, nor has the establishment of functional neuronal connectivity or neuron-glia interactions been demonstrated.

CHALLENGES AND FUTURE DIRECTIONS

Currently, brain organoids do not reproduce the requisite tissue complexity of the human brain, and models have yet to recapitulate the developmental stages of the brain of a young child for studying the postnatal manifestation of neurodevelopmental disorders. RTT patients develop normally from 6 to 18 months after birth, which is followed by a developmental trajectory regression where they lose their ability to control their hand movements, they stop walking and talking, and they develop phenotypes such as microcephaly, seizures, autism, prolonged QT intervals, and breathing problems including apneas. Symptoms range in severity with limited phenotype-genotype correlations. The expression of *MECP2* is tightly regulated both temporally during development and spatially throughout the brain. As *MECP2* is an X-linked disorder, it is subjected to X-chromosome inactivation, resulting in the skewing of either the wildtype or mutant allele. All these unusual characteristics make it very challenging to study the pathophysiology of disease in *in vitro* cellular expression systems and in mouse models as they do not completely recapitulate the disease that is observed in human subjects.

Rett syndrome patient iPSC-derived neurons and brain organoids are effective models to address several specific phenotypes such as synaptic dysfunction, glutamatergic neuron morphology, electrophysiological and synaptic dysfunction, GABA-ergic dysregulation, non-cell autonomous effects of astrocytes, transcriptional dysregulation, neurogenesis, and miRNA target sites. In addition to this, therapeutic molecules have also been tested, broadening our understanding of iPSC-derived models as well as the pathophysiology of RTT. However, one of the critical questions in the field is how developmental delay and regression can be interrogated using these models,

and whether they can inform us about how to reverse RTT in humans. The contributions by Guy et al. (2007), demonstrating phenotypic reversal in mice, provided much hope to the RTT community that the disorder was indeed reversable, albeit in murine models. 3D brain organoids that more closely resemble the human brain than the widely used mouse models, may be able to address this question. Cortical organoid studies have recapitulated the features of cortical development including temporal neurogenesis and functional cortical neurons, as well as the appearance of spontaneous glial cell populations (Kadoshima et al., 2013; Qian et al., 2016; Paşca, 2019; Xiang et al., 2020). Further, forebrain organoid development has allowed for the modeling of tangential migration of interneurons into the cortex by fusing dorsal forebrain organoids with ventral forebrain organoids (Kim et al., 2019; Xiang et al., 2020), which has enabled the study of human-specific features of brain development. Studies such as these that address the development of the brain in RTT-iPSC-derived neurons and organoids, together with the refinement of brain organoid technologies, will overcome the existing shortcomings and provide more insight into the developmental delay associated with MeCP2 deficiency. The organoid model has untapped potential for developing personalized therapeutic strategies for RTT and other monogenic neurodevelopmental disorders.

Both the cellular model and the organoid model have their specific utility and limitations. There may be no ideal models, but rather appropriate models that fulfill the requirements of the research question. This review outlines the major phenotypes that have been modeled in RTT-iPSC-derived cells and organoids and their application for drug screening. Impending optimization in modeling technology will enable the creation of high-fidelity disease models for the human brain, which in addition to modeling pediatric neurodevelopmental disorders, will allow the characterization of normal and abnormal neurogenic differentiation and tracking of the disease trajectory through pre and postnatal development.

AUTHOR CONTRIBUTIONS

FH wrote the manuscript. BC summarized studies used in the review. LR checked the genetic nomenclature. LCC, LR, PPLT, and WAG contributed to the drafts and revisions. PLTT and WAG framed the concept and structure of the review. All authors reviewed and approved the final manuscript.

FUNDING

PPLT was supported by NHMRC Research Fellowship (Grant 1110751). FH, BC, and WAG were supported by the Neil and Norma Hills Foundation.

ACKNOWLEDGMENTS

We would like to acknowledge the contributions of David Duruchukwu for his scientific discussions during the preparation of this manuscript.

SUPPLEMENTARY MATERIAL

The Supplementary Material for this article can be found online at: https://www.frontiersin.org/articles/10.3389/fnins.2021.698812/full#supplementary-material

REFERENCES

Alvarez-Saavedra, M., Sáez, M. A., Kang, D., Zoghbi, H. Y., and Young, J. I. (2007). Cell-specific expression of wild-type MeCP2 in mouse models of Rett syndrome yields insight about pathogenesis. *Hum. Mol. Genet.* 16, 2315–2325. doi: 10.1093/hmg/ddm185

Amenduni, M., De Filippis, R., Cheung, A. Y., Disciglio, V., Epistolato, M. C., Ariani, F., et al. (2011). iPS cells to model CDKL5-related disorders. *Eur. J. Hum. Genet.* 19, 1246–1255. doi: 10.1038/ejhg.2011.131

Amir, R. E., Van Den Veyver, I. B., Wan, M., Tran, C. Q., Francke, U., and Zoghbi, H. Y. (1999). Rett syndrome is caused by mutations in X-linked MECP2, encoding methyl-CpG-binding protein 2. *Nat. Genet.* 23, 185–188. doi: 10.1038/13810

Ananiev, G., Williams, E. C., Li, H., and Chang, Q. (2011). Isogenic pairs of wild type and mutant induced pluripotent stem cell (iPSC) lines from rett syndrome patients as in vitro disease model. *PLoS One* 6:e25255. doi: 10.1371/journal.pone.0025255

Andoh-Noda, T., Akamatsu, W., Miyake, K., Matsumoto, T., Yamaguchi, R., Sanosaka, T., et al. (2015). Differentiation of multipotent neural stem cells derived from Rett syndrome patients is biased toward the astrocytic lineage. *Mol. Brain* 8:31.

Armstrong, D., Dunn, J. K., Antalffy, B., and Trivedi, R. (1995). Selective dendritic alterations in the cortex of Rett syndrome. *J. Neuropathol. Exp. Neurol.* 54, 195–201. doi: 10.1097/00005072-199503000-00006

Baj, G., Patrizio, A., Montalbano, A., Sciancalepore, M., and Tongiorgi, E. (2014). Developmental and maintenance defects in Rett syndrome neurons identified by a new mouse staging system in vitro. *Front. Cell. Neurosci.* 8:18. doi: 10.3389/fncel.2014.00018

Ballas, N., Lioy, D. T., Grunseich, C., and Mandel, G. (2009). Non-cell autonomous influence of MeCP2-deficient glia on neuronal dendritic morphology. *Nat. Neurosci.* 12, 311–317. doi: 10.1038/nn.2275

Belichenko, P. V., Wright, E. E., Belichenko, N. P., Masliah, E., Li, H. H., Mobley, W. C., et al. (2009). Widespread changes in dendritic and axonal morphology in Mecp2-mutant mouse models of Rett syndrome: evidence for disruption of neuronal networks. *J. Comp. Neurol.* 514, 240–258. doi: 10.1002/cne.22009

Bhatia, S. N., and Ingber, D. E. (2014). Microfluidic organs-on-chips. *Nat. Biotechnol.* 32, 760–772. doi: 10.1038/nbt.2989

Blackman, M. P., Djukic, B., Nelson, S. B., and Turrigiano, G. G. (2012). A critical and cell-autonomous role for MeCP2 in synaptic scaling up. *J. Neurosci.* 32, 13529–13536. doi: 10.1523/jneurosci.3077-12.2012

Cakir, B., Xiang, Y., Tanaka, Y., Kural, M. H., Parent, M., Kang, Y.-J., et al. (2019). Engineering of human brain organoids with a functional vascular-like system. *Nat. Methods* 16, 1169–1175.

Carter, J., Lanham, D., Pham, D., Bibat, G., Naidu, S., and Kaufmann, W. E. (2008). Selective cerebral volume reduction in Rett syndrome: a multiple-approach MR imaging study. *Am. J. Neuroradiol.* 29, 436–441. doi: 10.3174/ajnr.a0857

Chahrour, M., Jung, S. Y., Shaw, C., Zhou, X., Wong, S. T., Qin, J., et al. (2008). MeCP2, a key contributor to neurological disease, activates and represses transcription. *Science* 320, 1224–1229. doi: 10.1126/science.1153252

Chao, H. T., Chen, H., Samaco, R. C., Xue, M., Chahrour, M., Yoo, J., et al. (2010). Dysfunction in GABA signalling mediates autism-like stereotypies

and Rett syndrome phenotypes. *Nature* 468, 263–269. doi: 10.1038/nature09582

Chapleau, C. A., Calfa, G. D., Lane, M. C., Albertson, A. J., Larimore, J. L., Kudo, S., et al. (2009). Dendritic spine pathologies in hippocampal pyramidal neurons from Rett syndrome brain and after expression of Rett-associated MECP2 mutations. *Neurobiol. Dis.* 35, 219–233. doi: 10.1016/j.nbd.2009.05.001

Cheung, A. Y., Horvath, L. M., Carrel, L., and Ellis, J. (2012). X-chromosome inactivation in rett syndrome human induced pluripotent stem cells. *Front. Psychiatry* 3:24. doi: 10.3389/fpsyt.2012.00024

Cheung, A. Y., Horvath, L. M., Grafodatskaya, D., Pasceri, P., Weksberg, R., Hotta, A., et al. (2011). Isolation of MECP2-null Rett Syndrome patient hiPS cells and isogenic controls through X-chromosome inactivation. *Hum. Mol. Genet.* 20, 2103–2115. doi: 10.1093/hmg/ddr093

Chin, E. W., Marcy, G., Yoon, S. I., Ma, D., Rosales, F. J., Augustine, G. J., et al. (2016). Choline ameliorates disease phenotypes in human iPSC models of rett syndrome. *Neuromol. Med.* 18, 364–377. doi: 10.1007/s12017-016-8421-y

Dani, V. S., Chang, Q., Maffei, A., Turrigiano, G. G., Jaenisch, R., and Nelson, S. B. (2005). Reduced cortical activity due to a shift in the balance between excitation and inhibition in a mouse model of Rett syndrome. *Proc. Natl. Acad. Sci. U.S.A.* 102, 12560–12565. doi: 10.1073/pnas.0506071102

De Boni, L., Gasparoni, G., Haubenreich, C., Tierling, S., Schmitt, I., Peitz, M., et al. (2018). DNA methylation alterations in iPSC-and hESC-derived neurons: potential implications for neurological disease modeling. *Clin. Epigenet.* 10, 1–13.

de Souza, J. S., Carromeu, C., Torres, L. B., Araujo, B. H., Cugola, F. R., Maciel, R. M., et al. (2017). IGF1 neuronal response in the absence of MECP2 is dependent on TRalpha 3. *Hum. Mol. Genet.* 26, 270–281.

de Souza, J. S., Ferreira, D. R., Herai, R., Carromeu, C., Torres, L. B., Araujo, B. H. S., et al. (2019). Altered gene expression of thyroid hormone transporters and deiodinases in iPS MeCP2-Knockout cells-derived neurons. *Mol. Neurobiol.* 56, 8277–8295. doi: 10.1007/s12035-019-01645-2

Djuric, U., Cheung, A. Y. L., Zhang, W., Mok, R. S., Lai, W., Piekna, A., et al. (2015). MECP2e1 isoform mutation affects the form and function of neurons derived from Rett syndrome patient iPS cells. *Neurobiol. Dis.* 76, 37–45. doi: 10.1016/j.nbd.2015.01.001

Eze, U. C., Bhaduri, A., Haeussler, M., Nowakowski, T. J., and Kriegstein, A. R. (2021). Single-cell atlas of early human brain development highlights heterogeneity of human neuroepithelial cells and early radial glia. *Nat. Neurosci.* 24, 584–594. doi: 10.1038/s41593-020-00794-1

Ferrón, S. R., Marqués-Torrejón, M. Á, Mira, H., Flores, I., Taylor, K., Blasco, M. A., et al. (2009). Telomere shortening in neural stem cells disrupts neuronal differentiation and neuritogenesis. *J. Neurosci.* 29, 14394–14407. doi: 10.1523/jneurosci.3836-09.2009

Fossati, V., Jain, T., and Sevilla, A. (2016). The silver lining of induced pluripotent stem cell variation. *Stem Cell Invest.* 3:86. doi: 10.21037/sci.2016.11.16

Gadalla, K. K. E., Vudhironarit, T., Hector, R. D., Sinnett, S., Bahey, N. G., Bailey, M. E. S., et al. (2017). Development of a novel AAV gene therapy cassette with improved safety features and efficacy in a mouse model of rett syndrome. *Mol. Ther. Methods Clin. Dev.* 5, 180–190. doi: 10.1016/j.omtm.2017.04.007

Gadalla, K. K., Bailey, M. E., Spike, R. C., Ross, P. D., Woodard, K. T., Kalburgi, S. N., et al. (2013). Improved survival and reduced phenotypic severity following AAV9/MECP2 gene transfer to neonatal and juvenile male Mecp2 knockout mice. *Mol. Ther.* 21, 18–30. doi: 10.1038/mt.2012.200

Garg, S. K., Lioy, D. T., Cheval, H., Mcgann, J. C., Bissonnette, J. M., Murtha, M. J., et al. (2013). Systemic delivery of MeCP2 rescues behavioral and cellular deficits in female mouse models of Rett syndrome. *J. Neurosci.* 33, 13612–13620. doi: 10.1523/jneurosci.1854-13.2013

Geens, M., Seriola, A., Barbé, L., Santalo, J., Veiga, A., Dée, K., et al. (2016). Female human pluripotent stem cells rapidly lose X chromosome inactivation marks and progress to a skewed methylation pattern during culture. *Mol. Hum. Reprod.* 22, 285–298.

Ghaffari, I., Yaghoobi, M. P., and Ghannad, M. (2018). Complete mechanical behavior analysis of FG Nano Beam under non-uniform loading using non-local theory. *Mater. Res. Express* 5:015016. doi: 10.1088/2053-1591/aaa206

Glasgow, S. D., Mcphedrain, R., Madranges, J. F., Kennedy, T. E., and Ruthazer, E. S. (2019). Approaches and limitations in the investigation of synaptic transmission and plasticity. *Front. Synaptic Neurosci.* 11:20. doi: 10.3389/fnsyn.2019.00020

Gold, W. A., Krishnarajy, R., Ellaway, C., and Christodoulou, J. (2018). Rett syndrome: a genetic update and clinical review focusing on comorbidities. *ACS Chem. Neurosci.* 9, 167–176. doi: 10.1021/acschemneuro.7b00346

Gold, W. A., Lacina, T. A., Cantrill, L. C., and Christodoulou, J. (2015). MeCP2 deficiency is associated with reduced levels of tubulin acetylation and can be restored using HDAC6 inhibitors. *J. Mol. Med. (Berl.)* 93, 63–72. doi: 10.1007/s00109-014-1202-x

Good, K. V., Vincent, J. B., and Ausió, J. (2021). MeCP2: the genetic driver of rett syndrome epigenetics. *Front. Genet.* 12:620859. doi: 10.3389/fgene.2021.620859

Guy, J., Gan, J., Selfridge, J., Cobb, S., and Bird, A. (2007). Reversal of neurological defects in a mouse model of Rett syndrome. *Science* 315, 1143–1147. doi: 10.1126/science.1138389

Hagberg, B., Aicardi, J., Dias, K., and Ramos, O. (1983). A progressive syndrome of autism, dementia, ataxia, and loss of purposeful hand use in girls: Rett's syndrome: report of 35 cases. *Ann. Neurol.* 14, 471–479. doi: 10.1002/ana.410140412

Hinz, L., Hoekstra, S. D., Watanabe, K., Posthuma, D., and Heine, V. M. (2019). Generation of isogenic controls for in vitro disease modelling of X-Chromosomal disorders. *Stem Cell Rev. Rep.* 15, 276–285. doi: 10.1007/s12015-018-9851-8

Hsu, W.-L., Ma, Y.-L., Liu, Y.-C., Tai, D. J. C., and Lee, E. H. Y. (2020). Restoring Wnt6 signaling ameliorates behavioral deficits in MeCP2 T158A mouse model of Rett syndrome. *Sci. Rep.* 10:1074.

Huang, T. W., Kochukov, M. Y., Ward, C. S., Merritt, J., Thomas, K., Nguyen, T., et al. (2016). Progressive changes in a distributed neural circuit underlie breathing abnormalities in mice lacking MeCP2. *J. Neurosci.* 36, 5572–5586. doi: 10.1523/jneurosci.2330-15.2016

Jo, J., Xiao, Y., Sun, A. X., Cukuroglu, E., Tran, H. D., Göke, J., et al. (2016). Midbrain-like organoids from human pluripotent stem cells contain functional dopaminergic and neuromelanin-producing neurons. *Cell Stem Cell* 19, 248–257. doi: 10.1016/j.stem.2016.07.005

Kadoshima, T., Sakaguchi, H., Nakano, T., Soen, M., Ando, S., Eiraku, M., et al. (2013). Self-organization of axial polarity, inside-out layer pattern, and species-specific progenitor dynamics in human ES cell–derived neocortex. *Proc. Natl. Acad. Sci. U.S.A.* 110, 20284–20289. doi: 10.1073/pnas.1315710110

Kim, J. J., Savas, J. N., Miller, M. T., Hu, X., Carromeu, C., Lavallée-Adam, M., et al. (2019). Proteomic analyses reveal misregulation of LIN28 expression and delayed timing of glial differentiation in human iPS cells with MECP2 loss-of-function. *PLoS One* 14:e0212553. doi: 10.1371/journal.pone.0212553

Kim, K. Y., Hysolli, E., and Park, I. H. (2011). Neuronal maturation defect in induced pluripotent stem cells from patients with Rett syndrome. *Proc. Natl. Acad. Sci. U.S.A.* 108, 14169–14174. doi: 10.1073/pnas.1018979108

Lancaster, M. A., and Knoblich, J. A. (2014). Organogenesis in a dish: modeling development and disease using organoid technologies. *Science* 345:1247125. doi: 10.1126/science.1247125

Lancaster, M. A., Renner, M., Martin, C. A., Wenzel, D., Bicknell, L. S., Hurles, M. E., et al. (2013). Cerebral organoids model human brain development and microcephaly. *Nature* 501, 373–379.

Landucci, E., Brindisi, M., Bianciardi, L., Catania, L. M., Daga, S., Croci, S., et al. (2018). iPSC-derived neurons profiling reveals GABAergic circuit disruption and acetylated alpha-tubulin defect which improves after iHDAC6 treatment in Rett syndrome. *Exp. Cell Res.* 368, 225–235. doi: 10.1016/j.yexcr.2018.05.001

Lengner, C. J., Gimelbrant, A. A., Erwin, J. A., Cheng, A. W., Guenther, M. G., Welstead, G. G., et al. (2010). Derivation of pre-X inactivation human embryonic stem cells under physiological oxygen concentrations. *Cell* 141, 872–883. doi: 10.1016/j.cell.2010.04.010

Lewis, J. D., Meehan, R. R., Henzel, W. J., Maurer-Fogy, I., Jeppesen, P., Klein, F., et al. (1992). Purification, sequence, and cellular localization of a novel chromosomal protein that binds to methylated DNA. *Cell* 69, 905–914. doi: 10.1016/0092-8674(92)90610-o

Lioy, D. T., Garg, S. K., Monaghan, C. E., Raber, J., Foust, K. D., Kaspar, B. K., et al. (2011). A role for glia in the progression of Rett's syndrome. *Nature* 475, 497–500.

Livide, G., Patriarchi, T., Amenduni, M., Amabile, S., Yasui, D., Calcagno, E., et al. (2015). GluD1 is a common altered player in neuronal differentiation from both MECP2-mutated and CDKL5-mutated iPS cells. *Eur. J. Hum. Genet.* 23, 195–201. doi: 10.1038/ejhg.2014.81

Liyanage, V. R. B., and Rastegar, M. (2014). Rett syndrome and MeCP2. *Neuromol. Med.* 16, 231–264.

Luo, Y., Li, J., Zhu, D., Fan, Y., Li, S., and Sun, X. (2014). High-resolution chromosomal microarray analysis of early-stage human embryonic stem cells reveals an association between X chromosome instability and skewed X inactivation. *Cell Biosci.* 4:74.

Luoni, M., Giannelli, S., Indrigo, M. T., Niro, A., Massimino, L., Iannielli, A., et al. (2020). Whole brain delivery of an instability-prone Mecp2 transgene improves behavioral and molecular pathological defects in mouse models of Rett syndrome. *Elife* 9:e52629.

Maezawa, I., Swanberg, S., Harvey, D., Lasalle, J. M., and Jin, L. W. (2009). Rett syndrome astrocytes are abnormal and spread MeCP2 deficiency through gap junctions. *J. Neurosci.* 29, 5051–5061. doi: 10.1523/jneurosci.0324-09.2009

Maherali, N., Sridharan, R., Xie, W., Utikal, J., Eminli, S., Arnold, K., et al. (2007). Directly reprogrammed fibroblasts show global epigenetic remodeling and widespread tissue contribution. *Cell Stem Cell* 1, 55–70. doi: 10.1016/j.stem.2007.05.014

Maliszewska-Cyna, E., Bawa, D., and Eubanks, J. (2010). Diminished prevalence but preserved synaptic distribution of N-methyl-D-aspartate receptor subunits in the methyl CpG binding protein 2 (MeCP2)-null mouse brain. *Neuroscience* 168, 624–632. doi: 10.1016/j.neuroscience.2010.03.065

Mansour, A. A., Gonçalves, J. T., Bloyd, C. W., Li, H., Fernandes, S., Quang, D., et al. (2018). An in vivo model of functional and vascularized human brain organoids. *Nat. Biotechnol.* 36, 432–441. doi: 10.1038/nbt.4127

Marchetto, M. C., Carromeu, C., Acab, A., Yu, D., Yeo, G. W., Mu, Y., et al. (2010). A model for neural development and treatment of Rett syndrome using human induced pluripotent stem cells. *Cell* 143, 527–539. doi: 10.1016/j.cell.2010.10.016

Martinez-Fernandez, A., Nelson, T. J., Ikeda, Y., and Terzic, A. (2010). c-MYC independent nuclear reprogramming favors cardiogenic potential of induced pluripotent stem cells. *J. Cardiovasc. Transl. Res.* 3, 13–23. doi: 10.1007/s12265-009-9150-5

Marton, R. M., and Paşca, S. P. (2020). Organoid and assembloid technologies for investigating cellular crosstalk in human brain development and disease. *Trends Cell Biol.* 30, 133–143. doi: 10.1016/j.tcb.2019.11.004

Mellios, N., Feldman, D. A., Sheridan, S. D., Ip, J. P. K., Kwok, S., Amoah, S. K., et al. (2018). MeCP2-regulated miRNAs control early human neurogenesis through differential effects on ERK and AKT signaling. *Mol. Psychiatry* 23, 1051–1065. doi: 10.1038/mp.2017.86

Muguruma, K., Nishiyama, A., Kawakami, H., Hashimoto, K., and Sasai, Y. (2015). Self-organization of polarized cerebellar tissue in 3D culture of human pluripotent stem cells. *Cell Rep.* 10, 537–550. doi: 10.1016/j.celrep.2014.12.051

Muotri, A., Maria, C. N. M., Nicole, G. C., Ruth, O., Gene, Y., Kinichi, N., et al. (2010). L1 retrotransposition in neurons is modulated by MeCP2. *Nature* 468:443. doi: 10.1038/nature09544

Nag, N., and Berger-Sweeney, J. E. (2007). Postnatal dietary choline supplementation alters behavior in a mouse model of Rett syndrome. *Neurobiol. Dis.* 26, 473–480. doi: 10.1016/j.nbd.2007.02.003

Nelson, E. D., Kavalali, E. T., and Monteggia, L. M. (2006). MeCP2-dependent transcriptional repression regulates excitatory neurotransmission. *Curr. Biol.* 16, 710–716. doi: 10.1016/j.cub.2006.02.062

Neul, J. L., Kaufmann, W. E., Glaze, D. G., Christodoulou, J., Clarke, A. J., Bahi-Buisson, N., et al. (2010). Rett syndrome: revised diagnostic criteria and nomenclature. *Ann. Neurol.* 68, 944–950. doi: 10.1002/ana.22124

Nguyen, A. T., Mattiassi, S., Loeblein, M., Chin, E., Ma, D., Coquet, P., et al. (2018). Human Rett-derived neuronal progenitor cells in 3D graphene scaffold as an in vitro platform to study the effect of electrical stimulation on neuronal differentiation. *Biomed. Mater. (Bristol Engl.)* 13:034111. doi: 10.1088/1748-605x/aaaf2b

Nott, A., Cheng, J., Gao, F., Lin, Y.-T., Gjoneska, E., Ko, T., et al. (2016). Histone deacetylase 3 associates with MeCP2 to regulate FOXO and social behavior. *Nat. Neurosci.* 19, 1497–1505.

Ohashi, M., Korsakova, E., Allen, D., Lee, P., Fu, K., Vargas, B. S., et al. (2018). Loss of MECP2 leads to activation of P53 and neuronal senescence. *Stem Cell Rep.* 10, 1453–1463. doi: 10.1016/j.stemcr.2018.04.001

Paşca, S. P. (2019). Assembling human brain organoids. *Science* 363, 126–127. doi: 10.1126/science.aau5729

Pomp, O., Dreesen, O., Leong, D. F., Meller-Pomp, O., Tan, T. T., Zhou, F., et al. (2011). Unexpected X chromosome skewing during culture and reprogramming of human somatic cells can be alleviated by exogenous telomerase. *Cell Stem Cell* 9, 156–165. doi: 10.1016/j.stem.2011.06.004

Popp, B., Krumbiegel, M., Grosch, J., Sommer, A., Uebe, S., Kohl, Z., et al. (2018). Need for high-resolution genetic analysis in iPSC: results and lessons from the ForIPS consortium. *Sci. Rep.* 8:17201.

Qian, X., Nguyen, H. N., Song, M. M., Hadiono, C., Ogden, S. C., Hammack, C., et al. (2016). Brain-region-specific organoids using mini-bioreactors for modeling ZIKV exposure. *Cell* 165, 1238–1254. doi: 10.1016/j.cell.2016.04.032

Sakaguchi, H., Kadoshima, T., Soen, M., Narii, N., Ishida, Y., Ohgushi, M., et al. (2015). Generation of functional hippocampal neurons from self-organizing human embryonic stem cell-derived dorsomedial telencephalic tissue. *Nat. Commun.* 6:8896.

Samaco, R. C., Mandel-Brehm, C., Chao, H. T., Ward, C. S., Fyffe-Maricich, S. L., Ren, J., et al. (2009). Loss of MeCP2 in aminergic neurons causes cell-autonomous defects in neurotransmitter synthesis and specific behavioral abnormalities. *Proc. Natl. Acad. Sci. U.S.A.* 106, 21966–21971. doi: 10.1073/pnas.0912257106

Schwartzentruber, J., Foskolou, S., Kilpinen, H., Rodrigues, J., Alasoo, K., Knights, A. J., et al. (2018). Molecular and functional variation in iPSC-derived sensory neurons. *Nat. Genet.* 50, 54–61.

Shi, Y., Sun, L., Wang, M., Liu, J., Zhong, S., Li, R., et al. (2020). Vascularized human cortical organoids (vOrganoids) model cortical development in vivo. *PLoS Biol.* 18:e3000705.

Sinnett, S. E., Hector, R. D., Gadalla, K. K. E., Heindel, C., Chen, D., Zaric, V., et al. (2017). Improved MECP2 gene therapy extends the survival of MeCP2-Null mice without apparent toxicity after intracisternal delivery. *Mol. Ther. Methods Clin. Dev.* 5, 106–115. doi: 10.1016/j.omtm.2017.04.006

Takahashi, K., and Yamanaka, S. (2006). Induction of pluripotent stem cells from mouse embryonic and adult fibroblast cultures by defined factors. *Cell* 126, 663–676. doi: 10.1016/j.cell.2006.07.024

Tang, X., Kim, J., Zhou, L., Wengert, E., Zhang, L., Wu, Z., et al. (2016). KCC2 rescues functional deficits in human neurons derived from patients with Rett syndrome. *Proc. Natl. Acad. Sci. U.S.A.* 113, 751–756. doi: 10.1073/pnas.1524013113

Tchieu, J., Kuoy, E., Chin, M. H., Trinh, H., Patterson, M., Sherman, S. P., et al. (2010). Female human iPSCs retain an inactive X chromosome. *Cell Stem Cell* 7, 329–342. doi: 10.1016/j.stem.2010.06.024

Tillotson, R., and Bird, A. (2020). The molecular basis of MeCP2 function in the brain. *J. Mol. Biol.* 432, 1602–1623. doi: 10.1016/j.jmb.2019.10.004

Tillotson, R., Selfridge, J., Koerner, M. V., Gadalla, K. K. E., Guy, J., De Sousa, D., et al. (2017). Radically truncated MeCP2 rescues Rett syndrome-like neurological defects. *Nature* 550, 398–401. doi: 10.1038/nature24058

Trujillo, C., Gao, R., Negraes, P., Chaim, I., Domissy, A., Vandenberghe, M., et al. (2018). Nested oscillatory dynamics in cortical organoids model early human brain network development. *BioRxiv* doi: 10.1101/358622

van Duinen, V., Trietsch, S. J., Joore, J., Vulto, P., and Hankemeier, T. (2015). Microfluidic 3D cell culture: from tools to tissue models. *Curr. Opin. Biotechnol.* 35, 118–126. doi: 10.1016/j.copbio.2015.05.002

Vallot, C., Patrat, C., Collier, A. J., Huret, C., Casanova, M., Liyakat Ali, T. M., et al. (2017). XACT noncoding RNA competes with XIST in the control of X chromosome activity during human early development. *Cell Stem Cell* 20, 102–111.

Velasco, S., Kedaigle, A. J., Simmons, S. K., Nash, A., Rocha, M., Quadrato, G., et al. (2019). Individual brain organoids reproducibly form cell diversity of the human cerebral cortex. *Nature* 570, 523–527. doi: 10.1038/s41586-019-1289-x

Volpato, V., and Webber, C. (2020). Addressing variability in iPSC-derived models of human disease: guidelines to promote reproducibility. *Dis. Models Mech.* 13:dmm042317.

Wan, M., Lee, S. S. J., Zhang, X., Houwink-Manville, I., Song, H.-R., Amir, R. E., et al. (1999). Rett syndrome and beyond: recurrent spontaneous and familial MECP2 mutations at CpG hotspots. *Am. J. Hum. Genet.* 65, 1520–1529. doi: 10.1086/302690

Wang, H. (2018). Modeling neurological diseases with human brain organoids. *Front. Synaptic Neurosci.* 10:15. doi: 10.3389/fnsyn.2018.00015

Williams, E. C., Zhong, X., Mohamed, A., Li, R., Liu, Y., Dong, Q., et al. (2014). Mutant astrocytes differentiated from Rett syndrome patients-specific iPSCs have adverse effects on wild-type neurons. *Hum. Mol. Genet.* 23, 2968–2980. doi: 10.1093/hmg/ddu008

Xiang, Y., Tanaka, Y., Patterson, B., Hwang, S.-M., Hysolli, E., Cakir, B., et al. (2020). Dysregulation of BRD4 function underlies the functional abnormalities of MeCP2 mutant neurons. *Mol. Cell* 79, 84–98.e89.

Xie, N., and Tang, B. (2016). The application of human iPSCs in neurological diseases: from bench to bedside. *Stem Cells Int.* 2016: 6484713.

Yamanaka, S. (2012). Induced pluripotent stem cells: past, present, and future. *Cell Stem Cell* 10, 678–684. doi: 10.1016/j.stem.2012.05.005

Yoo, M., Carromeu, C., Kwon, O., Muotri, A., and Schachner, M. (2017). The L1 adhesion molecule normalizes neuritogenesis in Rett syndrome-derived neural precursor cells. *Biochem. Biophys. Res. Commun.* 494, 504–510. doi: 10.1016/j.bbrc.2017.10.073

Zhang, L., He, J., Jugloff, D. G., and Eubanks, J. H. (2008). The MeCP2−null mouse hippocampus displays altered basal inhibitory rhythms and is prone to hyperexcitability. *Hippocampus* 18, 294–309. doi: 10.1002/hipo.20389

Zhang, Z. N., Freitas, B. C., Qian, H., Lux, J., Acab, A., Trujillo, C. A., et al. (2016). Layered hydrogels accelerate iPSC-derived neuronal maturation and reveal migration defects caused by MeCP2 dysfunction. *Proc. Natl. Acad. Sci. U.S.A.* 113, 3185–3190. doi: 10.1073/pnas.1521255113

Conflict of Interest: The authors declare that the research was conducted in the absence of any commercial or financial relationships that could be construed as a potential conflict of interest.

Publisher's Note: All claims expressed in this article are solely those of the authors and do not necessarily represent those of their affiliated organizations, or those of the publisher, the editors and the reviewers. Any product that may be evaluated in this article, or claim that may be made by its manufacturer, is not guaranteed or endorsed by the publisher.

frontiers in Neuroscience

ORIGINAL RESEARCH
published: 10 September 2021
doi: 10.3389/fnins.2021.682054

Social Deficits and Repetitive Behaviors Are Improved by Early Postnatal Low-Dose VPA Intervention in a Novel *shank3*-Deficient Zebrafish Model

Chunxue Liu[1†], Yi Wang[1†], Jingxin Deng[1], Jia Lin[2], Chunchun Hu[1], Qiang Li[2] and Xiu Xu[1*]*

[1] Department of Child Health Care, Children's Hospital of Fudan University, National Children's Medical Center, Shanghai, China, [2] Center for Translational Medicine, Institute of Pediatrics, Shanghai Key Laboratory of Birth Defects Prevention and Control, Children's Hospital of Fudan University, National Children's Medical Center, Shanghai, China

OPEN ACCESS

Edited by:
Xiaoyan Ke,
Nanjing Brain Hospital Affiliated to Nanjing Medical University, China

Reviewed by:
Sofia Lizarraga,
University of South Carolina, United States
Jessica L. MacDonald,
Syracuse University, United States

***Correspondence:**
Qiang Li
liq@fudan.edu.cn
Xiu Xu
xuxiu@shmu.edu.cn

[†] These authors have contributed equally to this work

Specialty section:
This article was submitted to Neurodevelopment, a section of the journal Frontiers in Neuroscience

Received: 17 March 2021
Accepted: 11 August 2021
Published: 10 September 2021

Citation:
Liu C, Wang Y, Deng J, Lin J, Hu C, Li Q and Xu X (2021) Social Deficits and Repetitive Behaviors Are Improved by Early Postnatal Low-Dose VPA Intervention in a Novel shank3-Deficient Zebrafish Model. Front. Neurosci. 15:682054. doi: 10.3389/fnins.2021.682054

Mutations of the *SHANK3* gene are found in some autism spectrum disorder (ASD) patients, and animal models harboring *SHANK3* mutations exhibit a variety of ASD-like behaviors, presenting a unique opportunity to explore the underlying neuropathological mechanisms and potential pharmacological treatments. The histone deacetylase (HDAC) valproic acid (VPA) has demonstrated neuroprotective and neuroregenerative properties, suggesting possible therapeutic utility for ASD. Therefore, *SHANK3*-associated ASD-like symptoms present a convenient model to evaluate the potential benefits, therapeutic window, and optimal dose of VPA. We constructed a novel *shank3*-deficient (*shank3ab*$^{-/-}$) zebrafish model through CRISPR/Cas9 editing and conducted comprehensive morphological and neurobehavioral evaluations, including of core ASD-like behaviors, as well as molecular analyses of synaptic proteins expression levels. Furthermore, different VPA doses and treatment durations were examined for effects on ASD-like phenotypes. Compared to wild types (WTs), *shank3ab*$^{-/-}$ zebrafish exhibited greater developmental mortality, more frequent abnormal tail bending, pervasive developmental delay, impaired social preference, repetitive swimming behaviors, and generally reduced locomotor activity. The expression levels of synaptic proteins were also dramatically reduced in *shank3ab*$^{-/-}$ zebrafish. These ASD-like behaviors were attenuated by low-dose (5 μM) VPA administered from 4 to 8 days post-fertilization (dpf), and the effects persisted to adulthood. In addition, the observed underexpression of *grm5*, encoding glutamate metabotropic receptor 5, was significantly improved in VPA-treated *shank3ab*$^{-/-}$ zebrafish. We report for the first time that low-dose VPA administered after neural tube closure has lasting beneficial effects on the social deficits and repetitive behavioral patterns in *shank3*-deficient ASD model zebrafish. These findings provide a promising strategy for ASD clinical drug development.

Keywords: *shank3*, valproic acid, zebrafish model, drug treatment, autism spectrum disorder

INTRODUCTION

Autism spectrum disorder (ASD) encompasses a group of neurodevelopmental syndromes characterized by deficits in social interaction and communication as well as repetitive behaviors and restricted interests (American Psychiatric Association, 2013). There is strong evidence for the involvement of inherited genetic factors in ASD (accounting for at least 80% of the variation in disease risk) (Jutla et al., 2019; Liu et al., 2021). Furthermore, mutations in numerous genes encoding synaptic proteins have been identified in patients with ASD and intellectual disability (Verpelli and Sala, 2012; Lai et al., 2014). According to a meta-analysis, monogenic mutations in *SHANK3*, which encodes the major postsynaptic density (PSD) scaffolding protein at excitatory glutamatergic synapses, are found in approximately 0.69% of ASD cases and up to 2.12% of all moderate to profound intellectual disability cases (Leblond et al., 2014). *De novo* mutations, interstitial deletions, and terminal deletions have been identified in ASD (Durand et al., 2007; Moessner et al., 2007; Gauthier et al., 2009; Boccuto et al., 2013; Leblond et al., 2014). Additionally, *SHANK3* mutations underlie Phelan–McDermid syndrome (PMS, also known as 22q13.3 deletion syndrome), a rare autosomal dominant neurodevelopmental disorder characterized by autistic-like behaviors, absent to severely delayed speech, developmental delay, and moderate to profound intellectual disability as well as neonatal hypotonia and minor dysmorphic facial features (Phelan et al., 1993; Wilson et al., 2003; Phelan, 2008; Bonaglia et al., 2011; Phelan and McDermid, 2012). The genomic rearrangements in PMS are diverse, ranging from simple 22q13 deletions (72%), ring chromosomes (14%), and unbalanced translocations (7%) to interstitial deletions (9%), all leading to *SHANK3* haploinsufficiency (Bonaglia et al., 2011). Although the severity of the developmental delay tends to vary with deletion size (Sarasua et al., 2011; Zwanenburg et al., 2016), individuals with the same size deletion may exhibit vastly different degrees of disability (Dhar et al., 2010). Thus, *SHANK3* deficits appear to profoundly disrupt the neural circuitry required for social behavior, communication, and cognition.

The *SHANK3* gene (also known as ProSAP2, at 22q13.33) is the best studied of the three *SHANK* family members, which encoding an extensive number of mRNA and protein isoforms *via* multiple intragenic promoters and alternative splicing (Durand et al., 2007; Wang et al., 2014b). In the brain, *Shank3* mRNA is enriched in the cortex, thalamus, striatum, hippocampus, dentate gyrus, and cerebellar granule cells (Peca et al., 2011; Wang et al., 2016; Monteiro and Feng, 2017), suggesting important functions in synaptic plasticity underlying cortical organization, sensory processing, behavioral control, and cognition.

Owing to the strong genetic association between *SHANK3* deficiency and ASD, many studies have focused on the neurodevelopmental functions of this particular gene. Numerous animal models of *SHANK3* deficiency, including zebrafish, *Drosophila*, rat, mouse, and monkey models, demonstrate ASD-like behaviors, suggesting a causative role of *SHANK3* deficiency in ASD (Peca et al., 2011; Wang et al., 2016; Monteiro and Feng, 2017). Wang et al. (2016) reported that homozygous *Shank3* knockout mice displayed core behavioral features of ASD as well as impaired mGluR5–Homer association at the PSD, resulting in corticostriatal circuit abnormalities that may underlie learning deficits and ASD-like behaviors. In addition, monkey models also displayed core ASD features including impaired social interactions, repetitive behaviors, delayed vocalization, and reduced brain network activities (Tu et al., 2019; Zhou et al., 2019). The zebrafish genome harbors two homologs of human *SHANK3*, *shank3a*, and *shank3b*. In our previous studies, we generated the first *shank3b* loss-of-function mutation in zebrafish and reported prominent ASD-like behaviors (Liu et al., 2018). However, we did not examine the effects of *shank3a* and *shank3b* double mutant combinations, which would be more analogous to mammalian models harboring a single *SHANK3* mutation, or assess potential pharmacological strategies to mitigate behavioral deficits.

Current treatment options for ASD are limited, especially pharmacotherapies (Wang et al., 2014a; Penagarikano et al., 2015). Evidence-based treatments for ASD children are restricted mainly to educational practices, and intensive behavioral interventions such as Treatment and Education of Autistic and Related Communication-Handicapped Children (TEACCH) and the Early Start Denver Model (ESDM) (Dawson et al., 2010; Hyman et al., 2020). Outcomes of these behavioral therapies vary markedly according to intervention intensity, disease severity, and a variety of other factors (Sandbank et al., 2020). Further, education and behavioral interventions do not target the underlying neurobiological mechanisms (Wang et al., 2014a; Weitlauf et al., 2014) and are costly both for educational institutions and primary caregivers (Lord et al., 2018, 2020). Similarly, current pharmacologic treatments address only the associated symptoms or comorbidities, including agitation and hyperactivity, rather than the core symptoms and underlying causes (Fung et al., 2016; Lord et al., 2018, 2020; Muhle et al., 2018). Risperidone and aripiprazole are approved by the United States Food and Drug Administration (FDA) to treat comorbidities common in ASD, including irritability, and agitation (Lord et al., 2018, 2020), but similar to behavioral interventions, these evidence-based pharmacologic treatments lack sufficient biological support.

Based on available evidence, behavioral interventions should be implemented as early and intensively as possible following ASD diagnosis to improve the cognitive and adaptive outcomes of preschoolers (Weitlauf et al., 2014; Muhle et al., 2018). The preschool years are critical for acquiring language and social skills, key areas of difficulty in ASD, as this period coincides with the temporal window of enhanced plasticity in relevant neural circuits (Franz and Dawson, 2019). Similar to early intervention, pharmaceutical treatments appear effective in animal models when administered early, and Muhle et al. (2018) even suggested greater emphasis on early drug treatment rather than strict adherence to the standard timeline of efficacy based on studies in adults and adolescents. For instance, early postnatal treatment improves social deficits in adult mice with mutations in the ASD risk gene *cntnap2* (Franz and Dawson, 2019). Pharmacological inhibitors of histone deacetylase (HDAC)

have garnered interest as possible ASD therapeutics due to demonstrated neuroprotective efficacy (Fischer et al., 2010). The class I HDAC inhibitor valproic acid (VPA) was found to reduce repetitive behaviors in a small randomized controlled trial involving 13 ASD children (Hollander et al., 2006). In addition, several studies have reported that VPA can attenuate irritability in young ASD patients (Hellings et al., 2005; DeFilippis and Wagner, 2016). Further, three daily VPA treatments transiently restored social preference deficits in adult *Shank3*-deficient mice, although the effect disappeared within a few days following treatment (Qin et al., 2018). Therefore, the effects of VPA on *shank3* mutant models warrant further study.

Here we investigated the developmental characteristics of *shank3*-deficient zebrafish, neurobehavioral features relevant to ASD, and the effects of various VPA treatment regimens. We speculated that VPA administration in the early postnatal period would be more effective at reversing the core ASD-like deficits in *shank3*-deficient zebrafish than juvenile or adult treatment.

MATERIALS AND METHODS

Zebrafish and Embryo Maintenance

Wild-type (WT) zebrafish of Tu strains were acquired from Children's Hospital of Fudan University. They were raised and maintained under standard laboratory conditions at 28.5°C in "system water" under a 14 h light/10 h dark cycle according to standard protocols (Kalueff et al., 2014; Evans and Erickson, 2019). Freshly fertilized eggs were collected from multiple breeding tanks containing 25 females and 25 males. All animal experimental procedures were in compliance with local and international regulations, and approved by the institutional animal care committee of Children's Hospital of Fudan University.

Generation of *shank3a* and *shank3b* Double Deficient Zebrafish Model

Zebrafish *shank3a* and *shank3b* genes and their exon/intron boundaries were identified by searching the NCBI database (gene ID: *shank3b*, NC_007115.7; *shank3a*, NC_007129.7). Mutations in *shank3a* and *shank3b* were generated using CRISPR/Cas9 editing as previously reported (Hwang et al., 2013; Mali et al., 2013). The CRISPR/Cas9 target of *shank3a* was 5′-GGACCCCAGCCCTCCTCCCGTGG-3′ and that of *shank3b* was 5′-GGGCGTGTTGTTGCCACGGCCGG-3′ (Liu et al., 2018; **Supplementary Table 1**). *In vitro*-transcribed RNA of the guide RNA (120 ng each) and Cas9 mRNA (500 pg) were microinjected into WT zebrafish embryos (F_0) at the one-cell stage. The progeny were propagated *via* a series of out-crossings with WT zebrafish and genotyping of each generation. Eventually, these animals were in-crossed to obtain the homozygous knockouts *shank3a*$^{-/-}$ and *shank3b*$^{-/-}$. The *shank3ab*$^{-/-}$ homozygous line was obtained by mutant crossing and subsequent genotyping.

Behavior Tests for Adult Zebrafish

All behavioral experiments were conducted on 2–3.5 month old male zebrafish between 10 a.m. and 4 p.m. Behaviors were recorded for 30 min after 1–2 min habituation period using a video camera (zebrabox) suspended above the test tank. Zebrafish were returned to their home tanks immediately after completion of the test. The raw data was analyzed using Viewpoint software.

Open Field Test

The free-swimming open field test was performed in novel tanks as previously described (Liu et al., 2018). Each tank was 30 cm × 30 cm × 30 cm, and its walls consisted of opaque partitions. Swim velocity was calculated as the total distance traveled divided by the total swim time.

For the danger awareness test, the tank was virtually divided into two equal areas, peripheral and center, and greater peripheral swimming distance relative to central swimming distance was measured as a metric of danger awareness.

For analyzing repetitive and stereotyped behaviors, we used a double-blind method to score the swimming pattern within each minute, and counted the number of the four stereotyped swimming pattern episodes separately.

Shoaling Test

The shoaling test assesses social cohesion in homogeneous groups of zebrafish (**Figure 3A**; Liu et al., 2018). A shoal refers to a loose aggregation of individuals who swim close to one another, whereas a school describes a group of fish exhibiting polarized, synchronized motion (Perathoner et al., 2016). The distance between each fish can reveal the degree of shoaling behavior (i.e., social cohesion). Six zebrafish were placed in a novel 30 cm × 30 cm × 30 cm tank with walls consisting of opaque partitions, and mean inter-individual distance was measured (Kim et al., 2017).

Social Preference Test

Sociability was evaluated as the difference score between the time spent in proximity to a conspecific sector and an empty sector (Busnelli et al., 2016). Briefly, social testing was conducted over 30 min in a standard mating tank of inner dimensions 21 cm × 10 cm × 7.5 cm. A transparent plexiglas divider was placed in the middle of the tank, which allowed sufficient visual presentation for forming a social preference, and a single *shank3* mutant or WT zebrafish was placed on the left side while a group of six conspecific zebrafish (conspecific sector) was placed in the right side (**Figure 3C**). Social preference behavior was quantified as a distance distribution or as presence in a zone adjacent to the group of conspecifics. The distance ratio was calculated as the distance swam in the conspecific sector divided by the total distance.

Kin Preference Test

Another test was performed to assess preference for kinship using various colored variants. The duration and frequency of contact was compared between conspecifics and a phenotypically distinct strain (**Figure 3E**) in mating tanks with dimensions and configuration the same as those used in the "social preference test." Briefly, two transparent separators divided the tank into three compartments, with a single test fish placed in the middle and Kin zebrafish placed on the right and non-Kin (red color)

zebrafish placed on the left. Kin preference was represented by the ratio of the time spent in the Kin-sector to the total time.

VPA Treatment and Phenotypic Assessments

To assess the extent to which VPA exposure affects morphology, 4 dpf WT or *shank3ab*$^{-/-}$ larvae were reared in Petri dishes containing blue egg water alone or blue egg water containing 5, 10, 20, or 50 μM sodium valproate (Cat No. 4543-10G, Sigma-Aldrich). The egg water with or without VPA was changed daily. At 8 dpf, larvae were observed under a microscope for mortality and any morphologic abnormalities, including distended abdominal and thoracic regions, lordosis, yolk sac edema, and pericardial edema. Adverse effects including mortality and malformation rates were calculated to determine the optimal VPA concentration for subsequent experiments (**Supplementary Figure 1**).

To examine the effects of early postnatal low-dose VPA exposure on autism-like behaviors, WT or *shank3ab*$^{-/-}$ larvae were exposed to blue egg water with or without 5 μM VPA from 4 to 8 dpf. At 8 dpf, each larva was pipetted into fresh paramecium liquid, and raised to 2.5 months old (juvenile) or 3.5 months old (adult). The juveniles were then examined for 30 min using the 1 versus 6 social preference assay, while adults were subjected to social preference, repetitive behavior, locomotor activity, and thigmotaxis tests to comprehensively evaluate the effects of VPA on autism-like behaviors.

Real-Time Quantitative PCR

Total RNA was extracted from 15 WT, *shank3a*$^{-/-}$, *shank3b*$^{-/-}$, and *shank3ab*$^{-/-}$ larvae each at 3.5–4.5 months post-fertilization (mpf) using the RNA Extraction Kit from Takara, and reverse transcribed to cDNA using the PrimeScript^{TM} reagent Kit with gDNA Eraser (Takara) according to the manufacturer's recommendations. The Cas9 target region of *shank3a* and *shank3b* were amplified in duplicate samples from *shank3ab*$^{-/-}$ zebrafish by real-time quantitative PCR (RT-qPCR) to confirm genotype (**Figures 1C,D** and **Supplementary Table 1**).

To assess the effect of VPA exposure on synaptic genes and class I *hdac* genes (as VPA belongs to class I HDAC inhibitor), groups of ∼15 WT and *shank3ab*$^{-/-}$ zebrafish larvae were exposed to vehicle or VPA from 4 to 8 dpf, reared under normal conditions, then sacrificed for whole-brain total RNA isolation. The expression levels of the following genes analyzed by RT-qPCR: NMDAR subunits (*grin1a*, *grin1b*, *grin2bb*, *grin2ca*, *grin2da*, *grin2aa*), AMPAR subunits (*gria1a*, *gria1b*, *gria2b*), mGluR subunits (*grm1a*, *grm1b*, *grm5a*), and class I *hdacs* (*hdac1*, *hdac3*, *hdac8*). We selected β-*actin* or *Rpl13α* as internal controls because both are expressed in the brain throughout development. Primer sequence are shown in **Supplementary Table 1**.

Western Blotting

Proteins (50 μg per sample) were separated by SDS-PAGE and transferred on polyvinylidene difluoride membranes. After blocking the membrane at room temperature for 2 h with 5% BSA or 7% skim milk, and incubated with primary antibodies at 4°C overnight at the following concentrations: NeuN (Abcam, ab177487, 1:1500), homer1 (Aviva systems biology, ARP40181_P050, 1:1000), and synaptophysin (Abcam, ab32594, 1:1500). The blots were washed in TBS containing 0.1% Tween-20 (TBST) and incubated with HRP-conjugated secondary antibodies (1:5000) for 1.5 h at room temperature. Following six washes in TBST, the blots were incubated with ECL reagent (BeyoECL Plus, P0018M) and exposed to Kodak X-ray film (Tanon 5200). The gray values of proteins were analyzed by ImageJ software (NIH, Bethesda, MD, United States[1]), and normalized to that of corresponding internal controls, β-actin (1:2000) or Vinculin (1:5000).

Statistical Analysis

Values are presented as mean ± SEM. All data were analyzed using SPSS 20.0. In all experiments, WT and *shank3*-deficient zebrafish were compared by two-sided unpaired Student's *t*-tests, while three or more groups were compared by analysis of variance (ANOVA). Genotypes within treatment groups were compared by one-way ANOVA. All experiments were conducted in triplicate using independently treated animals. A $P < 0.05$ was considered statistically significant for all tests.

RESULTS

Generation of *shank3a*$^{-/-}$ and *shank3ab*$^{-/-}$ Zebrafish

To model *shank3* deficiency in zebrafish, we generated a loss-of-function mutant using CRISPR/Cas9 mutagenesis technology (Hwang et al., 2013; Mali et al., 2013; Liu et al., 2018). Generation of the *shank3b*$^{-/-}$ line was described in our previous study (Liu et al., 2018). Briefly, *shank3b*$^{-/-}$ harbors an early stop codon (p. 17Lfs*54) due to a deletion of 5 bases and insertion of 13 bases, resulting in a frameshift mutation and a 90-amino acid truncated protein (**Figure 1B**). The *shank3a*$^{-/-}$ line carries a deletion of five bases leading to protein truncation (p. 555Rfs*82), including most of the shank3 domain (**Figure 1A**). The *shank3ab*$^{-/-}$ line was generated by crossing *shank3b*$^{-/-}$ and *shank3a*$^{-/-}$, and individuals were selected by genotyping. RT-qPCR confirmed that *shank3a* and *shank3b* mRNA expression levels were significantly reduced in *shank3a*$^{-/-}$ and *shank3b*$^{-/-}$ zebrafish, respectively, and that both genes were downregulated in *shank3ab*$^{-/-}$ zebrafish (**Figures 1C,D**).

Aberrant Morphology and Swimming Patterns of *shank3*-Deficient Zebrafish

The developmental progression and morphological characteristics of *shank3* mutants were evaluated on 1 day post-fertilization (1 dpf). All mutants demonstrated a higher rate of mortality compared to WTs (*shank3a*$^{-/-}$: 6%, 15/266; *shank3b*$^{-/-}$: 7%, 19/270; *shank3ab*$^{-/-}$: 15%, 18/118; WT: 3%, 10/340) (**Figure 2A**). In addition, the rate of severe developmental delay was significantly greater in the *shank3ab*$^{-/-}$

[1]http://rsb.info.nih.gov/ij/

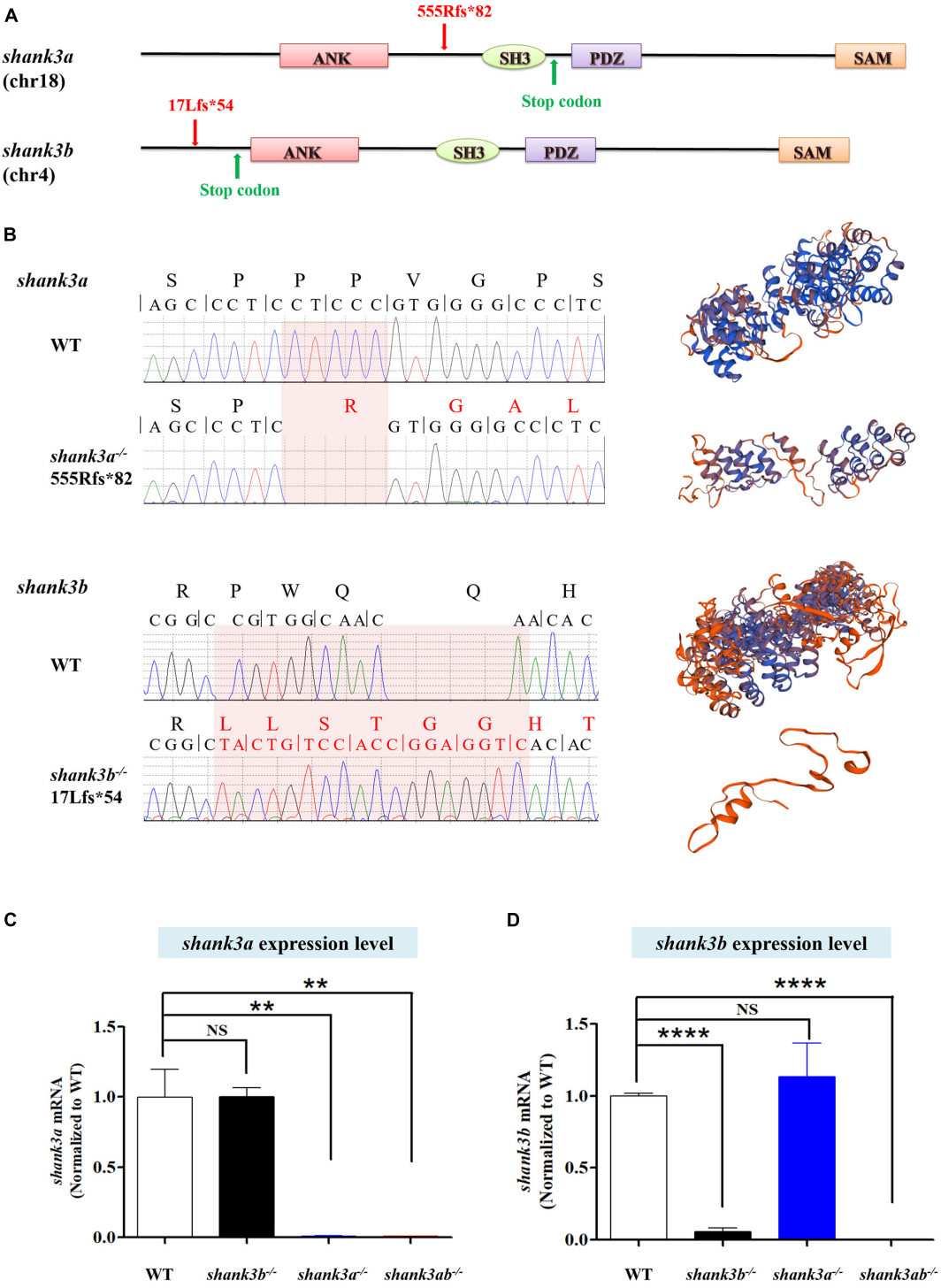

FIGURE 1 | Generation of *shank3a* and *shank3ab* mutants in zebrafish by CRISPR-Cas9 gene editing. **(A)** Structures of zebrafish *shank3a* and *shank3b* (Liu et al., 2018) gene and protein domains (ANK, ankyrin repeat domain; SH3, Src homology 3 domain; PDZ, PSD-95/discs large/ZO-1 domain; SAM, sterile alpha motif domain). Exon 9 is the target for CRISPR/Cas9 gene editing in zebrafish *shank3a* and exon 2 is the target for *shank3b*. The CRISPR/Cas9 induced frameshift mutations in shank3a (5-base deletion) and in *shank3b* (5-base deletion and 13-base insertion) which led to the truncation of the protein (Liu et al., 2018). **(B)** The mutations of *shank3a* and *shank3b* (Liu et al., 2018) were verified by Sanger sequencing. The predictions of protein spatial structures were both suggested that shank3a and shank3b proteins were likely to turn into truncated proteins (https://www.swissmodel.expasy.org/interactive/wUdwQQ/models/). **(C)** Reduced expression level of *shank3a* mRNA in the brain of *shank3a*$^{-/-}$ and *shank3ab*$^{-/-}$ adult (4 mpf) male zebrafish analyzed by RT-qPCR, while *shank3b*$^{-/-}$ was not affected. **(D)** Reduced expression level of *shank3b* mRNA in the brain of *shank3b*$^{-/-}$ and *shank3ab*$^{-/-}$ adult (4 mpf) male zebrafish analyzed by RT-qPCR, while *shank3a*$^{-/-}$ was not affected. Data are shown as mean ± SEM; $^{**}P < 0.01$. $^{****}P < 0.0001$.

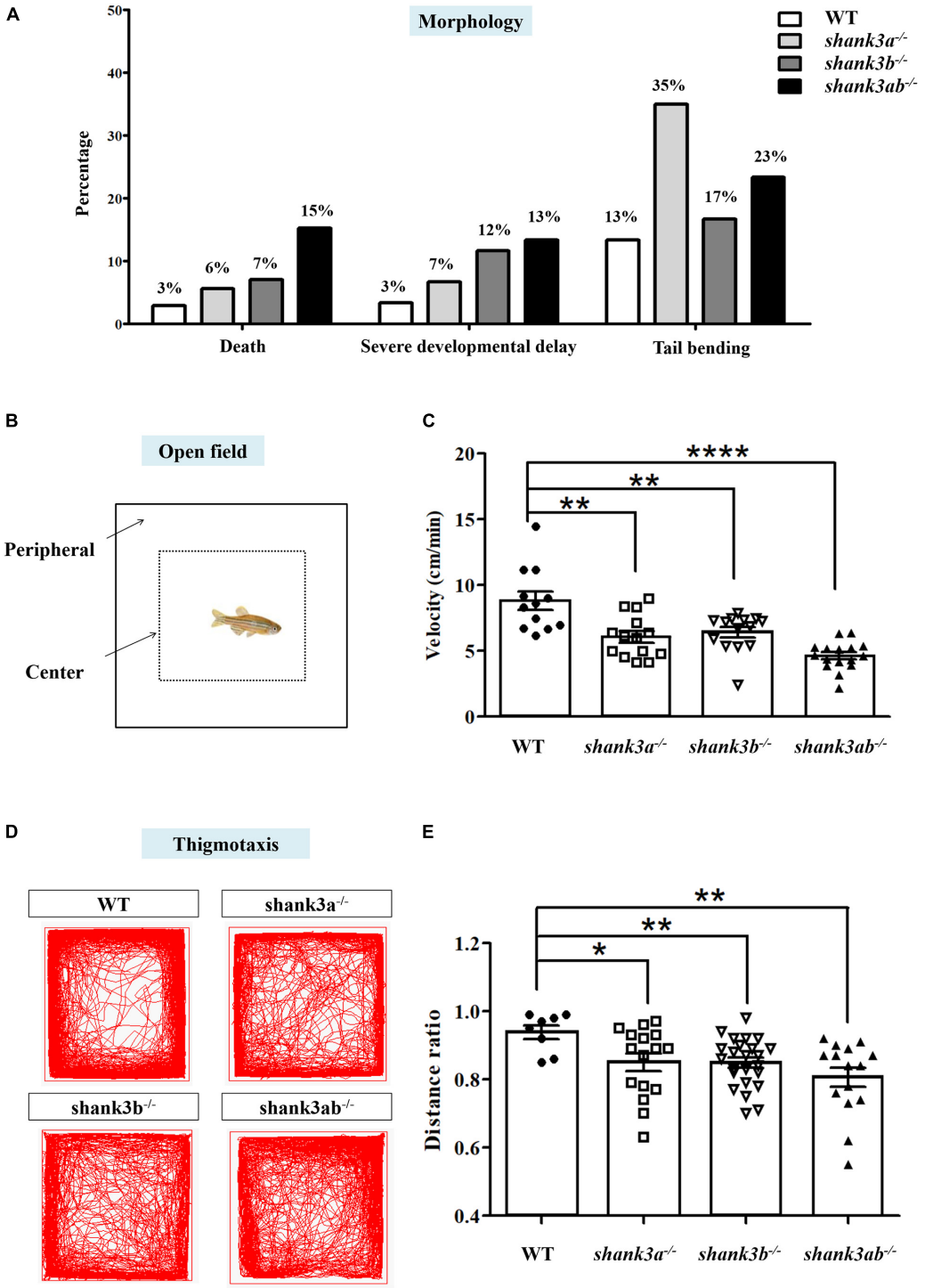

FIGURE 2 | Morphological characteristics and locomotion activity alteration in *shank3*-deficient zebrafish. **(A)** Abnormal morphological changes in *shank3a*$^{-/-}$, *shank3b*$^{-/-}$, and *shank3ab*$^{-/-}$ larvae at ∼1 dpf, including death (WT, *N* = 340; *shank3a*$^{-/-}$, *N* = 266; *shank3b*$^{-/-}$, *N* = 270; *shank3ab*$^{-/-}$, *N* = 118, severe developmental delay and tail bending (*N* = 60 each group). **(B)** Schematic diagram of the open field test and thigmotaxis test of adult male zebrafish (3.5 mpf). In the analysis of thigmotaxis test, the area of the peripheral zone is equal to the center zone (dotted line). **(C)** Compared with WT zebrafish (*N* = 12, 8.8 ± 2.4 cm/min), all *shank3*-deficient zebrafish displayed significantly decreased swimming velocity (*shank3a*$^{-/-}$, *N* = 14, 6.1 ± 1.6 cm/min; *shank3b*$^{-/-}$, *N* = 14, 6.4 ± 1.4 cm/min; *shank3ab*$^{-/-}$ zebrafish, *N* = 16, 4.6 ± 1.1 cm/min, respectively). **(D)** Representative traces of individual WT or *shank3*-deficient zebrafish in the thigmotaxis test. **(E)** Ratio for the distance traveled (periphery divided by the total zone) over 30 min in adult male zebrafish (3.5 mpf). WT, *N* = 8; *shank3a*$^{-/-}$, *N* = 16; *shank3b*$^{-/-}$, *N* = 24; *shank3ab*$^{-/-}$ zebrafish, *N* = 15. Data are shown as mean ± SEM; **P* < 0.05, ***P* < 0.01, ****P* < 0.001, *****P* < 0.0001.

group compared to all other genotypes (*shank3ab*$^{-/-}$: 13%, 8/60; *shank3a*$^{-/-}$: 7%, 4/60; *shank3b*$^{-/-}$: 12%, 7/60; WT: 3%, 2/60). Abnormal tail bending was more frequent in *shank3a*$^{-/-}$ zebrafish than other genotypes (*shank3a*$^{-/-}$: 35%, 21/60; *shank3b*$^{-/-}$: 17%, 10/60; *shank3ab*$^{-/-}$: 23%, 14/60; WT: 13%, 7/60).

The remaining *shank3a*$^{-/-}$, *shank3b*$^{-/-}$, and *shank3ab*$^{-/-}$ zebrafish were viable and fertile into adulthood. The locomotor activities of adult *shank3a*$^{-/-}$, *shank3b*$^{-/-}$, and *shank3ab*$^{-/-}$ zebrafish were examined in the open home tank as previously described (Liu et al., 2018; **Figure 2B**). Compared to WT zebrafish, all *shank3*-deficient zebrafish displayed significantly decreased swimming velocity, with *shank3ab*$^{-/-}$ zebrafish demonstrating the slowest swimming speed (*shank3ab*$^{-/-}$: 4.6 ± 1.1 cm/min; WT: 8.8 ± 2.4 cm/min; *shank3a*$^{-/-}$: 6.1 ± 1.6 cm/min; *shank3b*$^{-/-}$: 6.4 ± 1.4 cm/min) (**Figure 2C**).

Adult WT zebrafish typically avoid open areas near the water surface for protection against predation. To examine whether *shank3* deficiency modulates these avoidance behaviors, the relative proportions of swim time and distance in the pool periphery (thigmotaxis) versus the center (dotted line in **Figure 2B**) were calculated in a novel square tank with opaque walls. All *shank3*-deficient genotypes spent a significantly greater proportion of total swim time and traveled longer distances in the center of the tank compared to WT zebrafish, and *shank3ab*$^{-/-}$ zebrafish exhibited the greatest peripheral to center distance ratio of the three mutant genotypes (**Figures 2D,E**). This behavior can be interpreted as reduced alertness or reduced danger awareness (Mathur and Guo, 2010).

Core ASD-Like Behaviors of *shank3*-Deficient Adult Zebrafish

Since ASD diagnosis is based on behavioral criteria, a valid zebrafish model should exhibit core behavioral symptoms, including impaired social interactions and repetitive and stereotyped behaviors. The shoaling test showed that adult WT zebrafish spent the majority of swimming time in compact schools, while all three *shank3*-deficient genotypes swam in looser and larger schools with more frequent deviation (leaving the group), resulting in a greater average inter-fish distance compared to WT zebrafish (**Figure 3B**). This social deficit was particularly strong among the *shank3ab*$^{-/-}$ zebrafish group.

Social preference was further assessed by measuring conspecific proximity. WT zebrafish (3.5 mpf) maintain closer proximity with a conspecific group members on the right side (**Figure 3C**). In contrast, all *shank3*-deficient genotypes showed reduced frequency and duration of conspecific proximity, again with the *shank3ab*$^{-/-}$ genotype demonstrating the greatest average inter-conspecific distance (**Figure 3D**).

Wild type zebrafish also typically spend more time with a Kin group (conspecific and same color) than a non-Kin group in mixed populations. However, this Kin recognition and preference was markedly reduced in all *shank3*-deficient genotypes as measured by the proportion of time spent in close proximity with non-Kin (red-skinned) zebrafish among a mixed population (**Figure 3F**). Consistent with other social behavior tests, *shank3ab*$^{-/-}$ zebrafish spent the least amount of time in proximity to other conspecifics.

Repetitive and stereotyped behavior is another core symptom of ASD. Compared to adult WTs, *shank3ab*$^{-/-}$ zebrafish demonstrated greater behavioral perseveration, including repetitive stereotypic "figure 8" swimming, cycling behavior (swimming in circles), and other locomotor changes and patterns such as stereotyped "corner" or "wall" swimming (**Figures 3G,H**).

Dysregulation of Synapse-Related Protein Expression in *shank3*-Deficient Zebrafish

These behavioral abnormalities in *shank3*-deficient zebrafish suggest possible disruption of normal synaptic function, so we compared the expression levels of several important synaptic proteins among genotypes. Expression of the neuronal marker NeuN was reduced by 50% in the brains of adult *shank3ab*$^{-/-}$ zebrafish compared to age-matched WTs (**Figures 4A,B**). As SHANK3 is a major synaptic scaffolding protein enriched at the PSD of excitatory synapses (Jiang and Ehlers, 2013; Monteiro and Feng, 2017), we also examined expression of the postsynaptic marker homer1 and found an approximately 90% reduction in *shank3ab*$^{-/-}$ zebrafish relative to WTs (**Figures 4C,D**). It was reported that *Shank3* deficiency in mice disrupts the presynaptic neurexin-neuroligin-mediated signaling pathway required for synapse targeting and development (Arons et al., 2012), so we further compared the expression levels of presynaptic proteins among genotypes, including the ubiquitous synaptic vesicle protein synaptophysin (Kwon and Chapman, 2011). Indeed, synaptophysin expression level was reduced by ∼64% in *shank3ab*$^{-/-}$ zebrafish compared to WTs (**Figures 4E,F**). Thus, shank3 deficiency reduced the expressions of several pre- and postsynaptic proteins which are likely important to protein transmitter signaling.

Improved ASD Core Symptoms and *grm5* Receptor Expression by Early VPA Treatment

We then examined the efficacy of VPA to mitigate autism-like symptoms in these zebrafish models. In WT zebrafish, both *shank3a* and *shank3b* expression levels increased gradually from 3 to 7 dpf, a period of intense synaptogenesis (Liu et al., 2016). Exposure regimens of 3–7 and 4–8 dpf were thus judged as potentially suitable for optimal therapeutic effect. Based on preliminary observations, 4–8 dpf was chosen as the optimal exposure regimen (**Supplementary Figure 1**), and exposure concentrations (5, 20, and 50 μM) were then evaluated to identify the safety. We found that 5 μM completely eliminated mortality of *shank3ab*$^{-/-}$ larvae at 8 dpf and almost completely eliminated morphological dysgenesis (1.04%, 1/96) with no adverse effects on WT larvae (**Supplementary Figure 1**).

Once-daily administration of 5 μM VPA from 4 to 8 dpf (**Figure 5A**) significantly improved the social preference behavior of *shank3ab*$^{-/-}$ zebrafish both in juvenile and adulthood. In addition, VPA-treated *shank3ab*$^{-/-}$ juvenile (2.5 mpf) zebrafish

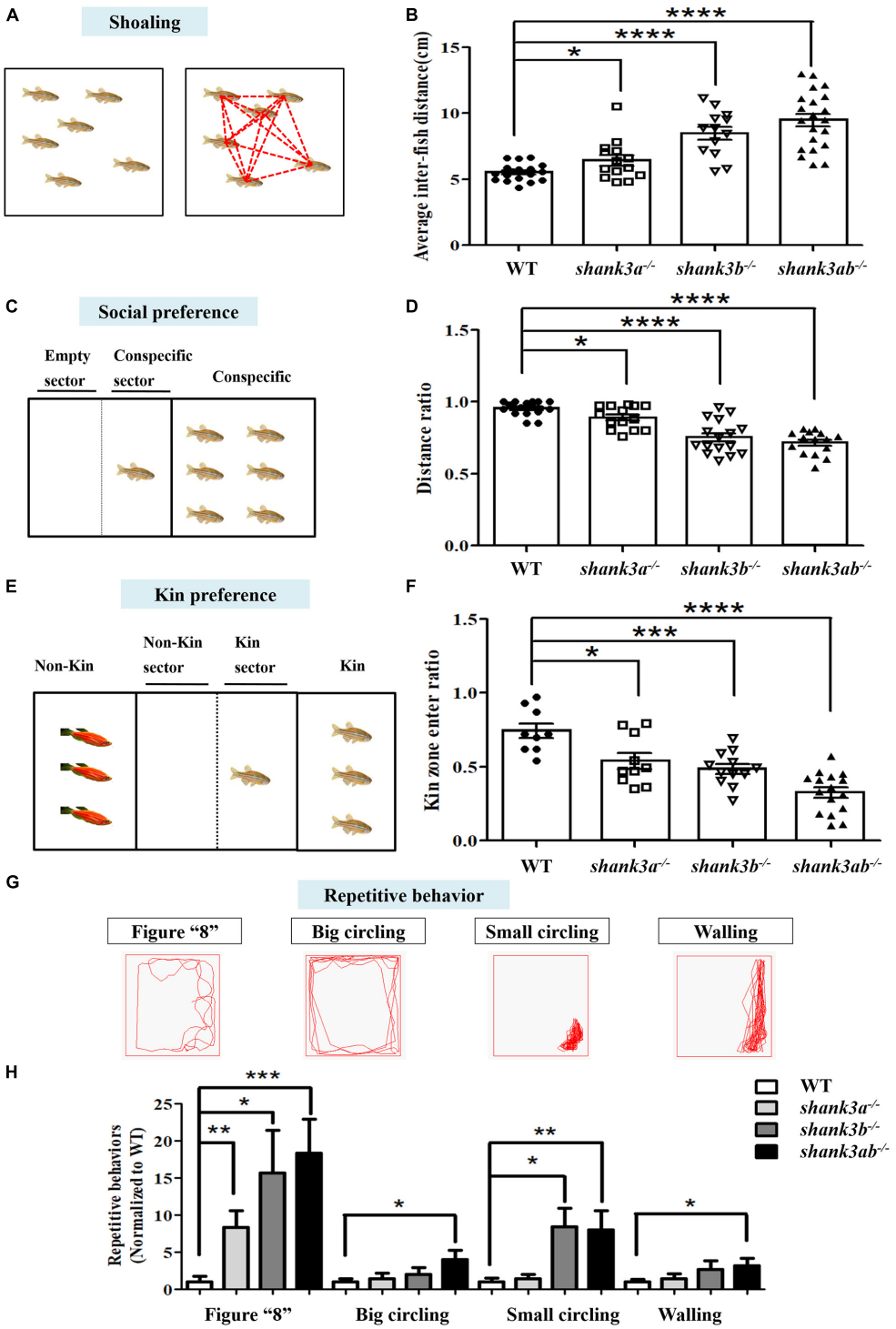

FIGURE 3 | Core behavioral features of ASD-like displayed in *shank3*-deficient zebrafish. **(A,B)** The shoaling test showed significantly increased average inter-fish distance of adult male *shank3*-deficient zebrafish (3.5 mpf). WT, $N = 18$; *shank3a*$^{-/-}$, $N = 14$; *shank3b*$^{-/-}$, $N = 13$; *shank3ab*$^{-/-}$ zebrafish, $N = 21$. **(C,D)** The social preference test showed distance ratio in the conspecific sector were significantly reduced in *shank3*-deficient zebrafish compared to WT adult male zebrafish (3.5 mpf). WT, $N = 16$; *shank3a*$^{-/-}$, $N = 14$; *shank3b*$^{-/-}$, $N = 16$; *shank3ab*$^{-/-}$ zebrafish, $N = 15$. **(E,F)** The Kin recognition and preference test showed significantly reduced ratio of Kin zone entering in *shank3*-deficient zebrafish compared to WT adult male zebrafish (3.5 mpf). WT, $N = 9$; *shank3a*$^{-/-}$, $N = 10$; *shank3b*$^{-/-}$, $N = 12$; *shank3ab*$^{-/-}$ zebrafish, $N = 16$. **(G)** Representative trace of different types of stereotyped behaviors of *shank3*-deficient adult male zebrafish (3.5 mpf). **(H)** *shank3*-deficient zebrafish had a significantly higher proportion of stereotyped movements than WT zebrafish. WT, $N = 12$; *shank3a*$^{-/-}$, $N = 14$; *shank3b*$^{-/-}$, $N = 14$; *shank3ab*$^{-/-}$ zebrafish, $N = 16$. Data are presented as mean ± SEM; $^{*}P < 0.05$, $^{**}P < 0.01$, $^{***}P < 0.001$, $^{****}P < 0.0001$.

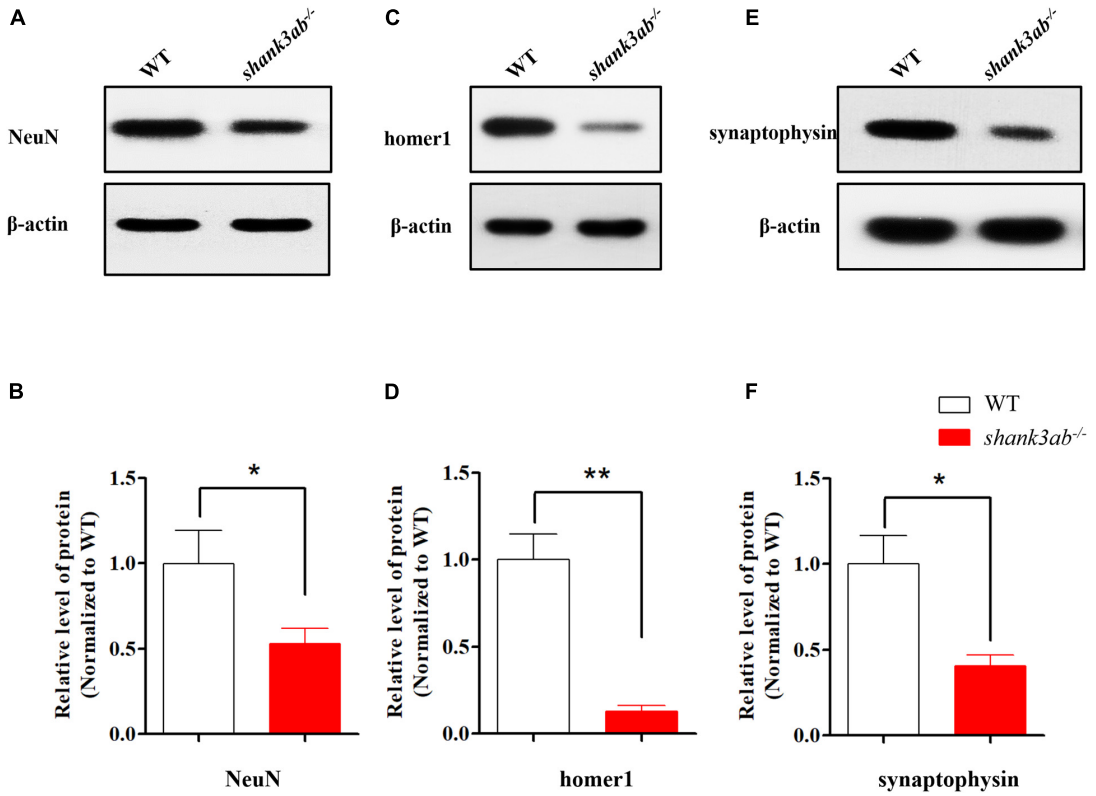

FIGURE 4 | *shank3* deficiency resulted in the reduction of synapse-related proteins in adult zebrafish brain. **(A,B)** Quantitative immunoblot blot analysis showed that the neuron protein NeuN was significantly decreased (50% of WT) in the *shank3ab*$^{-/-}$ male zebrafish brain relative to WT zebrafish (3.5 mpf). **(C,D)** The expression of post-synaptic homer1 protein was markedly reduced in *shank3ab*$^{-/-}$ male zebrafish brain compared with that of WT zebrafish (3.5 mpf, 10% of WT). **(E,F)** The expression of presynaptic synaptophysin protein was significantly reduced in *shank3ab*$^{-/-}$ male zebrafish brain compared with that of WT zebrafish (3.5 mpf, 36% of WT). *N* = 3 for each group. Data are presented as mean ± SEM; **P* < 0.05, ***P* < 0.01.

spent significantly more time exploring a tank section containing conspecifics compared to an empty zone as measured by the distance ratio (*shank3ab*$^{-/-}$: 0.84 ± 0.02; *shank3ab*$^{-/-}$ + VPA: 0.91 ± 0.02; *P* = 0.013) (**Figure 5B**). Moreover, VPA had no statistically significant effect on the social preference of WT zebrafish as measured by distance ratio (WT: 0.94 ± 0.02; WT + VPA: 0.95 ± 0.01; *P* = 0.558). This improvement was also observed in adult *shank3*-deficient zebrafish (3.5 mpf) (*shank3ab*$^{-/-}$: 0.79 ± 0.03; *shank3ab*$^{-/-}$ + VPA: 0.91 ± 0.02; *P* = 0.006) (**Figure 5C**). In fact, the deficit in social preference relative to WTs was completely reversed by postnatal VPA (WT: 0.94 ± 0.02; *shank3ab*$^{-/-}$ + VPA: 0.91 ± 0.02).

Compared to untreated *shank3ab*$^{-/-}$ zebrafish, those receiving early postnatal VPA treatment also showed reduced frequencies of stereotypic "figure 8" swim patterns (*P* = 0.035) (**Figure 5D**) and "wall" swimming (*P* < 0.0001) (**Figure 5E**). Taken together, these results suggest that early low-dose VPA treatment can induce sustained reversal of core ASD-like symptoms in *shank3*-deficient zebrafish. Conversely, VPA-treated WT zebrafish showed a greater frequency of stereotypic "figure 8" swimming (*P* = 0.018) (**Figure 5D**). Moreover, postnatal VPA treatment rescued the deficient avoidance behavior of *shank3ab*$^{-/-}$ adult zebrafish as evidenced by a significant increase in peripheral to central distance ratio (*shank3ab*$^{-/-}$: 0.77 ± 0.02; *shank3ab*$^{-/-}$ + VPA: 0.85 ± 0.02; *P* = 0.032; **Supplementary Figure 2A**). In contrast, VPA had no effect on the distance ratio of WT zebrafish (WT: 0.91 ± 0.02; WT + VPA: 0.88 ± 0.03) or the slower swim velocity of *shank3ab*$^{-/-}$ zebrafish (*shank3ab*$^{-/-}$: 6.38 ± 0.20 cm/s; *shank3ab*$^{-/-}$ + VPA: 5.71 ± 0.25 cm/s; *P* = 0.890) (**Supplementary Figure 2B**).

We also tested the effects of VPA treatment on synaptic proteins in *shank3ab*$^{-/-}$ zebrafish. As shown in **Figures 6A–F**, the expression levels of synaptic proteins (NeuN, homer1, and synaptophysin) were not significantly restored between WT and *shank3ab*$^{-/-}$ fish after exposed to VPA. To identify potential mechanisms underlying the amelioration of autism-like behaviors by early postnatal VPA, we first examined the expression levels of class I *hdac* genes (*hdac1*, *hdac2*, *hdac3*, and *hdac8*), as HDACs are the major known targets of this agent. Given the absence of *hdac2* gene in the zebrafish genome (Ko et al., 2019), we detected the expression levels of the rest three genes. However, RT-qPCR analysis revealed no changes in mRNA expression levels of *hdac1*, *hdac3*, and *hdac8* (**Supplementary Figure 2C**). We then examined the expression levels of glutamate receptors after cessation of treatment and found that VPA reversed the underexpression of *grm5a* observed in *shank3ab*$^{-/-}$

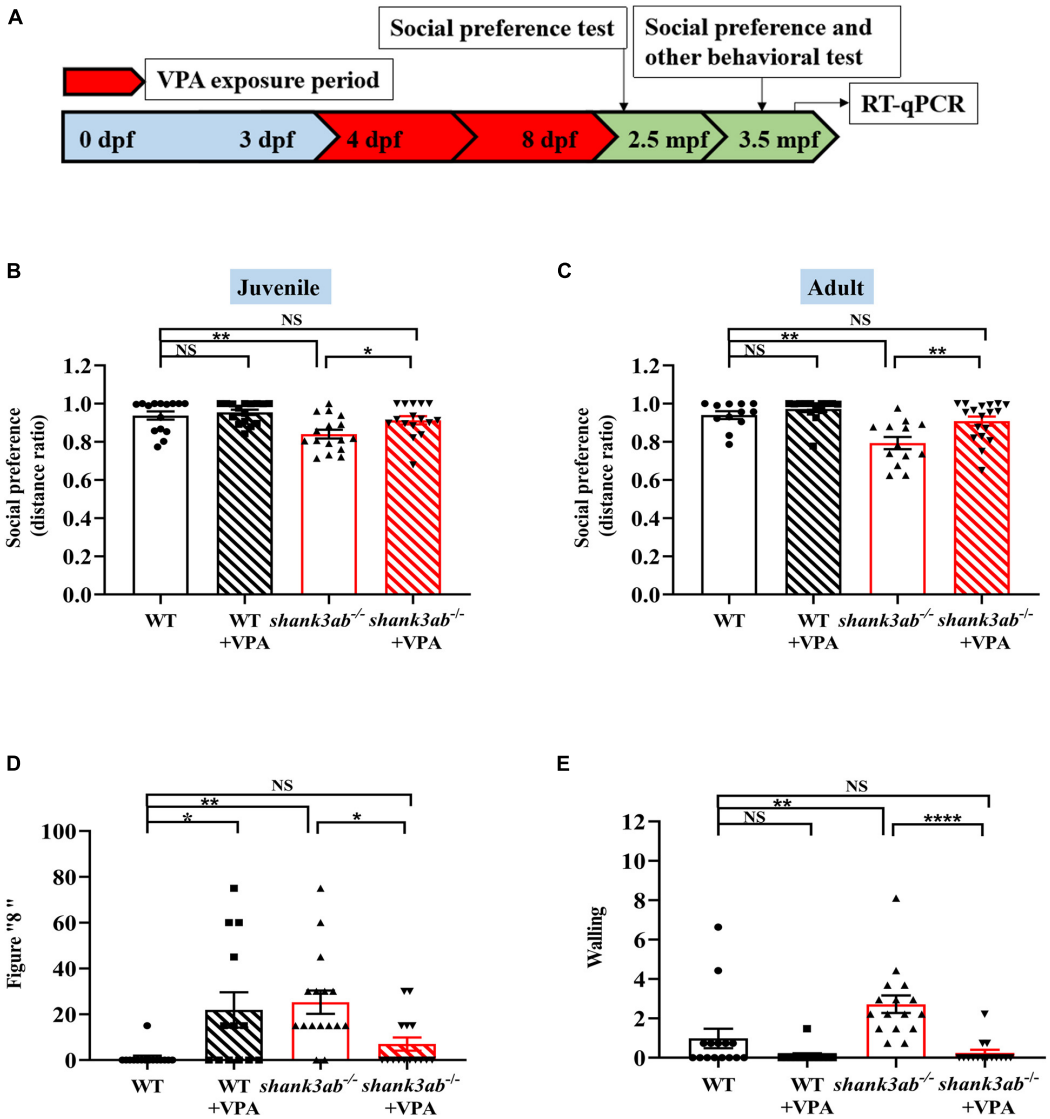

FIGURE 5 | Improved ASD core symptoms in *shank3*-deficient zebrafish upon early VPA treatment. **(A)** Schematic overview of the protocol used for the VPA exposure period, the evaluation of behavioral tests at juvenile (2.5 mpf) and adult (3.5 mpf), and RT-qPCR analysis at 4.5 mpf. Red color indicates the VPA exposure phases. **(B)** Social preference index (distance ratio) of social test on juvenile zebrafish, WT, $n = 15$; WT-VPA, $n = 16$; *shank3ab*$^{-/-}$, $n = 16$; *shank3ab*$^{-/-}$-VPA, $n = 16$. **(C)** Social preference index (distance ratio) of social test on adult zebrafish, WT, $n = 12$; WT-VPA, $n = 14$; *shank3ab*$^{-/-}$, $n = 13$; *shank3ab*$^{-/-}$-VPA, $n = 18$. **(D)** The VPA treatment reduced abnormal proportion of stereotypic figure "8" swimming and **(E)** back and forth swimming (walling) in *shank3ab*$^{-/-}$ zebrafish, WT, $n = 15$; WT-VPA, $n = 13$; *shank3ab*$^{-/-}$, $n = 16$; *shank3ab*$^{-/-}$-VPA, $n = 15$. Data are shown as mean ± SEM. Statistical analyses: **(B)** one-way ANOVA with LSD correction for multiple testing. **(C–E)** One-way ANOVA with Bonferroni correction for multiple testing. Data are presented as mean ± SEM; $^{*}P < 0.05$, $^{**}P < 0.01$, $^{****}P < 0.0001$.

zebrafish ($P < 0.05$) (**Figure 6G**) but had no effects on the mRNA levels of AMPAR subunits (*gria1a*, *gria1b*, *gria2b*) (**Supplementary Figure 2D**), and NMDAR subunits (*grin1a*, *grin1b*, *grin2bb*, *grin2ca*, *grin2da*, *grin2aa*) (**Supplementary Figure 2E**) compared to untreated zebrafish.

DISCUSSION

We described a novel *shank3*-deficient zebrafish, *shank3ab*$^{-/-}$, demonstrating stable autism-like behaviors from the juvenile stage through adulthood, including social deficits and stereotyped behaviors. These deficits were generally more severe than exhibited by either *shank3a* or *shank3b* mutants. All three mutants also exhibited higher postnatal mortality and rates of morphological dysgenesis than WTs, but adults were fertile. We also found there were decreases in several pre- and postsynaptic proteins in *shank3ab*$^{-/-}$ mutants. Low-dose VPA reversed some of these autism-like behaviors, consistent with the potential efficacy of this treatment strategy for ASD patients (Hellings et al., 2005; Hollander et al., 2006; DeFilippis and Wagner, 2016). Therefore, the *shank3ab*$^{-/-}$ zebrafish line is a robust model to

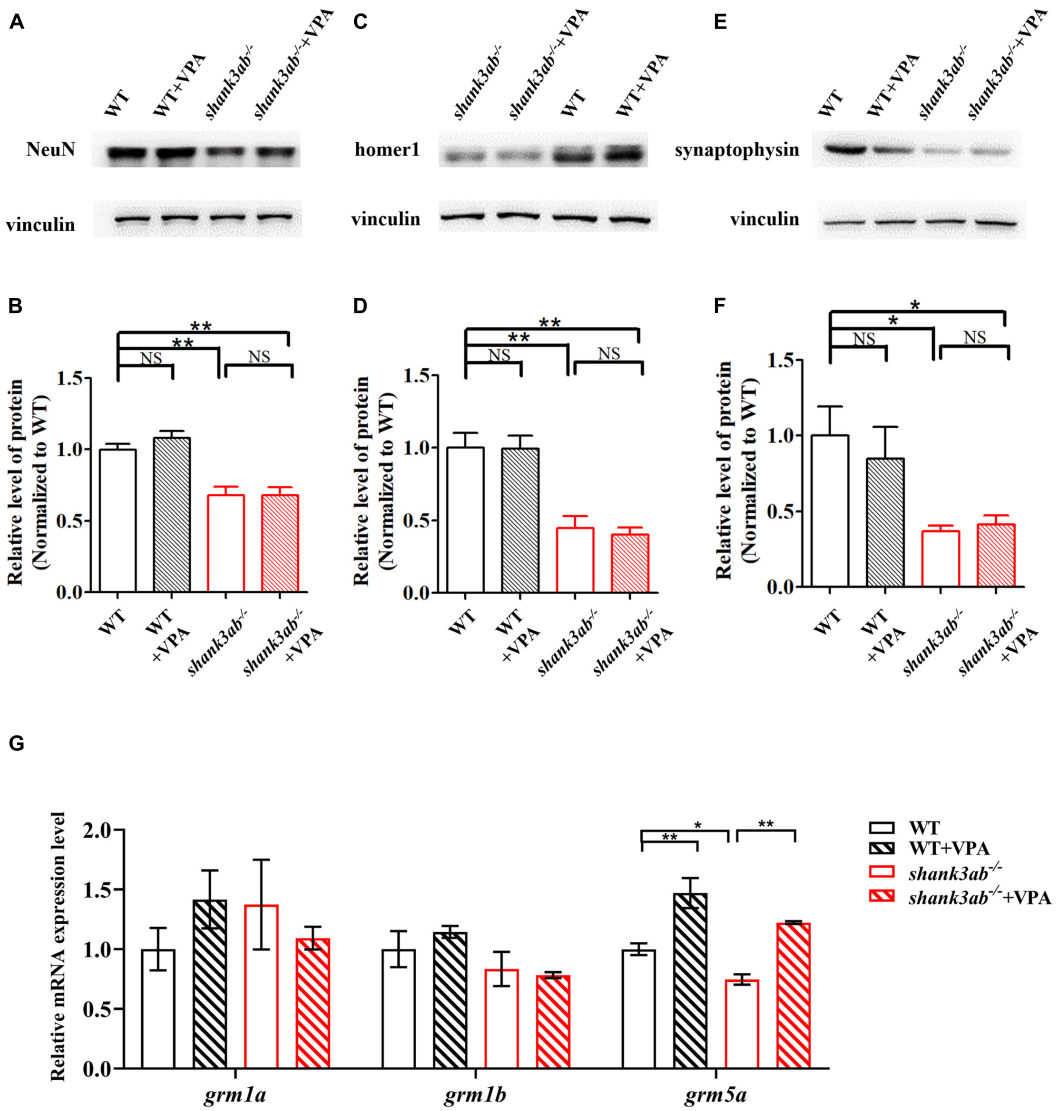

FIGURE 6 | Increased *grm5* expression level in *shank3*-deficient zebrafish upon early VPA treatment. **(A,B)** Quantitative immunoblot blot analysis showed that the expression level of neuron protein NeuN was not significantly restored in the brain of *shank3ab*$^{-/-}$ zebrafish treated with VPA relative to WT zebrafish (2 mpf). Similarly, the expressions of post-synaptic homer1 protein **(C,D)** and presynaptic synaptophysin protein **(E,F)** were not significantly increased in in the brain of *shank3ab*$^{-/-}$ zebrafish treated with VPA relative to WT zebrafish (2 mpf). **(G)** The relative mRNA expression levels of *grm1a*, *grm1b*, and *grm5a* at 4.5 mpf were detected. Each group $n = 3$. Data are shown as mean ± SEM. $^{*}P < 0.05$, $^{**}P < 0.01$.

explore the neurological mechanisms underlying ASD as well as potential pharmacological treatments.

Among molecular alterations, these *shank3*-deficient zebrafish exhibited a significant reduction in the expression levels of several synaptic proteins, including pre- and postsynaptic markers, which were consistent with previous mouse or *Drosophila* models. As a postsynaptic protein, change in postsynaptic homer1 protein was prominent in *shank3ab*$^{-/-}$ zebrafish, which was consistent with findings from other ASD mouse models (Tu et al., 1999; Wang et al., 2016). In addition, we also demonstrate reduced expression of the presynaptic protein synaptophysin, which was not previously detected in *Shank3* deficient mouse models. This finding suggests that *shank3* deficiency alters presynaptic formation and neurotransmission through direct or trans-synaptic mechanisms in zebrafish. The presynaptic functions of SHANK3 are not well characterized in comparison to postsynaptic functions. Several recent studies have suggested that SHANK3 is expressed in presynaptic terminals of rodent brain and dorsal root ganglion (DRG) neurons (Han et al., 2016). In a *Drosophila Shank* mutant (analogous to a *SHANK3* mutation in humans), Shank was found in both axons and the presynaptic sites of neuromuscular junctions (NMJs) (Wu et al., 2017). Moreover, ultrastructural analysis of synaptic boutons at *Shank* mutant calyces showed disorganization of both presynaptic and postsynaptic components, and lack of synaptic clefts (Wu et al., 2017). This first demonstration of reduced synaptophysin in a

vertebrate ASD model supports a presynaptic function for shank3 protein. The contribution of shank3-associated presynaptic deficits to ASD warrant further investigation. Generally, the overall morphology of the brain tissues were relatively normal in KO group as compared to WT group (**Supplementary Figure 3**). Moreover, the expression levels of synaptic proteins were not significantly restored between WT and *shank3ab*$^{-/-}$ fish after exposed to VPA (**Figure 6**). Similarly, in mouse model, neuronal morphology and density were not changed between WT and *Shank3*-deficient mice and also not altered by romidepsin (a highly potent class I inhibitor) treatment (Qin et al., 2018). Additionally, there were no apparent morphological changes in neurons treated with VPA compared with controls (Fujiki et al., 2013).

Postnatal low-dose VPA treatment profoundly and persistently improved social preference deficits, abnormal repetitive behaviors, and impaired thigmotaxis, suggesting activation of a compensatory mechanism under *shank3* deficiency. Shank3 facilitates both synaptogenesis and the synaptic plasticity processes underlying social learning and cognition (Duffney et al., 2015). In addition, the behavioral abnormalities exhibited by *Shank3*-deficient animal models have been attributed to altered glutamatergic signaling (Peca et al., 2011; Wang et al., 2011; Bozdagi et al., 2013; Jiang and Ehlers, 2013), and VPA has been reported to increase synaptic transmission (Rinaldi et al., 2007; Akhtar et al., 2009).

We also found that postnatal low-dose VPA significantly reduced stereotyped swimming patterns ("figure 8" and "walling"). One possible explanation for this effect is improved transcription of *grm5a*, as Wang et al. (2016) demonstrated that disrupted mGluR5 scaffolding and abnormal mGluR5 signaling contribute to the excessive self-grooming and other behavioral and functional abnormalities of *Shank3*-defcient mice. Moreover, pharmacological enhancement of mGluR5 receptors rescued behavioral deficits, including repetitive behaviors and social deficits, in *Shank3* knockout mice (Vicidomini et al., 2017). Collectively, an important inference from this study is that early VPA treatment can have long-lasting benefits on repetitive behaviors in *shank3*-deficient zebrafish, possibly by improving *grm5a* expression.

Valproic acid has anticonvulsant and mood stabilizing activities and are used to treat epilepsy and bipolar disorder. Generally, VPA is a HDAC inhibitor (Phiel et al., 2001), a GABA transaminase inhibitor, and a sodium channel blocker (Johannessen, 2000; Löscher, 2002; Owens and Nemeroff, 2003; Zanatta et al., 2019). Several studies confirmed the role of HDAC inhibitor of VPA. Fujiki et al. (2013) have reported that VPA, trichostatin A and sodium butyrate (all are HDAC inhibitors), but not valpromide, which is a structural analog of VPA having the same antiepileptic effect as VPA but lacking the HDAC inhibitor activity, have proapoptotic effects on neural progenitor cells (NPCs) of embryonic stem (ES) cell-derived glutamatergic neurons. In this study, we also have added a positive control – romidepsin, a highly potent class I HDAC inhibitor, to treat fish (**Supplementary Table 2** and **Figure 4**). WT or *shank3ab*$^{-/-}$ larvae were exposed to blue egg water with or without 0.05 or 0.1 μM romidepsin from 4 to 8 dpf. At 8 dpf, each larva was pipetted into fresh paramecium liquid, and raised to 2 months old (juvenile). Compared to *shank3ab*$^{-/-}$ zebrafish, romidepsin treated (0.05 or 0.1 μM) juvenile *shank3ab*$^{-/-}$ zebrafish exhibited significantly elevated social preference behaviors, which was consistent with *Shank3*-deficient mice model (Qin et al., 2018).

Valproic acid is a broad-spectrum inhibitor against class I (HDAC1, HDAC2, HDAC3, and HDAC8) HDAC (Chelladurai et al., 2020). Qin et al. (2018) reported that *Shank3*-deficient mice exhibited an abnormally low level of histone acetylation resulting from *HDAC2* upregulation in the prefrontal cortex (PFC) and β-catenin/HDAC2 played a causal role in social deficits of *Shank3*-deficiency mouse model and the therapeutic effect of romidepsin. While the levels of *HDAC1*, *HDAC3*, *and HDAC8* mRNA were largely unchanged. Given the absence of *hdac2* gene in the zebrafish genome (Ko et al., 2019), we detected the expression levels of the rest three genes. Similarly, RT-qPCR analysis revealed no changes in mRNA expression levels of *hdac1*, *hdac3*, and *hdac8* (**Supplementary Figure 2C**). In the further study, a VPA analog that does not have the HDAC inhibitory activity should be used as a control to detect the effects of the HDAC inhibitory activity of VPA.

This study also supports previous studies demonstrating that the early postnatal period is a critical therapeutic time window for long-lasting effects on core autistic symptoms (Dinstein et al., 2011). Hensch (2005) reported that novel interventions should be applied before irreversible neural function changes coinciding with the end of these critical periods. However, clinical studies have demonstrated that VPA exposure before the neural tube is closed (20–24 days of gestation in humans) increases the incidence of neurodevelopmental disorders including ASD (Rice and Barone, 2000; Jentink et al., 2010; Meador et al., 2013). Moreover, prenatal VPA exposure is actually used to establish rodent ASD models. Animals exposed to VPA during neural tube closure [E12.5 in rats according to Kim et al. (2011) and E10.5 in mice according to Kim et al. (2014)] showed an increased incidence of autism-like symptoms. When VPA was administered earlier than this critical time point, embryonic malformation was very likely to occur (Kim et al., 2019). In contrast, VPA administered after neural tube closure did not cause embryonic lethality or autism-like phenotypes (Kim et al., 2019). Furthermore, long-term VPA therapy had no noticeable noxious effect on cognition and learning in school children (Calandre et al., 1990). Thus, the optimal postnatal time window appears essential for VPA treatment efficacy against ASD.

Dose was the other key factor for effective VPA treatment. In animal models, fetal VPA exposure impairs cognitive outcome and increases malformation rate in a dose-dependent manner (Meador et al., 2013; Kaplan et al., 2015). Nicolini and Fahnestock (2018) reported ASD-like deficits following exposure of rat embryos to 350-600 mg/kg or of mouse embryos to 300-800 mg/kg VPA, while exposure to 25 μM from 10 to 24 hpf elicited social deficits in zebrafish (Baronio et al., 2018). VPA can also induce neuronal apoptosis (Ikonomidou et al., 1999). Conversely, low-dose VPA induced a dramatic rescue of core autistic deficits in *shank3*-deficient zebrafish, and this dose had no detectable effects on WT animals.

This study provides a new genetic zebrafish model of *shank3* deficiency which displayed distinctly abnormal social behaviors and increased stereotyped behaviors. Importantly, the autism-like behaviors could be improved by postnatal low-dose VPA treatment. These findings may suggest a path for further research to identify medicinal development and allow for more in-depth understandings of future clinical drug research.

DATA AVAILABILITY STATEMENT

The original contributions presented in the study are included in the article/**Supplementary Material**, further inquiries can be directed to the corresponding authors.

ETHICS STATEMENT

The animal study was reviewed and approved by Research Ethics Board of Children's Hospital of Fudan University.

AUTHOR CONTRIBUTIONS

XX and QL conceived the study. CL and YW performed the experiments, analyzed the data, and wrote the initial draft of the manuscript. All authors contributed to the interpretation of the results, provided critical feedback, helped shape the analysis and manuscript, and approved the submitted manuscript.

FUNDING

This study was supported by grants from "Haiju" International Joint Laboratory of National Children's Medical Center of Children's Hospital of Fudan University (No. EK1125180106), Industry-University-Research High-tech Transformation Incubation Project of Fudan University (FDEKCXY08), and Shanghai Key Clinical Specialty Construction Project to XX. This study was also supported by grants from the Shanghai Sailing Program (No. 19YF1403800) and Clinical Research of Shanghai Municipal Health Commission (No. 20204Y0102) to CL.

SUPPLEMENTARY MATERIAL

The Supplementary Material for this article can be found online at: https://www.frontiersin.org/articles/10.3389/fnins.2021.682054/full#supplementary-material

REFERENCES

American Psychiatric Association (2013). *Diagnostic and Statistical Manual of Mental Disorders*, 5th Edn. Washington, DC: American Psychiatric Association.

Akhtar, M. W., Raingo, J., Nelson, E. D., Montgomery, R. L., Olson, E. N., Kavalali, E. T., et al. (2009). Histone deacetylases 1 and 2 form a developmental switch that controls excitatory synapse maturation and function. *J. Neurosci.* 29, 8288–8297. doi: 10.1523/JNEUROSCI.009709.2009

Arons, M. H., Thynne, C. J., Grabrucker, A. M., Li, D., Schoen, M., Cheyne, J. E., et al. (2012). Autism-associated mutations in ProSAP2/Shank3 impair synaptic transmission and neurexin-neuroligin-mediated transsynaptic signaling. *J. Neurosci.* 32, 14966–14978. doi: 10.1523/JNEUROSCI.2215-12.2012

Baronio, D., Puttonen, H., Sundvik, M., Semenova, S., and Lehtonen, E. (2018). Embryonic exposure to valproic acid affects the histaminergic system and the social behaviour of adult zebrafish (Danio rerio). *Br. J. Pharmacol.* 175, 797–809. doi: 10.1111/bph.14124

Bonaglia, M. C., Giorda, R., Beri, S., De Agostini, C., Novara, F., Fichera, M., et al. (2011). Molecular mechanisms generating and stabilizing terminal 22q13 deletions in 44 subjects with Phelan/McDermid syndrome. *PLoS Genet* 7:e1002173. doi: 10.1371/journal.pgen.1002173

Bozdagi, O., Tavassoli, T., and Buxbaum, J. D. (2013). Insulin-like growth factor-1 rescues synaptic and motor deficits in a mouse model of autism and developmental delay. *Mol. Autism* 4:9. doi: 10.1186/2040-2392-4-9

Boccuto, L., Lauri, M., Sarasua, S. M., Skinner, C. D., Buccella, D., Dwivedi, A., et al. (2013). Prevalence of SHANK3 variants in patients with different subtypes of autism spectrum disorders. *Eur. J. Hum. Genet.* 21, 310–316. doi: 10.1038/ejhg.2012.175

Busnelli, M., Kleinau, G., Muttenthaler, M., Stoev, S., Manning, M., Bibic, L., et al. (2016). Design and characterization of superpotent bivalent ligands targeting oxytocin receptor dimers via a channel-like structure. *J. Med. Chem.* 59, 7152–7166. doi: 10.1021/acs.jmedchem.6b00564

Calandre, E. P., Dominguez-Granados, R., Gomez-Rubio, M., and Molina-Font, J. A. (1990). Cognitive effects of long-term treatment with phenobarbital and valproic acid in school children. *Acta Neurol. Scand.* 81, 504–506. doi: 10.1111/j.1600-0404.1990.tb01008.x

Chelladurai, P., Dabral, S., Basineni, S. R., Chen, C., Schmoranzer, M., Bender, N., et al. (2020). Isoform-specific characterization of class I histone deacetylases and their therapeutic modulation in pulmonary hypertension. *Sci. Rep.* 10:12864. doi: 10.1038/s41598-020-69737-x

Dawson, G., Rogers, S., Munson, J., Smith, M., Winter, J., Greenson, J., et al. (2010). Randomized, controlled trial of an intervention for toddlers with autism: the Early Start Denver Model. *Pediatrics* 125, e17–e23. doi: 10.1542/peds.2009-2958

DeFilippis, M., and Wagner, K. D. (2016). Treatment of autism spectrum disorder in children and adolescents. *Psychopharmacol. Bull.* 46, 18–41.

Dhar, S. U., Del, G. D., German, J. R., Peters, S. U., Ou, Z., Bader, P. I., et al. (2010). 22q13.3 deletion syndrome: clinical and molecular analysis using array CGH. *Am. J. Med. Genet A* 152A, 573–581. doi: 10.1002/ajmg.a.33253

Dinstein, I., Pierce, K., Eyler, L., Solso, S., Malach, R., Behrmann, M., et al. (2011). Disrupted neural synchronization in toddlers with autism. *Neuron* 70, 1218–1225. doi: 10.1016/j.neuron.2011.04.018

Duffney, L. J., Zhong, P., Wei, J., Matas, E., Cheng, J., Qin, L., et al. (2015). Autism-like deficits in Shank3-deficient mice are rescued by targeting actin regulators. *Cell Rep.* 11, 1400–1413. doi: 10.1016/j.celrep.2015.04.064

Durand, C. M., Betancur, C., Boeckers, T. M., Bockmann, J., Chaste, P., Fauchereau, F., et al. (2007). Mutations in the gene encoding the synaptic scaffolding protein SHANK3 are associated with autism spectrum disorders. *Nat. Genet.* 39, 25–27. doi: 10.1038/ng1933

Evans, C. R., and Erickson, N. (2019). Intersectionality and depression in adolescence and early adulthood: a MAIHDA analysis of the national longitudinal study of adolescent to adult health, 1995-2008. *Soc. Sci. Med.* 220, 1–11. doi: 10.1016/j.socscimed.2018.10.019

Fischer, A., Sananbenesi, F., Mungenast, A., and Tsai, L. H. (2010). Targeting the correct HDAC(s) to treat cognitive disorders. *Trends Pharmacol. Sci.* 31, 605–617. doi: 10.1016/j.tips.2010.09.003

Franz, L., and Dawson, G. (2019). Implementing early intervention for autism spectrum disorder: a global perspective. *Pediatr. Med.* 2:44. doi: 10.21037/pm.2019.07.09

Fujiki, R., Sato, A., Fujitani, M., and Yamashita, T. (2013). A proapoptotic effect of valproic acid on progenitors of embryonic stem cell-derived glutamatergic neurons. *Cell Death Dis.* 4:e677. doi: 10.1038/cddis.2013.205

Fung, L. K., Mahajan, R., Nozzolillo, A., Bernal, P., Krasner, A., Jo, B., et al. (2016). Pharmacologic treatment of severe irritability and problem behaviors in autism: a systematic review and meta-analysis. *Pediatrics* 137(Suppl. 2), S124–S135. doi: 10.1542/peds.2015-2851K

Gauthier, J., Spiegelman, D., Piton, A., Lafreniere, R. G., Laurent, S., St-Onge, J., et al. (2009). Novel de novo SHANK3 mutation in autistic patients. *Am. J. Med. Genet B Neuropsychiatr. Genet* 150B, 421–424. doi: 10.1002/ajmg.b.30822

Han, Q., Kim, Y. H., Wang, X., Liu, D., Zhang, Z. J., Bey, A. L., et al. (2016). SHANK3 deficiency impairs heat hyperalgesia and TRPV1 signaling in primary sensory neurons. *Neuron* 92, 1279–1293. doi: 10.1016/j.neuron.2016.11.007

Hellings, J. A., Weckbaugh, M., Nickel, E. J., Cain, S. E., Zarcone, J. R., Reese, R. M., et al. (2005). A double-blind, placebo-controlled study of valproate for aggression in youth with pervasive developmental disorders. *J. Child Adolesc. Psychopharmacol.* 15, 682–692. doi: 10.1089/cap.2005.15.682

Hensch, T. K. (2005). Critical period plasticity in local cortical circuits. *Nat. Rev. Neurosci.* 6, 877–888. doi: 10.1038/nrn1787

Hollander, E., Soorya, L., Wasserman, S., Esposito, K., and Chaplin, W. (2006). Divalproex sodium vs. placebo in the treatment of repetitive behaviours in autism spectrum disorder. *Int. J. Neuropsychopharmacol.* 9, 209–213. doi: 10.1017/S1461145705005791

Hwang, W. Y., Fu, Y., Reyon, D., Maeder, M. L., Tsai, S. Q., Sander, J. D., et al. (2013). Efficient genome editing in zebrafish using a CRISPR-Cas system. *Nat. Biotechnol.* 31, 227–229. doi: 10.1038/nbt.2501

Hyman, S. L., Levy, S. E., and Myers, S. M. (2020). Identification, evaluation, and management of children with autism spectrum disorder. *Pediatrics* 145:e20193447. doi: 10.1542/peds.2019-3447

Ikonomidou, C., Bosch, F., Miksa, M., Bittigau, P., Vockler, J., Dikranian, K., et al. (1999). Blockade of NMDA receptors and apoptotic neurodegeneration in the developing brain. *Science* 283, 70–74. doi: 10.1126/science.283.5398.70

Jentink, J., Loane, M. A., Dolk, H., Barisic, I., Garne, E., Morris, J. K., et al. (2010). Valproic acid monotherapy in pregnancy and major congenital malformations. *N. Engl. J. Med.* 362, 2185–2193. doi: 10.1056/NEJMoa0907328

Jiang, Y. H., and Ehlers, M. D. (2013). Modeling autism by SHANK gene mutations in mice. *Neuron* 78, 8–27. doi: 10.1016/j.neuron.2013.03.016

Jutla, A., Reed, H., and Veenstra-VanderWeele, J. (2019). The architecture of autism spectrum disorder risk: what do we know, and where do we go from here? *JAMA Psychiatry* 76, 1005–1006. doi: 10.1001/jamapsychiatry.2019.1375

Kalueff, A. V., Stewart, A. M., and Gerlai, R. (2014). Zebrafish as an emerging model for studying complex brain disorders. *Trends Pharmacol. Sci.* 35, 63–75. doi: 10.1016/j.tips.2013.12.002

Kaplan, Y. C., Nulman, I., and Koren, G. (2015). Dose-dependent risk of malformations with antiepileptic drugs: an analysis of data from the EURAP epilepsy and pregnancy registry. *Ther. Drug Monit.* 37, 557–558. doi: 10.1097/FTD.0000000000000193

Kim, J. W., Park, K., Kang, R. J., Gonzales, E. L., Oh, H. A., Seung, H., et al. (2019). Gene-environment interaction counterbalances social impairment in mouse models of autism. *Sci. Rep.* 9:11490. doi: 10.1038/s41598-019-47680-w

Kim, J. W., Seung, H., Kwon, K. J., Ko, M. J., Lee, E. J., Oh, H. A., et al. (2014). Subchronic treatment of donepezil rescues impaired social, hyperactive, and stereotypic behavior in valproic acid-induced animal model of autism. *PLoS One* 9:e104927. doi: 10.1371/journal.pone.0104927

Kim, K. C., Kim, P., Go, H. S., Choi, C. S., Yang, S. I., Cheong, J. H., et al. (2011). The critical period of valproate exposure to induce autistic symptoms in Sprague-Dawley rats. *Toxicol. Lett.* 201, 137–142. doi: 10.1016/j.toxlet.2010.12.018

Kim, O. H., Cho, H. J., Han, E., Hong, T. I., Ariyasiri, K., Choi, J. H., et al. (2017). Zebrafish knockout of Down syndrome gene, DYRK1A, shows social impairments relevant to autism. *Mol. Autism* 8:50. doi: 10.1186/s13229-017-0168-162

Ko, S., Russell, J. O., Tian, J., Gao, C., Kobayashi, M., Feng, R., et al. (2019). Hdac1 regulates differentiation of bipotent liver progenitor cells during regeneration via Sox9b and Cdk8. *Gastroenterology* 156, 187–202. doi: 10.1053/j.gastro.2018.09.039

Kwon, S. E., and Chapman, E. R. (2011). Synaptophysin regulates the kinetics of synaptic vesicle endocytosis in central neurons. *Neuron* 70, 847–854. doi: 10.1016/j.neuron.2011.04.001

Lai, M. C., Lombardo, M. V., and Baron-Cohen, S. (2014). Autism. *Lancet* 383, 896–910. doi: 10.1016/S0140-6736(13)61539-61531

Leblond, C. S., Nava, C., Polge, A., Gauthier, J., Huguet, G., Lumbroso, S., et al. (2014). Meta-analysis of SHANK mutations in autism spectrum disorders: a gradient of severity in cognitive impairments. *PLoS Genet* 10:e1004580. doi: 10.1371/journal.pgen.1004580

Liu, C. X., Li, C. Y., Hu, C. C., Wang, Y., Lin, J., Jiang, Y. H., et al. (2018). CRISPR/Cas9-induced shank3b mutant zebrafish display autism-like behaviors. *Mol. Autism* 9:23. doi: 10.1186/s13229-018-0204-x

Liu, C. X., Peng, X. L., Hu, C. C., Li, C. Y., and Li, Q. (2016). Developmental profiling of ASD-related shank3 transcripts and their differential regulation by valproic acid in zebrafish. *Dev. Genes Evol.* 226, 389–400. doi: 10.1007/s00427-016-0561-564

Liu, C. X., Li, D. Y., Yang, H. W., Li, H. P., Xu, Q., Zhou, B. R., et al. (2021). Altered striatum centered brain structures in SHANK3 deficient Chinese children with genotype and phenotype profiling. *Prog. Neurobiol.* 200:101985. doi: 10.1016/j.pneurobio.2020.101985

Lord, C., Brugha, T. S., Charman, T., Cusack, J., Dumas, G., Frazier, T., et al. (2020). Autism spectrum disorder. *Nat. Rev. Dis. Primers* 6:5. doi: 10.1038/s41572-019-0138-134

Lord, C., Elsabbagh, M., Baird, G., and Veenstra-Vanderweele, J. (2018). Autism spectrum disorder. *Lancet* 392, 508–520. doi: 10.1016/S0140-6736(18)31129-31122

Johannessen, C. U. (2000). Mechanisms of action of valproate: a commentatory. *Neurochem. Int.* 37, 103–110. doi: 10.1016/s0197-0186(00)00013-19

Löscher, W. (2002). Basic pharmacology of valproate: a review after 35 years of clinical use for the treatment of epilepsy. *CNS Drugs* 16, 669–694. doi: 10.2165/00023210-200216100-00003

Mali, P., Yang, L., Esvelt, K. M., Aach, J., Guell, M., DiCarlo, J. E., et al. (2013). RNA-guided human genome engineering via Cas9. *Science* 339, 823–826. doi: 10.1126/science.1232033

Mathur, P., and Guo, S. (2010). Use of zebrafish as a model to understand mechanisms of addiction and complex neurobehavioral phenotypes. *Neurobiol. Dis.* 40, 66–72. doi: 10.1016/j.nbd.2010.05.016

Meador, K. J., Baker, G. A., Browning, N., Cohen, M. J., Bromley, R. L., Clayton-Smith, J., et al. (2013). Fetal antiepileptic drug exposure and cognitive outcomes at age 6 years (NEAD study): a prospective observational study. *Lancet Neurol.* 12, 244–252. doi: 10.1016/S1474-4422(12)70323-X

Moessner, R., Marshall, C. R., Sutcliffe, J. S., Skaug, J., Pinto, D., Vincent, J., et al. (2007). Contribution of SHANK3 mutations to autism spectrum disorder. *Am. J. Hum. Genet.* 81, 1289–1297. doi: 10.1086/522590

Monteiro, P., and Feng, G. (2017). SHANK proteins: roles at the synapse and in autism spectrum disorder. *Nat. Rev. Neurosci.* 18, 147–157. doi: 10.1038/nrn.2016.183

Muhle, R. A., Reed, H. E., Stratigos, K. A., and Veenstra-VanderWeele, J. (2018). The emerging clinical neuroscience of autism spectrum disorder: a review. *JAMA Psychiatry* 75, 514–523. doi: 10.1001/jamapsychiatry.2017.4685

Nicolini, C., and Fahnestock, M. (2018). The valproic acid-induced rodent model of autism. *Exp. Neurol.* 299, 217–227. doi: 10.1016/j.expneurol.2017.04.017

Owens, M. J., and Nemeroff, C. B. (2003). Pharmacology of valproate. *Psychopharmacol. Bull.* 37(Suppl. 2), 17–24. doi: 10.2165/00023210-200216100-200216103

Peca, J., Feliciano, C., Ting, J. T., Wang, W., Wells, M. F., Venkatraman, T. N., et al. (2011). Shank3 mutant mice display autistic-like behaviours and striatal dysfunction. *Nature* 472, 437–442. doi: 10.1038/nature09965

Penagarikano, O., Lazaro, M. T., Lu, X. H., Gordon, A., Dong, H., and Lam, H. A. (2015). Exogenous and evoked oxytocin restores social behavior in the Cntnap2 mouse model of autism. *Sci. Transl. Med.* 7, 271r–278r. doi: 10.1126/scitranslmed.3010257

Perathoner, S., Cordero-Maldonado, M. L., and Crawford, A. D. (2016). Potential of zebrafish as a model for exploring the role of the amygdala in emotional memory and motivational behavior. *J. Neurosci. Res.* 94, 445–462. doi: 10.1002/jnr.23712

Phelan, K., and McDermid, H. E. (2012). The 22q13.3 deletion syndrome (Phelan-McDermid Syndrome). *Mol. Syndromol.* 2, 186–201. doi: 10.1159/000334260

Phelan, K., Rogers, R. C., and Boccuto, L. (1993). *Phelan-McDermid Syndrome*. Seattle (WA): University of Washington.

Phelan, M. C. (2008). Deletion 22q13.3 syndrome. *Orphanet J. Rare Dis.* 3:14. doi: 10.1186/1750-1172-3-14

Phiel, C. J., Zhang, F., Huang, E. Y., Guenther, M. G., Lazar, M. A., and Klein, P. S. (2001). Histone deacetylase is a direct target of valproic acid, a potent anticonvulsant, mood stabilizer, and teratogen. *J. Biol. Chem.* 276, 36734–36741. doi: 10.1074/jbc.M101287200

Qin, L., Ma, K., Wang, Z. J., Hu, Z., Matas, E., Wei, J., et al. (2018). Social deficits in Shank3-deficient mouse models of autism are rescued by histone deacetylase (HDAC) inhibition. *Nat. Neurosci.* 21, 564–575. doi: 10.1038/s41593-018-0110-118

Rice, D., and Barone, S. J. (2000). Critical periods of vulnerability for the developing nervous system: evidence from humans and animal models. *Environ. Health Perspect* 108(Suppl. 3), 511–533. doi: 10.1289/ehp.00108s3511

Rinaldi, T., Kulangara, K., Antoniello, K., and Markram, H. (2007). Elevated NMDA receptor levels and enhanced postsynaptic long-term potentiation induced by prenatal exposure to valproic acid. *Proc. Natl. Acad. Sci. U S A.* 104, 13501–13506. doi: 10.1073/pnas.0704391104

Sandbank, M., Bottema-Beutel, K., and Woynaroski, T. (2020). Intervention recommendations for children with autism in light of a changing evidence base. *JAMA Pediatr.* 175, 341–342. doi: 10.1001/jamapediatrics.2020.4730

Sarasua, S. M., Dwivedi, A., Boccuto, L., Rollins, J. D., Chen, C. F., Rogers, R. C., et al. (2011). Association between deletion size and important phenotypes expands the genomic region of interest in Phelan-McDermid syndrome (22q13 deletion syndrome). *J. Med. Genet.* 48, 761–766. doi: 10.1136/jmedgenet-2011-100225

Tu, J. C., Xiao, B., Naisbitt, S., Yuan, J. P., Petralia, R. S., Brakeman, P., et al. (1999). Coupling of mGluR/Homer and PSD-95 complexes by the Shank family of postsynaptic density proteins. *Neuron* 23, 583–592. doi: 10.1016/s0896-6273(00)80810-80817

Tu, Z., Zhao, H., Li, B., Yan, S., Wang, L., Tang, Y., et al. (2019). CRISPR/Cas9-mediated disruption of SHANK3 in monkey leads to drug-treatable autism-like symptoms. *Hum. Mol. Genet.* 28, 561–571. doi: 10.1093/hmg/ddy367

Verpelli, C., and Sala, C. (2012). Molecular and synaptic defects in intellectual disability syndromes. *Curr. Opin. Neurobiol.* 22, 530–536. doi: 10.1016/j.conb.2011.09.007

Vicidomini, C., Ponzoni, L., Lim, D., Schmeisser, M. J., Reim, D., Morello, N., et al. (2017). Pharmacological enhancement of mGlu5 receptors rescues behavioral deficits in SHANK3 knock-out mice. *Mol. Psychiatry* 22:784. doi: 10.1038/mp.2016.70

Wang, X., Bey, A. L., Chung, L., Krystal, A. D., and Jiang, Y. H. (2014a). Therapeutic approaches for shankopathies. *Dev. Neurobiol.* 74, 123–135. doi: 10.1002/dneu.22084

Wang, X., Bey, A. L., Katz, B. M., Badea, A., Kim, N., David, L. K., et al. (2016). Altered mGluR5-Homer scaffolds and corticostriatal connectivity in a Shank3 complete knockout model of autism. *Nat. Commun.* 7:11459. doi: 10.1038/ncomms11459

Wang, X., McCoy, P. A., Rodriguiz, R. M., Pan, Y., Je, H. S., Roberts, A. C., et al. (2011). Synaptic dysfunction and abnormal behaviors in mice lacking major isoforms of Shank3. *Hum. Mol. Genet.* 20, 3093–3108. doi: 10.1093/hmg/ddr212

Wang, X., Xu, Q., Bey, A. L., Lee, Y., and Jiang, Y. H. (2014b). Transcriptional and functional complexity of Shank3 provides a molecular framework to understand the phenotypic heterogeneity of SHANK3 causing autism and Shank3 mutant mice. *Mol. Autism* 5:30. doi: 10.1186/2040-2392-5-30

Weitlauf, A. S., McPheeters, M. L., Peters, B., Sathe, N., Travis, R., Aiello, R., et al. (2014). *Therapies for Children With Autism Spectrum Disorder: Behavioral Interventions Update*. Rockville, MD: Agency for Healthcare Research and Quality.

Wilson, H. L., Wong, A. C., Shaw, S. R., Tse, W. Y., Stapleton, G. A., Phelan, M. C., et al. (2003). Molecular characterisation of the 22q13 deletion syndrome supports the role of haploinsufficiency of SHANK3/PROSAP2 in the major neurological symptoms. *J. Med. Genet.* 40, 575–584. doi: 10.1136/jmg.40.8.575

Wu, S., Gan, G., Zhang, Z., Sun, J., Wang, Q., Gao, Z., et al. (2017). A presynaptic function of Shank protein in *Drosophila*. *J. Neurosci.* 37, 11592–11604. doi: 10.1523/JNEUROSCI.0893-17.2017

Zanatta, G., Sula, A., Miles, A. J., Ng, L., Torella, R., Pryde, D. C., et al. (2019). Valproic acid interactions with the NavMs voltage-gated sodium channel. *Proc. Natl. Acad. Sci. U S A.* 116, 26549–26554. doi: 10.1073/pnas.1909696116

Zhou, Y., Sharma, J., Ke, Q., Landman, R., Yuan, J., Chen, H., et al. (2019). Atypical behaviour and connectivity in SHANK3-mutant macaques. *Nature* 570, 326–331. doi: 10.1038/s41586-019-1278-1270

Zwanenburg, R. J., Ruiter, S. A., van den Heuvel, E. R., Flapper, B. C., and Van Ravenswaaij-Arts, C. M. (2016). Developmental phenotype in Phelan-McDermid (22q13.3 deletion) syndrome: a systematic and prospective study in 34 children. *J. Neurodev. Disord.* 8:16. doi: 10.1186/s11689-016-9150-9150

Conflict of Interest: The authors declare that the research was conducted in the absence of any commercial or financial relationships that could be construed as a potential conflict of interest.

Publisher's Note: All claims expressed in this article are solely those of the authors and do not necessarily represent those of their affiliated organizations, or those of the publisher, the editors and the reviewers. Any product that may be evaluated in this article, or claim that may be made by its manufacturer, is not guaranteed or endorsed by the publisher.

frontiers in Neuroscience

ORIGINAL RESEARCH
published: 29 September 2021
doi: 10.3389/fnins.2021.648143

Dynamic Functional Connectivity Reveals Abnormal Variability in the Amygdala Subregions of Children With Attention-Deficit/Hyperactivity Disorder

Yue Yang, Binrang Yang, Linlin Zhang, Gang Peng and Diangang Fang*

Children's Healthcare & Mental Health Center, Shenzhen Children's Hospital, Shenzhen, China

Objective: This study investigates whether the dynamic functional connectivity (dFC) of the amygdala subregions is altered in children with attention-deficit/hyperactivity disorder (ADHD).

Methods: The dFC of the amygdala subregions was systematically calculated using a sliding time window method, for 75 children with ADHD and 20 healthy control (HC) children.

Results: Compared with the HC group, the right superficial amygdala exhibited significantly higher dFC with the right prefrontal cortex, the left precuneus, and the left post-central gyrus for children in the ADHD group. The dFC of the amygdala subregions showed a negative association with the cognitive functions of children in the ADHD group.

Conclusion: Functional connectivity of the amygdala subregions is more unstable among children with ADHD. In demonstrating an association between the stability of functional connectivity of the amygdala and cognitive functions, this study may contribute by providing a new direction for investigating the internal mechanism of ADHD.

Keywords: ADHD, dynamic functional connectivity, anxiety, amygdala, rs-fMRI

OPEN ACCESS

Edited by:
Li Sun,
Peking University Sixth Hospital, China

Reviewed by:
Ya Wang,
Institute of Psychology, Chinese Academy of Sciences (CAS), China
Fei Li,
Shanghai Jiao Tong University, China
Lane Strathearn,
The University of Iowa, United States

****Correspondence:***
Binrang Yang
ybinrang@126.com

Specialty section:
This article was submitted to Neurodevelopment, a section of the journal Frontiers in Neuroscience

Received: *31 December 2020*
Accepted: *06 September 2021*
Published: *29 September 2021*

Citation:
Yang Y, Yang B, Zhang L, Peng G and Fang D (2021) Dynamic Functional Connectivity Reveals Abnormal Variability in the Amygdala Subregions of Children With Attention-Deficit/Hyperactivity Disorder. Front. Neurosci. 15:648143. doi: 10.3389/fnins.2021.648143

INTRODUCTION

Globally, nearly 1 in 20 youth suffers from attention-deficit/hyperactivity disorder (ADHD), making it one of the most prevalent psychiatric disorders among children (Polanczyk et al., 2007; Polanczyk et al., 2014). Inattention, hyperactivity, and impulsivity are the three recognized core symptoms of ADHD (American Psychiatric Association, 2013); however, research deems these

Abbreviations: ADHD, attention-deficit/hyperactivity disorder; BLA, basolateral amygdala; BOLD, blood oxygen level-dependent; CMA; centromedial amygdala; dFC, dynamic functional connectivity; DPABI, Data Processing and Analysis of Brain Imaging; FC, functional connectivity; FD, framewise displacement; FSIQ, full-scale intelligence quotient; HC, health control; K-SADS-PL, Schizophrenia for School-Aged Children Present and Lifetime Version; IS, interference score; PFC, prefrontal cortex; ROIs, regions of interest; rs-fMRI, Resting-state functional magnetic resonance imaging; SFA, superficial amygdala; TR, repetition time.

symptoms inadequate to explain the functional impairment of children (Anastopoulos et al., 2011; Skirrow and Asherson, 2013; Szuromi et al., 2013). Research on school-age children revealed that most children with ADHD have psychiatric comorbidities that worsen functional impairments (Cuffe et al., 2020). This condition includes markedly elevated rates of anxiety disorders, with common features such as excessive fear, anxiety, and avoidance behavior.

Studies on anxiety over the last few decades have further clarified the impairment associated with ADHD (Prevatt et al., 2015; Overgaard et al., 2016; D'Agati et al., 2019). Abundant evidence suggests that people with ADHD have elevated levels of anxiety. For instance, researchers found that up to 25% of children with ADHD have comorbid anxiety disorders (Wolraich et al., 2005). O'Rourke et al. (2020) believe that people with ADHD are at a greater risk of having anxiety symptoms and its associated features than people without ADHD. Similarly, Gau et al. (2010) noticed that children and adolescents with persistent ADHD have a higher risk of developing anxiety disorders than those without persistent ADHD. People suffering from ADHD and with high levels of anxiety have demonstrated significantly different performances than individuals with pure ADHD in terms of working memory deficits, symptoms of impulsivity, and cognitive efficiency (Schatz and Rostain, 2006; Sorensen et al., 2011; Prevatt et al., 2015). For example, a recent meta-analysis suggested that patients with both ADHD and an anxiety disorder had better response inhibition, compared with individuals afflicted only with ADHD (Maric et al., 2018). March et al. (2000) found that children with ADHD and anxiety exhibited more symptoms of inattentiveness than impulsivity. In a recent study, the researchers found that adolescents with higher trait anxiety performed better on indices of sustained attention, reaction time, and motor variability among people with ADHD but not among those without ADHD (Ruf et al., 2017).

It is important to study the complex mechanisms underlying ADHD, together with the functional impairments of the diseased brain, to ensure effective diagnosis, treatment, and prevention. Resting-state functional magnetic resonance imaging (rs-fMRI) is a safe and non-invasive tool that can detect spontaneous activity in the brain (Bin et al., 2018).The amygdala, which can respond to a wide range of emotional stimuli in time, has long been considered a critical component of emotional processing (Aghajani et al., 2014; Fox et al., 2015). In the study of pediatric anxiety, the amygdala is also the most frequently examined region of interest (ROI) (Hamm et al., 2014). The association between the functional connectivity (FC) of the amygdala and elevated anxiety levels has been identified in numerous clinical populations via this technology (Gold et al., 2016; Jalbrzikowski et al., 2017; Porta-Casteras et al., 2020). For example, Jalbrzikowski et al. (2017) specified that increased FC based on the centromedial amygdala (CMA)–rostral anterior cingulate cortex is associated with greater anxiety symptoms during early adulthood, whereas increased structural connectivity in the CMA–anterior ventromedial prefrontal cortex (PFC) white matter is associated with greater anxiety during late childhood (Jalbrzikowski et al., 2017). In another study involving children aged 7 to 9 years, researchers found that high childhood anxiety is associated with abnormal function and volume of the amygdala (Qin et al., 2014). The amygdala has also been found to contribute to cognitive functions such as working memory and executive functions (Schaefer et al., 2006; Schaefer and Gray, 2007). Previous studies have proven that the amygdala of patients with ADHD is significantly abnormal in terms of function and volume compared with those of normal people (Yu et al., 2016; Tajima-Pozo et al., 2018). Hence, the relationship among the amygdala, anxiety, and cognitive functions may provide essential insights into the psychopathology of ADHD. However, the amygdala is a complex structure and may functionally segregate into several subregions (Han et al., 2014). According to an rs-fMRI study, the FC patterns of each of the amygdala subregions in healthy humans is distinctive (Roy et al., 2009). Thus far, there have been few similar studies on children with ADHD.

Reliance on the implicit assumption that participants' brain activity remained static throughout the rs-fMRI scan was a common feature of many previously mentioned studies. However, a growing body of research confirms that brain activity changes dynamically over time (Yao et al., 2017; Liao et al., 2019; Li et al., 2019). Most rs-fMRI studies in the ADHD domain currently focus on the characteristics of the static state of brain activity but fail to demonstrate the dynamic temporal changes in spontaneous brain activity among humans. Using the sliding window approach, researchers have inspected the dynamic mechanisms of voluntary brain activity in humans (Voytek and Knight, 2015) and non-human primates (Hutchison et al., 2013). The abnormalities concerning the variance of dynamic FC (dFC) in patients with common neuropsychiatric diseases, such as schizophrenia (Guo et al., 2018), Alzheimer's disease (Gu et al., 2020), major depressive disorders (Yao et al., 2019), and autism spectrum disorder (Li et al., 2020), have been effectively revealed by the sliding window method. These studies suggest that changes in dFC may be biological markers of specific diseases. In this approach, a fixed-length time window is selected and used to calculate the FC metric. The window then slides to the next time window after a predetermined duration, leading to many FC metrics that can elucidate the temporal features of FC over the entire duration of the scan (Yue et al., 2018). By calculating the time-varying covariance of interregional neural signals, dFC can describe precisely the collaboration of brain regions; that is, the higher the value of the dFC, the more unstable the FC (Yao et al., 2017). Therefore, further investigation of the overall dFC between brain regions may be necessary. In this regard, several studies have found abnormal dFC in ADHD patients. For example, a recent study found that patients with ADHD had significantly changed dFC of the cingulo-opercular network and sensorimotor network (Sun et al., 2021). Another research reported that the default-mode and task-positive networks in people with ADHD exhibit a quasi-periodic clustering recurrence pattern during the entire rs-fMRI scan, suggesting that dFC alterations in people with ADHD may be a neuroimaging marker for ADHD (Kaboodvand et al., 2020). However, no systematic study on the dynamic characteristics of abnormal amygdala-related neural networks in people with ADHD has emerged thus far.

To address this gap, we first used the sliding window method to study the abnormal dFC of the amygdala subregions of children with ADHD, specifically focusing on anxiety symptoms and cognitive functions, and further studied the relationship between the dFC of the amygdala subregions and anxiety symptoms and cognitive functions. Based on previous studies, we hypothesized that (1) higher dFCs of the amygdala subregions can be observed in children with ADHD; (2) higher dFC is positively associated with anxiety symptoms among children with ADHD; and (3) higher dFC is negatively associated with the cognitive functions of children with ADHD.

MATERIALS AND METHODS

Participants

In total, 76 drug-naive ADHD boys aged 8 to 10 years were recruited from Shenzhen Children's Hospital. All patients were interviewed by two experienced psychiatrists, fulfilling the diagnostic criteria for ADHD based on clinical interviews that follow the *Diagnostic and Statistical Manual of Mental Disorders, Fourth Edition*. The Schedule for Affective Disorder and Schizophrenia for School-Aged Children Present and Lifetime Version (K-SADS-PL) was used to interview the participants and their parents (Kaufman et al., 1997). Meanwhile, 20 boys aged 8 to 10 years were recruited from the Children's Health Care Department of the same hospital for the healthy control (HC) group. Children in this group, together with their parents, were also interviewed using the K-SADS-PL to ensure that they did not meet the diagnosis of ADHD or any other mental disorders. Notably, all participants were Han Chinese.

The inclusion criteria also included normal vision and hearing and a Full-Scale Intelligence Quotient (FSIQ) $\geq$ 70 estimated by the Wechsler Intelligence Scale for Children, Fourth Edition. Participants who currently or previously had psychological disorders or who had serious physical disorders, neurological disorders, or brain injuries were excluded from this study. This study was approved by the Medical Research Ethics Committee of the Shenzhen Children's Hospital. All children agreed to participate, and written informed consent was obtained from their parents.

Measures of Anxiety Symptoms

Conner's Parent Rating Scale (Conners et al., 1998) is a widely used scale for screening children's behavioral problems, especially ADHD, and comprises items that assess anxiety. The scale's Chinese version has good reliability and validity and is used to evaluate children between 3 and 16 years old (Conners et al., 1998). This scale constitutes five factors: behavioral problems, learning problems, psychosomatic disorders, hyperactivity impulse, and anxiety. This study chose four items to assess the anxiety symptoms of children, namely, "fear of new environments, places, new people, and going to school," being "more afraid of loneliness, illness, or death than others," "bashfulness," and having a "feeling that he or she is threatened frequently." The questionnaire, which was completed by the parents according to their observations of their child, adopted a four-level scoring method (0, 1, 2, and 3).

Cognitive Measures

The neuropsychological test battery consisted of the Stroop color-word and N-back tests. The two tests were considered representative of two areas of cognitive function: response inhibition and working memory.

The Stroop test, translated from the Victorian version (Lee and Chan, 2010), consists of three cards printed with colors, representing color, word, and color–word tasks. The color task consists of colored dots; the word task comprises ordinary words that are unrelated to the meaning of color; the color–word task consists of words written in color that indicate the meaning of the color, but the color of these words differ from the meaning of the word itself. All these tasks require participants to read the color of dots or words and the researcher to record the time it takes participants to read through each card and the number of mistakes they make. Interference control ability is represented by the interference score (IS), that is, the time taken to complete the color–word task minus the time taken to complete the word–word task, or the number of errors made in the color–word task minus the number of errors made in the word–word task.

The N-back task consists of three subtasks, namely, 0-back, 1-back, and 2-back tasks. The 0-back task requires participants to press the left mouse button when a gray square appears at the top left of the central fixation (" + ") and to press the right mouse button when the square appears at the top right or right bottom of central fixation (" + "). The 1-back (2-back) task requires participants to identify whether the orientation of the X square displayed on the screen is the same as that of the X-1 (X-2) square. If the orientation is the same, they press the right mouse button; otherwise, they press the left button.

rs-fMRI Data Acquisition

The rs-fMRI data for all participants were obtained using a 3.0-T system scanner (Siemens Magnetom Skyra), and all participants were instructed to close their eyes, relax, stay awake, and try not to move their head during the scan. Participants were checked after the scan to ensure that they remained awake during the procedure. The rs-fMRI data were obtained using an echo-planar imaging sequence with the following parameters: repetition time (TR) = 2,000 ms; echo time = 30 ms; flip angle = 90°; field of view = 220 × 220 mm^2; matrix size = 94 × 94; 32 axial slices; and slice thickness = 3 mm and 130 volumes.

Preprocessing

rs-fMRI data preprocessing was performed using the Data Processing and Analysis of Brain Imaging (DPABI) toolbox (http://rfmri.org/dpabi; Yan et al., 2016). The first 10 volumes were discarded to allow the machine to reach magnetization equilibrium and enable participants to adapt to the MRI scanning environment. The remaining volumes were processed based on the following steps: slice timing, head motion correction, normalization to a Montreal Neurological Institute template via the gray matter segment, and resampling to isotropic 3-mm voxels. Multiple nuisance covariates (i.e., the estimated motion

parameters based on the Friston-24 model (Friston et al., 1996), the linear drift, the white matter signal, and the cerebrospinal fluid signal) were regressed out from the data. Finally, the rs-fMRI time series were temporal bandpass filtered ($0.01 < f < 0.10$ Hz).

Head Motion

Following Jenkinson's relative root-mean-square algorithm (Jenkinson et al., 2002), the mean framewise displacement (FD) generated during the scanning process was excluded. Notably, the participant was excluded if the mean FD exceeded 0.2 mm. Based on this criterion, one participant was excluded, and the study had a final total sample of 75 ADHD and 20 HC children. We used mean FD as a covariable in the subsequent statistical analysis to further reduce the impact of head movement on the findings.

Dynamic Functional Connectivity Analysis

To examine whole-brain dFC, using a seed method based on the anatomical ROIs, we used six previously validated seed ROIs in the bilateral amygdala (Zimmermann et al., 2018). These regions were divided into the basolateral amygdala (BLA), CMA, and superficial amygdala (SFA; radius = 6 mm; the detailed coordinates of each seed are provided in **Supplementary Table S1**). The mean blood oxygen level–dependent (BOLD) time series of each seed region was extracted from the rs-fMRI data of each participant (Chao-Gan and Yu-Feng, 2010) and correlated with the BOLD time series of each voxel in the brain to generate six three-dimensional dFC maps.

A sliding window method was used in this study to formulate dFC maps for each participant. This method can elucidate the temporal features of FC over the entire duration of the scan and calculate the time-varying covariance of interregional neural signals, which is the variance of dFC. The window length is a key parameter based on the sliding window method. According to Leonardi and van de Ville (2015), the minimum window length should not be less than $1/f_{\min}$ because a very short window length may cause spurious fluctuations. Additionally, the $f_{\min}$ denotes the minimum frequency of the time courses. Conversely, if a window length is too long, the dynamic characteristics of the time series would be rendered unobservable. Hence, we decided to use a Hamming window with a width of 50 TRs (100S) and a step of 1 TR. Moreover, the entire rs-fMRI time series was segmented into 71 windows for each participant. The resting-state r value matrix was obtained by computing the partial correlation coefficients, and the z value matrix was obtained via Fisher-z transformation. Before the statistical analyses, the result maps were smoothed out with a 4-mm full-width at the half-maximum Gaussian kernel. Furthermore, to exclude the influence of window width on the results, the window width was set as 32/64 TR to repeat the calculations. The results were similar with the results of the 50TR and are detailed in the **Supplementary Materials Figure S1**.

Statistical Analyses

The Statistical Package for the Social Sciences 21.0 was used to analyze the demographic and clinical data. A two-sample t test was used to evaluate differences in age, grade, FSIQ, mean FD, anxiety scores, and cognitive scores between the ADHD and HC groups. Moreover, dFC maps were analyzed using the two-sample t test based on DPABI to distinguish dynamic changes in FC between the two groups. Previous studies based on rs-fMRI have shown that FC in the brain is significantly associated with intelligence (Song et al., 2008; Pamplona et al., 2015). Therefore, we included the FSIQ as a covariate, in addition to mean FD and age. The Gaussian random field theory was applied for multiple comparison corrections (two-tailed, voxel $p < 0.001$, cluster $p < 0.05$) in DPABI (Yan et al., 2016). Furthermore, we conducted partial correlation analyses between anxiety scores/cognitive scores and dFC, which showed significant difference between the groups in the two-sample t test, while using mean FD, age, and FSIQ as covariates, to examine the association between the dFC of the amygdala subregions and the anxiety symptoms and cognitive functions of children with ADHD. $p < 0.05$ was considered statistically significant. However, the two groups had an imbalanced number of participants, and this may have resulted in low statistical power. To test the reproducibility of this study's results, we selected an equal number of children from the ADHD group as in the control group and rematched the children by age, grade, and FSIQ. The two-sample t tests were performed, and the same statistical method was used.

RESULTS

Demographic Information

Altogether, 75 children with ADHD and 20 HC children were recruited to participate in this study, and their demographic and clinical information is provided in **Table 1**. A comparison between the two groups showed no statistical difference in age, education level, and psychosomatic disorders, whereas

TABLE 1 | The participants' demographic and clinical information.

	ADHD (n = 75)	HC (n = 20)	p values
Age, mean ± SD (y)	8.86 ± 0.58	8.93 ± 0.68	0.75
Grade, mean ± SD	2.88 ± 0.73	2.63 ± 0.77	0.14
FSIQ, mean ± SD	86.07 ± 8.05	95.85 ± 10.20	< 0.01
Mean FD, mean ± SD	0.07 ± 0.03	0.10 ± 0.06	0.01
Anxiety scores, mean ± SD	0.66 ± 0.54	0.14 ± 0.19	< 0.01
Behavioral problems, mean ± SD	1.14 ± 0.51	0.41 ± 0.35	< 0.01
Learning problems, mean ± SD	1.91 ± 0.63	0.57 ± 0.45	< 0.01
Psychosomatic disorders, mean ± SD	0.26 ± 0.31	0.23 ± 0.30	0.71
Hyperactivity–impulse scores, mean ± SD	1.59 ± 0.68	0.39 ± 0.43	< 0.01
IS(time), mean ± SD	19.43 ± 11.46	11.08 ± 4.00	< 0.01
IS(error), mean ± SD	2.22 ± 2.72	1.20 ± 1.61	0.04
Correct rate of working memory, mean ± SD			
0-back	0.87 ± 0.14	0.94 ± 0.08	0.01
1-back	0.63 ± 0.21	0.80 ± 0.17	< 0.01
2-back	0.41 ± 0.15	0.56 ± 0.14	< 0.01

ADHD means attention-deficit/hyperactivity disorder; FD, framewise displacement; FSIQ, Full-Scale Intelligence Quotient; HC, health control; IS, interference score.

significant differences were observed in the mean FD, FSIQ, behavioral problems, learning problems, hyperactivity–impulse scores, anxiety scores, IS, and N-back scores of the two groups. As expected, the FSIQ and the N-back scores of the ADHD group were significantly lower than those of the HC group, whereas their behavioral problems, learning problems, hyperactivity–impulse scores, IS, and anxiety scores were higher.

Group dFC Comparisons

For the patients with ADHD (vs. the HC group), the dFC of the amygdala subregions showed significant differences in some areas, and the right SFA exhibited a significantly higher dFC in the right PFC, the left precuneus, and the left post-central gyrus. However, no regional differences in dFC were found between the children with ADHD and those in the HC group with regard to the bilateral BLA, CMA, and the left SFA. Detailed information is shown in **Figure 1** and **Table 2**. After we rematched the subjects (**Supplementary Materials Table S1**), the results of the group dFC comparisons were slightly different (**Supplementary Materials Figure S2**). However, the dFC between the right SFA and the right PFC for the ADHD group was still higher than that for the HC group.

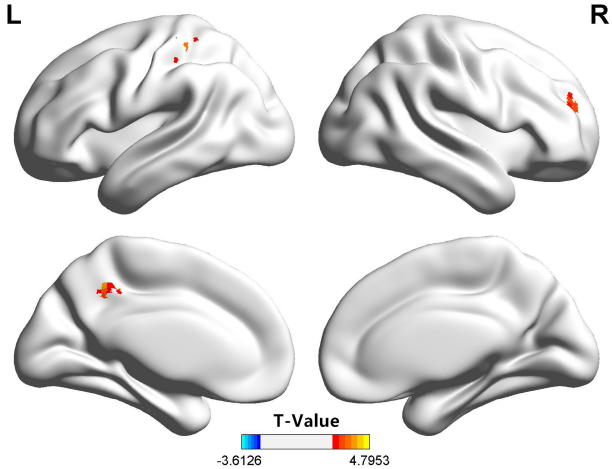

FIGURE 1 | Compared with the HC group, the right SFA of the children in the ADHD group exhibited significantly higher dFC with the right PFC, the left precuneus, and the left post-central gyrus. ADHD, attention-deficit/hyperactivity disorder; dFC, dynamic functional connectivity; HC, health control; PFC, prefrontal cortex; SFA, superficial amygdala.

TABLE 2 | Brain areas with significant dFC differences between children in the ADHD and HC groups.

Regions	Brodmann areas	Voxels size	Peak MNI coordinates			*t* value
			x	*Y*	*z*	
Right PFC	10	45	30	48	24	3.49
Left precuneus	5/7/31	42	−12	−48	45	4.01
Left post-central gyrus	2/3/4	53	−24	−36	48	4.31

ADHD means attention-deficit/hyperactivity disorder; HC, health control; MNI, Montreal Neurological Institute; PFC, prefrontal cortex; SFA, superficial amygdala.

Correlation Analysis

For patients with ADHD, the dFC between the right SFA and the right PFC showed a negative correlation with the 2-back scores (r = -0.234, p = 0.043) and a positive correlation with the IS (error) ($r = -0.247$, $p = 0.041$) (**Figure 2**). However, no significant results were found regarding the anxiety symptoms.

DISCUSSION

To our knowledge, this study is the first to use the dFC method to explore the amygdala subregion network of children with ADHD. We observed that compared with the HC group, the right SFA of the ADHD group showed a higher dFC; this highlights greater temporal variability in FC with the right PFC, the left precuneus, and the left postcentral gyrus. Another key finding is the correlation between the subregion of the amygdala and cognitive functions of patients with ADHD. The dFC of the amygdala subregions showed a specific association with working memory and response inhibition among patients with ADHD. These outcomes suggest that the FC of the amygdala is more unstable among children with ADHD, and the dFC of the amygdala subregion network is related to the cognitive functions of children with ADHD.

Unlike the resting-state FC, the stability of the FC is reflected by the dFC. The findings of this study may provide new insights into the abnormal brain activity of children with ADHD. Previous studies that analyzed the amygdala as a whole failed to recognize its structural complexity. Instead, research demonstrated that different subregions of the amygdala perform different functions (Han et al., 2014). Primarily, BLA is involved in associative learning processes as it receives incoming signals from the cortex and subcortical regions, including the PFC, thalamus, and hippocampus (Roy et al., 2009; Bzdok et al., 2013). Meanwhile, CMA is involved in attention regulation, motor generation, and autonomous emotional responses (Pessoa, 2011; Bzdok et al., 2013), whereas SFA addresses olfactory and reward-related information (Heimer and Van Hoesen, 2006; Bzdok et al., 2013).

In this study, the right SFA of the ADHD group showed a significantly higher FC variability in the right PFC, the left precuneus, and the left post-central gyrus. Previous studies suggested that the PFC is fundamentally involved in mechanisms underlying anxiety (Bishop, 2007; Hare et al., 2008). In the brain, the PFC and amygdala are interconnected and work in concert to control the expression of emotions, such as fear and anxiety (Likhtik et al., 2014). The PFC exerts inhibitory top-down control over amygdala activities under physiological conditions, preventing inappropriate emotional expressions (Rosenkranz et al., 2003). Several studies have shown that the PFC is necessary for the neurobiology of ADHD (Cheng et al., 2017; Chen et al., 2020; Liu et al., 2020). Posner et al. (2011) detected a stronger FC between the amygdala and PFC in adolescents with ADHD. In contrast to previous studies, our study further analyzed the dFC of the amygdala subregion, taking into account its heterogeneity. We analyzed the dFC of the amygdala, and the elevated dFC represented poor stability of FC; this means that

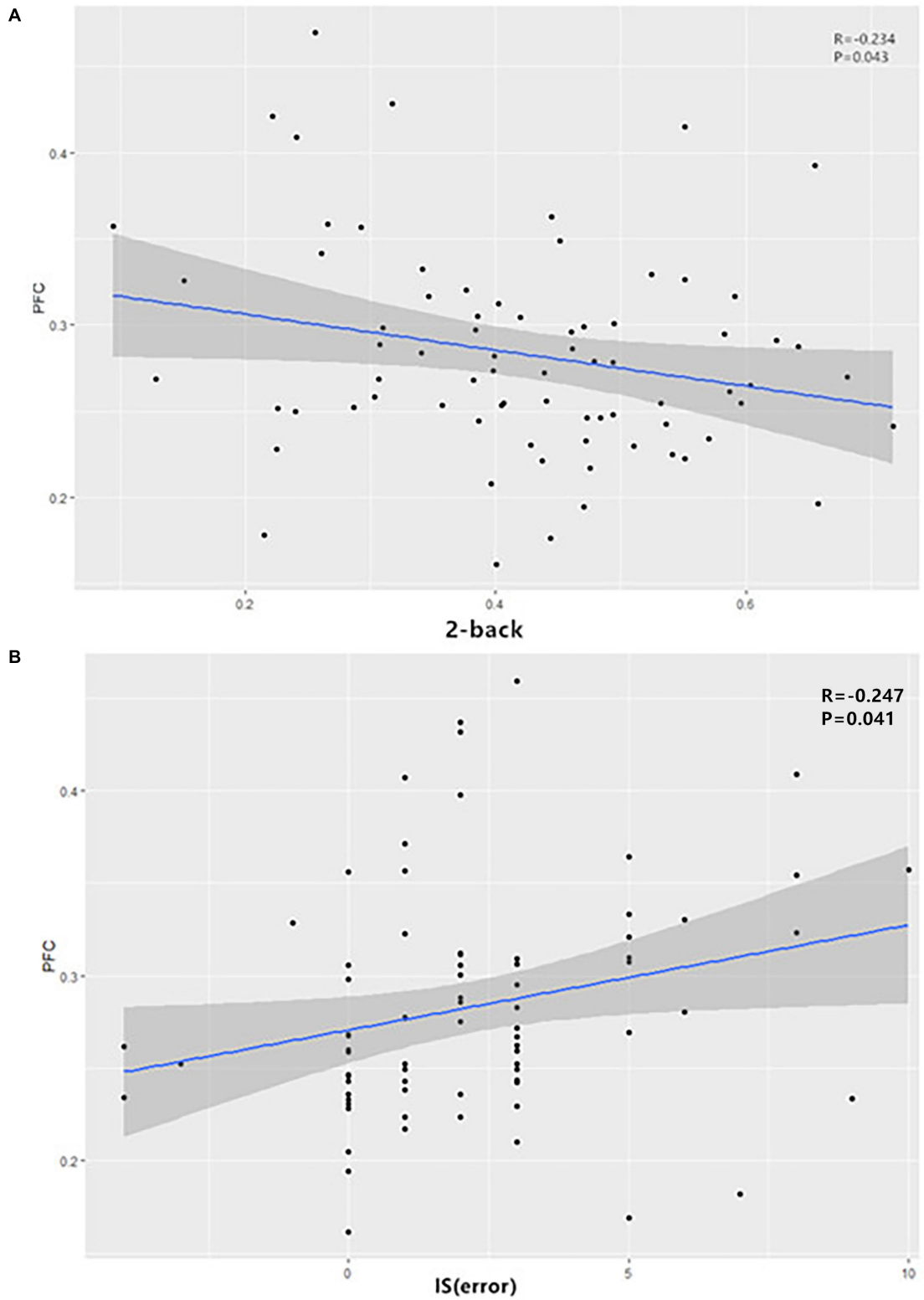

FIGURE 2 | In ADHD patients, the dFC between the right SFA and the right PFC showed **(A)** a negative correlation with the 2-back scores and **(B)** a positive correlation with IS (error). ADHD, attention-deficit/hyperactivity disorder; dFC, dynamic functional connectivity; IS, interference score; SFA, superficial amygdala.

the interaction between the amygdala and PFC is unstable in children with ADHD.

Generally, the precuneus belongs to the parietal lobe, which is involved in a variety of complex functions and is critical for emotion processing (Cavanna and Trimble, 2006), mediation of subjective happiness, and somatomotor processing (Sato et al., 2015). The amygdala is involved in several of these functions, including emotional processing. The results obtained in our study, along with the proven psychological functions of these regions, suggest that the unstable functional connection between the amygdala and the parietal lobe may be a potential cause of ADHD. A survey of adolescents with ADHD signified that there was significantly less activation in the parietal lobe when these adolescents were asked to perform a mental rotation task that required spatial working memory; this may indicate parietal dysfunction in patients with ADHD (Vance et al., 2007). Hale et al. (2015) believe that parietal electroencephalogram asymmetry is associated with mood and anxiety disorders. However, in our study, we did not find a relationship between anxiety symptoms and brain regions. This may be because (1) in this study, the factors from Conner's Parent Rating Scale were used to represent anxiety symptoms, which had no correlation with the three brain regions; and (2) the sample size of this study is relatively small.

This study also finds a relationship between the dFC of the amygdala subregions and the cognitive functions of patients with ADHD. Specifically, for patients with ADHD, the dFC between the right SFA and the right PFC showed a negative correlation with the 2-back scores and a positive correlation with the IS (error). This means that the more unstable the functional connection between SFA and PFC, the worse the cognitive function of patients with ADHD. Halperin and Schulz (2006) believe that the structure and function of the PFC are intimately involved in the manifestation of ADHD symptoms. A previous study found a reduced activation in the left PFC of children with ADHD during an inhibition task (Miao et al., 2017). Among people with ADHD, an increasing number of studies have shown that there are functional changes in the PFC. For example, a study found that young people with ADHD show decreased FC of the left dorsolateral PFC for high-load visuospatial working memory (Bedard et al., 2014). Another study found that a higher brain signal variability in the medial prefrontal areas is related to overall ADHD symptom severity and inattention across children with an ADHD diagnosis (Nomi et al., 2018), which is consistent with our findings. However, a previous study showed that increased brain signal variability is associated with improved task performance (Garrett et al., 2013). This contradicts our results and might be explained by the Yerkes–Dodson curve. There is an optimal value for brain functioning. It is possible that the signal variability in the PFC of people with ADHD exceeds this optimal value and thus appears to impair cognitive performance.

This study's outcomes should be interpreted with caution because of the following limitations. First, the scanning time was relatively short, which might reduce the reliability of the rs-fMRI data. Each participant underwent an rs-fMRI scan for 260 s, whereas similar studies were typically performed for 5 to 8 min (Yu et al., 2016). Second, several methods, with unverified consistencies, have been proposed to calculate the dFC. However, this study used the sliding time window method only to explore the differences in the amygdala subregion network of children with ADHD. Various methods can be used to confirm the results of this study in future work. Third, the number of participants in the two groups was imbalanced, and the sample size of this study was relatively small, resulting in low statistical power. This disparity arose because of (1) the difficulty of recruiting participants who were willing to provide experimental data and (2) the use of stringent inclusion and exclusion criteria. Randomized controlled trials with larger sample sizes are warranted in the future to verify the findings of this study.

Despite these limitations, the following two advantages enhance the reliability of the results. Previous studies have outlined that stimulants can change the brain structure and function of patients with ADHD (An et al., 2013; Querne et al., 2017; Walhovd et al., 2020) and the dose of the stimulant correlates with the size of the amygdala (Becker et al., 2015). The participants selected for this study were not on any stimulants. Furthermore, researchers confirmed differences in FC among children with ADHD belonging to different age groups (Tang et al., 2018). This study minimized the confounding effect of age by including children between 8 and 10 years old and controlling for the participants' ages in the statistical analysis.

In summary, we investigated the dynamic variability of amygdala-based FC and its association with anxiety symptoms and the cognitive function of children with ADHD. The results of this study suggest that the dFC of the amygdala subregion of children with ADHD is significantly different from that of healthy children, and higher dFCs are negatively associated with the cognitive functions of children with ADHD. In demonstrating an association between the variability of amygdala FC and cognitive functions, this study may contribute by providing a new direction for studying the internal mechanism of ADHD.

DATA AVAILABILITY STATEMENT

The raw data supporting the conclusions of this article will be made available by the authors, without undue reservation.

ETHICS STATEMENT

The studies involving human participants were reviewed and approved by Medical Research Ethics Committee of Shenzhen Children's Hospital. Written informed consent to participate in this study was provided by the participants' legal guardian/next of kin.

AUTHOR CONTRIBUTIONS

YY and BY: conceptualization. LZ and DF: methodology and investigation. YY, BY, and GP: validation. YY and GP: formal analysis. BY and GP: resources and writing—review and editing. YY and DF: data curation. YY, LZ, and GP: writing—original draft preparation. BY: project administration and funding acquisition. All authors discussed the results and reviewed the manuscript.

FUNDING

This study was supported by the Natural Science Foundation of China (Grant No. 81271512) and the Sanming Project of Medicine in Shenzhen (SZSM 201612036).

ACKNOWLEDGMENTS

We would like to thank all the participants in the present study.

SUPPLEMENTARY MATERIAL

The Supplementary Material for this article can be found online at: https://www.frontiersin.org/articles/10.3389/fnins.2021.648143/full#supplementary-material

Supplementary Figure S1 | Brain areas with significant dFC differences between children in the ADHD and HC groups (the window width was set as 32/64 TR). ADHD, attention-deficit/hyperactivity disorder; HC, health control; TR, repetition time.

REFERENCES

Aghajani, M., Veer, I. M., van Tol, M. J., Aleman, A., van Buchem, M. A., Veltman, D. J., et al. (2014). Neuroticism and extraversion are associated with amygdala resting-state functional connectivity. *Cogn. Affect. Behav. Neurosci.* 14, 836–848.

American Psychiatric Association (2013). *Diagnostic and Statistical Manual of Mental Disorders (DSM-5®)*. Washington, DC: American Psychiatric Publishing.

An, L., Cao, X.-H., Cao, Q.-J., Sun, L., Yang, L., Zou, Q.-H., et al. (2013). Methylphenidate normalizes resting-state brain dysfunction in boys with attention deficit hyperactivity disorder. *Neuropsychopharmacology* 38, 1287–1295. doi: 10.1038/npp.2013.27

Anastopoulos, A. D., Smith, T. F., Garrett, M. E., Morrissey-Kane, E., Schatz, N. K., Sommer, J. L., et al. (2011). Self-regulation of emotion, functional impairment, and comorbidity among childrenWith AD/HD. *J. Atten. Disord.* 15, 583–592. doi: 10.1177/1087054710370567

Becker, B., Wagner, D., Koester, P., Tittgemeyer, M., Mercer-Chalmers-Bender, K., Hurlemann, R., et al. (2015). Smaller amygdala and medial prefrontal cortex predict escalating stimulant use. *Brain* 138, 2074–2086. doi: 10.1093/brain/awv113

Bedard, A. C., Newcorn, J. H., Clerkin, S. M., Krone, B., Fan, J., Halperin, J. M., et al. (2014). Reduced prefrontal efficiency for visuospatial working memory in attention-deficit/hyperactivity disorder. *J. Am. Acad. Child. Adolesc. Psychiatry* 53, 1020–1030. doi: 10.1016/j.jaac.2014.05.011

Bin, L., Xiao, C., Le, L., Yangqian, S., Ningxuan, C., Ting, M., et al. (2018). Aberrant dynamics of spontaneous brain activity and its integration in patients with autism spectrum disorder. *Chin. Sci. Bull.* 63, 1452–1463.

Bishop, S. J. (2007). Neurocognitive mechanisms of anxiety: an integrative account. *Trends Cogn. Sci.* 11, 307–316. doi: 10.1016/j.tics.2007.05.008

Bzdok, D., Laird, A. R., Zilles, K., Fox, P. T., and Eickhoff, S. B. (2013). An investigation of the structural, connectional, and functional subspecialization in the human amygdala. *Hum. Brain. Mapp.* 34, 3247–3266. doi: 10.1002/hbm.22138

Cavanna, A. E., and Trimble, M. R. (2006). The precuneus: a review of its functional anatomy and behavioural correlates. *Brain* 129, 564–583.

Chao-Gan, Y., and Yu-Feng, Z. (2010). DPARSF: a MATLAB toolbox for "pipeline" data analysis of resting-state fMRI. *Front. Syst. Neurosci.* 4:13. doi: 10.3389/fnsys.2010.00013

Chen, T., Yuan, H., Sun, Y. B., Song, Y. C., Lu, M., Ni, X., et al. (2020). Metabolomics study of the prefrontal cortex in a rat model of attention deficit hyperactivity disorder reveals the association between cholesterol metabolism disorder and hyperactive behavior. *Biochem. Biophys. Res. Commun.* 523, 315–321. doi: 10.1016/j.bbrc.2019.12.016

Cheng, J., Liu, A., Shi, M. Y., and Yan, Z. (2017). Disrupted glutamatergic transmission in prefrontal cortex contributes to behavioral abnormality in an animal model of ADHD. *Neuropsychopharmacology* 42, 2096–2104. doi: 10.1038/npp.2017.30

Conners, C. K., Sitarenios, G., Parker, J. D. A., and Epstein, J. N. (1998). The revised Conners' Parent Rating Scale (CPRS-R):factor structure, reliability, and criterion validity. *J. Abnorm. Child. Psychol.* 26, 257–268. doi: 10.1023/a:1022602400621

Cuffe, S. P., Visser, S. N., Holbrook, J. R., Danielson, M. L., Geryk, L. L., Wolraich, M. L., et al. (2020). ADHD and psychiatric comorbidity: functional outcomes in a school-based sample of children. *J. Atten. Disord.* 24, 1345–1354. doi: 10.1177/1087054715613437

D'Agati, E., Curatolo, P., and Mazzone, L. (2019). Comorbidity between ADHD and anxiety disorders across the lifespan. *Int. J. Psychiatry Clin. Pract.* 23, 238–244.

Fox, A. S., Oler, J. A., Tromp do, P. M., Fudge, J. L., and Kalin, N. H. (2015). Extending the amygdala in theories of threat processing. *Trends Neurosci.* 38, 319–329. doi: 10.1016/j.tins.2015.03.002

Friston, K. J., Williams, S., Howard, R., Frackowiak, R. S., and Turner, R. (1996). Movement-related effects in fMRI time-series. *Magn. Reson. Med.* 35, 346–355.

Garrett, D. D., Samanez-Larkin, G. R., MacDonald, S. W., Lindenberger, U., McIntosh, A. R., and Grady, C. L. (2013). Moment-to-moment brain signal variability: a next frontier in human brain mapping? *Neurosci. Biobehav. Rev.* 37, 610–624. doi: 10.1016/j.neubiorev.2013.02.015

Gau, S. S.-F., Ni, H.-C., Shang, C.-Y., Soong, W.-T., Wu, Y.-Y., Lin, L.-Y., et al. (2010). Psychiatric comorbidity among children and adolescents with and without persistent attention-deficit hyperactivity disorder. *Aust. N. Z. J. Psychiatry.* 44, 135–143.

Gold, A. L., Shechner, T., Farber, M. J., Spiro, C. N., Leibenluft, E., Pine, D. S., et al. (2016). Amygdala-cortical connectivity: associations with anxiety, development, and threat. *Depress. Anxiety* 33, 917–926.

Gu, Y., Lin, Y., Huang, L., Ma, J., Zhang, J., Xiao, Y., et al. (2020). Abnormal dynamic functional connectivity in Alzheimer's disease. *CNS Neurosci. Ther.* 26, 962–971.

Guo, S., Zhao, W., Tao, H., Liu, Z., and Palaniyappan, L. (2018). The instability of functional connectivity in patients with schizophrenia and their siblings: a dynamic connectivity study. *Schizophr. Res.* 195, 183–189. doi: 10.1016/j.schres.2017.09.035

Hale, T. S., Wiley, J. F., Smalley, S. L., Tung, K. L., Kaminsky, O., McGough, J. J., et al. (2015). A parietal biomarker for ADHD liability: as predicted by the distributed effects perspective model of ADHD. *Front. Psychiatry* 6:63. doi: 10.3389/fpsyt.2015.00063

Halperin, J. M., and Schulz, K. P. (2006). Revisiting the role of the prefrontal cortex in the pathophysiology of attention-deficit/hyperactivity disorder. *Psychol. Bull.* 132, 560–581.

Hamm, L. L., Jacobs, R. H., Johnson, M. W., Fitzgerald, D. A., Fitzgerald, K. D., Langenecker, S. A., et al. (2014). Aberrant amygdala functional connectivity at rest in pediatric anxiety disorders. *Biol. Mood. Anxiety Disord.* 4:15. doi: 10.1186/s13587-014-0015-4

Han, H. J., Lee, K., Kim, H. T., and Kim, H. (2014). Distinctive amygdala subregions involved in emotion-modulated Stroop interference. *Soc. Cogn. Affect. Neurosci.* 9, 689–698. doi: 10.1093/scan/nst021

Hare, T. A., Tottenham, N., Galvan, A., Voss, H. U., Glover, G. H., and Casey, B. J. (2008). Biological substrates of emotional reactivity and regulation in adolescence during an emotional go-nogo task. *Biol. Psychiatry* 63, 927–934. doi: 10.1016/j.biopsych.2008.03.015

Heimer, L., and Van Hoesen, G. W. (2006). The limbic lobe and its output channels: implications for emotional functions and adaptive behavior. *Neurosci. Biobehav. Rev.* 30, 126–147. doi: 10.1016/j.neubiorev.2005.06.006

Hutchison, R. M., Womelsdorf, T., Gati, J. S., Everling, S., and Menon, R. S. (2013). Resting-state networks show dynamic functional connectivity in awake humans and anesthetized macaques. *Hum. Brain Mapp.* 34, 2154–2177. doi: 10.1002/hbm.22058

Jalbrzikowski, M., Larsen, B., Hallquist, M. N., Foran, W., Calabro, F., and Luna, B. (2017). Development of white matter microstructure and intrinsic functional connectivity between the amygdala and ventromedial prefrontal cortex: associations with anxiety and depression. *Biol. Psychiatry* 82, 511–521. doi: 10.1016/j.biopsych.2017.01.008

Jenkinson, M., Bannister, P., Brady, M., and Smith, S. (2002). Improved optimization for the robust and accurate linear registration and motion correction of brain images. *NeuroImage* 17, 825–841. doi: 10.1016/s1053-8119(02)91132-8

Kaboodvand, N., Iravani, B., and Fransson, P. (2020). Dynamic synergetic configurations of resting-state networks in ADHD. *Neuroimage* 207:116347. doi: 10.1016/j.neuroimage.2019.116347

Kaufman, J., Birmaher, B., Brent, D., Rao, U., Flynn, C., Moreci, P., et al. (1997). Schedule for affective disorders and schizophrenia for school-age children-present and lifetime version (K-SADS-PL): initial reliability and validity data. *J. Am. Acad. Child. Adolesc. Psychiatry* 36, 980–988. doi: 10.1097/00004583-199707000-00021

Lee, T. M. C., and Chan, C. C. H. (2010). Stroop interference in Chinese and English. *J. Clin. Exp. Neuropsychol.* 22, 465–471.

Leonardi, N., and van de Ville, D. (2015). On spurious and real fluctuations of dynamic functional connectivity during rest. *NeuroImage* 104, 430–436. doi: 10.1016/j.neuroimage.2014.09.007

Li, J., Duan, X., Cui, Q., Chen, H., and Liao, W. (2019). More than just statics: temporal dynamics of intrinsic brain activity predicts the suicidal ideation in depressed patients. *Psychol. Med.* 49, 852–860. doi: 10.1017/S0033291718001502

Li, Y., Zhu, Y., Nguchu, B. A., Wang, Y., Wang, H., Qiu, B., et al. (2020). Dynamic functional connectivity reveals abnormal variability and hyper-connected pattern in autism spectrum disorder. *Autism Res.* 13, 230–243. doi: 10.1002/aur.2212

Liao, W., Li, J., Ji, G. J., Wu, G. R., Long, Z., Xu, Q., et al. (2019). Endless fluctuations: temporal dynamics of the amplitude of low frequency fluctuations. *IEEE Trans. Med. Imaging* 38, 2523–2532. doi: 10.1109/TMI.2019.2904555

Likhtik, E., Stujenske, J. M., Topiwala, M. A., Harris, A. Z., and Gordon, J. A. (2014). Prefrontal entrainment of amygdala activity signals safety in learned fear and innate anxiety. *Nat. Neurosci.* 17, 106–113. doi: 10.1038/nn.3582

Liu, L., Zhao, Q., Yu, X., Xu, D., Li, H., Ji, N., et al. (2020). Monoaminergic genetic variants, prefrontal cortex-amygdala circuit, and emotional symptoms in children with ADHD: exploration based on the gene-brain-behavior relationship. *J. Atten. Disord.* 25, 1272–1283. doi: 10.1177/1087054719897838

March, J. S., Swanson, J. M., Arnold, L. E., Hoza, B., Conners, C. K., Hinshaw, S. P., et al. (2000). Anxiety as a predictor and outcome variable in the multimodal treatment study of children with ADHD (MTA). *J. Abnorm. Child. Psychol.* 28, 527–541. doi: 10.1023/a:1005179014321

Maric, M., Bexkens, A., and Bogels, S. M. (2018). Is clinical anxiety a risk or a protective factor for executive functioning in youth with ADHD? A meta-regression analysis. *Clin. Child. Fam. Psychol. Rev.* 21, 340–353.

Miao, S., Han, J., Gu, Y., Wang, X., Song, W., Li, D., et al. (2017). Reduced prefrontal cortex activation in children with attention-deficit/hyperactivity disorder during go/no-go task: a functional near-infrared spectroscopy study. *Front. Neurosci.* 11:367. doi: 10.3389/fnins.2017.00367

Nomi, J. S., Schettini, E., Voorhies, W., Bolt, T. S., Heller, A. S., and Uddin, L. Q. (2018). Resting-state brain signal variability in prefrontal cortex is associated with ADHD symptom severity in children. *Front. Hum. Neurosci.* 12:90. doi: 10.3389/fnhum.2018.00090

O'Rourke, S. R., Bray, A. C., and Anastopoulos, A. D. (2020). Anxiety symptoms and disorders in college students with ADHD. *J. Atten. Disord.* 24, 1764–1774.

Overgaard, K. R., Aase, H., Torgersen, S., and Zeiner, P. (2016). Co-occurrence of ADHD and anxiety in preschool children. *J. Atten. Disord.* 20, 573–580.

Pamplona, G. S., Santos Neto, G. S., Rosset, S. R., Rogers, B. P., and Salmon, C. E. (2015). Analyzing the association between functional connectivity of the brain and intellectual performance. *Front. Hum. Neurosci.* 9:61. doi: 10.3389/fnhum.2015.00061

Pessoa, L. (2011). Reprint of: emotion and cognition and the amygdala: from "what is it?" to "what's to be done?" *Neuropsychologia* 49, 681–694. doi: 10.1016/j.neuropsychologia.2011.02.030

Polanczyk, G. V., Willcutt, E. G., Salum, G. A., Kieling, C., and Rohde, L. A. (2014). ADHD prevalence estimates across three decades: an updated systematic review and meta-regression analysis. *Int. J. Epidemiol.* 43, 434–442. doi: 10.1093/ije/dyt261

Polanczyk, G., De Lima, M. S., Horta, B. L., Biederman, J., and Rohde, L. A. (2007). The worldwide prevalence of ADHD: a systematic review and metaregression analysis. *Am. J. Psychiatry* 164, 942–948.

Porta-Casteras, D., Fullana, M. A., Tinoco, D., Martinez-Zalacain, I., Pujol, J., Palao, D. J., et al. (2020). Prefrontal-amygdala connectivity in trait anxiety and generalized anxiety disorder: testing the boundaries between healthy and pathological worries. *J. Affect. Disord.* 267, 211–219. doi: 10.1016/j.jad.2020.02.029

Posner, J., Nagel, B. J., Maia, T. V., Mechling, A., Oh, M., Wang, Z., et al. (2011). Abnormal amygdalar activation and connectivity in adolescents with attentiondeficit/hyperactivity disorder. *J. Am. Acad. Child. Adolesc. Psychiatry* 50, 828–837.

Prevatt, F., Dehili, V., Taylor, N., and Marshall, D. (2015). Anxiety in college students With ADHD: relationship to cognitive functioning. *J. Atten. Disord.* 19, 222–230.

Qin, S., Young, C. B., Duan, X., Chen, T., Supekar, K., and Menon, V. (2014). Amygdala subregional structure and intrinsic functional connectivity predicts individual differences in anxiety during early childhood. *Biol. Psychiatry* 75, 892–900. doi: 10.1016/j.biopsych.2013.10.006

Querne, L., Fall, S., Le Moing, A. G., Bourel-Ponchel, E., Delignieres, A., Simonnot, A., et al. (2017). Effects of methylphenidate on default-mode network/task-positive network synchronization in children With ADHD. *J. Atten. Disord.* 21, 1208–1220. doi: 10.1177/1087054713517542

Rosenkranz, J. A., Moore, H., and Grace, A. A. (2003). The prefrontal cortex regulates lateral amygdala neuronal plasticity and responses to previously conditioned stimuli. *J. Neurosci.* 23, 11054–11064. doi: 10.1523/JNEUROSCI.23-35-11054.2003

Roy, A. K., Shehzad, Z., Margulies, D. S., Kelly, A. C., Uddin, L. Q., Gotimer, K., et al. (2009). Functional connectivity of the human amygdala using resting state fMRI. *Neuroimage* 45, 614–626.

Ruf, B. M., Bessette, K. L., Pearlson, G. D., and Stevens, M. C. (2017). Effect of trait anxiety on cognitive test performance in adolescents with and without attention-deficit/hyperactivity disorder. *J. Clin. Exp. Neuropsychol.* 39, 434–448.

Sato, W., Kochiyama, T., Uono, S., Kubota, Y., Sawada, R., Yoshimura, S., et al. (2015). The structural neural substrate of subjective happiness. *Sci. Rep.* 5:16891. doi: 10.1038/srep16891

Schaefer, A., and Gray, J. R. (2007). A role for the human amygdala in higher cognition. *Rev. Neurosci.* 18, 355–364.

Schaefer, A., Braver, T. S., Reynolds, J. R., Burgess, G. C., Yarkoni, T., and Gray, J. R. (2006). Individual differences in amygdala activity predict response speed during working memory. *J. Neurosci.* 26, 10120–10128. doi: 10.1523/JNEUROSCI.2567-06.2006

Schatz, D. B., and Rostain, A. L. (2006). ADHD with comorbid anxiety: a review of the current literature. *J. Atten. Disord.* 10, 141–149.

Skirrow, C., and Asherson, P. (2013). Emotional lability, comorbidity and impairment in adults with attention-deficit hyperactivity disorder. *J. Affect. Disord.* 147, 80–86.

Song, M., Zhou, Y., Li, J., Liu, Y., Tian, L., Yu, C., et al. (2008). Brain spontaneous functional connectivity and intelligence. *Neuroimage* 41, 1168–1176.

Sorensen, L., Plessen, K. J., Nicholas, J., and Lundervold, A. J. (2011). Is behavioral regulation in children with ADHD aggravated by comorbid anxiety disorder? *J. Atten. Disord.* 15, 56–66.

Sun, Y., Lan, Z., Xue, S.-W., Zhao, L., Xiao, Y., Kuai, C., et al. (2021). Brain state-dependent dynamic functional connectivity patterns in attention-deficit/hyperactivity disorder. *J. Psychiatr. Res.* 138, 569–575. doi: 10.1016/j.jpsychires.2021.05.010

Szuromi, B., Bitter, I., and Czobor, P. (2013). Functional impairment in adults positively screened for attention-deficit hyperactivity disorder: the role of symptom presentation and executive functioning. *Compr. Psychiatry* 54, 974–981. doi: 10.1016/j.comppsych.2013.04.002

Tajima-Pozo, K., Yus, M., Ruiz-Manrique, G., Lewczuk, A., Arrazola, J., and Montanes-Rada, F. (2018). Amygdala abnormalities in adults with ADHD. *J. Atten. Disord.* 22, 671–678.

Tang, C., Wei, Y., Zhao, J., and Nie, J. (2018). Different developmental pattern of brain activities in ADHD: a study of resting-state fMRI. *Dev. Neurosci.* 40, 246–257.

Vance, A., Silk, T. J., Casey, M., Rinehart, N. J., Bradshaw, J. L., Bellgrove, M. A., et al. (2007). Right parietal dysfunction in children with attention deficit hyperactivity disorder, combined type: a functional MRI study. *Mol. Psychiatry* 12, 826–832.

Voytek, B., and Knight, R. T. (2015). Dynamic network communication as a unifying neural basis for cognition, development, aging, and disease. *Biol. Psychiatry* 77, 1089–1097. doi: 10.1016/j.biopsych.2015.04.016

Walhovd, K. B., Amlien, I., Schrantee, A., Rohani, D. A., Groote, I., Bjornerud, A., et al. (2020). Methylphenidate effects on cortical thickness in children and adults with attention-deficit/hyperactivity disorder: a randomized clinical trial. *AJNR Am. J. Neuroradiol.* 41, 758–765. doi: 10.3174/ajnr.A6560

Wolraich, M. L., Wibbelsman, C. J., Brown, T. E., Evans, S. W., Gotlieb, E. M., Knight, J. R., et al. (2005). Attention-deficit/hyperactivity disorder among adolescents: a review of the diagnosis, treatment, and clinical implications. *Pediatrics* 115, 1734–1746.

Yan, C.-G., Wang, X.-D., Zuo, X.-N., and Zang, Y.-F. (2016). DPABI: data processing & analysis for (resting-state) brain imaging. *Neuroinformatics* 14, 339–351.

Yao, Z., Liao, M., Hu, T., Zhang, Z., Zhao, Y., Zheng, F., et al. (2017). An effective method to identify adolescent generalized anxiety disorder by temporal features of dynamic functional connectivity. *Front. Hum. Neurosci.* 11:492. doi: 10.3389/fnhum.2017.00492

Yao, Z., Shi, J., Zhang, Z., Zheng, W., Hu, T., Li, Y., et al. (2019). Altered dynamic functional connectivity in weakly-connected state in major depressive disorder. *Clin. Neurophysiol.* 130, 2096–2104. doi: 10.1016/j.clinph.2019.08.009

Yu, X., Liu, L., Chen, W., Cao, Q., Zepf, F. D., Ji, G., et al. (2016). Integrity of amygdala subregion-based functional networks and emotional lability in drug-naive boys with ADHD. *J. Atten. Disord.* 24, 1661–1673. doi: 10.1177/1087054716661419

Yue, J. L., Li, P., Shi, L., Lin, X., Sun, H. Q., and Lu, L. (2018). Enhanced temporal variability of amygdala-frontal functional connectivity in patients with schizophrenia. *Neuroimage Clin.* 18, 527–532. doi: 10.1016/j.nicl.2018.02.025

Zimmermann, J., Deris, N., Montag, C., Reuter, M., Felten, A., Becker, B., et al. (2018). A common polymorphism on the oxytocin receptor gene (rs2268498) and resting-state functional connectivity of amygdala subregions-A genetic imaging study. *Neuroimage.* 179, 1–10.

Conflict of Interest: The authors declare that the research was conducted in the absence of any commercial or financial relationships that could be construed as a potential conflict of interest.

The reviewer LS declared a past collaboration with one of the author BY to the handling editor.

Publisher's Note: All claims expressed in this article are solely those of the authors and do not necessarily represent those of their affiliated organizations, or those of the publisher, the editors and the reviewers. Any product that may be evaluated in this article, or claim that may be made by its manufacturer, is not guaranteed or endorsed by the publisher.

frontiers in Neuroscience

ORIGINAL RESEARCH
published: 06 October 2021
doi: 10.3389/fnins.2021.711542

Modulation of Dorsolateral Prefrontal Cortex Glutamate/Glutamine Levels Following Repetitive Transcranial Magnetic Stimulation in Young Adults With Autism

*Iska Moxon-Emre[1], Zafiris J. Daskalakis[2,3], Daniel M. Blumberger[2,3], Paul E. Croarkin[4], Rachael E. Lyon[1], Natalie J. Forde[1,5], Hideaki Tani[1], Peter Truong[6], Meng-Chuan Lai[1,3,7,8], Pushpal Desarkar[2,3], Napapon Sailasuta[6], Peter Szatmari[1,3,7] and Stephanie H. Ameis[1,3,7]**

[1] Cundill Centre for Child and Youth Depression, The Margaret and Wallace McCain Centre for Child, Youth & Family Mental Health, Campbell Family Mental Health Research Institute, Centre for Addiction and Mental Health, Toronto, ON, Canada, [2] Temerty Centre for Therapeutic Brain Intervention, Campbell Family Mental Health Research Institute, Centre for Addiction and Mental Health, Toronto, ON, Canada, [3] Department of Psychiatry, Temerty Faculty of Medicine, University of Toronto, Toronto, ON, Canada, [4] Division of Child and Adolescent Psychiatry, Department of Psychiatry and Psychology, Mayo Clinic, Rochester, MN, United States, [5] Radboud University Medical Centre, Donders Institute for Brain, Cognition and Behaviour, Nijmegen, Netherlands, [6] Research Imaging Centre, Centre for Addiction and Mental Health, Toronto, ON, Canada, [7] Department of Psychiatry, Research Institute, The Hospital for Sick Children, Toronto, ON, Canada, [8] Department of Psychology, University of Toronto, Toronto, ON, Canada

OPEN ACCESS

Edited by:
Li Yang,
Peking University Sixth Hospital, China

Reviewed by:
Ashwin S. Shetty,
Harvard University, United States
Lonnie Sears,
University of Louisville, United States
Xingbao Li,
Medical University of South Carolina, United States

***Correspondence:**
Stephanie H. Ameis
stephanie.ameis@camh.ca

Specialty section:
This article was submitted to Neurodevelopment, a section of the journal Frontiers in Neuroscience

Received: *18 May 2021*
Accepted: *13 September 2021*
Published: *06 October 2021*

Citation:
Moxon-Emre I, Daskalakis ZJ, Blumberger DM, Croarkin PE, Lyon RE, Forde NJ, Tani H, Truong P, Lai M-C, Desarkar P, Sailasuta N, Szatmari P and Ameis SH (2021) Modulation of Dorsolateral Prefrontal Cortex Glutamate/Glutamine Levels Following Repetitive Transcranial Magnetic Stimulation in Young Adults With Autism. Front. Neurosci. 15:711542. doi: 10.3389/fnins.2021.711542

Altered excitatory and inhibitory neurotransmission has been implicated in autism spectrum disorder (ASD). Interventions using repetitive transcranial magnetic stimulation (rTMS) to enhance or inhibit cortical excitability are under study for various targets, though the mechanistic effects of rTMS have yet to be examined in ASD. Here, we examined whether an excitatory rTMS treatment course modulates glutamatergic (Glx) or γ-aminobutyric acid (GABA) metabolite levels in emerging adults with ASD. Twenty-eight participants with ASD and executive function impairment [23.3 ± 4.69 years; seven-female] underwent two magnetic resonance spectroscopy (MRS) scans of the left dorsolateral prefrontal cortex (DLPFC). MRS scans were acquired before and after participants with ASD were randomized to receive a 20-session course of active or sham rTMS to the DLPFC. Baseline MRS data was available for 19 typically developing controls [23.8 ± 4.47 years; six-female]. Metabolite levels for Glx and GABA+ were compared between ASD and control groups, at baseline, and metabolite level change, pre-to-post-rTMS treatment, was compared in ASD participants that underwent active vs. sham rTMS. Absolute change in Glx was greater in the active vs. sham-rTMS group [$F_{(1,19)} = 6.54$, $p = 0.02$], though the absolute change in GABA+ did not differ between groups. We also examined how baseline metabolite levels related to pre/post-rTMS metabolite level change, in the active vs. sham groups. rTMS group moderated the relation between baseline Glx and pre-to-post-rTMS Glx change, such that baseline Glx predicted Glx change in the active-rTMS group only [$b = 1.52$, $SE = 0.32$, $t_{(18)} = 4.74$, $p < 0.001$]; Glx levels increased when baseline levels were lower, and decreased when baseline levels were higher. Our results indicate that an interventional course of excitatory

rTMS to the DLPFC may modulate local Glx levels in emerging adults with ASD, and align with prior reports of glutamatergic alterations following rTMS. Interventional studies that track glutamatergic markers may provide mechanistic insights into the therapeutic potential of rTMS in ASD.

Clinical Trial Registration: Clinicaltrials.gov (ID: NCT02311751), https://clinicaltrials.gov/ct2/show/NCT02311751?term=ameis&rank=1; NCT02311751.

Keywords: autism spectrum disorder, repetitive transcranial magnetic simulation, dorsolateral prefrontal cortex, magnetic resonance spectography, Glx, GABA, MEGA-PRESS

INTRODUCTION

Autism spectrum disorder (ASD) is a neurodevelopmental disorder characterized by complex phenotypic and neurobiological heterogeneity. A number of studies point to the possible convergence of altered excitatory glutamatergic and inhibitory γ-aminobutyric acid (GABA) mediated neurotransmission in ASD (Ford and Crewther, 2016; Ajram et al., 2019). Glutamate and GABA are fundamentally important for the development of neuronal circuitry, and maintenance of cognition and behavior (Lujan et al., 2005). Importantly, glutamate and GABA are not independent neural chemicals; within GABAergic interneurons, glutamine is synthesized into glutamate, which is subsequently synthesized into GABA by the glutamate decarboxylase (GAD) enzyme (Bak et al., 2006). The rate-limiting GAD enzyme may be altered in ASD (Yip et al., 2007). Thus, relative levels of glutamate and GABA may differ among individuals with ASD, as glutamate, glutamine and GABA are continually in flux.

Magnetic resonance spectroscopy (MRS) is one of the few non-invasive techniques able to probe biochemistry in the human brain through measurement of metabolites associated with neurophysiological processes (Rae, 2014). Though findings are mixed, a number of MRS studies report altered GABA and Glx (glutamate + glutamine) levels, across various brain regions, in participants with ASD compared to typically developing controls (TDC) (Ford and Crewther, 2016; Ajram et al., 2019). Within prefrontal regions, lower GABA and/or Glx levels have been detected in samples of children with ASD vs. TDC (Harada et al., 2011; Kubas et al., 2012). There are comparatively fewer studies that evaluate GABA and Glx levels in autistic adults. Both lower (Bernardi et al., 2011; Horder et al., 2013, 2018; Tebartz van Elst et al., 2014) and higher Glx (Page et al., 2006; Brown et al., 2013) levels have been reported in available studies of adults with ASD vs. TDC, though no GABA differences have been found. Of note, studies that include samples spanning across the child, youth and young adult age ranges have not shown differences in GABA or Glx levels in ASD vs. TDC (Ajram et al., 2019), suggesting that age may have influenced prior neurometabolite findings.

Various pharmacological agents that affect glutamate/GABA signaling are currently under study as interventions in ASD [e.g., Memantine, riluzole, arbaclofen (Lai et al., 2020), cannabinoid compounds (Pretzsch et al., 2019a,b)]. Identifying non-invasive approaches that modulate this neurotransmitter pathway, and metrics that can track successful modulation, represent important steps to development of biomedical interventions in this area. Repetitive transcranial magnetic stimulation (rTMS) is a non-invasive interventional tool that involves stimulating the cortex with trains of magnetic pulses (George et al., 2009). Although TMS studies implicate aberrant cortical plasticity in ASD (Oberman et al., 2012; Oberman et al., 2016), we are not aware of any study that has examined rTMS effects on neurometabolite levels in this population.

Repetitive transcranial magnetic stimulation may drive changes in excitatory and inhibitory tone through a variety of mechanisms, such as changes to glutamatergic synapses, GABAergic neurons, brain derived neurotrophic factor, or promotion of neurogenesis (Dayan et al., 2013; Polania et al., 2018). However, the neurobiological effect of rTMS may depend upon the individual characteristics of the brain undergoing stimulation (Silvanto et al., 2008). For example, in major depressive disorder (MDD), rTMS is thought to restore normative brain function through facilitating the re-emergence of intrinsic cerebral rhythms (Leuchter et al., 2013). Further, a study in a non-clinical sample suggested that although rTMS paradigms can increase cortical inhibition, the extent of change may depend on baseline inhibition (i.e., larger increases in individuals with lower baseline inhibition found) (Daskalakis et al., 2006).

The potential utility of rTMS in the treatment of neuropsychiatric conditions stems, in part, from its ability to enhance or inhibit cortical excitability in targeted brain regions. Preliminary evidence suggests that rTMS to the dorsolateral prefrontal cortex (DLPFC) may have value as an interventional tool to alter repetitive or stereotyped behaviors, social functioning (Barahona-Correa et al., 2018), depressive symptoms (Gwynette et al., 2020), or executive functioning (Sokhadze et al., 2014) in ASD.

Our recent randomized double-blind sham-controlled pilot trial of 20 sessions of 20 Hz (excitatory) rTMS to bilateral DLPFC, tested the feasibility and preliminary efficacy of rTMS for the treatment of executive function deficits in emerging adults with ASD. Stimulation parameters for our trial targeting executive function impairment were chosen according to the best available evidence for improving cognitive function in clinical populations at the time of trial design. For example, a systematic review that assessed the potential for rTMS to improve cognitive outcome across various clinical populations found that a course of high frequency stimulation to DLPFC was most promising for improving executive function (Guse et al., 2010).

Preliminary studies in ASD had also suggested that bilateral DLPFC stimulation at 90% resting motor threshold (RMT) may improve performance on cognitive domains (Sokhadze et al., 2014) and that a course of high frequency bilateral prefrontal cortex stimulation was feasibly implemented in an ASD sample at 90% RMT (Enticott et al., 2014). Our pilot rTMS clinical trial in ASD used the exact same stimulation protocol (20 sessions of 20 Hz rTMS to bilateral DLPFC at 90% RMT) as a prior positive clinical trial that tested the efficacy and feasibility of rTMS to improve working memory in schizophrenia (Barr et al., 2013). Individuals with ASD are predisposed to seizures and often take medications similar to individuals with schizophrenia. Therefore, we specifically chose to model our pilot clinical trial parameters to be consistent with a protocol that had improved working memory deficits (our main clinical outcome measure of the trial), and that was safely and feasibly implemented in a complex clinical population (Barr et al., 2013). Additionally, we used target site and intensity parameters that had been safely implemented in prior published rTMS studies in ASD samples (Enticott et al., 2014; Sokhadze et al., 2014). Though we did not find significant differences in executive function performance following active versus sham treatment across our clinical trial sample, executive functioning improved following active rTMS in the subset of participants in our sample with more pronounced baseline functional impairments (Ameis et al., 2020).

In the present study, we analyzed available ^{1}H MRS data measuring GABA+ (GABA+ macromolecules) and Glx levels in individuals with ASD that participated in our 4-week pilot clinical trial studying the effects of rTMS to DLPFC on executive function deficits (Ameis et al., 2020). MRS data was collected as part of the trial to explore changes in inhibitory and excitatory neurotransmission following rTMS. No *a priori* hypotheses for MRS data were registered prior to the clinical trial. Owing to the mixed evidence for neurometabolite alterations in ASD, we first examined whether GABA+ or Glx levels within the DLPFC differed in ASD vs. age-matched TDCs, at baseline. However, the primary objective of our study was to test the hypothesis that GABA+ and Glx levels within the DLPFC would change following active vs. sham rTMS in participants with ASD. Based on the potential for state-dependent effects following rTMS (Daskalakis et al., 2006; Kearney-Ramos et al., 2019), we also explored whether the direction of metabolite level change was influenced by baseline metabolite levels.

MATERIALS AND METHODS

Participants

Baseline Autism Spectrum Disorder Group

Forty participants with ASD, characterized previously (Ameis et al., 2017, 2020), were recruited from the Centre for Addiction and Mental Health (CAMH, Toronto, Canada), local community clinics, and advertisements (local and online). Among the 40 participants that completed the rTMS clinical trial, 33 participants underwent MRS at least once, and 28 had useable baseline scans (see **Supplementary Table 1** and **Table 1**). Characteristics of the participants with and without useable MRS scans are provided in **Supplementary Table 2**. This study was part of a pilot clinical trial designed to investigate the potential of rTMS as an intervention for executive function deficits in ASD. The study was approved by the CAMH research ethics board (REB; protocol #119-2013) and registered with Clinicaltrials.gov (ID: NCT02311751). The inclusion/exclusion criteria for trial participants with ASD were described previously (Ameis et al., 2017, 2020). Briefly, participants with ASD were included if they were aged 16-35 years, fluent in English, had a DSM-IV-TR diagnosis of autistic disorder, Asperger's disorder, or pervasive developmental disorder-not otherwise specified (PDD-NOS), or a DSM-5 diagnosis of ASD. Prior clinical diagnoses were confirmed on clinical interview and using the Autism Diagnostic Observation Schedule-2 (ADOS-2), Module 4 (administered by a trained child and youth psychiatrist, SHA) (Lord et al., 2000). Capacity to consent, clinical stability, an IQ $\geq$ 70 on the General Abilities Index (GAI) from the Wechsler Adult Intelligence Scale-Fourth Edition (WAIS-IV) (Benson et al., 2010), and a T score $>$ 65 on any subscale of the Behavior Rating Inventory of Executive Function (BRIEF)-self report version (Gioia et al., 2002), indicating clinically significant impairment in executive functioning, were also required for inclusion. Adaptive functioning was assessed with the Vineland Adaptive Behavior Scale-II (VABS-II) (Sparrow and Cicchetti, 1985). Co-occurring mental health conditions were assessed using the Mini International Neuropsychiatric Interview (MINI) (Sheehan et al., 1998). Participants were excluded if they had prior major medical or neurological illnesses, were taking anticonvulsants or benzodiazepines ($\geq$2 mg lorazepam equivalent), were pregnant or had potential for pregnancy, had history of substance use/dependence within the last 6 months or a positive urine toxicology screen, had history of rTMS treatment, were unable to commit to the rTMS protocol, or unable to consent to participation. No changes in psychotropic medication were permitted within 4 weeks of randomization to the end of treatment. Psychiatric comorbidities, and psychotropic medications are detailed in **Supplementary Table 3**.

Baseline Comparison/Control Group

Twenty age- and sex-matched TDCs were recruited from local and online advertisements; all participants underwent MRS once, and 19 had useable baseline scans (**Supplementary Table 1** and **Table 1**). Control participants were included if they were aged 16–35 years, fluent in English, and had capacity to consent. TDC participants were excluded if they had a history of substance use/dependence within the last 6 months, a positive urine toxicology screen, any major medical or neurological illness, a diagnosed learning disorder, an IQ $<$ 70, were pregnant, or if they were found to have a psychiatric diagnosis during the MINI assessment. Participant characteristics are detailed in **Table 1**.

Repetitive Transcranial Magnetic Stimulation Intervention Group

Demographic and clinical characteristics for the 28 participants with ASD with available MRS data that were treated with active (n = 16) vs. sham (n = 12) rTMS, are provided in **Table 2**. The breakdown of participants with MRS scans, within each

TABLE 1 | Characteristics of the baseline sample (TDC vs. all ASD participants).

	TDC ($n = 19$)	ASD ($n = 28$)	Test	*p*-value
Age				
Mean (*SD*)	23.8 (4.47)	23.3 (4.69)	$t_{(40)} = 0.40$	0.69
Median [Min, Max]	23.0 [16.0, 34.0]	22.0 [16.0, 33.0]		
Sex				
Number of males (%)	13 (68.4%)	21 (75.0%)	$X^2 = 0.03$	0.87
Psychotropic Medication[a],*				
Number of participants on (%)	0 (0%)	17 (60.7%)	Fisher's Exact	**<0.001**
MINI[a]				
Comorbidity				
Number of participants (%)	0 (0%)	16 (57.1%)	Fisher's Exact	**<0.001**
Depression – current (2 weeks)				
Number of participants (%)	0 (0%)	7 (25.0%)	Fisher's Exact	**0.03**
Depression – recurrent				
Number of participants (%)	0 (0%)	2 (7.1%)	Fisher's Exact	0.15
Years of Education[a]				
Mean (*SD*)	15.4 (2.31)	14.2 (3.01)	$t_{(43)} = 1.56$	0.13
Median [Min, Max]	16.0 [10.0, 19.0]	13.5 [10.0, 22.0]		
IQ – General Abilities Index[b]				
Mean (*SD*)	111 (9.37)	112 (17.8)	$t_{(42)} = -0.23$	0.82
Median [Min, Max]	111 [94.0, 136]	111 [77.0, 141]		
BRIEF Metacognition Index[a]				
Mean (*SD*)	45.7 (6.88)	70.6 (8.21)	$U = 1.5$	**<0.001**
Median [Min, Max]	45.0 [36.0, 59.0]	68.5 [59.0, 84.0]		
BRIEF Global Composite[a]				
Mean (*SD*)	43.5 (5.89)	68.0 (8.18)	$t_{(43)} = -11.81$	**<0.001**
Median [Min, Max]	43.5 [35.0, 55.0]	66.5 [52.0, 86.0]		
Adaptive Functioning Composite				
Mean (*SD*)	–	75.5 (9.88)	–	–
Median [Min, Max]	–	74.5 [58.0, 104]		
WM Fraction				
Mean (*SD*)	0.415 (0.0663)	0.395 (0.0841)	$F_{(1,44)} = 0.63$	0.43
Median [Min, Max]	0.407 [0.311, 0.528]	0.397 [0.222, 0.585]		
GM Fraction				
Mean (*SD*)	0.459 (0.0392)	0.461 (0.0512)	$F_{(1,44)} < 0.001$	0.98
Median [Min, Max]	0.467 [0.373, 0.507]	0.466 [0.340, 0.557]		
CSF Fraction				
Mean (*SD*)	0.116 (0.0341)	0.129 (0.0300)	$F_{(1,44)} = 1.80$	0.19
Median [Min, Max]	0.123 [0.0567, 0.163]	0.128 [0.0742, 0.208]		
GABA+				
Mean (*SD*)	0.182 (0.0219)	0.175 (0.0292)	$F_{(1,44)} = 0.59$	0.45
Median [Min, Max]	0.181 [0.134, 0.230]	0.168 [0.133, 0.253]		
Glx				
Mean (*SD*)	0.121 (0.0172)	0.120 (0.0208)	$F_{(1,44)} = 0.03$	0.86
Median [Min, Max]	0.123 [0.0912, 0.157]	0.116 [0.0846, 0.166]		
GABA+/Glx ratio				
Mean (*SD*)	1.52 (0.256)	1.48 (0.198)	$F_{(1,44)} = 0.44$	0.51
Median [Min, Max]	1.46 [1.24, 2.37]	1.46 [1.21, 1.92]		

[a]*Data was missing from 1 control participant.*
[b]*Data was missing from 2 control participants.*
Psychotropic medication is detailed in **Supplementary Table 3.*
Age, years of education, IQ and BRIEF scores were compared between groups using Welch's t-tests or Mann–Whitney's U tests when data was not normally distributed. Sex (which was determined based on participant self report) was compared with a Chi-Square Test. Fisher's Exact tests were used when values in any cell were <5. Statistical tests for biological measures (i.e., tissue fractions and metabolite levels) represent groups comparisons, covarying for age.
ASD, autism spectrum disorder; BRIEF, behavior rating inventory of executive function; TDC, typically developing controls; MINI, Mini International Neuropsychiatric Interview; WM, white matter; GM, gray matter; CSF, cerebrospinal fluid. Bold values denote statistical significance at $p < 0.05$.

TABLE 2 | Characteristics of the clinical trial sample (participants with ASD in the active vs. sham rTMS groups).

	Active rTMS (*n* = 16)	**Sham rTMS (*n* = 12)**	**Test**	***p*-value**
Age				
Mean (*SD*)	23.1 (4.66)	23.4 (4.93)	$t_{(23)} = -0.16$	0.88
Median [Min, Max]	21.5 [16.0, 33.0]	23.5 [16.0, 31.0]		
Sex				
Number of males (%)	13 (81.2%)	8 (66.7%)	Fisher's Exact	0.42
Psychotropic Medication*				
Number of participants on (%)	12 (75.0%)	5 (41.7%)	Fisher's Exact	**<0.001**
MINI				
Comorbidity				
Number of participants (%)	10 (62.5%)	6 (50.0%)	Fisher's Exact	**0.04**
Depression – current (2 weeks)				
Number of participants (%)	2 (12.5%)	5 (41.7%)	Fisher's Exact	**<0.001**
Depression – recurrent				
Number of participants (%)	0 (0%)	2 (16.7%)	Fisher's Exact	**0.004**
Years of Education				
Mean (*SD*)	14.9 (3.11)	13.3 (2.70)	$U = 129$	0.13
Median [Min, Max]	15.0 [10.0, 22.0]	12.0 [10.0, 18.0]		
IQ – General Abilities Index				
Mean (*SD*)	112 (19.5)	112 (16.1)	$t_{(26)} = 0.009$	0.99
Median [Min, Max]	114 [77.0, 140]	111 [92.0, 141]		
BRIEF Metacognition Index				
Mean (SD)	70.8 (7.63)	70.3 (9.27)	$t_{(21)} = 0.15$	0.89
Median [Min, Max]	69.5 [59.0, 84.0]	68.0 [59.0, 84.0]		
BRIEF Global Composite				
Mean (*SD*)	67.1 (7.99)	69.3 (8.61)	$U = 87.5$	0.71
Median [Min, Max]	66.5 [52.0, 86.0]	65.5 [61.0, 83.0]		
Adaptive Functioning Composite				
Mean (*SD*)	75.8 (8.13)	75.2 (12.2)	$t_{(18)} = 0.16$	0.88
Median [Min, Max]	75.5 [61.0, 89.0]	72.0 [58.0, 104]		

	Pre (*n* = 16)	**Post (*n* = 12)**	**Pre (*n* = 12)**	**Post (*n* = 12)**		
WM fraction						
Mean (*SD*)	0.399 (0.0857)	0.432 (0.105)	0.390 (0.0853)	0.406 (0.102)	$F_{(1,25)} = 0.25$	0.62
Median [Min, Max]	0.397 [0.222, 0.534]	0.423 [0.310, 0.600]	0.389 [0.268, 0.585]	0.383 [0.270, 0.588]		
GM fraction						
Mean (*SD*)	0.460 (0.0527)	0.438 (0.0729)	0.462 (0.0515)	0.453 (0.0673)	$F_{(1,25)} = 0.13$	0.72
Median [Min, Max]	0.465 [0.370, 0.542]	0.450 [0.321, 0.542]	0.466 [0.340, 0.557]	0.452 [0.337, 0.546]		
CSF fraction						
Mean (*SD*)	0.128 (0.0301)	0.123 (0.0365)	0.131 (0.0311)	0.130 (0.0327)	$F_{(1,26)} = 0.16$	0.69
Median [Min, Max]	0.119 [0.0948, 0.208]	0.117 [0.0794, 0.209]	0.141 [0.0742, 0.166]	0.138 [0.0754, 0.168]		
GABA+						
Mean (*SD*)	0.181 (0.0315)	0.193 (0.0364)	0.168 (0.0254)	0.189 (0.0502)	$F_{(1,26)} = 0.33$	0.57
Median [Min, Max]	0.176 [0.141, 0.253]	0.198 [0.118, 0.239]	0.164 [0.133, 0.219]	0.170 [0.131, 0.292]		
Glx						
Mean (*SD*)	0.119 (0.0226)	0.130 (0.0281)	0.121 (0.0189)	0.121 (0.0254)	$F_{(1,25)} = 0.23$	0.64
Median [Min, Max]	0.112 [0.0846, 0.166]	0.130 [0.0938, 0.175]	0.120 [0.0919, 0.162]	0.123 [0.0731, 0.163]		
GABA+/Glx ratio						
Mean (*SD*)	1.54 (0.224)	1.51 (0.297)	1.39 (0.120)	1.58 (0.287)	$F_{(1,25)} = 0.38$	0.55
Median [Min, Max]	1.52 [1.21, 1.92]	1.45 [1.13, 2.25]	1.38 [1.21, 1.56]	1.48 [1.27, 2.21]		

Psychotropic medication is detailed in **Supplementary Table 3.*

Age, years of education, IQ, BRIEF, and Adaptive Functioning scores were compared between groups using Welch's t-tests or Mann–Whitney's U tests when data was not normally distributed. Fisher's Exact tests were used when values in any cell were <5.

Statistical tests for biological measures (i.e., tissue fractions and metabolite levels) represent main effects of Group, from the 2 × 2 mixed-model ANCOVAs [group (active vs. sham rTMS) × time (pre- vs. post-rTMS)] covarying for age.

rTMS, repetitive transcranial magnetic stimulation; MINI, Mini International Neuropsychiatric Interview; WM, white matter; GM, gray matter; CSF, cerebrospinal fluid, BRIEF, behavior rating inventory of executive function. Bold values denote statistical significance at $p < 0.05$.

treatment group, is detailed in **Supplementary Table 1**. Of note, the number of participants with both pre- and post-rTMS scans was slightly smaller (active: $n = 12$; sham: $n = 10$) (**Supplementary Table 4**). Both cohorts were included, for reasons detailed in the statistical analyses section below.

Clinical Trial Design

Participants with ASD were enrolled in a double-blind, sham-controlled trial (recruitment between November 2014 and June 2017), and were randomly allocated in a 1:1 ratio to receive active or sham rTMS treatment. Briefly, active (20 Hz, delivered at 90% RMT intensity) and sham rTMS were administered bilaterally to DLPFC (Talairach [x, y, z] = [–] 50, 30, 36), 5 days per week for 4 weeks, totaling 20 sessions, at CAMH. Stimulation was administered at 20 Hz with 25 stimulation trains of 30 stimuli each. The inter-train interval was 30 s, at equivalent stimulation parameters (Barr et al., 2013) of 750 pulses/hemisphere, totaling 1500 pulses/session. The rTMS treatment sessions lasted ∼30–45 min. 90% RMT was selected as this was the intensity used in the pilot clinical trial that our study was modeled after (Barr et al., 2013). Further, all published trials of rTMS to DLPFC in ASD available at the time of study design had stimulated at 90% RMT (Sokhadze et al., 2009, 2012, 2014; Baruth et al., 2010; Casanova et al., 2012). TDC participants were not included in the clinical trial, and thus did not receive rTMS. At the beginning of the trial, each participant was randomized to receive left or right-sided stimulation first followed by stimulation of the contralateral hemisphere (this order was maintained for all sessions). We implemented the same sham condition approach used by the study we modeled our clinical trial after; a single-wing tilt position of the coil to mimic the active rTMS condition, as this produces scalp muscle contraction with minimal direct effects on the brain (Barr et al., 2013). To test the integrity of our blinding, we asked participants following the first and last rTMS session if they believed they received active stimulation, and responses did not differ between active/sham groups (Ameis et al., 2020). Detailed clinical trial information, including sample size, randomization details (Ameis et al., 2017), and the CONSORT diagram (Ameis et al., 2020) have been published previously. Clinical trial participants underwent MRS within 1 week prior to commencing rTMS, and within 1 week following the last rTMS session.

Magnetic Resonance Spectroscopy Data Acquisition

GABA-edited proton MRS data were acquired using a MEshcher-GArwood Point RESolved Spectroscopy (MEGA-PRESS) sequence on a 3 Tesla GE MR750 (General Electric, Milwaukee, WI, United States) scanner. Each spectrum was recorded from a single 20 mm × 40 mm × 30 mm voxel, prescribed in the left DLPFC (**Figure 1A**). MEGA-PRESS data acquisition is single voxel method. Due to the low concentration of GABA in the brain tissue (GM GABA concentration = 1.30 + –0.36 μmol/g of brain tissue, WM GABA = 0.16 + –0.16 μmol/g tissue) (Choi et al., 2006), a large voxel is required in order to acquire enough metabolite signal for analysis. Due to imaging time-constraints in our clinical trial, we were unable to acquire MRS data from both hemispheres. Given this, we selected the left DLPFC for MRS voxel placement as left-DLPFC stimulation is more common across rTMS studies, including those with pre/post MRS data which have mainly acquired a single left hemisphere voxel (Michael et al., 2003; Luborzewski et al., 2007; Zheng et al., 2010; Croarkin et al., 2016; Dubin et al., 2016; Baeken et al., 2017; Levitt et al., 2019). Shimming was performed using GE's manufacturer automated shimming routine (AUTOSHIM). Data acquisition parameters were: TE = 68 ms, TR = 1500 ms, 512 averages (256 editing-ON and 256 editing-OFF), ON/OFF editing RF pulses were centered at 1.9/7.5 ppm, and editing RF width = 14.4 ms. To facilitate internal tissue water referencing, unsuppressed water averages were acquired prior to the water-suppressed scans.

Structural Imaging, Voxel Co-registration and Tissue Segmentation

Structural images were acquired at 3T, using 3D fast spoiled gradient-echo imaging (FSPGR) (Low et al., 1993) with the following parameters: TI = 650 ms, TE = 3 ms, TR = 6.7 ms, flip angle = 8^o, FOV = 256 × 256 mm, resulting voxel size = 0.9 mm isotropic without gap, and scan time of ∼5 min. High-resolution T_1 images were acquired sagittally and reformatted to axial and coronal oblique images parallel to the anterior commissure - posterior commissure (AC-PC) line. To ensure consistent voxel positioning in the left DLPFC, guidelines were to place the voxel on a double oblique image parallel to and between the superior and inferior frontal gyrus; these instructions were followed for all acquired scans. Grey matter (GM), white matter (WM), and cerebrospinal fluid (CSF) composition within the single voxel MEGA-PRESS data were determined using the GannetCoRegister module in Gannet (Harris et al., 2015) and FSL-FMRIB's Automatic Segmentation Tool (FAST) (Zhang et al., 2001). Briefly, raw MRS data acquisition parameters (voxel size, orientation, and location stored in the MRS raw data headers) were determined to create a binary mask of the voxel locations, and co-registered to the T1-weighted images. This mask was then applied using FSL-FAST to determine GM/WM/CSF fractions (**Figure 1B**, **Tables 1**, **2**, and **Supplementary Table 4**). Water-scaled metabolite concentrations were corrected for voxel tissue composition; observed metabolite concentrations (not corrected for metabolite relaxation times) were obtained, relative to the fully relaxed water concentration in tissue [M] by accounting for the volume fractions, water relaxation times (T1, T2) and water concentrations of the WM, GM, and CSF compartments, as per Gasparovic et al. (2006). Equations used for metabolite correction, and water relaxation times of the tissue compartments, are detailed in the **Supplementary Methods**.

Magnetic Resonance Spectroscopy Data Processing

The Gannet 3.0 (Edden et al., 2014) processing pipeline was used to perform the following processing steps: frequency and phase correction by spectral registration, exponential line broadening

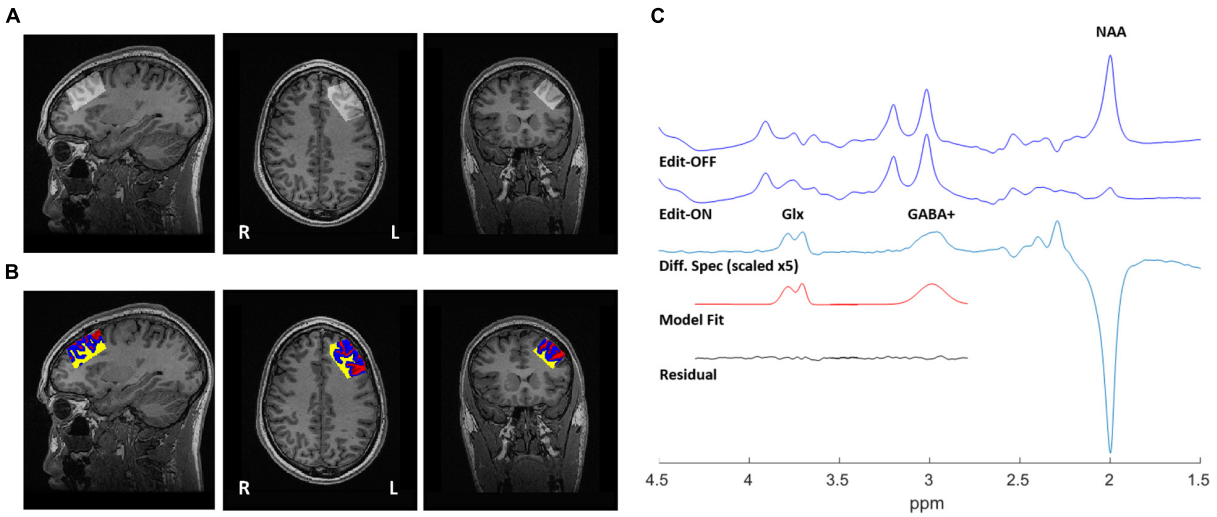

FIGURE 1 | 1H-MRS voxel position, tissue segmentation, and representative spectra from a single participant. **(A)** 20 mm × 40 mm × 30 mm voxel, placed in the left dorsolateral prefrontal cortex (DLPFC). **(B)** Segmentation of T1-weighted MRI, used to correct water-scaled metabolite concentrations for voxel tissue composition. Gray matter (blue), white matter (yellow), and CSF (red). **(C)** Sample output from the MEGA-PRESS sequence, with representative fits of GABA+ and Glx peaks shown in the edited spectrum.

(3 Hz) and a fast Fourier transform. The full-width at half-maximum (FWHM) of the modeled water signal was used to obtain the linewidth of the water reference. Once the OFF was subtracted from the ON acquisitions, a single reliable GABA+ peak at 3.01 ppm (representing the GABA peak co-edited with macromolecule [MM] signal), and a Glx doublet (co-edited glutamine + glutamate) peak at ∼3.75 ppm were fitted. Gaussian line shape fitting, with modifications to obtain GABA+ area outputs, were performed as in prior publications (Dubin et al., 2016; Da Silva et al., 2019). GABA+ and Glx levels were normalized by the area of the water model peak. An example spectra is provided in **Figure 1C**, and all (overlaid) spectra are provided in **Supplementary Figure 1**. GABA+ /Glx ratios were calculated to evaluate the inhibition/excitation balance within the voxel. The editing OFF acquisition was also processed using the FID-A toolkit (Simpson et al., 2017), which combined the receiver coil data, removed averages with significant motion, and performed spectral registration to frequency and phase correct the data prior to separating and combining the editing OFF averages. This output was then analyzed using the LCModel (version 6.3-0E) (Provencher, 1993) over the frequency range of 0.2–4.0 ppm. Metabolite reference spectra were generated using GAMMA library (Smith et al., 1994). The reference basis set consisted of 19 metabolites, as detailed in **Supplementary Methods**, and the corrected metabolite pseudo concentrations are shown in **Supplementary Table 5**.

Quality Control

Seventy nine MRS scans from 53 participants (33 ASD; 20 control) were assessed for quality control. Reasons and details for scan exclusion (n = 3 baseline, n = 5 post-rTMS) are provided in **Supplementary Table 1**. We note that useable MRS data was not available for all rTMS trial participants due to imaging time-constraints, difficulties with scanning a complex clinical population, and due to our adherence to rigorous quality control of MRS data.

Statistical Analysis

Analysis of Baseline Metabolite Levels in Autism Spectrum Disorder vs. Typically Developing Controls

Demographic variables, tissue composition and metabolites were compared between participants with ASD and TDCs. Tissue composition (GM, WM, and CSF fraction) and baseline metabolites (GABA+, Glx and GABA+ /Glx ratio) were compared between the ASD and TDC groups using a series of ANCOVAs, including age as a covariate. Group differences in NAA, GPC, mI, Glu, and Cr were also assessed.

Analysis of Magnetic Resonance Spectroscopy-Derived Metabolites at Pre- vs. Post-repetitive Transcranial Magnetic Stimulation in Clinical Trial Participants With Autism Spectrum Disorder

The effect of rTMS (active vs. sham) on metabolites was assessed in participants with ASD that completed the rTMS clinical trial. Pre/post-rTMS tissue composition (GM, WM, and CSF fractions) and metabolites (GABA+, Glx, and GABA+/Glx) were each compared between active and sham groups using 2 × 2 mixed-effect ANCOVAs, with rTMS group (active vs. sham rTMS) as a between-subjects factor, time (pre- vs. post-rTMS) as a within-subjects factor, and age as a covariate. Participants with MRS available at a single time point were included in these models, as single data points contribute to the overall group mean effects (cohort detailed in **Table 2**). To capture change in neurometabolite levels, irrespective of direction, the absolute value change for each metabolite (GABA+ and Glx levels, and

GABA+ /Glx ratio) from pre- to post-rTMS was compared between active vs. sham groups, using ANCOVAs including age as a covariate. Only participants with MRS data available at both time points were included in these analyses (**Supplementary Table 4** cohort). For metabolites that demonstrated change following rTMS, exploratory regressions were performed to test whether rTMS group moderated the relation between metabolite level change and baseline metabolite level. Simple effects of this moderation were tested using Aiken and West method (Aiken and West, 1991).

Baseline and pre/post analyses yielding significant p-values were corrected for multiple comparisons using the Benjamini Hochberg procedure (Benjamini and Hochberg, 1995), where appropriate (e.g., across GABA+, Glx and GABA+/Glx ratio analyses), and effect sizes were calculated.

RESULTS

Analysis of Baseline Metabolite Levels in Autism Spectrum Disorder vs. Typically Developing Controls

Autism spectrum disorder and TDC participants had comparable demographic characteristics and voxel tissue composition, as detailed in **Table 1**. We did not find a significant effect of diagnostic group for metabolites at baseline; ASD and TDC participants did not differ in GABA+, Glx, or the GABA+/Glx ratio [all $F_{(1,44)} < 0.60$, all $p > 0.05$] (**Table 1**). No diagnostic group differences were observed for NAA, GPC, mI, Glu, and Cr [all $F_{(1,44)} < 3.21$, all $p > 0.05$] (**Supplementary Table 5**).

Analysis of Magnetic Resonance Spectroscopy-Derived Metabolites Pre- vs. Post-repetitive Transcranial Magnetic Stimulation in Clinical Trial Participants With Autism Spectrum Disorder

Autism spectrum disorder participants in the active vs. sham rTMS groups with usable MRS data were found to have comparable demographic characteristics, as detailed in **Table 2**. However, participants with usable MRS data in the active group featured increased comorbidity on the MINI ($p = 0.04$, Fisher's Exact), and were more often taking psychotropic medications ($p < 0.001$, Fisher's Exact). Tissue fractions were comparable between active and sham rTMS groups, and over time there was no main effect of rTMS group for WM [$F_{(1,25)} = 0.25$, $p = 0.62$], GM [$F_{(1,25)} = 0.13$, $p = 0.73$] or CSF [$F_{(1,25)} = 0.16$, $p = 0.69$], and no interaction between group and time, for WM [$F_{(1,25)} = 0.09$, $p = 0.77$], GM [$F_{(1,25)} = 0.11$, $p = 0.75$], or CSF [$F_{(1,25)} = 0.07$, $p = 0.79$] fractions (**Table 2**).

Mean GABA+ and Glx levels, and the GABA+/Glx ratio did not differ from pre- to post-rTMS in either group; there was no main effect of rTMS group for GABA+ [$F_{(1,26)} = 0.33$, $p = 0.57$], Glx [$F_{(1,25)} = 0.23$, $p = 0.64$], or GABA+/Glx ratio [$F_{(1,25)} = 0.38$, $p = 0.55$], no main effect of time for GABA+ [$F_{(1,24)} = 3.37$, $p = 0.08$], Glx [$F_{(1,26)} = 0.72$, $p = 0.40$], or GABA+/Glx ratio [$F_{(1,25)} = 0.84$, $p = 0.37$], and no interaction between rTMS group and time, for GABA+ [$F_{(1,24)} = 0.46$, $p = 0.50$], Glx [$F_{(1,26)} = 0.72$, $p = 0.40$], or GABA+/Glx ratio [$F_{(1,25)} = 3.71$, $p = 0.07$] (**Table 2** and **Figures 2A–C**). Individual participant data are also shown as pre-/post-rTMS values (**Figures 2D–F**).

The absolute change in Glx level was greater in the active vs. sham rTMS group [$F_{(1,19)} = 6.54$, $p = 0.02$ (FDR_{corr} $p = 0.06$), Cohen's $f = 0.59$], whereas rTMS groups did not differ on change in absolute GABA+ level [$F_{(1,19)} = 0.89$, $p = 0.36$] or GABA+/Glx ratio [$F_{(1,19)} = 0.005$, $p = 0.94$] (**Figures 2G–I**). Given the apparent unequal variances between our absolute value Glx change data, we performed a Levene's test to assess homogeneity of variance across active/sham groups, confirming the variances differed between groups [$F_{(1,20)} = 9.68$, $p < 0.05$]. Welch's t-test was then used to test for between-group differences, as appropriate when variances differ between groups; absolute Glx level change remained significantly different between active/sham groups [$t_{(16)} = 16.22$, $p = 0.02$]. To further confirm our results, we log-transformed our absolute value Glx change data, and confirmed the Levene's test was not significant for our transformed data [$F_{(1,20)} = 0.04$, $p = 0.85$] before proceeding. We then re-ran our original analysis using the log-transformed data (in order to include age as a covariate as per our original analysis), and found absolute Glx level change remained significantly different between active/sham groups [$F_{(1,19)} = 6.2$, $p = 0.02$].

Repetitive transcranial magnetic stimulation group significantly moderated the relationship between baseline Glx and pre/post-rTMS Glx change [$F_{(1,17)} = 4.78$, $p = 0.04$, Cohen's $f = 0.53$] (**Figure 3A**). Simple effects analysis (Aiken and West, 1991) revealed that baseline Glx predicted pre/post-rTMS Glx change in the active [$b = 1.52$, $SE = 0.32$, $t_{(17)} = 4.74$, $p < 0.001$] but not the sham rTMS group [$b = 0.13$, $SE = 0.55$, $t_{(17)} = 0.24$, $p = 0.81$].

For visualization purposes, participants were divided according to the baseline Glx level by median split (median Glx level across all ASD participants = 0.12), and pre/post-rTMS Glx level for each participant was plotted. Participants in the active rTMS group whose baseline Glx levels were below the median had post-rTMS Glx levels that were higher, whereas participants whose baseline Glx levels were above the median had post-rTMS Glx levels that were similar or lower (**Figure 3B**). In contrast, post-rTMS Glx levels for participants in the sham rTMS group remained similar to their baseline Glx levels (**Figure 3B**).

Given that the DLPFC was stimulated bilaterally, yet MRS was acquired unilaterally, significant analyses were re-analyzed, adjusting for stimulation site order instead of age. Results remained unchanged; the absolute change in Glx level was greater in the active vs. sham rTMS group [$F_{(1,19)} = 6.46$, $p = 0.02$ (FDR_{corr} $p = 0.06$), Cohen's $f = 0.58$]. rTMS group significantly moderated the relationship between baseline Glx and pre/post-rTMS Glx change [$F_{(1,17)} = 4.97$, $p = 0.04$, Cohen's $f = 0.54$], and simple effects analysis revealed that baseline Glx predicted pre/post-rTMS Glx change in the active [$b = 1.50$, $SE = 0.37$, $t_{(17)} = 4.02$, $p < 0.001$] but not the sham-rTMS group [$b = 0.07$, $SE = 0.56$, $t_{(17)} = 0.14$, $p = 0.89$].

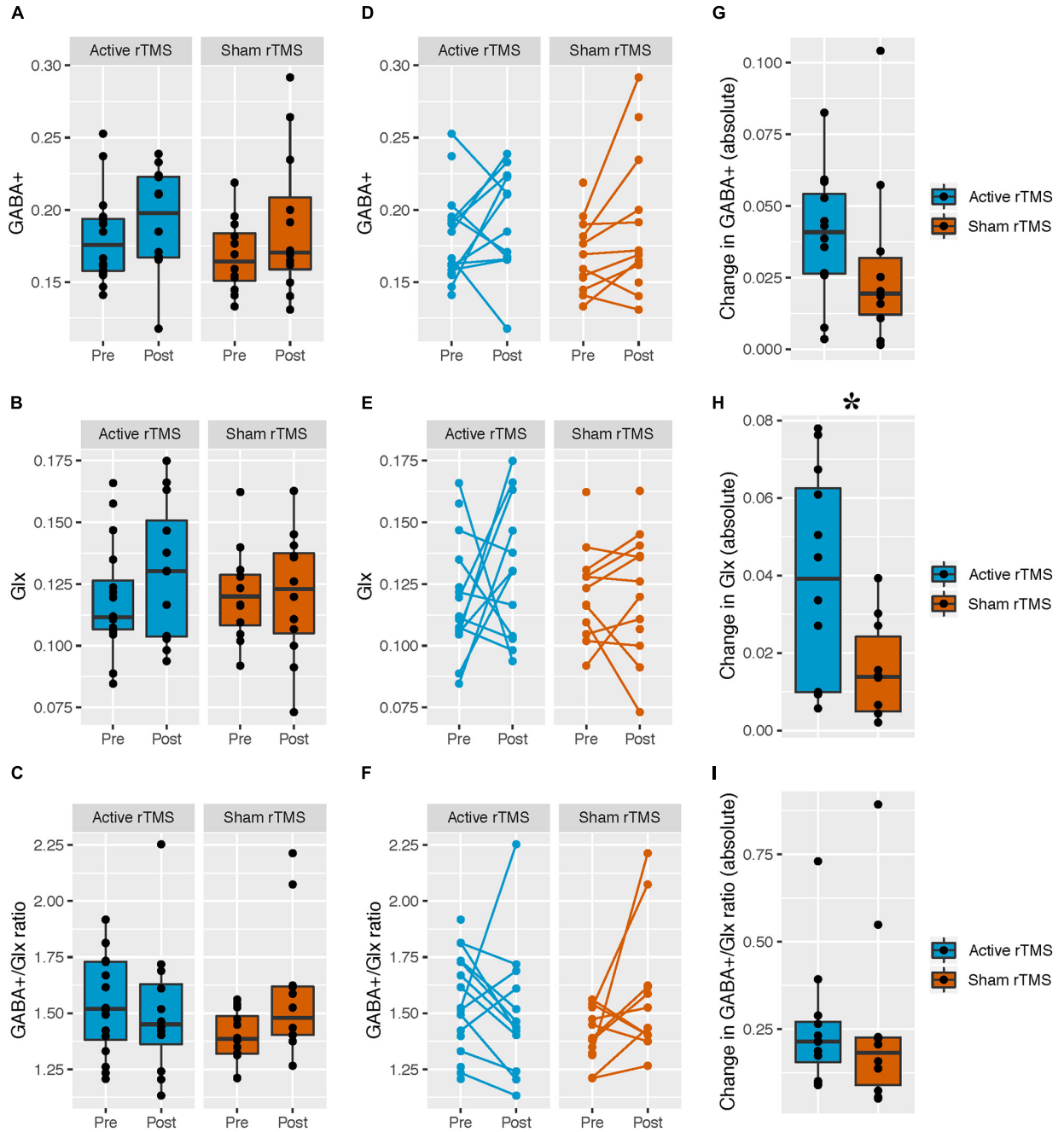

FIGURE 2 | Pre- and post-rTMS GABA+, Glx, and GABA+/Glx ratio, in the left dorsolateral prefrontal cortex (DLPFC). **(A–C)** Levels of pre- and post-rTMS metabolites (GABA+, Glx) and the GABA+/Glx ratio, in the full ASD sample with MRS data; active rTMS (pre: $n = 16$; post: $n = 12$), sham rTMS (pre: $n = 12$; post: $n = 12$). Black lines denote the group medians. **(D–F)** Each participant is indicated by a pre-/post-rTMS pair of points, connected by a line. Unconnected points are from participants with MRS scans at a single time point. Active rTMS (pre: $n = 16$; post: $n = 12$), sham rTMS (pre: $n = 12$; post: $n = 12$). **(G–I)** The absolute value of the change in metabolites from pre- to post-rTMS in the ASD sample with matched pre- and post-rTMS scans only; active rTMS ($n = 12$), sham rTMS ($n = 10$). Black lines denote the group medians. *The absolute value change in Glx level was greater in the active compared to the sham rTMS group [$F_{(1,19)} = 6.54$, $p = 0.02$].

Although no formal analyses were undertaken to assess corresponding behavior changes with metabolite level change, qualitative data relating pre-post rTMS Glx level change to change in executive function outcome measures are provided in **Supplementary Figure 2**.

DISCUSSION

Using MRS, we compared GABA+ and Glx levels in young adults with ASD and clinically significant executive function deficits, prior to (baseline) and following their participation in

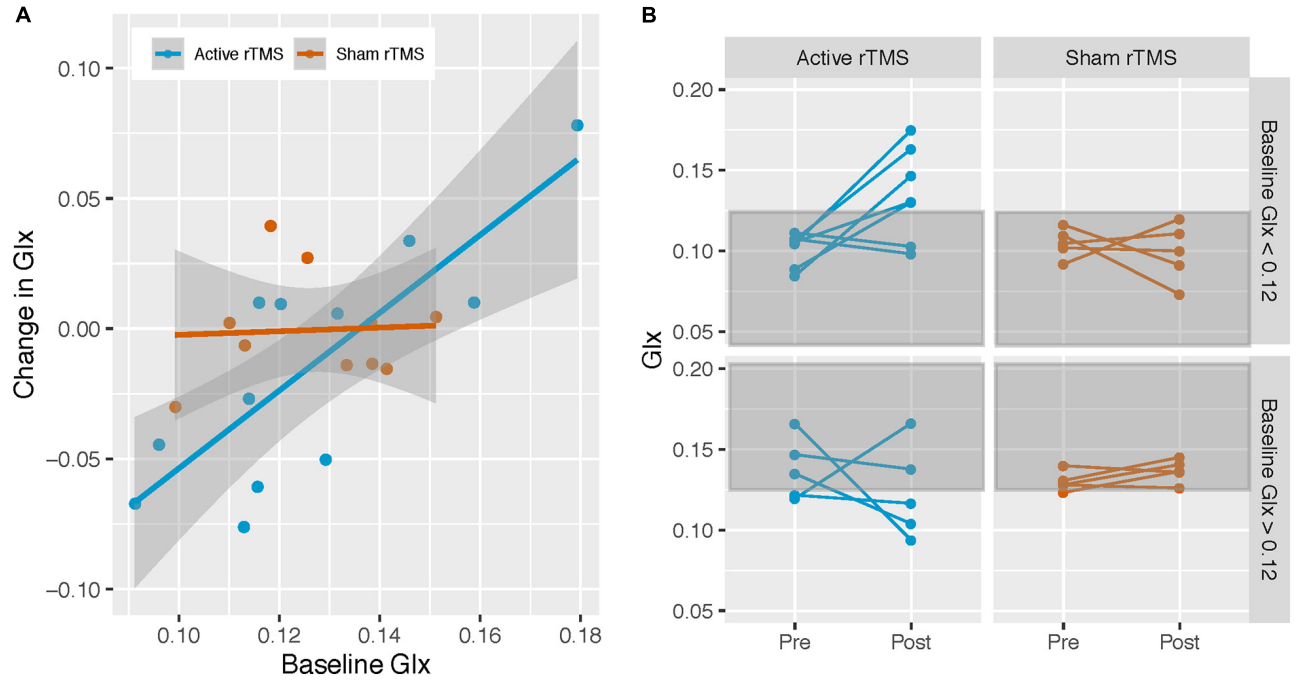

FIGURE 3 | Active rTMS modulates Glx levels. **(A)** Associations between Glx levels at baseline, and change in Glx from pre- to post-rTMS in the left dorsolateral prefrontal cortex (DLPFC), in the active and sham rTMS groups; active rTMS ($n = 12$), sham rTMS ($n = 10$). Baseline Glx was associated with Glx change in the active rTMS group only: $b = 1.49$, $SE = 0.31$, $t_{(18)} = 4.77$, $p < 0.001$. **(B)** To visually demonstrate that Glx level increased in participants with lower baseline Glx levels, and that Glx level decreased in participants with higher baseline Glx levels, in the active rTMS group only, participants were stratified according to the median split of the baseline Glx level (median Glx level for entire ASD sample = 0.12) and their pre-/post-rTMS pair of points were plotted.

a pilot randomized, double-blind, sham-controlled rTMS trial (20 sessions of active vs. sham rTMS to DLPFC) that tested the feasibility and preliminary efficacy of rTMS for the treatment of executive function deficits. Baseline metabolite levels from the entire ASD group were also compared to a TDC group with data available for the same baseline time-point. Our results suggest that while levels of GABA+, Glx, and their ratio, in the left DLPFC, may not differ in emerging adults with vs. without ASD, active rTMS can modulate Glx levels in individuals with ASD, and that the direction of change is associated with baseline Glx levels. Our results build on prior evidence in non-ASD samples that MRS appears to be sensitive to changes in cortical metabolism following rTMS.

Our findings based on the comparison of neurometabolite levels at baseline in ASD vs. TDC align with several studies, particularly in adult samples, that did not detect GABA + and/or Glx differences between participants with ASD vs. TDCs in prefrontal brain regions [i.e., the left DLPFC (Horder et al., 2013; Endres et al., 2017), right DLPFC (Kirkovski et al., 2018), dorsomedial prefrontal cortex (Ajram et al., 2017; Pretzsch et al., 2019a), and medial prefrontal cortex (Aoki et al., 2012; Carvalho Pereira et al., 2018)]. In contrast, our findings do not align with two studies conducted in children, which report reduced GABA+ and/or Glx levels in the frontal lobe of ASD vs. TDC participants (Harada et al., 2011; Kubas et al., 2012), suggesting that alterations could be more pronounced at the diagnostic group level earlier in development. GABA is critical for the functional maturation of the central nervous system, and dysfunctional GABA is thought to play a role in multiple neurodevelopmental disorders, including ASD (Smith-Hicks, 2013). Thus, even if GABA levels normalize by adulthood in individuals with ASD, it remains possible that the presence of altered GABA levels during childhood could contribute to atypical neurodevelopment. Moreover, aberrant excitatory-inhibitory neurotransmission in ASD may not manifest as uniformly higher or lower metabolite levels, which could conceal group-wise ASD-TDC differences. Interestingly, associations between GABA+ levels and scores on the Autism Spectrum Questionnaire (Brix et al., 2015) and Autism Diagnostic Interview–Revised (Carvalho Pereira et al., 2018) have been reported, despite the absence of between group (ASD vs. TDC) GABA+ level differences. Therefore, the capacity to alter metabolite levels within the GABA/glutamate neurotransmitter pathways may remain an important therapeutic target in individuals with ASD, irrespective of the presence or absence of ASD-TDC group differences.

In the current study, we found increased Glx level change following active but not sham rTMS. Our findings align with a number of prior MRS studies, conducted across healthy, depressed and schizophrenia samples, that demonstrate excitatory rTMS to left DLPFC alters the glutamatergic system (Michael et al., 2003; Luborzewski et al., 2007; Croarkin et al., 2016; Dlabac-de Lange et al., 2017). In our clinical trial sample of ASD participants with executive function impairment, Glx level change following active rTMS was associated with baseline

Glx levels. A recent MRS study in participants with ASD also found that Glx level change following an intervention with cannabivarin (CBDV) (a cannabinoid compound) was associated with baseline Glx level in the basal ganglia (Pretzsch et al., 2019b). Moreover, neither our rTMS intervention, nor the CBVD intervention (Pretzsch et al., 2019b) had any impact on GABA+ levels in ASD. GABA, glutamate and glutamine are constantly in flux, and the final conversion to GABA is dependent upon the GAD enzyme. Within the GABA/glutamate metabolic pathways, Glx level change may be achieved more readily, as both glutamate and glutamine exist earlier along the conversion chain, and the enzyme required for the final conversion to GABA may be altered in some individuals with ASD (Yip et al., 2007). However, our findings may not be specific to ASD (or individuals with ASD and executive function impairments). Namely, a study conducted in healthy participants found that active (20 Hz) but not sham rTMS to left DLPFC increased Glx in the cingulate cortex, and that increases were most prominent in participants with lower baseline Glx (Michael et al., 2003). The observed modulation of Glx following active rTMS found here aligns with the concept of homeostatic plasticity (Daskalakis et al., 2006). Given that rTMS modifies brain physiology, it follows that its effect would depend upon an individual's unique physiology during stimulation. In light of evidence that unilateral rTMS can alter contralateral cortical excitability (Plewnia et al., 2003), stimulation site order could conceivably induce different physiological effects in each hemisphere; however, our findings remained unchanged when we controlled for stimulation site order. Moreover, while unilateral (left DLPFC) stimulation is more common in the literature (Michael et al., 2003; Luborzewski et al., 2007; Zheng et al., 2010; Croarkin et al., 2016; Dubin et al., 2016; Baeken et al., 2017; Levitt et al., 2019), there is prior evidence that bilateral stimulation to DLPFC increases Glx levels in the left DLPFC of individuals with schizophrenia (Dlabac-de Lange et al., 2017). However, as with our study, Dlabac-de Lange et al. (2017) did not collect MRS data from the right DLPFC, despite stimulating the DLPFC bilaterally.

Some limitations to the present study warrant mention. First, our pilot clinical trial sample size is limited and usable MRS data for the rTMS intervention group was available for 28/40 participants from the full clinical trial. Pre/post MRS data was further limited to 22/40 clinical trial participants. We note that our sample size was smaller than anticipated due to the challenges of collecting pre/post imaging data in a complex clinical sample and based on our adherence to rigorous quality control of MRS data (which we consider a relative strength of our study). The published study from our pilot clinical trial found that participants with ASD and executive function deficits that also had lower adaptive (everyday) functioning exhibited improvements in spatial working memory following active rTMS (Ameis et al., 2020). Though we had hoped to relate metabolite change with behavior, owing to the sample size of participants with complete pre/post MRS data, we did not undertake statistical analyses to evaluate the relations between metabolites, cognition, and behavior due to concerns that the sample is underpowered to undertake such analyses and multiple testing may contribute to spurious findings. Therefore, the clinical meaningfulness of our presented findings remains unclear. While our findings are promising and align with previous evidence of excitatory rTMS effects on Glx, our results in ASD must be considered preliminary and are in need of replication in a larger sample with the opportunity to examine relationships with clinical outcomes. Second, our findings may not be broadly generalizable. Specifically, this study included emerging adults with ASD with clinically significant executive function impairments, thus our findings may not be generalizable to individuals across the autism spectrum. Relatedly, as the TDC group did not receive rTMS, we were not able to test whether rTMS-induced modulation of Glx is unique to our ASD sample. However, rTMS effects on Glx have been reported previously in non-ASD samples (Michael et al., 2003). Moreover, concurrent medication in the ASD groups may have affected GABA+ and Glx levels, though sample size constraints precluded investigations of medication effects. It would be valuable for future studies to compare metabolite levels across ASD and clinical samples taking similar medications (e.g., stimulants, SSRIs). We chose not to covary for medication in our analyses, as medications used were highly heterogeneous, with potential for variable effects on the excitation-inhibition system. Further, we did not collect race/ethnicity data as part of our clinical trial. We primarily recruited participants from a publicly funded mental health clinic at our Center with specific policies in place to ensure equitable access to care across the city of Toronto. We therefore expect our sample would be broadly in line with the diverse composition of the city of Toronto. Third, neurometabolites were evaluated from a single voxel in the left DLPFC, yet rTMS was administered to bilateral DLPFC in a sequential order throughout the clinical trial. Future bilateral rTMS studies in ASD should acquire MRS data bilaterally to help tease apart potential hemispheric differences in neurophysiological effects following rTMS. Fourth, the relative amounts of glutamine and glutamate that contribute to the Glx signal could not be differentiated with the MEGA-PRESS sequence used. However, it is likely that the Glx signal predominantly reflects glutamate as glutamate is present in higher concentrations than glutamine in the brain, and glutamine can be below the detection limit of MRS (e.g., <1 mM) (Hancu and Port, 2011). The stability of water-referenced GABA and Glx using MEGA-PRESS has been demonstrated in the same individual over a 3-month period (Ferland et al., 2019), and a large multi-site study demonstrated that water-referenced GABA is a viable and reliable method to quantify GABA levels *in vivo* (Mikkelsen et al., 2019). Of note, GABA+ measurements reflect GABA plus underlying macromolecules, and it is unknown if/how macromolecules are altered in pathology. Fifth, metabolite levels are typically assessed within 24 h post-rTMS, though Glx levels in depressed adolescents have been shown to increase for up to 6-months post stimulation (Croarkin et al., 2016). Thus, we may not have captured the full extent of metabolite level change induced by rTMS, and future studies including a longer follow-up period will be required to clarify this. Lastly, due to the small number of females included in our sample, we were unable to assess how sex/gender modulate the present findings. Notably, the active rTMS group had

a larger (though non-significant) proportion of females than the sham rTMS group. The published study from this pilot clinical trial found an interaction effect between rTMS group, time and sex on executive functioning, such that executive functioning improved to a greater extent in females in the active vs. sham group (Ameis et al., 2020). Recent neuroimaging work suggests that imbalanced excitation-inhibition within social-cognitive brain regions may be more pronounced in males vs. females with ASD (Trakoshis et al., 2020). Thus, future clinical trials should consider sex/gender, when possible. Future trials should also consider relations between neurometabolite levels and depressive symptoms in young adults with ASD, especially given recent preliminary evidence that rTMS to the DLPFC may improve depressive symptoms in adults with ASD (Gwynette et al., 2020).

Given that modulation of corticospinal excitability is thought to involve glutamatergic and/or GABAergic receptor pathways (Huang et al., 2007; Stagg et al., 2009), it is promising that we found rTMS to be a useful probe and modulator of the glutamatergic system in individuals with ASD. The current finding that rTMS yields a change in Glx that is measurable with MRS builds on prior similar findings in non-ASD samples and is encouraging for future studies aimed at better understanding the mechanism of action of rTMS in the service of harnessing its interventional potential. Uncovering how baseline metabolite levels relate to metabolite level change and clinical outcomes across different clinical populations could meaningfully inform future rTMS study designs in ASD and beyond.

DATA AVAILABILITY STATEMENT

The datasets presented in this article are not readily available because we do not have consent to share this data.

ETHICS STATEMENT

The studies involving human participants were reviewed and approved by The Centre for Addiction and Mental Health (CAMH) Research Ethics Board (REB; protocol #119-2013). This study was registered with Clinicaltrials.gov (ID: NCT02311751). All participants provided written informed consent to participate in the current study. Written informed consent from the participants' legal guardian/next of kin was not required to participate in this study in accordance with the national legislation and the institutional requirements.

AUTHOR CONTRIBUTIONS

SHA, PS, ZJD, DMB, PD, NS, M-CL, PEC and IM-E contributed to the design of this work. REL, M-CL, and SHA collected the data. PT and PS advised on the MRS analyses. IM-E, NJF, and HT analyzed the data. IM-E and SHA interpreted the data and drafted this work. All the authors reviewed, edited, and approved a final version.

FUNDING

This publication was made possible through the American Academy of Child and Adolescent Psychiatry (AACAP) Pilot Research Award for Child and Adolescent Psychiatry Residents and Junior Faculty (to SHA), supported by CFAK; its contents are the responsibility of the authors and do not necessarily reflect the official views of AACAP. This research was also supported by: the University of Toronto, Temerty Faculty of Medicine, Dean's Fund New Staff Grant, the Innovation Fund from the Alternate Funding Plan of the Academic Health Sciences Centres of Ontario, an Ontario Mental Health Foundation (OMHF) Project A Grant and OMHF New investigator Fellowship (to SHA).

SUPPLEMENTARY MATERIAL

The Supplementary Material for this article can be found online at: https://www.frontiersin.org/articles/10.3389/fnins.2021.711542/full#supplementary-material

REFERENCES

Aiken, L. S., and West, S. G. (1991). *Multiple Regression: Testing and Interpreting Interactions*. Thousand Oaks: Sage Publications, Inc.

Ajram, L. A., Horder, J., Mendez, M. A., Galanopoulos, A., Brennan, L. P., Wichers, R. H., et al. (2017). Shifting brain inhibitory balance and connectivity of the prefrontal cortex of adults with autism spectrum disorder. *Transl. Psychiatry* 7:e1137. doi: 10.1038/tp.2017.104

Ajram, L. A., Pereira, A. C., Durieux, A. M. S., Velthius, H. E., Petrinovic, M. M., and McAlonan, G. M. (2019). The contribution of [1H] magnetic resonance spectroscopy to the study of excitation-inhibition in autism. *Prog. Neuropsychopharmacol. Biol. Psychiatry* 89, 236–244. doi: 10.1016/j.pnpbp.2018.09.010

Ameis, S. H., Blumberger, D. M., Croarkin, P. E., Mabbott, D. J., Meng-Chuan, L., Desarkar, P., et al. (2020). Treatment of executive function deficits in autism spectrum disorder with repetitive transcranial magnetic stimulation: a double-blind, sham-controlled, pilot trial. *Brain Stimul.* 13, 539–547.

Ameis, S. H., Daskalakis, Z. J., Blumberger, D. M., Desarkar, P., Drmic, I., Mabbott, D. J., et al. (2017). Repetitive transcranial magnetic stimulation for the treatment of executive function deficits in autism spectrum disorder: clinical trial approach. *J. Child Adolesc. Psychopharmacol.* 27, 413–421. doi: 10.1089/cap.2016.0146

Aoki, Y., Abe, O., Yahata, N., Kuwabara, H., Natsubori, T., Iwashiro, N., et al. (2012). Absence of age-related prefrontal NAA change in adults with autism spectrum disorders. *Transl. Psychiatry* 2:e178. doi: 10.1038/tp.2012.108

Baeken, C., Lefaucheur, J. P., and Van Schuerbeek, P. (2017). The impact of accelerated high frequency rTMS on brain neurochemicals in treatment-resistant depression: insights from (1)H MR spectroscopy. *Clin. Neurophysiol.* 128, 1664–1672. doi: 10.1016/j.clinph.2017.06.243

Bak, L. K., Schousboe, A., and Waagepetersen, H. S. (2006). The glutamate/GABA-glutamine cycle: aspects of transport, neurotransmitter homeostasis and ammonia transfer. *J. Neurochem.* 98, 641–653. doi: 10.1111/j.1471-4159.2006.03913.x

Barahona-Correa, J. B., Velosa, A., Chainho, A., Lopes, R., and Oliveira-Maia, A. J. (2018). repetitive transcranial magnetic stimulation for treatment of

autism spectrum disorder: a systematic review and meta-analysis. *Front. Integr. Neurosci.* 12:27. doi: 10.3389/fnint.2018.00027

Barr, M. S., Farzan, F., Rajji, T. K., Voineskos, A. N., Blumberger, D. M., Arenovich, T., et al. (2013). Can repetitive magnetic stimulation improve cognition in schizophrenia? Pilot data from a randomized controlled trial. *Biol. Psychiatry* 73, 510–517. doi: 10.1016/j.biopsych.2012.08.020

Baruth, J. M., Casanova, M. F., El-Baz, A., Horrell, T., Mathai, G., Sears, L., et al. (2010). Low-frequency repetitive transcranial magnetic stimulation (rTMS) modulates evoked-gamma frequency oscillations in autism spectrum disorder (ASD). *J. Neurother.* 14, 179–194. doi: 10.1080/10874208.2010.501500

Benjamini, Y., and Hochberg, Y. (1995). Controlling the false discovery rate: a practical and powerful approach to multiple testing. *J. R. Stat. Soc. Series B (Methodol.)* 57, 289–300.

Benson, N., Hulac, D. M., and Kranzler, J. H. (2010). Independent examination of the wechsler adult intelligence scale-fourth edition (WAIS-IV): what does the WAIS-IV measure? *Psychol. Assess.* 22, 121–130. doi: 10.1037/a0017767

Bernardi, S., Anagnostou, E., Shen, J., Kolevzon, A., Buxbaum, J. D., Hollander, E., et al. (2011). In vivo 1H-magnetic resonance spectroscopy study of the attentional networks in autism. *Brain Res.* 1380, 198–205. doi: 10.1016/j.brainres.2010.12.057

Brix, M. K., Ersland, L., Hugdahl, K., Gruner, R., Posserud, M. B., Hammar, A., et al. (2015). Brain MR spectroscopy in autism spectrum disorder-the GABA excitatory/inhibitory imbalance theory revisited. *Front. Hum. Neurosci.* 9:365. doi: 10.3389/fnhum.2015.00365

Brown, M. S., Singel, D., Hepburn, S., and Rojas, D. C. (2013). Increased glutamate concentration in the auditory cortex of persons with autism and first-degree relatives: a (1)H-MRS study. *Autism Res.* 6, 1–10. doi: 10.1002/aur.1260

Carvalho Pereira, A., Violante, I. R., Mouga, S., Oliveira, G., and Castelo-Branco, M. (2018). Medial frontal lobe neurochemistry in autism spectrum disorder is marked by reduced N-Acetylaspartate and unchanged gamma-aminobutyric acid and glutamate + glutamine levels. *J. Autism Dev. Disord.* 48, 1467–1482. doi: 10.1007/s10803-017-3406-8

Casanova, M. F., Baruth, J. M., El-Baz, A., Tasman, A., Sears, L., and Sokhadze, E. (2012). Repetitive transcranial magnetic stimulation (rTMS) modulates event-related potential (ERP) indices of attention in autism. *Transl. Neurosci.* 3, 170–180. doi: 10.2478/s13380-012-0022-0

Choi, I. Y., Lee, S. P., Merkle, H., and Shen, J. (2006). In vivo detection of gray and white matter differences in GABA concentration in the human brain. *Neuroimage* 33, 85–93. doi: 10.1016/j.neuroimage.2006.06.016

Croarkin, P. E., Nakonezny, P. A., Wall, C. A., Murphy, L. L., Sampson, S. M., Frye, M. A., et al. (2016). Transcranial magnetic stimulation potentiates glutamatergic neurotransmission in depressed adolescents. *Psychiatry Res. Neuroimaging* 247, 25–33. doi: 10.1016/j.pscychresns.2015.11.005

Da Silva, T., Hafizi, S., Rusjan, P. M., Houle, S., Wilson, A. A., Prce, I., et al. (2019). GABA levels and TSPO expression in people at clinical high risk for psychosis and healthy volunteers: a PET-MRS study. *J. Psychiatry Neurosci.* 44, 111–119. doi: 10.1503/jpn.170201

Daskalakis, Z. J., Moller, B., Christensen, B. K., Fitzgerald, P. B., Gunraj, C., and Chen, R. (2006). The effects of repetitive transcranial magnetic stimulation on cortical inhibition in healthy human subjects. *Exp. Brain Res.* 174, 403–412. doi: 10.1007/s00221-006-0472-0

Dayan, E., Censor, N., Buch, E. R., Sandrini, M., and Cohen, L. G. (2013). Noninvasive brain stimulation: from physiology to network dynamics and back. *Nat. Neurosci.* 16, 838–844. doi: 10.1038/nn.3422

Dlabac-de Lange, J. J., Liemburg, E. J., Bais, L., van de Poel-Mustafayeva, A. T., de Lange-de Klerk, E. S. M., Knegtering, H., et al. (2017). Effect of Bilateral Prefrontal rTMS on left prefrontal NAA and Glx levels in schizophrenia patients with predominant negative symptoms: an exploratory study. *Brain Stimul.* 10, 59–64. doi: 10.1016/j.brs.2016.08.002

Dubin, M. J., Mao, X., Banerjee, S., Goodman, Z., Lapidus, K. A., Kang, G., et al. (2016). Elevated prefrontal cortex GABA in patients with major depressive disorder after TMS treatment measured with proton magnetic resonance spectroscopy. *J. Psychiatry Neurosci.* 41, E37–E45. doi: 10.1503/jpn.150223

Edden, R. A., Puts, N. A., Harris, A. D., Barker, P. B., and Evans, C. J. (2014). Gannet: a batch-processing tool for the quantitative analysis of gamma-aminobutyric acid-edited MR spectroscopy spectra. *J. Magn. Reson Imaging* 40, 1445–1452. doi: 10.1002/jmri.24478

Endres, D., Tebartz, van Elst, L., Meyer, S. A., Feige, B., Nickel, K., et al. (2017). Glutathione metabolism in the prefrontal brain of adults with high-functioning autism spectrum disorder: an MRS study. *Mol. Autism* 8:10. doi: 10.1186/s13229-017-0122-3

Enticott, P. G., Fitzgibbon, B. M., Kennedy, H. A., Arnold, S. L., Elliot, D., Peachey, A., et al. (2014). A double-blind, randomized trial of deep repetitive transcranial magnetic stimulation (rTMS) for autism spectrum disorder. *Brain Stimul.* 7, 206–211. doi: 10.1016/j.brs.2013.10.004

Ferland, M. C., Therrien-Blanchet, J. M., Lefebvre, G., Klees-Themens, G., Proulx, S., and Theoret, H. (2019). Longitudinal assessment of (1)H-MRS (GABA and Glx) and TMS measures of cortical inhibition and facilitation in the sensorimotor cortex. *Exp. Brain Res.* 237, 3461–3474. doi: 10.1007/s00221-019-05691-z

Ford, T. C., and Crewther, D. P. (2016). A comprehensive review of the (1)H-MRS metabolite spectrum in autism spectrum disorder. *Front. Mol. Neurosci.* 9:14. doi: 10.3389/fnmol.2016.00014

Gasparovic, C., Song, T., Devier, D., Bockholt, H. J., Caprihan, A., Mullins, P. G., et al. (2006). Use of tissue water as a concentration reference for proton spectroscopic imaging. *Magn. Reson. Med.* 55, 1219–1226. doi: 10.1002/mrm.20901

George, M. S., Padberg, F., Schlaepfer, T. E., O'Reardon, J. P., Fitzgerald, P. B., Nahas, Z. H., et al. (2009). Controversy: repetitive transcranial magnetic stimulation or transcranial direct current stimulation shows efficacy in treating psychiatric diseases (depression, mania, schizophrenia, obsessive-complusive disorder, panic, posttraumatic stress disorder). *Brain Stimul.* 2, 14–21. doi: 10.1016/j.brs.2008.06.001

Gioia, G. A., Isquith, P. K., Retzlaff, P. D., and Espy, K. A. (2002). Confirmatory factor analysis of the behavior rating inventory of executive function (BRIEF) in a clinical sample. *Child Neuropsychol.* 8, 249–257. doi: 10.1076/chin.8.4.249.13513

Guse, B., Falkai, P., and Wobrock, T. (2010). Cognitive effects of high-frequency repetitive transcranial magnetic stimulation: a systematic review. *J. Neural Transm. (Vienna)* 117, 105–122. doi: 10.1007/s00702-009-0333-7

Gwynette, M. F., Lowe, D. W., Henneberry, E. A., Sahlem, G. L., Wiley, M. G., Alsarraf, H., et al. (2020). Treatment of adults with autism and major depressive disorder using transcranial magnetic stimulation: an open label pilot study. *Autism Res.* 13, 346–351. doi: 10.1002/aur.2266

Hancu, I., and Port, J. (2011). The case of the missing glutamine. *NMR Biomed.* 24, 529–535. doi: 10.1002/nbm.1620

Harada, M., Taki, M. M., Nose, A., Kubo, H., Mori, K., Nishitani, H., et al. (2011). Non-invasive evaluation of the GABAergic/glutamatergic system in autistic patients observed by MEGA-editing proton MR spectroscopy using a clinical 3 tesla instrument. *J. Autism Dev. Disord.* 41, 447–454. doi: 10.1007/s10803-010-1065-0

Harris, A. D., Puts, N. A., and Edden, R. A. (2015). Tissue correction for GABA-edited MRS: considerations of voxel composition, tissue segmentation, and tissue relaxations. *J. Magn. Reson. Imaging* 42, 1431–1440. doi: 10.1002/jmri.24903

Horder, J., Lavender, T., Mendez, M. A., O'Gorman, R., Daly, E., Craig, M. C., et al. (2013). Reduced subcortical glutamate/glutamine in adults with autism spectrum disorders: a [(1)H]MRS study. *Transl. Psychiatry* 3:e279. doi: 10.1038/tp.2013.53

Horder, J., Petrinovic, M. M., Mendez, M. A., Bruns, A., Takumi, T., Spooren, W., et al. (2018). Glutamate and GABA in autism spectrum disorder-a translational magnetic resonance spectroscopy study in man and rodent models. *Transl. Psychiatry* 8:106. doi: 10.1038/s41398-018-0155-1

Huang, Y. Z., Chen, R. S., Rothwell, J. C., and Wen, H. Y. (2007). The after-effect of human theta burst stimulation is NMDA receptor dependent. *Clin. Neurophysiol.* 118, 1028–1032. doi: 10.1016/j.clinph.2007.01.021

Kearney-Ramos, T. E., Dowdle, L. T., Mithoefer, O. J., Devries, W., George, M. S., and Hanlon, C. A. (2019). State-dependent effects of ventromedial prefrontal cortex continuous thetaburst stimulation on cocaine cue reactivity in chronic cocaine users. *Front. Psychiatry* 10:317. doi: 10.3389/fpsyt.2019.00317

Kirkovski, M., Suo, C., Enticott, P. G., Yucel, M., and Fitzgerald, P. B. (2018). Short communication: sex-linked differences in gamma-aminobutyric acid (GABA)

are related to social functioning in autism spectrum disorder. *Psychiatry Res. Neuroimaging* 274, 19–22. doi: 10.1016/j.pscychresns.2018.02.004

Kubas, B., Kulak, W., Sobaniec, W., Tarasow, E., Lebkowska, U., and Walecki, J. (2012). Metabolite alterations in autistic children: a 1H MR spectroscopy study. *Adv. Med. Sci.* 57, 152–156. doi: 10.2478/v10039-012-0014-x

Lai, M. C., Anagnostou, E., Wiznitzer, M., Allison, C., and Baron-Cohen, S. (2020). Evidence-based support for autistic people across the lifespan: maximising potential, minimising barriers, and optimising the person-environment fit. *Lancet Neurol.* 19, 434–451. doi: 10.1016/S1474-4422(20)30034-X

Leuchter, A. F., Cook, I. A., Jin, Y., and Phillips, B. (2013). The relationship between brain oscillatory activity and therapeutic effectiveness of transcranial magnetic stimulation in the treatment of major depressive disorder. *Front. Hum. Neurosci.* 7:37. doi: 10.3389/fnhum.2013.00037

Levitt, J. G., Kalender, G., O'Neill, J., Diaz, J. P., Cook, I. A., Ginder, N., et al. (2019). Dorsolateral prefrontal gamma-aminobutyric acid in patients with treatment-resistant depression after transcranial magnetic stimulation measured with magnetic resonance spectroscopy. *J. Psychiatry Neurosci.* 44, 386–394. doi: 10.1503/jpn.180230

Lord, C., Risi, S., Lambrecht, L., Cook, E. H. Jr., Leventhal, B. L., DiLavore, P. C., et al. (2000). The autism diagnostic observation schedule-generic: a standard measure of social and communication deficits associated with the spectrum of autism. *J. Autism Dev. Disord.* 30, 205–223.

Low, R. N., Francis, I. R., Herfkens, R. J., Jeffrey, R. B. Jr., Glazer, G. M., Foo, T. K., et al. (1993). Fast multiplanar spoiled gradient-recalled imaging of the liver: pulse sequence optimization and comparison with spin-echo MR imaging. *AJR Am. J. Roentgenol.* 160, 501–509. doi: 10.2214/ajr.160.3.8381572

Luborzewski, A., Schubert, F., Seifert, F., Danker-Hopfe, H., Brakemeier, E. L., Schlattmann, P., et al. (2007). Metabolic alterations in the dorsolateral prefrontal cortex after treatment with high-frequency repetitive transcranial magnetic stimulation in patients with unipolar major depression. *J. Psychiatr. Res.* 41, 606–615. doi: 10.1016/j.jpsychires.2006.02.003

Lujan, R., Shigemoto, R., and Lopez-Bendito, G. (2005). Glutamate and GABA receptor signalling in the developing brain. *Neuroscience* 130, 567–580. doi: 10.1016/j.neuroscience.2004.09.042

Michael, N., Gosling, M., Reutemann, M., Kersting, A., Heindel, W., Arolt, V., et al. (2003). Metabolic changes after repetitive transcranial magnetic stimulation (rTMS) of the left prefrontal cortex: a sham-controlled proton magnetic resonance spectroscopy (1H MRS) study of healthy brain. *Eur. J. Neurosci.* 17, 2462–2468. doi: 10.1046/j.1460-9568.2003.02683.x

Mikkelsen, M., Rimbault, D. L., Barker, P. B., Bhattacharyya, P. K., Brix, M. K., Buur, P. F., et al. (2019). Big GABA II: water-referenced edited MR spectroscopy at 25 research sites. *Neuroimage* 191, 537–548. doi: 10.1016/j.neuroimage.2019.02.059

Oberman, L., Eldaief, M., Fecteau, S., Ifert-Miller, F., Tormos, J. M., and Pascual-Leone, A. (2012). Abnormal modulation of corticospinal excitability in adults with Asperger's syndrome. *Eur. J. Neurosci.* 36, 2782–2788. doi: 10.1111/j.1460-9568.2012.08172.x

Oberman, L. M., Ifert-Miller, F., Najib, U., Bashir, S., Heydrich, J. G., Picker, J., et al. (2016). Abnormal mechanisms of plasticity and metaplasticity in autism spectrum disorders and fragile X syndrome. *J. Child. Adolesc. Psychopharmacol.* 26, 617–624. doi: 10.1089/cap.2015.0166

Page, L. A., Daly, E., Schmitz, N., Simmons, A., Toal, F., Deeley, Q., et al. (2006). In vivo 1H-magnetic resonance spectroscopy study of amygdala-hippocampal and parietal regions in autism. *Am. J. Psychiatry* 163, 2189–2192. doi: 10.1176/appi.ajp.163.12.2189

Plewnia, C., Lotze, M., and Gerloff, C. (2003). Disinhibition of the contralateral motor cortex by low-frequency rTMS. *Neuroreport* 14, 609–612. doi: 10.1097/00001756-200303240-00017

Polania, R., Nitsche, M. A., and Ruff, C. C. (2018). Studying and modifying brain function with non-invasive brain stimulation. *Nat. Neurosci.* 21, 174–187. doi: 10.1038/s41593-017-0054-4

Pretzsch, C. M., Freyberg, J., Voinescu, B., Lythgoe, D., Horder, J., Mendez, M. A., et al. (2019a). Effects of cannabidiol on brain excitation and inhibition systems; a randomised placebo-controlled single dose trial during magnetic resonance spectroscopy in adults with and without autism spectrum disorder. *Neuropsychopharmacology* 44, 1398–1405. doi: 10.1038/s41386-019-0333-8

Pretzsch, C. M., Voinescu, B., Lythgoe, D., Horder, J., Mendez, M. A., Wichers, R., et al. (2019b). Effects of cannabidivarin (CBDV) on brain excitation and inhibition systems in adults with and without Autism Spectrum Disorder (ASD): a single dose trial during magnetic resonance spectroscopy. *Transl. Psychiatry* 9:313. doi: 10.1038/s41398-019-0654-8

Provencher, S. W. (1993). Estimation of metabolite concentrations from localized in vivo proton NMR spectra. *Magn. Reson Med.* 30, 672–679. doi: 10.1002/mrm.1910300604

Rae, C. D. (2014). A guide to the metabolic pathways and function of metabolites observed in human brain 1H magnetic resonance spectra. *Neurochem. Res.* 39, 1–36. doi: 10.1007/s11064-013-1199-5

Sheehan, D. V., Lecrubier, Y., Sheehan, K. H., Amorim, P., Janavs, J., Weiller, E., et al. (1998). The mini-international neuropsychiatric interview (M.I.N.I.): the development and validation of a structured diagnostic psychiatric interview for DSM-IV and ICD-10. *J. Clin. Psychiatry* 59 (Suppl. 20), 22–33;quiz 34-57.,

Silvanto, J., Muggleton, N., and Walsh, V. (2008). State-dependency in brain stimulation studies of perception and cognition. *Trends Cogn. Sci.* 12, 447–454. doi: 10.1016/j.tics.2008.09.004

Simpson, R., Devenyi, G. A., Jezzard, P., Hennessy, T. J., and Near, J. (2017). Advanced processing and simulation of MRS data using the FID appliance (FID-A)-An open source, MATLAB-based toolkit. *Magn. Reson. Med.* 77, 23–33. doi: 10.1002/mrm.26091

Smith, S. A., Levante, T. O., Meier, B. H., and Ernst, R. R. (1994). Computer simulations in magnetic resonance. An object-oriented programming approach. *J. Magn. Reson. A* 106, 75–105.

Smith-Hicks, C. L. (2013). GABAergic dysfunction in pediatric neurodevelopmental disorders. *Front. Cell Neurosci.* 7:269. doi: 10.3389/fncel.2013.00269

Sokhadze, E. M., Baruth, J. M., Sears, L., Sokhadze, G. E., El-Baz, A. S., and Casanova, M. F. (2012). Prefrontal neuromodulation using rTMS improves error monitoring and correction function in autism. *Appl. Psychophysiol. Biofeedback* 37, 91–102. doi: 10.1007/s10484-012-9182-5

Sokhadze, E. M., El-Baz, A., Baruth, J., Mathai, G., Sears, L., and Casanova, M. F. (2009). Effects of low frequency repetitive transcranial magnetic stimulation (rTMS) on gamma frequency oscillations and event-related potentials during processing of illusory figures in autism. *J. Autism Dev. Disord.* 39, 619–634. doi: 10.1007/s10803-008-0662-7

Sokhadze, E. M., El-Baz, A. S., Sears, L. L., Opris, I., and Casanova, M. F. (2014). rTMS neuromodulation improves electrocortical functional measures of information processing and behavioral responses in autism. *Front. Syst. Neurosci.* 8:134. doi: 10.3389/fnsys.2014.00134

Sparrow, S. S., and Cicchetti, D. V. (1985). Diagnostic uses of the vineland adaptive behavior scales. *J. Pediatr. Psychol.* 10, 215–225. doi: 10.1093/jpepsy/10.2.215

Stagg, C. J., Wylezinska, M., Matthews, P. M., Johansen-Berg, H., Jezzard, P., Rothwell, J. C., et al. (2009). Neurochemical effects of theta burst stimulation as assessed by magnetic resonance spectroscopy. *J. Neurophysiol.* 101, 2872–2877. doi: 10.1152/jn.91060.2008

Tebartz van Elst, L., Maier, S., Fangmeier, T., Endres, D., Mueller, G. T., et al. (2014). Disturbed cingulate glutamate metabolism in adults with high-functioning autism spectrum disorder: evidence in support of the excitatory/inhibitory imbalance hypothesis. *Mol. Psychiatry* 19, 1314–1325. doi: 10.1038/mp.2014.62

Trakoshis, S., Martinez-Canada, P., Rocchi, F., Canella, C., You, W., Chakrabarti, B., et al. (2020). Intrinsic excitation-inhibition imbalance affects medial prefrontal cortex differently in autistic men versus women. *Elife* 9:e55684. doi: 10.7554/eLife.55684

Yip, J., Soghomonian, J. J., and Blatt, G. J. (2007). Decreased GAD67 mRNA levels in cerebellar Purkinje cells in autism: pathophysiological implications. *Acta Neuropathol.* 113, 559–568. doi: 10.1007/s00401-006-0176-3

Zhang, Y., Brady, M., and Smith, S. (2001). Segmentation of brain MR images through a hidden Markov random field model and the expectation-maximization algorithm. *IEEE Trans. Med. Imaging* 20, 45–57. doi: 10.1109/42.906424

Zheng, H., Zhang, L., Li, L., Liu, P., Gao, J., Liu, X., et al. (2010). High-frequency rTMS treatment increases left prefrontal myo-inositol in young patients with

treatment-resistant depression. *Prog. Neuropsychopharmacol. Biol. Psychiatry* 34, 1189–1195. doi: 10.1016/j.pnpbp.2010.06.009

Conflict of Interest: ZJD received research support and in-kind equipment support for an investigator-initiated study from Brainsway Ltd. He has also received in-kind equipment support from Magventure for investigator-initiated research. DMB received research support and in-kind equipment support for an investigator-initiated study from Brainsway Ltd., and he is the site principal investigator for three sponsor-initiated studies for Brainsway Ltd. He receives in-kind equipment support from Magventure for investigator-initiated research. He received medication supplies for an investigator-initiated trial from Indivior. He has participated in an advisory board for Janssen. PEC has received research grant support from Pfizer Inc.; equipment support from Neuronetics Inc.; and received supplies and genotyping services from Assurex Health Inc., for investigator-initiated studies. He is the primary investigator for a multicenter study funded by Neuronetics Inc., and a site primary investigator for a study funded by NeoSync Inc. He has served as a paid consultant for Procter & Gamble Company and Myriad Neuroscience.

The remaining authors declare that the research was conducted in the absence of any commercial or financial relationships that could be construed as a potential conflict of interest.

Publisher's Note: All claims expressed in this article are solely those of the authors and do not necessarily represent those of their affiliated organizations, or those of the publisher, the editors and the reviewers. Any product that may be evaluated in this article, or claim that may be made by its manufacturer, is not guaranteed or endorsed by the publisher.

frontiers in Neuroscience

ORIGINAL RESEARCH
published: 28 October 2021
doi: 10.3389/fnins.2021.751364

Common and Distinct Disruptions of Cortical Surface Morphology Between Autism Spectrum Disorder Children With and Without *SHANK3* Deficiency

Dongyun Li[1], Chunxue Liu[1], Ziyi Huang[2,3], Huiping Li[1], Qiong Xu[1], Bingrui Zhou[1], Chunchun Hu[1], Ying Zhang[1], Yi Wang[1], Jingxin Nie[3], Zhongwei Qiao[4], Dazhi Yin[2]* and Xiu Xu[1]**

[1] Department of Child Health Care, Children's Hospital of Fudan University, Shanghai, China, [2] Shanghai Key Laboratory of Brain Functional Genomics (Ministry of Education), School of Psychology and Cognitive Science, Affiliated Mental Health Center, East China Normal University, Shanghai, China, [3] School of Psychology, South China Normal University, Guangzhou, China, [4] Department of Radiology, Children's Hospital of Fudan University, Shanghai, China

SH3 and Multiple Ankyrin Repeat Domains 3 (*SHANK3*)-caused autism spectrum disorder (ASD) may present a unique opportunity to clarify the heterogeneous neuropathological mechanisms of ASD. However, the specificity and commonality of disrupted large-scale brain organization in *SHANK3*-deficient children remain largely unknown. The present study combined genetic tests, neurobehavioral evaluations, and magnetic resonance imaging, aiming to explore the disruptions of both local and networked cortical structural organization in ASD children with and without *SHANK3* deficiency. Multiple surface morphological parameters such as cortical thickness (CT) and sulcus depth were estimated, and the graph theory was adopted to characterize the topological properties of structural covariance networks (SCNs). Finally, a correlation analysis between the alterations in brain morphological features and the neurobehavioral evaluations was performed. Compared with typically developed children, increased CT and reduced nodal degree were found in both ASD children with and without *SHANK3* defects mainly in the lateral temporal cortex, prefrontal cortex (PFC), temporo-parietal junction (TPJ), superior temporal gyrus (STG), and limbic/paralimbic regions. Besides commonality, our findings showed some distinct abnormalities in ASD children with *SHANK3* defects compared to those without. Locally, more changes in the STG and orbitofrontal cortex were exhibited in ASD children with *SHANK3* defects, while more changes in the TPJ and inferior parietal lobe (IPL) in those without *SHANK3* defects were observed. For the SCNs, a trend toward regular network topology was observed in ASD children with *SHANK3* defects, but not in those without. In addition, ASD children with *SHANK3* defects showed more alterations of nodal degrees in the anterior and posterior cingulate cortices and right insular, while there were more disruptions in the sensorimotor areas and the left insular and dorsomedial PFC in ASD without *SHANK3*

OPEN ACCESS

Edited by:
Li Yang,
Peking University Sixth Hospital, China

Reviewed by:
Hsiao-Tuan Chao,
Baylor College of Medicine, United States
Ashwin S. Shetty,
Harvard University, United States
Vanesa Lerma,
Baylor College of Medicine, United States, in collaboration with reviewer H-TC

***Correspondence:**
Zhongwei Qiao
qiaozhwei@163.com
Dazhi Yin
dzyin@psy.ecnu.edu.cn
Xiu Xu
xuxiu@shmu.edu.cn

Specialty section:
This article was submitted to Neurodevelopment, a section of the journal Frontiers in Neuroscience

Received: *01 August 2021*
Accepted: *29 September 2021*
Published: *28 October 2021*

Citation:
Li D, Liu C, Huang Z, Li H, Xu Q, Zhou B, Hu C, Zhang Y, Wang Y, Nie J, Qiao Z, Yin D and Xu X (2021) Common and Distinct Disruptions of Cortical Surface Morphology Between Autism Spectrum Disorder Children With and Without SHANK3 Deficiency. Front. Neurosci. 15:751364. doi: 10.3389/fnins.2021.751364

defects. Our findings indicate dissociable disruptions of local and networked brain morphological features in ASD children with and without *SHANK3* deficiency. Moreover, this monogenic study may provide a valuable path for parsing the heterogeneity of brain disturbances in ASD.

Keywords: surface-based morphometry, structural covariance networks, autism spectrum disorder, *SHANK3*, children

INTRODUCTION

SH3 and Multiple Ankyrin Repeat Domains 3 (*SHANK3*) is a master postsynaptic density scaffolding protein that is crucial for synaptogenesis, dendritic spine maturation, and synapse formation (Jiang and Ehlers, 2013; Monteiro and Feng, 2017). Mutations in genes coding for synaptic proteins consist of the most well-characterized genetic deficits reported in autism spectrum disorder (ASD; de la Torre-Ubieta et al., 2016). Haploinsufficiency of the *SHANK3* gene is a key contributor of autistic features in the 22q13.3 deletion syndrome (i.e., Phelan–McDermid syndrome; Phelan, 2008; Bonaglia et al., 2011; Phelan and McDermid, 2012). Supported by the fact of an approximately 2% prevalence in ASD patients with cognitive deficits, the *SHANK3* gene is considered as one of the most common genetic causes for ASDs (Betancur and Buxbaum, 2013; Leblond et al., 2014).

Magnetic resonance imaging (MRI), as a noninvasive examination tool, has been extensively applied to human ASD to delineate the brain morphometry and connectivity (Hazlett et al., 2005; Muller and Fishman, 2018; van Rooij et al., 2018). Numerous neuroimaging data in literature indicated alterations in brain morphology [e.g., cortical surface area, cortical thickness (CT), and gray matter volume] mainly in the frontal cortex, temporal cortex, and limbic/paralimbic regions (Hazlett et al., 2005; Ecker et al., 2015; Li et al., 2017). However, the majority of previous findings are inconsistent. The main reason could be the etiological and clinical heterogeneity of ASD. To address these caveats, one of the promising strategies is to conduct the study in a homogenous subgroup of ASD with confirmed genetic etiology. *SHANK3*-caused ASD thus presents a unique opportunity to understand the underlying neuropathological mechanisms.

Previous MRI studies in *SHANK*3-deficit patients are mostly single cases or case series with unsystematic approaches by visual MRI inspection resulting in a variety of gray and white matter structures found to be abnormal (Philippe et al., 2008; Soorya et al., 2013; Srivastava et al., 2019). A latest research from our team applying automated and unbiased whole-brain analyses to a relatively large sample revealed changes of striatum-centered gray matter volume in *SHANK3*-deficient children, suggesting possible alterations in large-scale brain networks (Liu et al., 2021). Although the volumetric morphometry is widely used to assess the brain structural alterations, it may still present some limitations that can be surpassed with surface-based morphometry (SBM). The cerebral cortex is arranged in a highly folded sheet with the majority of the cortical surface area buried in folds (Fischl et al., 1999). Surface-based algorithms can account for a better dissociation of information content and new forms of analyses regarding measuring cortical complexity in 3D space (Ghosh et al., 2010; Oosterhof et al., 2011). The surface measures such as gyrification index (GI) and sulcus depth (SD) allow the characterization of the cortical complexity, implicating the association with neurodevelopmental disorders, schizophrenia, and other cognitive disorders including ASD (Van Essen et al., 2006; Yang et al., 2016; Tang et al., 2021). However, little is known so far about the features of cortical surface morphology in patients with *SHANK3* deficit.

Beyond local morphological analysis, graph theoretical approaches to structural covariance networks (SCNs) offer a useful way to characterize the topological organization of the brain structure. The basic assumption underlying SCNs is that morphological correlations are related to axonal connectivity between brain regions with shared trophic, genetic, and neurodevelopmental influences (Alexander-Bloch et al., 2013b; Seidlitz et al., 2018). Researchers recently began to study the associations between the SCNs and the intrinsic functional networks for salience, executive function, and default mode in both neurotypical children and adults (Zielinski et al., 2010; Bruno et al., 2017). In individuals with ASD, previous investigations of SCNs have reported a decrease in various regional or nodal topological properties mainly in the regions of insula, hippocampus, caudate, prefrontal cortex (PFC), and the regions related to social and sensorimotor processing as well as speech and language (Vissers et al., 2012; Sharda et al., 2016). To date, however, no study has uncovered how the topological architecture of SCNs disrupted in *SHANK3*-deficient ASD. This approach could help to further elucidate the role of dysconnectivity in both of the ASD with and without *SHANK3* deficiency.

In the present study, we employed SBM as well as SCN approaches to explore the disruptions of cortical surface morphology (i.e., both local features and anatomical networks) in ASD children with and without *SHANK3* deficiency. We hypothesized that there might be common as well as distinct disruptions of both local and networked cortical structural organization in ASD children with and without *SHANK3* deficiency, which may help to parse the heterogeneity of brain disturbances in ASD.

MATERIALS AND METHODS

Participants

All participants were recruited at the Children's Hospital of Fudan University [details about recruitment can be found in Liu et al. (2021)]. In total, 69 children in three groups [SHANK3

group, idiopathic ASD control, and typically developing (TD) control] were scanned and eight subjects were excluded for the analysis due to the poor quality of images. Children with recognizable lesions or abnormalities on scans, cerebral palsy, or other neurologic or degenerative diseases were excluded. SHANK3 group: 12 participants were enrolled with *SHANK3* deletion and/or mutation but without any other pathogenic or likely pathogenic variations [genetic testing details can be found in Liu et al. (2021)]. Idiopathic ASD control group: 24 ASD children without *SHANK3* deficiency or known genetic etiology were recruited. TD control group: 25 children underwent MRI scan because of the first episode of febrile convulsion and paroxysmal dizziness or headache, but otherwise normal developing children were used as normal controls.

Autism spectrum disorder diagnosis was based on the DSM-5 (Grzadzinski et al., 2013), ADOS-2 (Gotham et al., 2007), and Autism Diagnostic Interview-Revised (Lord et al., 1994) administrated by certified clinicians. Developmental and cognitive levels were evaluated by Griffiths Mental Development Scales (Griffiths; Benatti et al., 1986) conducted by licensed and certified clinicians.

Image Acquisition and Preprocessing

T1-weighted images were acquired employing a high-resolution 3D T1-weighted BRAVO (BRA in Volume imaging) sequence with the GE 3.0 Tesla Discovery MR750 system (GE Medical Systems, Milwaukee, WI, United States) with a 32-channel head coil at the Radiology Department after parental consent. Sequence parameters were the following: repetition time (TR) = 8.2 ms; echo time (TE) = 3.2 ms; flip angle = 12°; voxel size = 1 mm × 1 mm × 1 mm; gap = 0; FOV = 256 mm × 256 mm; and matrix = 256 × 256. Participants were routinely sedated in the "Sedation Center" under the supervision of a licensed clinician or anesthesiologist. Children are given chloral hydrate at a dose of 50 mg/kg orally approximately 1 h prior to the MRI scan. Vital signs were monitored and recorded during the scan.

The images were imported in the CAT12[1] toolboxes implemented in the Statistical Parametric Mapping software package (SPM12)[2] on the platform of Matlab (Version R2014b, MathWorks Inc., Natick, MA, United States). All the T1-weighted images were then segmented into gray matter, white matter, and cerebrospinal fluid and spatially normalized using the DARTEL algorithm (Ashburner, 2007). Gray matter-segmented images were submitted to the Check Sample Homogeneity by using the function embedded in CAT-12. Then, the segmented images were smoothed with a 6-mm full-width at half-maximum (FWHM) Gaussian kernel. At the end of this preprocessing, modulated, smoothed, normalized images were obtained for statistical analysis. Besides, the image quality rating (IQR) generated by CAT12 served as the parameter for imaging quality control.

This study was approved by the ethics committee of Children's Hospital of Fudan University, and all of the procedures were in accordance with the Declaration of Helsinki.

[1]http://dbm.neuro.uni-jena.de/cat/

[2]http://www.fil.ion.ucl.ac.uk/spm/software/spm12/

Surface-Based Morphometry Analysis

To characterize cortical morphological features, an SBM analysis was conducted using the CAT12 toolbox to estimate CT and the central surface of hemispheres based on the projection-based thickness (PBT) approach (Dahnke et al., 2013). The left and right CT maps and the additional surface parameters, including fractal dimension (FD), GI, and SD, were resampled to the HCP 32k surface mesh and smoothed with a 15-mm FWHM Gaussian kernel for the CT estimates and 20-mm FWHM for the rest parameters as suggested by CAT 12. CT is obtained by projecting the local maxima of white matter distance after tissue segmentation onto other gray matter voxels, which measures the distance between the inner and outer surfaces (Dahnke et al., 2013). FD is defined as the slope of a logarithmic plot of surface area versus a measure of the bandwidth of frequencies in the reconstructed surface shape based on a spherical harmonic reconstruction approach, measuring the surface complexity (Yotter et al., 2011). Local GI is defined as the estimations of "smoothed absolute mean curvature" within a spherical surface mesh, revealing the degree of cortical convolution (Luders et al., 2006). SD is defined as the square root-transformed Euclidean distance between the central surface (half way between the inner and outer surfaces) and its convex hull.

Structural Covariance Networks Approach

Considering the popularity in previous studies, here we merely selected the CT for structural covariance estimation (He et al., 2007; Alexander-Bloch et al., 2013a). The effects of age, gender, and overall mean CT were regressed from the mean thickness of each brain region, and the residuals were used for the subsequent steps of the analysis. Structural covariance analysis was conducted in the regions of interest (ROIs) defined by the HCP-MMP1.0 atlas (Glasser et al., 2016) which contains 180 regions for each hemisphere. Pearson correlations were applied between the CT of each possible pair of ROIs to generate a 360 × 360 cortical covariance matrix for each group (**Figure 1**). Considering that the network organization of the human brain is economic and small-world, the covariance matrix was then binarized and sparsified (i.e., 15%) according to previous studies (Bassett et al., 2008; Yin et al., 2019). The graph theory was finally used to characterize the topological properties of the SCNs. Here, we employed a network efficiency measure to quantify the small-world property of the SCNs following our previous work (Yin et al., 2014). This efficiency metric can deal with disconnected graphs and provides a clear physical meaning for the topological characterization of the networks (Latora and Marchiori, 2001). The global efficiency (GE) of graph G can be calculated as

$$\mathrm{GE} = \frac{1}{N(N-1)} \sum_{i \neq j \in G} \frac{1}{L_{ij}}$$

where N is the number of nodes; L_{ij} is the shortest path length between nodes i and j in graph G (i.e., the minimal number of edges that has to be traveled to go from nodes i to j).

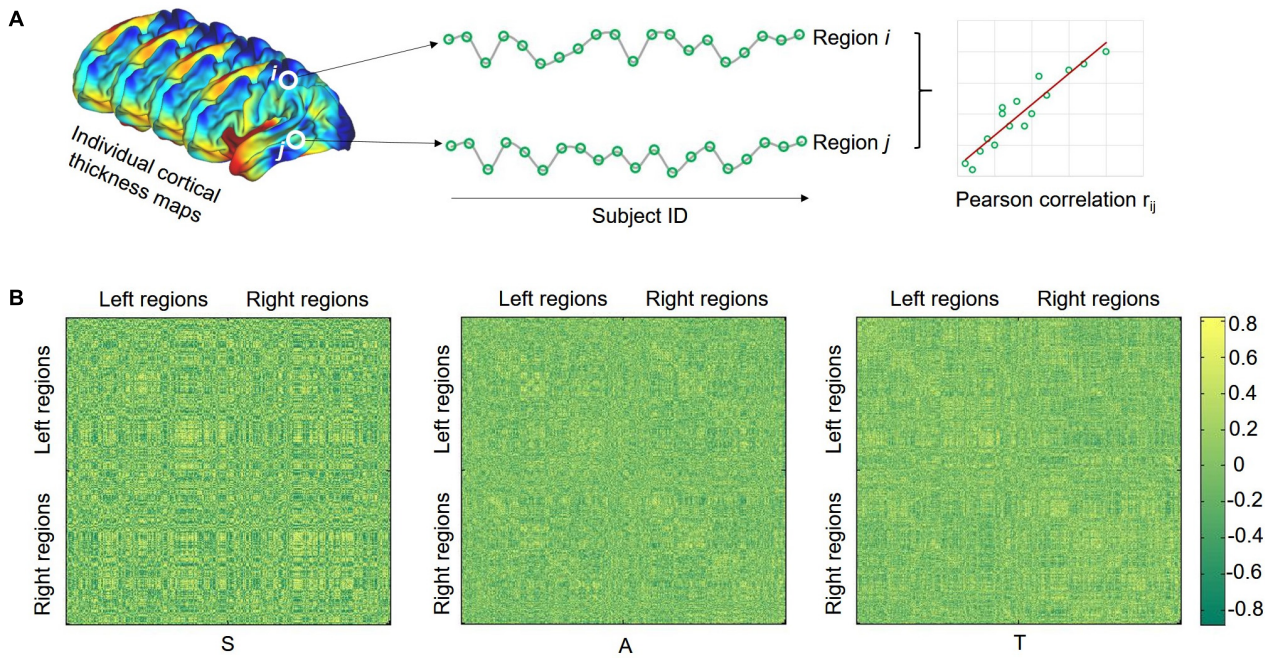

FIGURE 1 | Illustration of calculating structural covariance connectivity between two regions **(A)** and structural covariance matrix for each group **(B)**. S, SHANK3 group; A, ASD group; and T, typical developing group.

The local efficiency (LE) of graph G is measured as

$$\mathrm{LE} = \frac{1}{N}\sum_{i \in G} \mathrm{GE}\left(G_i\right)$$

where G_i denotes the subgraph composed of the nearest neighbors of node i.

Practically, a network can be categorized as a small-world network if GE is slightly less than and LE is much greater than the matched random networks with the same number of nodes, edges, and degree distribution. For comparison purposes, we generated random networks using the random rewiring procedure that preserves degree distribution as the real network (Maslov and Sneppen, 2002). Thus, a small-world network should meet the following criteria: *LE (real)/LE (random)* > 1 and *GE (real)/GE (random)* ≈ 1 (Wang et al., 2009). To explore small-world efficiency, we also calculated the normalized *GE = GE (real)/GE (random)* and normalized *LE = LE (real)/LE (random)*.

In addition, we calculated the nodal degree, which is commonly used to identify network hubs. Degree is defined as the number of immediate neighbors of a given node.

Statistical Analysis

Demographic and clinical data were analyzed using the statistical package SPSS 20.0. The threshold for all statistical significance was set at $p < 0.05$. Age, sex, developmental quotient, and total cranial volume were included as nuisance covariates.

For SBM, analysis of covariance (ANCOVA) was applied to the global mean values of each morphological parameter for the three groups followed by *post-hoc t*-tests. Age, sex, and total cranial volume were included as covariates. At the vertex-wise level, one-way ANOVA was conducted among the three groups and significant clusters with false discovery

TABLE 1 | Summary of clinical characteristics of studying subjects.

	SHANK3 group	ASD group	TD group	*p* value
Number of participants	12	24	25	
Gender, *n* (M/F)	6:6	20:4	19:6	0.095[a]
Age (*M* + *SD*)	4.9 ± 3.2	4.0 ± 1.9	4.9 ± 2.4	0.322[b]
ADOS-2 Scale (individuals)				
ASD severity	6.5 ± 1.67	6.68 ± 1.28	NA	0.570
SA	16.3 ± 3.86	15.59 ± 4.04	NA	0.720
RRB	1.58 ± 1.50	1.63 ± 1.17	NA	0.702
ADOS total score	17.92 ± 5.03	17.23 ± 4.46	NA	0.874
Griffith Scale (individuals)	11	20	NA	
Gross motor	50.3 ± 15.08	73.39 ± 16.87	NA	<0.0001****
Social	37.16 ± 17.22	60.20 ± 17.25	NA	0.002**
Language	17.79 ± 9.11	45.81 ± 19.35	NA	<0.0001[b]****
Fine motor	33.09 ± 18.65	57.71 ± 16.12	NA	0.0004***
Performance	33.34 ± 25.80	58.16 ± 22.47	NA	0.006**

Unpaired student's t-test (two-tailed).
[a] χ^2 *test.*
[b] *one-way ANOVA.*
***$p < 0.01$, ***$p < 0.001$, and ****$p < 0.0001$.*
ADOS-2, Autism Diagnostic Observation Schedule-The Second Edition; SA, social affect; RRB, restricted and repetitive behavior; and NA, not applicable.

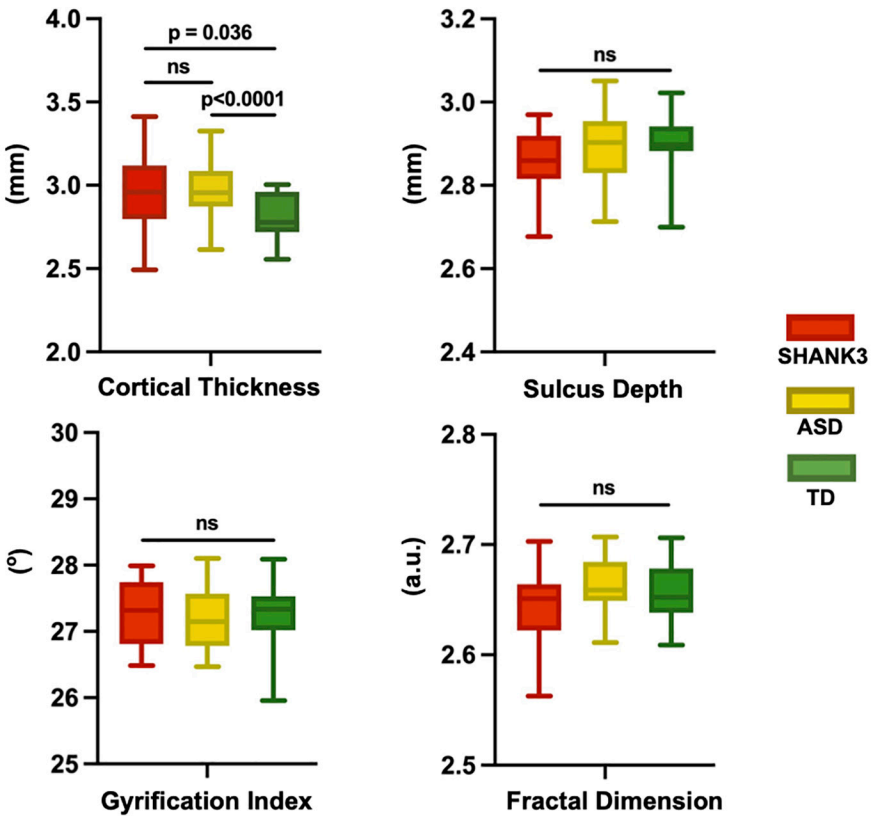

FIGURE 2 | Global leveled ANCOVA analysis showed significant difference of cortical thickness among the three groups. *Post-hoc t*-tests revealed significantly decreased cortical thickness in the ASD group but increased cortical thickness in the SHANK3 group compared to the TD group. No significant differences were found for the fractal dimension and sulcus depth among the three groups for ANCOVA analysis. ns, not significant; a.u., arbitrary unit.

rate (FDR) corrected were further picked up in CAT12. For each metric, *post-hoc t*-tests between each two groups were performed taking the significant result of ANOVA as the explicit mask. Age, sex, and total intracranial volume were included as nuisance covariates. Significance was set at $p < 0.05$ (FDR corrected).

For SCNs, a nonparametric permutation test was carried out to identify statistical significance of the between-group differences in network metrics. Briefly, we first calculated the difference of each network metric between groups. A null distribution of the difference for each metric was then obtained by randomly reallocating each subject's set of regional CT estimates to one or the other of the two groups and recomputing the difference of each metric between two randomized groups. Note that we calculated the network metrics for each randomized group using the same sparsity threshold as in the real brain networks. This randomization procedure was repeated 1,000 times, and the 95 percentile points of each distribution were used as the critical values for a one-tailed test of the null hypothesis with a probability of type I error of 0.05 (He et al., 2008). For the between-group comparisons of nodal degree, the FDR correction method was applied to correct multiple comparisons for $N = 360$ regions.

Spearman rank correlation analysis was conducted between the altered brain morphological features in SHANK3 and ASD groups and the clinical characteristics. Significance correction for multiple comparisons was applied using FDR correction ($p < 0.05$).

RESULTS

Participant Characteristics

No significant differences in age (for the SHANK3 group, mean ± SD: 4.9 ± 3.2 years; for the ASD group, mean ± SD: 4.0 ± 1.9 years; and for the typically developed group, mean ± SD: 4.9 ± 2.4 years) and sex (for the SHANK3 group, 6 males and 6 females; for the ASD group, 20 males and 4 females; and for the typically developed group, 19 males and 6 females) between groups (all p values > 0.05). Compared to idiopathic ASD children, the SHANK3 group achieved similar scores in each domain and severity of ADOS-2 but exhibited a significantly worse performance in all of the developmental domains of Griffith (gross motor: $p < 0.0001$; social: $p = 0.002$; language: $p < 0.0001$; fine motor: $p = 0.0004$; adaptability: $p = 0.006$). Detailed demographic

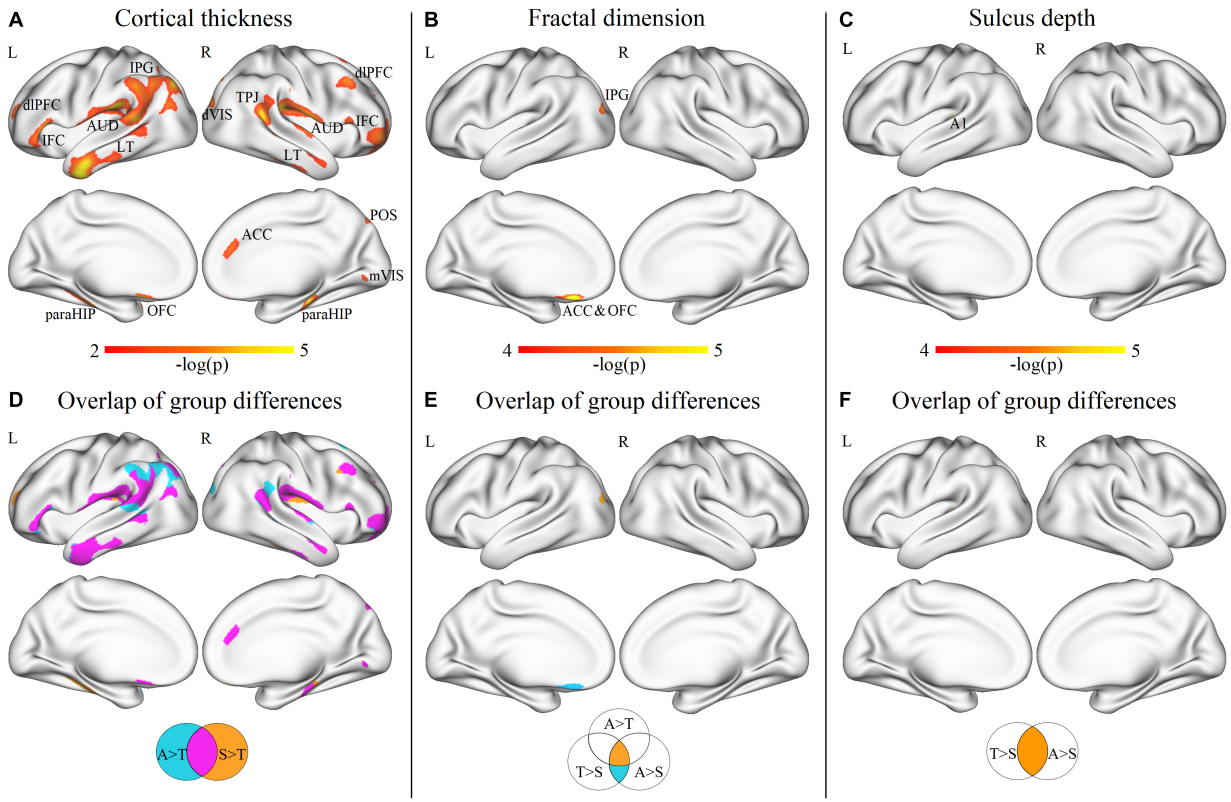

FIGURE 3 | Vertex-wise ANOVA results and the overlap areas of intergroup differences. Significant differences of cortical thickness **(A)**, fractal dimension **(B)**, and sulcus depth **(C)** among ASD, SHANK3, and TD groups; the overlap areas of intergroup differences in cortical thickness **(D)**, fractal dimension **(E)**, and sulcus depth **(F)**. dlPFC, dorsolateral prefrontal cortex; IFC, inferior frontal cortex; AUD, auditory areas; LT, lateral temporal cortex; IPG, inferior parietal gyrus; dVIS, dorsal visual streams; TPJ, temporo-parieto-occipital junction; paraHIP, parahippocampus; OFC, orbitofrontal cortex; ACC, anterior cingulate cortex; mVIS, medial visual areas; POS, parieto-occipital sulcus; and A1, primary auditory cortex. A, ASD; T, TD; and S, SHANK3.

information and clinical characteristics by group are presented in **Table 1**.

Inter-Group Differences in Surface-Based Morphometric Features

No group differences were found in all of the imaging quality control parameters, including the six absolute head motion parameters and IQR (for the SHANK3 group, mean ± SD: 0.907 ± 0.006; for the ASD group, mean ± SD: 0.906 ± 0.005; and for the typically developed group, mean ± SD: 0.908 ± 0.006; $p > 0.05$).

At the global level, we found that the averaged CT is 2.96 ± 0.57 mm for the SHANK3 group, 2.58 ± 0.55 mm for the ASD group, and 2.81 ± 0.5 mm for the TD group; the averaged FD in the SHANK3 group was 2.64 ± 0.34, in the ASD group 2.66 ± 0.35, and in the TD group 2.65 ± 0.35; the average SD in the SHANK3 group was 2.86 ± 0.77 mm, in the ASD group 2.89 ± 0.85 mm, and in the TD group 2.90 ± 0.85 mm; the average GI in the SHANK3 group was 27.29 ± 0.5°, in the ASD group 27.19 ± 0.45°, and in the TD group 27.28 ± 0.46°. For the individual raw values, please see **Supplementary Table 1**. ANCOVA analysis revealed a significant difference of CT among the three groups ($F = 8.64$, $p = 0.001$). In the *post-hoc* analysis, the ASD group showed significantly decreased CT than the TD group ($t = 3.86$, $p < 0.0001$) and the SHANK3 group showed increased CT than the TD group ($t = 2.18$, $p = 0.036$; **Figure 2**). No significant difference was found between the SHANK3 group and the ASD group for CT. In addition, no significant differences were found for the FD and SD among the three groups with ANCOVA analysis (**Figure 2**).

At the vertex level, through the vertex-wise ANOVA analysis of CT, we found significant differences among the three groups mainly in the regions of the dorsolateral prefrontal cortex, inferior frontal cortex (IFC), auditory areas, lateral temporal cortex (LT), inferior parietal gyrus, dorsal visual streams, temporo-parieto-occipital junction (TPJ), parahippocampus (paraHIP), orbitofrontal cortex (OFC), anterior cingulate cortex (ACC), medial visual areas, and parieto-occipital sulcus ($p < 0.05$, FDR corrected; **Figure 3A**). In the *post-hoc* analysis, the SHANK3 and ASD groups showed significantly increased CT mainly in the lateral temporal, prefrontal, primary auditory (part of superior temporal gyrus, STG), and temporo-parietal junction (TPJ) as well as limbic/paralimbic regions including the ACC, OFC, temporal pole, and paraHIP, compared with TD controls

($p < 0.05$, FDR corrected; **Figure 3D**). Notably, the SHANK3 group showed more disruptions in STG than the ASD group, while the latter showed more disruptions in the TPJ and inferior parietal lobule (IPL; **Figure 3D**). No significant difference was found between the SHANK3 group and the ASD group for CT. For the FD, ANOVA analysis revealed significant differences among the three groups mainly in the regions of the IPL, ACC, and OFC (**Figure 3B**). In the *post-hoc* analysis, the ASD group showed increased FD in a small region of the left IPL when compared with the SHANK3 and TD groups, while the SHANK3 group showed decreased FD in the left OFC in comparison with ASD and TD groups (**Figure 3E**). For the SD, the SHANK3 group showed decreased SD in the left primary auditory region (part of STG; **Figures 3C,F**) when compared with the ASD and TD groups. No group differences were found in local GI.

Inter-Group Differences in Topological Properties of Structural Covariance Networks

At the global level, we found that the *SHANK3*-deficient children exhibited a decrease in GE ($p = 0.001$) and an increase in LE ($p = 0.021$) compared to TD controls, while ASD children showed no significant differences in either global or LE compared with TD ($p > 0.05$). Compared with ASD children, *SHANK3*-deficient children exhibited a decrease in GE ($p = 0.001$) and an increase in LE ($p = 0.015$). In contrast, we found a significant increase in normalized LE in *SHANK3*-deficient compared with ASD groups, as well as in ASD compared with TD groups, while no significant differences were observed in normalized GE among the three groups (**Figure 4**).

For regional network analysis, group differences in nodal degree between every two groups were detected (all $p < 0.05$, FDR corrected). In contrast with TD controls, ASD without *SHANK3* deficiency showed significantly decreased nodal degrees mainly in sensorimotor areas, the left insular, and the right ACC and dorsomedial PFC (**Figure 5A**), while ASD with *SHANK3* deficiency showed decreased nodal degrees mainly in the left ACC, and the right insular cortex, posterior cingulate cortex (PCC), and medial visual cortex (**Figure 5B**). To overlap the between-group results, we observed a common reduction of the nodal degree in the prefrontal, IPL, and insular areas in both ASD with and without *SHANK3* deficiency compared with TD controls (**Figure 5D**). To compare with the ASD group, the SHANK3 group showed an increment of nodal degree in the ACC, premotor cortex, primary auditory cortex (part of STG), and visual areas in contrast with the ASD group (**Figure 5C**). Notably, the regions of disruptions of nodal degree in these two groups were geometrically close but distinct in the paracentral lobule, IFC, LT, and superior and IPL (**Figure 5D**).

Correlations Between Clinical Characteristics and Cortical Morphology

Spearman rank correlation analysis was conducted to explore the relationship between the disruptions of cortical morphological features and clinical assessments in ASD and SHANK3 groups, and then FDR correction was performed (corrected $p < 0.05$).

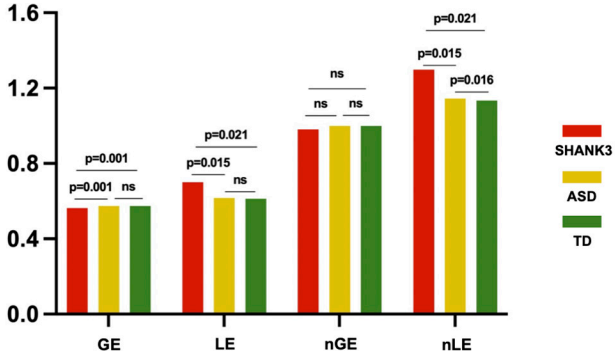

FIGURE 4 | Intergroup differences in global efficiency and local efficiency between the SHANK3, ASD, and TD groups. The orange color indicates the SHANK3 group, the yellow color indicates the ASD group, and the green color indicates the TD group; network sparsity = 15%. ns, not significant; GE, global efficiency; LE, local efficiency; nGE, normalized global efficiency; and nLE, normalized local efficiency.

The disruptions of FD in a region of the left IPL in both ASD children with and without *SHANK3* deficiencies were related to general DQ ($r = 0.597$, $p < 0.001$), gross motor ($r = 0.466$, $p = 0.011$), social ($r = 0.507$, $p = 0.005$), language ($r = 0.535$, $p = 0.003$), fine motor ($r = 0.517$, $p = 0.004$), and performance ($r = 0.545$, $p = 0.002$; **Figure 6**). Correlations between other cortical morphological features (incl. CT, SD, and GI) and the clinical assessments were not significant.

DISCUSSION

Our study demonstrated some common and distinct disruptions of both local and networked cortical structural organization in ASD children with and without *SHANK3* defects. Locally, increased CT was found in both ASD children with and without *SHANK3* defects mainly in the LT, PFC, TPJ, STG, and limbic/paralimbic regions. As to the networked cortical organizations, the majority of the above regions were observed with reduction of the nodal degree. Fitting with the idea that *SHANK3* deficiency shares some common patterns of cortical structural alterations with ASD, *SHANK3* deficiency thus provides a unique opportunity to understand the underlying neuropathological mechanisms as a homogenous subgroup of ASD.

The social deficits and repetitive and stereotyped behaviors are the core symptoms of ASD (Grzadzinski et al., 2013). It is well known that language expression is the vital part of social interaction. The clinical manifestations of *SHANK3* deficiency include ASD, global developmental delay, delayed or absent speech, intellectual disability, and motor abnormalities (Soorya et al., 2013; Leblond et al., 2014). The penetrance of the ASD phenotype in patients with *SHANK3* deficiency has been reported from 84.4 to 92.8% (Soorya et al., 2013; Liu et al., 2021). In consistency with these previous reports, our current clinical assessment data demonstrated that both ASD children with and without *SHANK3* defects showed social

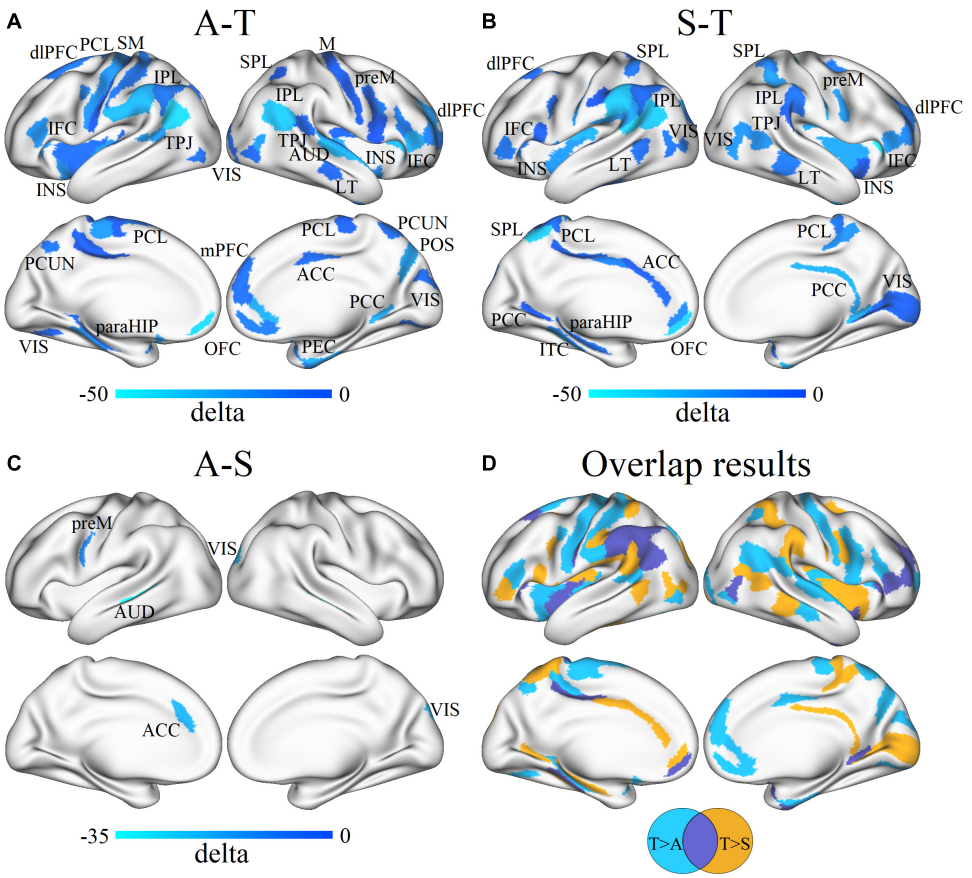

FIGURE 5 | Differences in the group mean of nodal degree between ASD, SHANK3, and TD groups and the overlap results. Group differences in nodal degree between ASD and TD **(A)**, SHANK3 and TD **(B)**, and ASD and SHANK3 **(C)**, and overlap results between the group differences **(D)**. Blue and light blue colors indicate ASD < TD in **(A)**, SHANK3 < TD in **(B)**, and ASD < SHANK3 in **(C)**, respectively. dlPFC, dorsolateral prefrontal cortex; PCL, paracentral lobule; SM, somatosensory and motor cortex; IFC, inferior frontal cortex; INS, insular; IPL, inferior parietal lobule; TPJ, temporo-parieto-occipital junction; VIS, visual areas; SPL, superior parietal lobule; M, motor cortex; preM, premotor cortex; AUD, auditory areas; LT, lateral temporal cortex; ACC, anterior cingulate cortex; PCC, posterior cingulate cortex; PCUN, precuneus; POS, parieto-occipital sulcus; paraHIP, parahippocampus; OFC, orbitofrontal cortex; and PEC, perirhinal and ectorhinal_cortex. A, ASD; T, TD; and S, SHANK3.

interaction impairments and repetitive behaviors (ADOS-2) as well as language developmental delay (Griffith language domain). Along with the clinical data, increased CT as well as networked alterations were revealed in the PFC, TPJ, STG, and limbic/paralimbic regions. The PFC, TPJ, and STG are the most consistently reported neural correlates of social-cognitive functions (Wolf et al., 2018).

Superior temporal gyrus, responsible for language comprehension, face processing, and social cognition, has been proved to be associated with ASD (Bigler et al., 2007; Jou et al., 2010; Ameis and Catani, 2015). As the area where the temporal and parietal lobes meet, the TPJ incorporated information from the thalamus, the limbic system, and somatosensory systems and plays an important role in social perception as well as theory of mind (ToM; Poletti et al., 2012; Bitsch et al., 2018). Neuropsychological studies suggested that individuals with ASD showed ToM deficits which result in the disabilities to initiate and sustain reciprocal social interactions (DiLalla et al., 2017; Tordjman et al., 2019). The PFC, even in cross-species ASD models, has been proved to be the critical hub for emotional and social behavior, as well as executive functions (Chini and Hanganu-Opatz, 2021; Yan and Rein, 2021). Additionally, the limbic/paralimbic structural alterations in ASD suggested that the paralimbic–limbic system is closely related to repetitive and stereotyped behaviors (Catani et al., 2013; Li et al., 2018).

From the perspective of the brain network, we found that the SHANK3 group showed a significant increase in LE compared with ASD and TD groups. Instead, the GE in the SHANK3 group is slightly lower than that in ASD and TD groups. No significant differences in either local or GE were observed between ASD and TD groups. This result suggests that the configuration of the SCN in *SHANK3* children shifts toward a topology of regular network, which is a nonoptimal network configuration. Actually, the trend toward a regular network topology has often been observed in other neuropsychiatric disorders (De Vico Fallani et al., 2007; Yin et al., 2014). In contrast, the ASD children without *SHANK3* defects appear to reserve a relatively intact global topology in SCN.

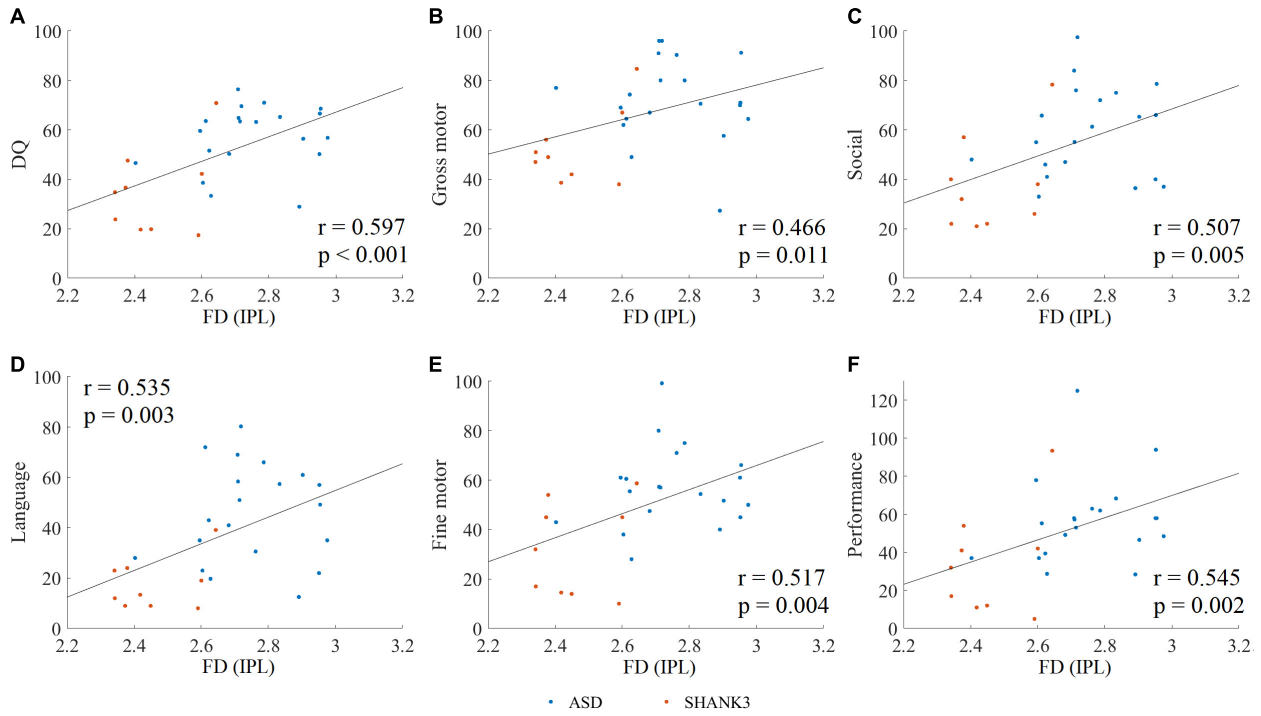

FIGURE 6 | Spearman rank correlation between clinical assessments and altered fractal dimension (FD) in ASD and SHANK3 groups. The Spearman rank correlation between the altered FD and DQ scores **(A)**, gross motor **(B)**, social **(C)**, language **(D)**, fine motor **(E)**, and performance **(F)**. IPL, inferior parietal lobule. A, ASD; S, SHANK3; and T, TD.

At the nodal level, our results revealed a common reduction of the nodal degree as the networked parameter alterations in the PFC, IPL, and insular cortex in both ASD children with and without *SHANK3* defects. These findings were consistent with our previous assumptions that there might be possible alterations in large-scale brain networks in ASD children with and without *SHANK3* defects (Liu et al., 2021). IPL and dorsolateral PFC are the core components of the frontoparietal network (FPN) or also known as central executive network (CEN) which is crucial for attention sustenance, decision-making, working memory, and cognitive control (Seeley et al., 2007; van Oort et al., 2017). FPN/CEN is one of the three networks in the "triple-network model," along with the salience network (SN) and the default mode network (DMN; van Oort et al., 2017; Wei et al., 2019). Disruption of FPN may account for the impairment in cognitive flexibility in ASD (Holiga et al., 2019), and reshaping of FPN connectivity might improve the cognitive–behavioral problems in ASD (De Luca et al., 2021). TPJ and PFC are part of DMN which is implicated in self-monitoring, ToM, and social cognition (Buckner et al., 2008; Sarasua et al., 2014). Functional connectivity studies have provided evidence for abnormal connectivity pattern of DMN and its subnetworks in individuals with ASD (von dem Hagen et al., 2013; Abbott et al., 2016). SN, which is composed of insula and ACC, orients attention toward salient information and facilitates switching between the FPN and DMN (Hermans et al., 2014; van Oort et al., 2020). Children with ASD exhibited both functional "over-" and "under-" connectivities in between the SN, DMN, and CEN (Lawrence et al., 2020; van Oort et al., 2020). Our morphological and network-based structural disruptions are consistent with these prior studies which may reflect a structural basis for the functional imbalance between these large-scale brain networks.

Interestingly, besides the common alterations, our study revealed some distinct abnormalities in ASD children with *SHANK3* defects compared to those without. Locally, more changes in STG and OFC were exhibited in ASD children with *SHANK3* defects, while those without *SHANK3* defects showed more changes in TPJ and IPL. On the networked level, ASD children with *SHANK3* defects showed more alterations of nodal degrees in ACC and PCC and right insula, while ASD without *SHANK3* defects exhibited more disruptions in the sensorimotor areas, the left insula, and dorsomedial PFC. SHANK3 protein is expressed highest in the cortico-striatal glutamatergic synapses (Shepherd, 2013; Monteiro and Feng, 2017). The medial orbitofrontal cortico-striatal loop originates in the OFC then projects to the caudate, putamen, and pallidum and then closes with projections returning to the OFC which shares reciprocal connections with ACC, PCC, STG, hippocampus, and parahippocampal cortex (Elliott et al., 2000; Jarbo and Verstynen, 2015). The current results supported the assumption of our previous study which suggested dysfunction of cortico-striatal connectivity in children with *SHANK3* defects (Liu et al., 2021).

Although large-scale studies sequenced numerous patient samples, there was only a maximum of 30% of ASD cases

identified with genetic causes with no single gene contributing to greater than 2% of cases (Boyle et al., 2017; Dias and Walsh, 2020). One of the major reasons for the explanation is generally acknowledged as the etiological and clinical heterogeneity of ASD. Our monogenetic subgroup of ASD children with *SHANK3* defects exhibited both common and distinct disruptions in local and networked structural organization compared to those idiopathic ASD, suggesting both common and distinct neuropathological mechanisms underlying ASD with and without *SHANK3* deficiency. Differentiating the heterogeneity in ASD is critical to both clinicians and researchers to understand the phenotype and pathophysiology of the syndrome (Agelink van Rentergem et al., 2021; Ziats et al., 2021). Our study of monogenic ASD patients may thus offer new insights into the diverse findings of previous neuroimaging studies of idiopathic ASD.

There were several limitations of the current study. Although the sample size of the SHANK3 group used in the current study is relatively large compared with previous studies (Monteiro and Feng, 2017), it is still small due to the rare condition of *SHANK3* mutations. In particular, even though the PBT method is better than other approaches on the basis of root mean square error, it still represents a thickness measurement error of 0.39 ± 0.02 mm (Dahnke et al., 2013). This may potentially confound the observed between-group differences in CT. Future studies with expanded sample size need to verify the current results. Besides, the current MRI scans were mainly structural so that future studies of functional connectivity may allow for more in-depth understanding of our conclusions. Despite these limitations, our results provide some new guidance to further understand the symptoms presented by ASD children both with and without *SHANK3* defects.

CONCLUSION

Besides commonality, our findings have revealed dissociable patterns of alterations in both local and networked features of brain morphology between ASD children with and without *SHANK3* defects, which suggests new insight into the understanding of neuropathological mechanisms underlying ASD. Moreover, this monogenic study may provide a valuable path for parsing the heterogeneity of brain disturbances in ASD.

DATA AVAILABILITY STATEMENT

The datasets presented in this study can be found in online repositories. The names of the repository/repositories and accession number(s) can be found in the article/ **Supplementary Material**.

ETHICS STATEMENT

The studies involving human participants were reviewed and approved by Ethics Committee of Children's Hospital of Fudan University. Written informed consent to participate in this study was provided by the participants' legal guardian/next of kin.

AUTHOR CONTRIBUTIONS

DL analyzed and interpreted the data and wrote and reviewed the manuscript. XX designed the research, interpreted the data, and reviewed the manuscript. DY analyzed and interpreted the data and reviewed the manuscript. ZQ interpreted the data and reviewed the manuscript. CL collected and analyzed the clinical data. ZH analyzed and interpreted the imaging data. HL, QX, BZ, CH, YZ, and YW prepared the data and reviewed the manuscript. JN reviewed the manuscript. All authors contributed to the article and approved the submitted version.

FUNDING

This study was supported in part by the National Natural Science Foundation of China (NSFC, Nos. 81701129, 82171540, and 31600869); Original Research Fund of Fudan University (No. IDF156012/004); and HaiJu Joint Laboratory Project of Children's Hospital of Fudan University (EK1125180106). We also would like to acknowledge the support of The Open Research Fund of Shanghai Key Laboratory of Brain Functional Genomics of East China Normal University.

SUPPLEMENTARY MATERIAL

The Supplementary Material for this article can be found online at: https://www.frontiersin.org/articles/10.3389/fnins.2021.751364/full#supplementary-material

REFERENCES

Abbott, A. E., Nair, A., Keown, C. L., Datko, M., Jahedi, A., Fishman, I., et al. (2016). Patterns of atypical functional connectivity and behavioral links in autism differ between default, salience, and executive networks. *Cereb. Cortex* 26, 4034–4045. doi: 10.1093/cercor/bhv191

Agelink van Rentergem, J. A., Deserno, M. K., and Geurts, H. M. (2021). Validation strategies for subtypes in psychiatry: a systematic review of research on autism spectrum disorder. *Clin. Psychol. Rev.* 87:102033. doi: 10.1016/j.cpr.2021.102033

Alexander-Bloch, A., Giedd, J. N., and Bullmore, E. (2013a). Imaging structural co-variance between human brain regions. *Nat. Rev. Neurosci.* 14, 322–336. doi: 10.1038/nrn3465

Alexander-Bloch, A., Raznahan, A., Bullmore, E., and Giedd, J. (2013b). The convergence of maturational change and structural covariance in human cortical networks. *J. Neurosci.* 33, 2889–2899. doi: 10.1523/JNEUROSCI.3554-12.2013

Ameis, S. H., and Catani, M. (2015). Altered white matter connectivity as a neural substrate for social impairment in autism spectrum disorder. *Cortex* 62, 158–181. doi: 10.1016/j.cortex.2014.10.014

Ashburner, J. (2007). A fast diffeomorphic image registration algorithm. *Neuroimage* 38, 95–113. doi: 10.1016/j.neuroimage.2007.07.007

Bassett, D. S., Bullmore, E., Verchinski, B. A., Mattay, V. S., Weinberger, D. R., and Meyer-Lindenberg, A. (2008). Hierarchical organization of human cortical networks in health and schizophrenia. *J. Neurosci.* 28, 9239–9248. doi: 10.1523/JNEUROSCI.1929-08.2008

Benatti, A., Ferrari, F., Giustardi, A., Filippi, A., Pinelli, M., Bosi, R., et al. (1986). Griffith test in the evaluation of psychomotor development in the 1st year of life. a longitudinal study. *Pediatr. Med. Chir.* 8, 757–761.

Betancur, C., and Buxbaum, J. D. (2013). SHANK3 haploinsufficiency: a "common" but underdiagnosed highly penetrant monogenic cause of autism spectrum disorders. *Mol. Autism* 4:17. doi: 10.1186/2040-2392-4-17

Bigler, E. D., Mortensen, S., Neeley, E. S., Ozonoff, S., Krasny, L., Johnson, M., et al. (2007). Superior temporal gyrus, language function, and autism. *Dev. Neuropsychol.* 31, 217–238. doi: 10.1080/87565640701190841

Bitsch, F., Berger, P., Nagels, A., Falkenberg, I., and Straube, B. (2018). The role of the right temporo-parietal junction in social decision-making. *Hum. Brain Mapp.* 39, 3072–3085. doi: 10.1002/hbm.24061

Bonaglia, M. C., Giorda, R., Beri, S., De Agostini, C., Novara, F., Fichera, M., et al. (2011). Molecular mechanisms generating and stabilizing terminal 22q13 deletions in 44 subjects with Phelan/McDermid syndrome. *PLoS Genet.* 7:e1002173. doi: 10.1371/journal.pgen.1002173

Boyle, E. A., Li, Y. I., and Pritchard, J. K. (2017). An expanded view of complex traits: from polygenic to omnigenic. *Cell* 169, 1177–1186. doi: 10.1016/j.cell.2017.05.038

Bruno, J. L., Hosseini, S. M. H., Saggar, M., Quintin, E. M., Raman, M. M., and Reiss, A. L. (2017). Altered brain network segregation in fragile X syndrome revealed by structural connectomics. *Cereb. Cortex* 27, 2249–2259. doi: 10.1093/cercor/bhw055

Buckner, R. L., Andrews-Hanna, J. R., and Schacter, D. L. (2008). The brain's default network: anatomy, function, and relevance to disease. *Ann. N. Y. Acad. Sci.* 1124, 1–38. doi: 10.1196/annals.1440.011

Catani, M., Dell'acqua, F., and Thiebaut de Schotten, M. (2013). A revised limbic system model for memory, emotion and behaviour. *Neurosci. Biobehav. Rev.* 37, 1724–1737. doi: 10.1016/j.neubiorev.2013.07.001

Chini, M., and Hanganu-Opatz, I. L. (2021). Prefrontal cortex development in health and disease: lessons from rodents and humans. *Trends Neurosci.* 44, 227–240. doi: 10.1016/j.tins.2020.10.017

Dahnke, R., Yotter, R. A., and Gaser, C. (2013). Cortical thickness and central surface estimation. *Neuroimage* 65, 336–348. doi: 10.1016/j.neuroimage.2012.09.050

de la Torre-Ubieta, L., Won, H., Stein, J. L., and Geschwind, D. H. (2016). Advancing the understanding of autism disease mechanisms through genetics. *Nat. Med.* 22, 345–361. doi: 10.1038/nm.4071

De Luca, R., Naro, A., Colucci, P. V., Pranio, F., Tardiolo, G., Billeri, L., et al. (2021). Improvement of brain functional connectivity in autism spectrum disorder: an exploratory study on the potential use of virtual reality. *J. Neural Transm.* 128, 371–380. doi: 10.1007/s00702-021-02321-3

De Vico Fallani, F., Astolfi, L., Cincotti, F., Mattia, D., Marciani, M. G., Salinari, S., et al. (2007). Cortical functional connectivity networks in normal and spinal cord injured patients: evaluation by graph analysis. *Hum. Brain Mapp.* 28, 1334–1346. doi: 10.1002/hbm.20353

Dias, C. M., and Walsh, C. A. (2020). Recent advances in understanding the genetic architecture of autism. *Annu. Rev. Genom. Hum Genet.* 21, 289–304. doi: 10.1146/annurev-genom-121219-082309

DiLalla, L. F., McCrary, M., and Diaz, E. (2017). A review of endophenotypes in schizophrenia and autism: the next phase for understanding genetic etiologies. *Am. J. Med. Genet. C Semin. Med. Genet.* 175, 354–361. doi: 10.1002/ajmg.c.31566

Ecker, C., Bookheimer, S. Y., and Murphy, D. G. (2015). Neuroimaging in autism spectrum disorder: brain structure and function across the lifespan. *Lancet Neurol.* 14, 1121–1134. doi: 10.1016/S1474-4422(15)00050-2

Elliott, R., Dolan, R. J., and Frith, C. D. (2000). Dissociable functions in the medial and lateral orbitofrontal cortex: evidence from human neuroimaging studies. *Cereb. Cortex* 10, 308–317. doi: 10.1093/cercor/10.3.308

Fischl, B., Sereno, M. I., Tootell, R. B., and Dale, A. M. (1999). High-resolution intersubject averaging and a coordinate system for the cortical surface. *Hum. Brain Mapp.* 8, 272–284. doi: 10.1002/(sici)1097-019319998:4<272::aid-hbm10<3.0.co;2-4

Ghosh, S. S., Kakunoori, S., Augustinack, J., Nieto-Castanon, A., Kovelman, I., Gaab, N., et al. (2010). Evaluating the validity of volume-based and surface-based brain image registration for developmental cognitive neuroscience studies in children 4 to 11 years of age. *Neuroimage* 53, 85–93. doi: 10.1016/j.neuroimage.2010.05.075

Glasser, M. F., Coalson, T. S., Robinson, E. C., Hacker, C. D., Harwell, J., Yacoub, E., et al. (2016). A multi-modal parcellation of human cerebral cortex. *Nature* 536, 171–178. doi: 10.1038/nature18933

Gotham, K., Risi, S., Pickles, A., and Lord, C. (2007). The autism diagnostic observation schedule: revised algorithms for improved diagnostic validity. *J. Autism Dev. Disord.* 37, 613–627. doi: 10.1007/s10803-006-0280-1

Grzadzinski, R., Huerta, M., and Lord, C. (2013). DSM-5 and autism spectrum disorders (ASDs): an opportunity for identifying ASD subtypes. *Mol. Autism* 4:12. doi: 10.1186/2040-2392-4-12

Hazlett, H. C., Poe, M., Gerig, G., Smith, R. G., Provenzale, J., Ross, A., et al. (2005). Magnetic resonance imaging and head circumference study of brain size in autism: birth through age 2 years. *Arch. Gen. Psychiatry* 62, 1366–1376. doi: 10.1001/archpsyc.62.12.1366

He, Y., Chen, Z., and Evans, A. (2008). Structural insights into aberrant topological patterns of large-scale cortical networks in Alzheimer's disease. *J. Neurosci.* 28, 4756–4766. doi: 10.1523/JNEUROSCI.0141-08.2008

He, Y., Chen, Z. J., and Evans, A. C. (2007). Small-world anatomical networks in the human brain revealed by cortical thickness from MRI. *Cereb. Cortex* 17, 2407–2419. doi: 10.1093/cercor/bhl149

Hermans, E. J., Henckens, M. J., Joels, M., and Fernandez, G. (2014). Dynamic adaptation of large-scale brain networks in response to acute stressors. *Trends Neurosci.* 37, 304–314. doi: 10.1016/j.tins.2014.03.006

Holiga, S., Hipp, J. F., Chatham, C. H., Garces, P., Spooren, W., D'Ardhuy, X. L., et al. (2019). Patients with autism spectrum disorders display reproducible functional connectivity alterations. *Sci. Transl. Med.* 11:eaat9223. doi: 10.1126/scitranslmed.aat9223

Jarbo, K., and Verstynen, T. D. (2015). Converging structural and functional connectivity of orbitofrontal, dorsolateral prefrontal, and posterior parietal cortex in the human striatum. *J. Neurosci.* 35, 3865–3878. doi: 10.1523/JNEUROSCI.2636-14.2015

Jiang, Y. H., and Ehlers, M. D. (2013). Modeling autism by SHANK gene mutations in mice. *Neuron* 78, 8–27. doi: 10.1016/j.neuron.2013.03.016

Jou, R. J., Minshew, N. J., Keshavan, M. S., Vitale, M. P., and Hardan, A. Y. (2010). Enlarged right superior temporal gyrus in children and adolescents with autism. *Brain Res.* 1360, 205–212. doi: 10.1016/j.brainres.2010.09.005

Latora, V., and Marchiori, M. (2001). Efficient behavior of small-world networks. *Phys. Rev. Lett.* 87:198701. doi: 10.1103/PhysRevLett.87.198701

Lawrence, K. E., Hernandez, L. M., Bowman, H. C., Padgaonkar, N. T., Fuster, E., Jack, A., et al. (2020). Sex differences in functional connectivity of the salience, default mode, and central executive networks in youth with ASD. *Cereb. Cortex* 30, 5107–5120. doi: 10.1093/cercor/bhaa105

Leblond, C. S., Nava, C., Polge, A., Gauthier, J., Huguet, G., Lumbroso, S., et al. (2014). Meta-analysis of SHANK mutations in autism spectrum disorders: a gradient of severity in cognitive impairments. *PLoS Genet.* 10:e1004580. doi: 10.1371/journal.pgen.1004580

Li, D., Karnath, H. O., and Xu, X. (2017). Candidate biomarkers in children with autism spectrum disorder: a review of MRI studies. *Neurosci. Bull.* 33, 219–237. doi: 10.1007/s12264-017-0118-1

Li, S. J., Wang, Y., Qian, L., Liu, G., Liu, S. F., Zou, L. P., et al. (2018). Alterations of white matter connectivity in preschool children with autism spectrum disorder. *Radiology* 288, 209–217. doi: 10.1148/radiol.2018170059

Liu, C., Li, D., Yang, H., Li, H., Xu, Q., Zhou, B., et al. (2021). Altered striatum centered brain structures in SHANK3 deficient Chinese children with genotype and phenotype profiling. *Prog. Neurobiol.* 200:101985. doi: 10.1016/j.pneurobio.2020.101985

Lord, C., Rutter, M., and Le Couteur, A. (1994). Autism diagnostic interview-revised: a revised version of a diagnostic interview for caregivers of individuals with possible pervasive developmental disorders. *J. Autism Dev. Disord.* 24, 659–685. doi: 10.1007/BF02172145

Luders, E., Thompson, P. M., Narr, K. L., Toga, A. W., Jancke, L., and Gaser, C. (2006). A curvature-based approach to estimate local gyrification on the cortical surface. *Neuroimage* 29, 1224–1230. doi: 10.1016/j.neuroimage.2005.08.049

Maslov, S., and Sneppen, K. (2002). Specificity and stability in topology of protein networks. *Science* 296, 910–913. doi: 10.1126/science.1065103

Monteiro, P., and Feng, G. (2017). SHANK proteins: roles at the synapse and in autism spectrum disorder. *Nat. Rev. Neurosci.* 18, 147–157. doi: 10.1038/nrn.2016.183

Muller, R. A., and Fishman, I. (2018). Brain connectivity and neuroimaging of social networks in autism. *Trends Cogn. Sci.* 22, 1103–1116. doi: 10.1016/j.tics.2018.09.008

Oosterhof, N. N., Wiestler, T., Downing, P. E., and Diedrichsen, J. (2011). A comparison of volume-based and surface-based multi-voxel pattern analysis. *Neuroimage* 56, 593–600. doi: 10.1016/j.neuroimage.2010.04.270

Phelan, K., and McDermid, H. E. (2012). The 22q13.3 deletion syndrome (phelan-mcdermid syndrome). *Mol. Syndromol.* 2, 186–201. doi: 10.1159/000334260

Phelan, M. C. (2008). Deletion 22q13.3 syndrome. *Orphanet. J. Rare Dis.* 3:14. doi: 10.1186/1750-1172-3-14

Philippe, A., Boddaert, N., Vaivre-Douret, L., Robel, L., Danon-Boileau, L., Malan, V., et al. (2008). Neurobehavioral profile and brain imaging study of the 22q13.3 deletion syndrome in childhood. *Pediatrics* 122:e376–e382. doi: 10.1542/peds.2007-2584

Poletti, M., Enrici, I., and Adenzato, M. (2012). Cognitive and affective theory of mind in neurodegenerative diseases: neuropsychological, neuroanatomical and neurochemical levels. *Neurosci. Biobehav. Rev.* 36, 2147–2164. doi: 10.1016/j.neubiorev.2012.07.004

Sarasua, S. M., Dwivedi, A., Boccuto, L., Chen, C. F., Sharp, J. L., Rollins, J. D., et al. (2014). 22q13.2q13.32 genomic regions associated with severity of speech delay, developmental delay, and physical features in phelan-mcdermid syndrome. *Genet. Med.* 16, 318–328. doi: 10.1038/gim.2013.144

Seeley, W. W., Menon, V., Schatzberg, A. F., Keller, J., Glover, G. H., Kenna, H., et al. (2007). Dissociable intrinsic connectivity networks for salience processing and executive control. *J. Neurosci.* 27, 2349–2356. doi: 10.1523/JNEUROSCI.5587-06.2007

Seidlitz, J., Vasa, F., Shinn, M., Romero-Garcia, R., Whitaker, K. J., Vertes, P. E., et al. (2018). Morphometric similarity networks detect microscale cortical organization and predict inter-individual cognitive variation. *Neuron* 97, 231–247. doi: 10.1016/j.neuron.2017.11.039

Sharda, M., Khundrakpam, B. S., Evans, A. C., and Singh, N. C. (2016). Disruption of structural covariance networks for language in autism is modulated by verbal ability. *Brain Struct. Funct.* 221, 1017–1032. doi: 10.1007/s00429-014-0953-z

Shepherd, G. M. (2013). Corticostriatal connectivity and its role in disease. *Nat. Rev. Neurosci.* 14, 278–291. doi: 10.1038/nrn3469

Soorya, L., Kolevzon, A., Zweifach, J., Lim, T., Dobry, Y., Schwartz, L., et al. (2013). Prospective investigation of autism and genotype-phenotype correlations in 22q13 deletion syndrome and SHANK3 deficiency. *Mol. Autism* 4:18. doi: 10.1186/2040-2392-4-18

Srivastava, S., Scherrer, B., Prohl, A. K., Filip-Dhima, R., Kapur, K., Kolevzon, A., et al. (2019). Volumetric analysis of the basal ganglia and cerebellar structures in patients with phelan-mcdermid syndrome. *Pediatr. Neurol.* 90, 37–43. doi: 10.1016/j.pediatrneurol.2018.09.008

Tang, X., Zhang, Y., Liu, D., Hu, Y., Jiang, L., and Zhang, J. (2021). Association of gyrification pattern, white matter changes, and phenotypic profile in patients with Parkinson disease. *Neurology* 96:e2387–e2394. doi: 10.1212/WNL.0000000000011894

Tordjman, S., Celume, M. P., Denis, L., Motillon, T., and Keromnes, G. (2019). Reframing schizophrenia and autism as bodily self-consciousness disorders leading to a deficit of theory of mind and empathy with social communication impairments. *Neurosci. Biobehav. Rev.* 103, 401–413. doi: 10.1016/j.neubiorev.2019.04.007

Van Essen, D. C., Dierker, D., Snyder, A. Z., Raichle, M. E., Reiss, A. L., and Korenberg, J. (2006). Symmetry of cortical folding abnormalities in Williams syndrome revealed by surface-based analyses. *J. Neurosci.* 26, 5470–5483. doi: 10.1523/JNEUROSCI.4154-05.2006

van Oort, J., Kohn, N., Vrijsen, J. N., Collard, R., Duyser, F. A., Brolsma, S. C. A., et al. (2020). Absence of default mode downregulation in response to a mild psychological stressor marks stress-vulnerability across diverse psychiatric disorders. *Neuroimage Clin.* 25:102176. doi: 10.1016/j.nicl.2020.102176

van Oort, J., Tendolkar, I., Hermans, E. J., Mulders, P. C., Beckmann, C. F., Schene, A. H., et al. (2017). How the brain connects in response to acute stress: a review at the human brain systems level. *Neurosci. Biobehav. Rev.* 83, 281–297. doi: 10.1016/j.neubiorev.2017.10.015

van Rooij, D., Anagnostou, E., Arango, C., Auzias, G., Behrmann, M., Busatto, G. F., et al. (2018). Cortical and subcortical brain morphometry differences between patients with autism spectrum disorder and healthy individuals across the lifespan: results from the ENIGMA ASD working group. *Am. J. Psychiatry* 175, 359–369. doi: 10.1176/appi.ajp.2017.17010100

Vissers, M. E., Cohen, M. X., and Geurts, H. M. (2012). Brain connectivity and high functioning autism: a promising path of research that needs refined models, methodological convergence, and stronger behavioral links. *Neurosci. Biobehav. Rev.* 36, 604–625. doi: 10.1016/j.neubiorev.2011.09.003

von dem Hagen, E. A., Stoyanova, R. S., Baron-Cohen, S., and Calder, A. J. (2013). Reduced functional connectivity within and between 'social' resting state networks in autism spectrum conditions. *Soc. Cogn. Affect. Neurosci.* 8, 694–701. doi: 10.1093/scan/nss053

Wang, J., Wang, L., Zang, Y., Yang, H., Tang, H., Gong, Q., et al. (2009). Parcellation-dependent small-world brain functional networks: a resting-state fMRI study. *Hum. Brain Mapp.* 30, 1511–1523. doi: 10.1002/hbm.20623

Wei, Y., de Lange, S. C., Scholtens, L. H., Watanabe, K., Ardesch, D. J., Jansen, P. R., et al. (2019). Genetic mapping and evolutionary analysis of human-expanded cognitive networks. *Nat. Commun.* 10:4839. doi: 10.1038/s41467-019-12764-8

Wolf, D., Mittelberg, I., Rekittke, L. M., Bhavsar, S., Zvyagintsev, M., Haeck, A., et al. (2018). Interpretation of social interactions: functional imaging of cognitive-semiotic categories during naturalistic viewing. *Front. Hum. Neurosci.* 12:296. doi: 10.3389/fnhum.2018.00296

Yan, Z., and Rein, B. (2021). Mechanisms of synaptic transmission dysregulation in the prefrontal cortex: pathophysiological implications. *Mol. Psychiatry* (in press). doi: 10.1038/s41380-021-01092-3

Yang, D. Y., Beam, D., Pelphrey, K. A., Abdullahi, S., and Jou, R. J. (2016). Cortical morphological markers in children with autism: a structural magnetic resonance imaging study of thickness, area, volume, and gyrification. *Mol. Autism* 7:11. doi: 10.1186/s13229-016-0076-x

Yin, D., Chen, X., Zeljic, K., Zhan, Y., Shen, X., Yan, G., et al. (2019). A graph representation of functional diversity of brain regions. *Brain Behav.* 9:e01358. doi: 10.1002/brb3.1358

Yin, D., Song, F., Xu, D., Sun, L., Men, W., Zang, L., et al. (2014). Altered topological properties of the cortical motor-related network in patients with subcortical stroke revealed by graph theoretical analysis. *Hum. Brain Mapp.* 35, 3343–3359. doi: 10.1002/hbm.22406

Yotter, R. A., Nenadic, I., Ziegler, G., Thompson, P. M., and Gaser, C. (2011). Local cortical surface complexity maps from spherical harmonic reconstructions. *Neuroimage* 56, 961–973. doi: 10.1016/j.neuroimage.2011.02.007

Ziats, C. A., Patterson, W. G., and Friez, M. (2021). Syndromic autism revisited: review of the literature and lessons learned. *Pediatr. Neurol.* 114, 21–25. doi: 10.1016/j.pediatrneurol.2020.06.011

Zielinski, B. A., Gennatas, E. D., Zhou, J., and Seeley, W. W. (2010). Network-level structural covariance in the developing brain. *Proc. Natl. Acad. Sci. U.S.A.* 107, 18191–18196. doi: 10.1073/pnas.1003109107

Conflict of Interest: The authors declare that the research was conducted in the absence of any commercial or financial relationships that could be construed as a potential conflict of interest.

Publisher's Note: All claims expressed in this article are solely those of the authors and do not necessarily represent those of their affiliated organizations, or those of the publisher, the editors and the reviewers. Any product that may be evaluated in this article, or claim that may be made by its manufacturer, is not guaranteed or endorsed by the publisher.

frontiers in Neuroscience

ORIGINAL RESEARCH
published: 15 November 2021
doi: 10.3389/fnins.2021.739580

Adaptive Immune Deficiency Impairs Neural Activity After Training and Retrieval

Huiping Li[1], Zhongxiao Fu[2], Meixin Hu[1] and Xiu Xu[1]**

[1] Department of Child Health Care, Children's Hospital of Fudan University, National Children's Medical Center, Shanghai, China, [2] Department of Neuroscience, University of Virginia, Charlottesville, VA, United States

Neuroimmune interactions have been studied for decades. Several neurodevelopmental disorders have been associated with immune dysfunction. However, the effects of immune system on neuronal function remain unknown. Herein, based on c-Fos protein expression, we characterized the brain areas that are activated after contextual fear conditioning (CFC) training or retrieval in severe combined immune deficiency (SCID) and wild-type mice. Further, we analyzed the interregional correlations of c-Fos activity that are affected by deficiency in adaptive immunity. Results showed significantly lower c-Fos density in learning and memory-associated brain regions of SCID mice after memory retrieval, but not during the CFC training. Moreover, SCID mice exhibited remarkably discordant interregional neuronal activities of learning neuron circuits after CFC training, which could be the cause of inefficient activation of the memory circuit after retrieval. These results provide a new perspective on how adaptive immunity affects neuronal function. Adaptive immune deficiency impairs the coordination of neural activity after training and retrieval, which might be a potential therapeutic target for neurodevelopmental disorders.

Keywords: adaptive immune, c-Fos, neural activity, contextual fear conditioning, neurodevelopmental disorders

OPEN ACCESS

Edited by:
Xiaoyan Ke,
Nanjing Brain Hospital Affiliated to Nanjing Medical University, China

Reviewed by:
Cesar Canales,
University of California, Davis, United States
Emanuela Zuccaro,
University of Padua, Italy

****Correspondence:***
Huiping Li
lihuiping@fudan.edu.cn
Xiu Xu
xuxiu@fudan.edu.cn

Specialty section:
This article was submitted to Neurodevelopment, a section of the journal Frontiers in Neuroscience

Received: *11 July 2021*
Accepted: *18 October 2021*
Published: *15 November 2021*

Citation:
Li H, Fu Z, Hu M and Xu X (2021) Adaptive Immune Deficiency Impairs Neural Activity After Training and Retrieval. Front. Neurosci. 15:739580. doi: 10.3389/fnins.2021.739580

INTRODUCTION

A wide range of neurodevelopmental disorders, including autism spectrum disorder (Hughes et al., 2018) and neurodevelopmental delay (Bodnar et al., 2020), have been associated with immune system dysregulation. Advances in our understanding of neuroimmune interactions have led to fundamental changes in the concepts of immunology and neuroscience. The immune system is not self-regulated, but functions in close association with the nervous system (Dantzer, 2018). The nervous system regulates immune factors through neuroendocrine mediators and peripheral nerve endings innervating immune organs. Reciprocally, immune cells and mediators play a regulatory role in the nervous system and participate in the elimination and plasticity of synapses during development, as well as in synaptic plasticity during adulthood (Tanabe and Yamashita, 2018; Morimoto and Nakajima, 2019).

Studies have demonstrated that adaptive immunity is implicated in brain functions, including learning and memory retrieval (Brynskikh et al., 2008; Baruch and Schwartz, 2013; Radjavi et al., 2014). The first evidence came from experiments that examined the cognitive ability of wild-type (WT) and severe combined immune deficiency (SCID, deficient in both T cell and B cell responses) mice, by using the Morris water maze, a hippocampal-dependent visuospatial learning/memory task (Kipnis et al., 2004). SCID mice manifested significant impairment of spatial memory compared to their WT counterparts, and the brain function in SCID mice was restored when adaptive immunity was enhanced. Subsequently, researchers found that depletion of adaptive immune cells in naive mice also impairs spatial memory, supporting the notion that immunity plays a lifelong role in maintaining brain functions (Wolf et al., 2009; Derecki et al., 2010). However, the mechanism by which adaptive immunity affects memory is poorly understood.

Memory is a complex process through which information acquired during learning is stored. Synaptic and system changes are involved in the memory processes. The synaptic change is completed within hours of training and involves the stabilization of synaptic connectivity in localized circuits (Takeuchi et al., 2014). System changes are a more prolonged process that involves gradual reorganization of the brain regions that support memory (Frankland and Bontempi, 2005). Contextual fear conditioning (CFC) behavioral tests have been well studied as hippocampus-dependent spatial and associative learning tasks that activate hippocampal–cortical memory networks (Cowansage et al., 2014). Episodic memories initially require rapid synaptic plasticity within the hippocampus for their formation and are gradually consolidated in neocortical networks for permanent storage (Kitamura et al., 2017). Evidence shows that the hippocampus, amygdala, retrosplenial cortex (RSP), and prefrontal cortex are key regions supporting memory consolidation and retrieval processes (Tonegawa et al., 2018; de Sousa et al., 2019).

c-Fos is one of the first transcription factors whose induction was shown to be activity-dependent and is routinely used as an indicator of neuronal activation (Gallo et al., 2018; Silva et al., 2019). Fear memory paradigms have been shown to produce changes in c-Fos expression in different structures (Maviel et al., 2004; Lopez et al., 2012; Pignatelli et al., 2019). In this study, using c-Fos protein expression pattern, we characterized the brain areas that are activated in WT and SCID mice after CFC training or retrieval and evaluated the interregional correlations of c-Fos activity affected by adaptive immunity deficiency. Our results helped to uncover the immunity-neuron interaction and the potential therapy for neurodevelopmental disorders with immune dysfunction.

MATERIALS AND METHODS

Mouse Strains and Housing

B6.CB17-*Prkdc*^{scid}/SzJ (SCID, JAX 001913) and WT mice (C57BL/6J background) purchased from the Jackson Laboratory were maintained in the animal facility for at least 1 week prior to the start of the experiments. Mice were maintained and bred in-house under standard 12-h light–dark cycle conditions. They were given standard rodent chow and sterilized tap water *ad libitum*, unless stated otherwise. Male mice at 10–20 weeks of age were used for the behavioral experiments. Experimenters were blinded to the experimental groups during scoring and quantification. All experiments were approved by the Institutional Animal Care and Use Committee of the University of Virginia.

Contextual Fear Conditioning Training and Retrieval

The equipment used was purchased from Coulbourn Instruments (United States). **Figure 1A** illustrates the experimental design. During training, mice were introduced to a new context (test chamber), following which a stimulus was delivered in the form of a foot shock. The walls of the test chamber were painted white, and the chamber was scented with 0.25% benzaldehyde. Each mouse was placed in the test chamber for 3 min. After 3 min, electric foot shock (2 s, 0.50 mA) was delivered thrice during 198–200, 258–260, and 318–320 s. The mice were left in the test chamber for an additional 30 s before they were returned to their home cages.

At 1 day or 4 weeks posttraining, CFC-trained mice were returned to the test chamber for memory retrieval. The test at 1 day posttraining was referred to as recent retrieval. The test at 4 weeks posttraining was called remote retrieval. Mice were kept in the test cage for 3 min and returned back to their home cage without delivering the electric foot shock.

Immunohistochemistry

Mice were euthanized by Euthasol overdose (10% vol/vol in saline, intraperitoneally) at 90 min (for c-Fos) and 60 min (for Arc) after training or retrieval. The animals were transcardially perfused with ice-cold phosphate-buffered saline (PBS) containing heparin (10 U mL^{-1}) followed by 4% paraformaldehyde (PFA). Brains were dissected out and kept in 4% PFA overnight at 4°C. The fixed brains were washed with PBS and cryoprotected by immersing them in 30% sucrose solution for 48 h at 4°C. The fixed brain tissue was frozen in Tissue-Plus OCT compound (Thermo Scientific) and sliced into 40-μm-thick free-floating coronal sections using a cryostat (Leica). Brain sections were stored in PBS containing 0.02% sodium azide at 4°C until further use.

Brain sections were blocked with 1% bovine serum albumin (BSA), 2% normal serum (either goat or chicken), 0.2% Triton X-100, and 0.1% Tween 20 in PBS for 1 h at room temperature (RT). Sections were then incubated with appropriate primary antibodies in PBS containing 5% BSA and 0.2% Triton X-100 overnight at 4°C. The primary antibodies used were as follows: rabbit anti-c-Fos (1:1,000, Synaptic Systems, 226003), mouse anti-NeuN (1:300; Millipore, MAB377, clone A60), or rabbit anti-Arc (1:100, Santa Cruz, sc-15325). Brain sections were then washed three times for 15 min at RT with PBS containing 0.2% Triton X-100 and 0.1% Tween 20. This

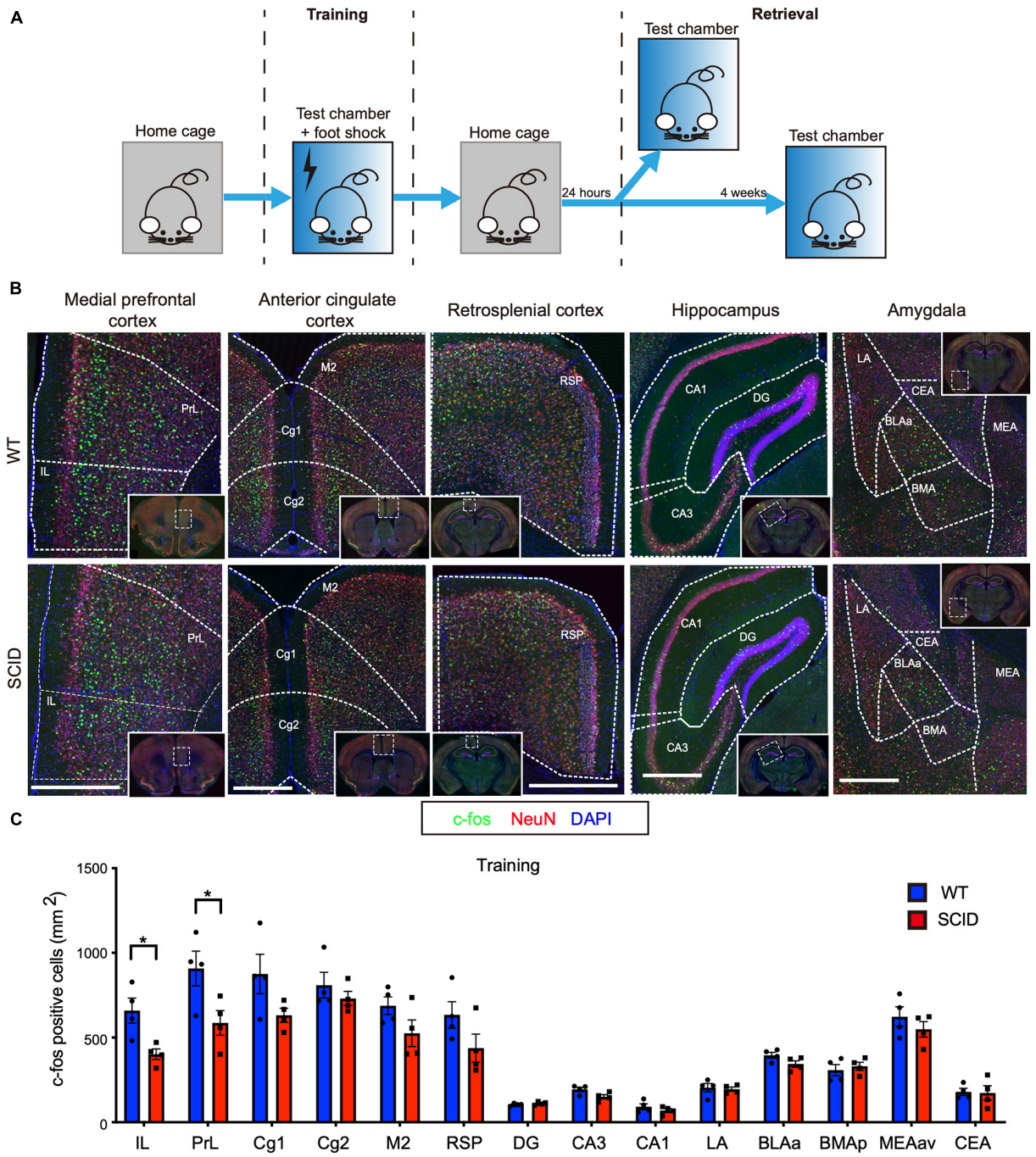

FIGURE 1 | Limited differences in c-Fos expression between SCID and WT mice brain after contextual fear conditioning training. **(A)** General scheme of contextual fear conditioning training and retrieval. **(B)** Representative immunofluorescence images of the brain sections from WT (top) and SCID (bottom) mice 90 min after CFC training. c-Fos is in green, NeuN in red, and DAPI in blue. Brain regions: medial prefrontal cortex, anterior cingulate cortex, retrosplenial cortex, hippocampus, and amygdala. Scale bar, 500 μm. Low-power images were presented in the white solid line frames, with white dotted frames that showed the regions zoomed in. White dotted line outlined most of the brain regions for quantification. **(C)** c-Fos–positive cell density in different brain regions of WT and SCID mice (n = 4, data represent mean ± SEM, $^*p < 0.05$).

was followed by incubation at RT for 1 or 1.5 h with species-matched fluorescently conjugated secondary antibodies (1:1,000, Invitrogen) diluted in PBS containing 0.2% Triton X-100. Nuclei were stained with 4′,6-diamidino-2-phenylindole (DAPI, 1:10,000, Sigma-Aldrich) at RT for 15 min. The sections were washed with PBS three times for 15 min and mounted with Aqua-Mount (Thermo Scientific TA-125-AM) under coverslips.

Image Acquisition and Analysis

For detecting c-Fos–positive cells, samples from the same experiment were stained and analyzed simultaneously using same settings on the Olympus FV1200 laser scanning confocal microscope with a 10× objective and 0.40 NA. Quantification of c-Fos expression was performed using the Fiji software (NIH). The following brain regions were analyzed using specific coordinates: infralimbic cortex (IL) and prelimbic cortex (PrL) at +1.98 to +1.54 mm from bregma; cingulate cortex (Cg1, Cg2, and M2) at +1.10 to +0.26 mm from bregma; hippocampus and RSP at −1.58 to −2.06 mm from bregma; and amygdala at −1.46 to −2.06 mm from bregma. Brain areas were manually outlined based on the DAPI and NeuN signals following the Allen Brain Reference Atlas and measured automatically by Fiji. The c-Fos–positive nuclei for each brain region were counted using the "Analyze Particles" tool in Fiji. Only the c-Fos–positive nuclei within a specific size range were counted, and a constant threshold level of staining was used to distinguish c-Fos–positive cells as follows: a fluorescence area between 18.07 and 117.78 μm^2 and mean intensity greater than 60 (arbitrary units) were counted. This method has been described previously (Lopatina et al., 2014; Zhong et al., 2014). The density of c-Fos–positive cells (c-Fos per mm^2) in each brain region was averaged from three sections per animal and at least four mice for each group.

Statistical Analysis

Statistical analysis was performed using Prism 8.0 (GraphPad Software, Inc.). Comparison between two groups was performed using a two-tailed unpaired Student *t*-test. Pearson correlation coefficients were calculated for pairwise comparisons of c-Fos density among all 14 brain regions analyzed. Correlations were displayed as a color-coded correlation matrix generated using a custom R-code (R version 3.6.3).

RESULTS

c-Fos Expression in Severe Combined Immune Deficiency and Wild-Type Mice After Contextual Fear Conditioning Training

Contextual fear conditioning behavioral test, a hippocampus-dependent spatial and associative learning/memory task, was used to compare the spatial learning/memory of SCID and WT mice. The CFC training was performed by transferring each mouse from the home cage to the test chamber where the animals received an electric foot shock (**Figure 1A**). SCID and WT mice were euthanized 90 min after CFC training. To investigate the brain regions that are activated during the training, brain slices were stained for c-Fos and NeuN. We quantified the density of c-Fos–positive cells in 14 brain regions that are known to play a crucial role in contextual fear learning and memory (Tovote et al., 2015). **Figure 1B** shows the density of c-Fos–positive cells in the IL, PrL, anterior cingulate cortex (Cg1, Cg2, and M2), RSP, hippocampus (DG, CA1, and CA3), and amygdala.

Although strong c-Fos expression was observed in these 14 brain regions of SCID mice, c-Fos expression was slightly higher in the WT mice brain. However, significant differences were observed only in the IL and PrL ($p < 0.05$, **Figure 1C**). IL and PrL regions have well-established roles in the fear memory circuit (Frankland and Bontempi, 2005).

Inefficient c-Fos Expression in Severe Combined Immune Deficiency Mice Following Memory Retrieval

To assess brain activity during recent memory retrieval, CFC-trained SCID and WT mice were transferred to the test cage at 1 day post-CFC training (**Figure 1A**). In the retrieval experiment, no electric shock was given to the animals. The animals were euthanized 90 min later, and c-Fos expression in the brain was evaluated (**Figure 2A**). Significant differences were observed in the hippocampus (DG, CA1, and CA3; $p < 0.001$, $p < 0.05$, and $p < 0.05$, respectively) and RSP ($p < 0.01$) (**Figure 2B**). Furthermore, the density of Acr (another immediate early gene)–positive cells at RSP and DG regions was lower in SCID mice than WT, which was consistent with c-Fos expression ($p < 0.05$) (**Figures 2C,D**).

Remote memory retrieval was performed at 4 weeks post-CFC training (**Figure 1A**). CFC-trained SCID and WT mice were placed in the test cage without giving the electric shock. Results showed significantly lower c-Fos levels in SCID mice, especially in the medial PrL, RSP, and CA1 (**Figures 3A,B**).

Lack of Adaptive Immunity Impairs the Interregional Activation of Learning and Memory Neuron Circuits

To gain insight into the functional connections within the learning and memory neuron circuits, we computed the correlation between each pair of brain regions in each group. The interregional correlation matrix for each experimental group led to the identification of sets of regions whose c-Fos density covaried across mice.

Results showed that in WT mice after CFC training, there was a strong connection between the brain regions that are important for learning and memory (**Figure 4A**, left). However, SCID mice showed remarkably discordant activation between the hippocampus–prefrontal cortex, hippocampus–amygdala, and prefrontal cortex–amygdala (**Figure 4A**, right). With the withdrawal of DG activation in memory retrieval, the prefrontal cortex to process memories might mirror that of the hippocampus to process recent memories. Inefficient activation of the cortex regions during the CFC training affected the memory retrieval, especially remote memory retrieval (**Figures 4B,C**).

DISCUSSION

To assess brain function and memory processes in mice lacking adaptive immunity, we compared c-Fos expression in 14 brain regions of SCID and WT mice that are known to be involved

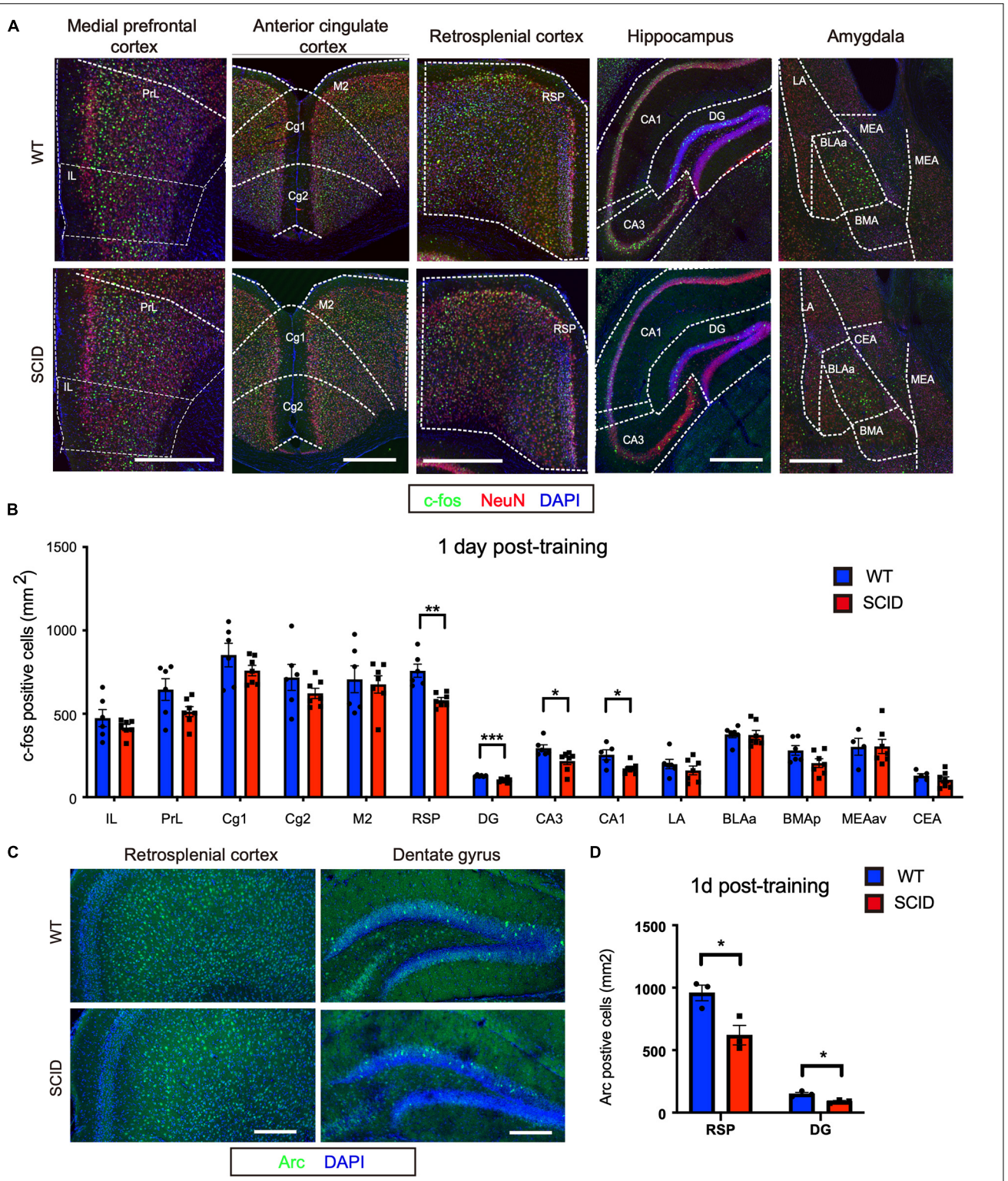

FIGURE 2 | Inefficient neuronal activity in the hippocampus and retrosplenial cortex of SCID mice after recent memory retrieval. **(A)** Representative immunofluorescence images of five brain regions from WT and SCID mice after recent memory retrieval (1 day after CFC training). c-Fos is in green, NeuN in red, and DAPI in blue. Scale bar, 500 μm. **(B)** c-Fos–positive cell density in different brain regions of WT and SCID mice after recent memory retrieval (n = 6–7 per group, data represent mean ± SEM, $^{*}p < 0.05$). **(C)** Representative immunofluorescence images of retrosplenial cortex and dentate gyrus from WT and SCID mice 60 min after recent memory retrieval. Arc is in green, and DAPI in blue. Scale bar, 200 μm. **(D)** Quantified Acr-positive cells at RSP and DG regions after recent memory retrieval (n = 3 per group; data represent mean ± SEM, $^{*}p < 0.05$, $^{**}p < 0.01$, $^{***}p < 0.001$).

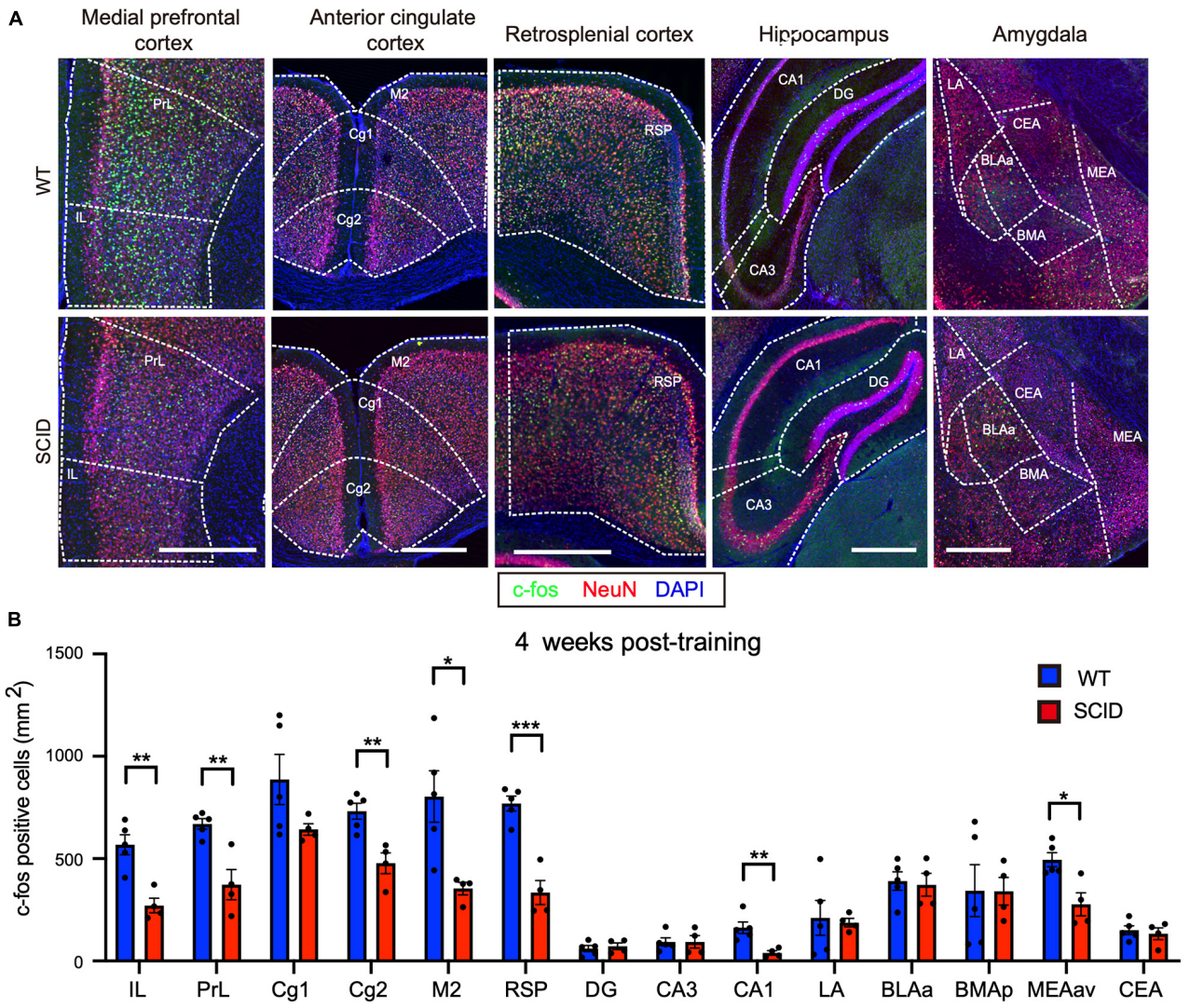

FIGURE 3 | Significantly lower neuronal activity in memory-associated brain regions of SCID mice after remote memory retrieval. **(A)** Representative immunofluorescence images of five different brain regions from WT and SCID mice after remote memory retrieval (4 weeks after CFC training). c-Fos is in green, NeuN in red, and DAPI in blue. Scale bar, 500 μm. **(B)** c-Fos–positive cell density in the brain regions of WT and SCID mice after remote memory retrieval (n = 4–5 per group; data represent mean ± SEM, $^{*}p < 0.05$, $^{**}p < 0.01$, $^{***}p < 0.001$).

in the acquisition of contextual memories. IL and PrL showed remarkably lower c-Fos expression during learning in SCID mice. In recent memory retrieval test at 1 day post-CFC training, remarkable differences in c-Fos density in the RSP and hippocampus were observed between SCID and WT mice. In the remote memory retrieval test at 4 weeks post-CFC training, the prefrontal cortex, RSP, CA1, and medial nuclei of the amygdala of the SCID mice showed significantly lower c-Fos expression than WT mice.

Memories are thought to be initially stored within the hippocampal–amygdala network (recent memory) and, over time, slowly consolidate within the neocortex for permanent storage (remote memory) (Frankland and Bontempi, 2005; Lopez et al., 2012; Tonegawa et al., 2018; Todd et al., 2019). Consistent with previous studies, our study found that in WT mice, the DG-CA3 hippocampal network was active during learning and recent memory retrieval (1 day posttraining), whereas it was not activated by remote memory retrieval (4 weeks posttraining). Hippocampal CA1 activity was involved in both recent and remote memory retrieval. In our study, significantly lower neuronal activity was observed in the hippocampus and neocortex of the SCID mice during memory retrieval.

Furthermore, interregional activation patterns showed that SCID mice have abnormalities in neural circuits, which might be the cause of memory dysfunctions. The low neuronal activity in SCID mice was limited to IL and PrL regions during the learning stage. However, remarkable discordant activation was observed between the hippocampus–prefrontal cortex, hippocampus–amygdala, and prefrontal cortex–amygdala. IL and PrL, as part of the prefrontal cortex, are highly interconnected with the

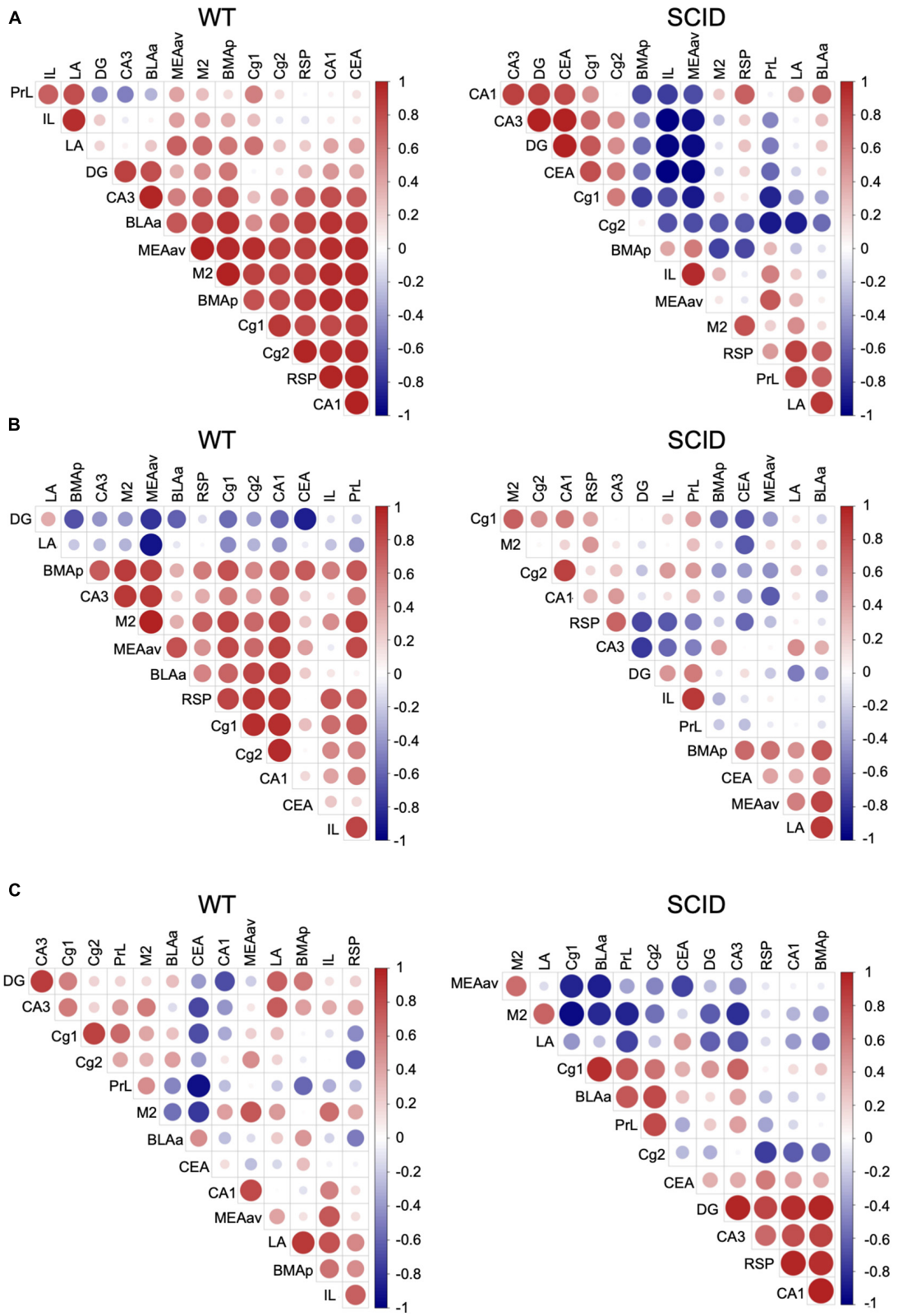

FIGURE 4 | Variations in interregional correlation of c-Fos activation between WT and SCID mice. Pearson correlation matrices showing interregional correlations of c-Fos activation density. Axes represent the brain regions. The different colors represent Pearson correlation coefficients (scale, right). Panel **(A)** is for WT and SCID mice after the CFC training. Panel **(B)** represents WT and SCID mice after recent retrieval. Panel **(C)** represents WT and SCID mice after remote retrieval.

hippocampus, sensory cortex, motor cortex, and limbic cortex; therefore, they are ideally suited to integrate and synthesize information from a large number of different sources (Euston et al., 2012). Kitamura et al. (2017) found that neocortical prefrontal memory engram cells are rapidly generated during initial learning through inputs from both the hippocampus and the basolateral amygdala and became functionally mature with time, which is critical for remote contextual fear memory. The insufficient activation of IL and PrL by the hippocampus–prefrontal cortex circuitry does not affect the learning ability of SCID mice, but could have a potential effect on memory retrieval. The importance of interregional coactivation in neuron circuits has been demonstrated using chemogenetic neuronal inhibition and computational modeling (Kitamura et al., 2017; Roy et al., 2017; Pignatelli et al., 2019).

The findings of this study have to be seen in light of some limitations. In the CFC behavior test, SCID mice did not show significant difference for freezing time between genders. Considering stable behavior phenotype, we used only male mice in the study. However, immune deficiency and neurodevelopmental disorders affect both male and female. It is better to include female mice in a future study. The second limitation concerns that the study did not provide mechanistic insights into the impairments of neural activity in SCID mice after training and retrieval. Further studies will be aimed at understanding the molecular basis that underlies how adaptive immunity impairs neural activity.

Overall, our results provide new details about how adaptive immunity affects neuronal function. Mice lacking components of adaptive immunity have problems with neuronal activation and interregional coordination of neuron circuits during training and memory retrieval. Our results uncover the neural–immune interactions and will help in developing novel therapies for neurodevelopmental disorders due to immune dysfunction.

DATA AVAILABILITY STATEMENT

The raw data supporting the conclusions of this article will be made available by the authors, without undue reservation.

ETHICS STATEMENT

The animal study was reviewed and approved by the Institutional Animal Care and Use Committee of the University of Virginia.

AUTHOR CONTRIBUTIONS

HL performed and analyzed IHC experiments and took the lead in writing the manuscript. ZF performed the behavioral tests. MH took part in c-Fos data analysis. XX conceived the project and provided advice. All authors provided feedback and contribution to the final manuscript.

FUNDING

This work was supported by the National Key Research and Development Program of China (No. 2016YFC1306205) and Key Subject Construction Project of Shanghai Municipal Health Commission (No. shslczdzk02903).

ACKNOWLEDGMENTS

We thank Jiawei Lu and Yunzhou Huang (Lu Ming Biotech Co., Ltd., Shanghai, China) for assistance with the analysis of the Pearson correlation coefficients. We would like to thank Editage (www.editage.com) for English language editing.

REFERENCES

Baruch, K., and Schwartz, M. (2013). CNS-specific T cells shape brain function via the choroid plexus. *Brain Behav. Immun.* 34, 11–16. doi: 10.1016/j.bbi.2013.04.002

Bodnar, T. S., Raineki, C., Wertelecki, W., Yevtushok, L., Plotka, L., Granovska, I., et al. (2020). Immune network dysregulation associated with child neurodevelopmental delay: modulatory role of prenatal alcohol exposure. *J. Neuroinflammation* 17:39. doi: 10.1186/s12974-020-1717-8

Brynskikh, A., Warren, T., Zhu, J., and Kipnis, J. (2008). Adaptive immunity affects learning behavior in mice. *Brain Behav. Immun.* 22, 861–869. doi: 10.1016/j.bbi.2007.12.008

Cowansage, K. K., Shuman, T., Dillingham, B. C., Chang, A., Golshani, P., and Mayford, M. (2014). Direct reactivation of a coherent neocortical memory of context. *Neuron* 84, 432–441. doi: 10.1016/j.neuron.2014.09.022

Dantzer, R. (2018). Neuroimmune interactions: from the brain to the immune system and vice versa. *Physiol. Rev.* 98, 477–504. doi: 10.1152/physrev.00039.2016

de Sousa, A. F., Cowansage, K. K., Zutshi, I., Cardozo, L. M., Yoo, E. J., Leutgeb, S., et al. (2019). Optogenetic reactivation of memory ensembles in the retrosplenial cortex induces systems consolidation. *Proc. Natl. Acad. Sci. U.S.A.* 116, 8576–8581. doi: 10.1073/pnas.1818432116

Derecki, N. C., Cardani, A. N., Yang, C. H., Quinnies, K. M., Crihfield, A., Lynch, K. R., et al. (2010). Regulation of learning and memory by meningeal immunity: a key role for IL-4. *J. Exp. Med.* 207, 1067–1080. doi: 10.1084/jem.20091419

Euston, D. R., Gruber, A. J., and McNaughton, B. L. (2012). The role of medial prefrontal cortex in memory and decision making. *Neuron* 76, 1057–1070. doi: 10.1016/j.neuron.2012.12.002

Frankland, P. W., and Bontempi, B. (2005). The organization of recent and remote memories. *Nat. Rev. Neurosci.* 6, 119–130. doi: 10.1038/nrn1607

Gallo, F. T., Katche, C., Morici, J. F., Medina, J. H., and Weisstaub, N. V. (2018). Immediate early genes, memory and psychiatric disorders: focus on c-Fos, Egr1 and Arc. *Front. Behav. Neurosci.* 12:79. doi: 10.3389/fnbeh.2018.00079

Hughes, H. K., Mills Ko, E., Rose, D., and Ashwood, P. (2018). Immune dysfunction and autoimmunity as pathological mechanisms in autism spectrum disorders. *Front. Cell Neurosci.* 12:405. doi: 10.3389/fncel.2018.00405

Kipnis, J., Cohen, H., Cardon, M., Ziv, Y., and Schwartz, M. (2004). T cell deficiency leads to cognitive dysfunction: implications for therapeutic vaccination for schizophrenia and other psychiatric conditions. *Proc. Natl. Acad. Sci. U.S.A.* 101, 8180–8185. doi: 10.1073/pnas.0402268101

Kitamura, T., Ogawa, S. K., Roy, D. S., Okuyama, T., Morrissey, M. D., Smith, L. M., et al. (2017). Engrams and circuits crucial for systems consolidation of a memory. *Science* 356, 73–78. doi: 10.1126/science.aam6808

Lopatina, O., Yoshihara, T., Nishimura, T., Zhong, J., Akther, S., Fakhrul, A. A., et al. (2014). Anxiety- and depression-like behavior in mice lacking the CD157/BST1 gene, a risk factor for Parkinson's disease. *Front. Behav. Neurosci.* 8:133. doi: 10.3389/fnbeh.2014.00133

Lopez, J., Herbeaux, K., Cosquer, B., Engeln, M., Muller, C., Lazarus, C., et al. (2012). Context-dependent modulation of hippocampal and cortical

recruitment during remote spatial memory retrieval. *Hippocampus* 22, 827–841. doi: 10.1002/hipo.20943

Maviel, T., Durkin, T. P., Menzaghi, F., and Bontempi, B. (2004). Sites of neocortical reorganization critical for remote spatial memory. *Science* 305, 96–99. doi: 10.1126/science.1098180

Morimoto, K., and Nakajima, K. (2019). Role of the immune system in the development of the central nervous system. *Front. Neurosci.* 13:916. doi: 10.3389/fnins.2019.00916

Pignatelli, M., Ryan, T. J., Roy, D. S., Lovett, C., Smith, L. M., Muralidhar, S., et al. (2019). Engram cell excitability state determines the efficacy of memory retrieval. *Neuron* 101, 274.e275–284.e275. doi: 10.1016/j.neuron.2018.11.029

Radjavi, A., Smirnov, I., and Kipnis, J. (2014). Brain antigen-reactive CD4+ T cells are sufficient to support learning behavior in mice with limited T cell repertoire. *Brain Behav. Immun.* 35, 58–63. doi: 10.1016/j.bbi.2013.08.013

Roy, D. S., Kitamura, T., Okuyama, T., Ogawa, S. K., Sun, C., Obata, Y., et al. (2017). Distinct neural circuits for the formation and retrieval of episodic memories. *Cell* 170, 1000.e1019–1012.e1019. doi: 10.1016/j.cell.2017.07.013

Silva, B. A., Burns, A. M., and Graff, J. (2019). A cFos activation map of remote fear memory attenuation. *Psychopharmacology* 236, 369–381. doi: 10.1007/s00213-018-5000-y

Takeuchi, T., Duszkiewicz, A. J., and Morris, R. G. (2014). The synaptic plasticity and memory hypothesis: encoding, storage and persistence. *Philos. Trans. R. Soc. Lond. B Biol. Sci.* 369:20130288. doi: 10.1098/rstb.2013.0288

Tanabe, S., and Yamashita, T. (2018). The role of immune cells in brain development and neurodevelopmental diseases. *Int. Immunol.* 30, 437–444. doi: 10.1093/intimm/dxy041

Todd, T. P., Fournier, D. I., and Bucci, D. J. (2019). Retrosplenial cortex and its role in cue-specific learning and memory. *Neurosci. Biobehav. Rev.* 107, 713–728. doi: 10.1016/j.neubiorev.2019.04.016

Tonegawa, S., Morrissey, M. D., and Kitamura, T. (2018). The role of engram cells in the systems consolidation of memory. *Nat. Rev. Neurosci.* 19, 485–498. doi: 10.1038/s41583-018-0031-2

Tovote, P., Fadok, J. P., and Luthi, A. (2015). Neuronal circuits for fear and anxiety. *Nat. Rev. Neurosci.* 16, 317–331. doi: 10.1038/nrn3945

Wolf, S. A., Steiner, B., Akpinarli, A., Kammertoens, T., Nassenstein, C., Braun, A., et al. (2009). CD4-positive T lymphocytes provide a neuroimmunological link in the control of adult hippocampal neurogenesis. *J. Immunol.* 182, 3979–3984. doi: 10.4049/jimmunol.0801218

Zhong, J., Liang, M., Akther, S., Higashida, C., Tsuji, T., and Higashida, H. (2014). c-Fos expression in the paternal mouse brain induced by communicative interaction with maternal mates. *Mol. Brain* 7:66. doi: 10.1186/s13041-014-0066-x

Conflict of Interest: The authors declare that the research was conducted in the absence of any commercial or financial relationships that could be construed as a potential conflict of interest.

Publisher's Note: All claims expressed in this article are solely those of the authors and do not necessarily represent those of their affiliated organizations, or those of the publisher, the editors and the reviewers. Any product that may be evaluated in this article, or claim that may be made by its manufacturer, is not guaranteed or endorsed by the publisher.

frontiers in Neuroscience

ORIGINAL RESEARCH
published: 24 November 2021
doi: 10.3389/fnins.2021.760779

Application of Clustering Method to Explore the Correlation Between Dominant Flora and the Autism Spectrum Disorder Clinical Phenotype in Chinese Children

*Biyuan Chen[1], Na You[2], Bangquan Pan[2], Xueyi He[2] and Xiaobing Zou[1]**

[1] Child Development and Behavior Center, Third Affiliated Hospital of Sun Yat-sen University, Guangzhou, China, [2] School of Mathematics, Sun Yat-sen University, Guangzhou, China

OPEN ACCESS

Edited by:
Xiaoyan Ke,
Nanjing Brain Hospital Affiliated to Nanjing Medical University, China

Reviewed by:
Chenjie Shen,
Massachusetts Institute of Technology, United States
Zhengmao Hu,
Central South University, China

****Correspondence:***
Xiaobing Zou
zouxb@mail.sysu.edu.cn

Specialty section:
This article was submitted to Neurodevelopment, a section of the journal Frontiers in Neuroscience

Received: *18 August 2021*
Accepted: *21 October 2021*
Published: *24 November 2021*

Citation:
Chen B, You N, Pan B, He X and Zou X (2021) Application of Clustering Method to Explore the Correlation Between Dominant Flora and the Autism Spectrum Disorder Clinical Phenotype in Chinese Children. Front. Neurosci. 15:760779. doi: 10.3389/fnins.2021.760779

Autism spectrum disorder (ASD) is characterized by deficits in social interactions and repetitive, stereotypic behaviors. Evidence shows that bidirectional communication of the gut-brain axis plays an important role. Here, we recruited 62 patients with ASD in southern China, and performed a cross-sectional study to test the relationship between repeated behavior, gut microbiome composition, and alpha diversity. We divided all participants into two groups based on the clustering results of their microbial compositions and found *Veillonella* and *Ruminococcus* as the seed genera in each group. Repetitive behavior differed between clusters, and cluster 2 had milder repetitive symptoms than Cluster 1. Alpha diversity between clusters was significantly different, indicating that cluster 1 had lower alpha diversity and more severe repetitive, stereotypic behaviors. Repetitive behavior had a negative correlation with alpha diversity. We demonstrated that the difference in intestinal microbiome composition and altered alpha diversity can be associated with repetitive, stereotypic behavior in autism. The role of *Ruminococcus* and *Veillonella* in ASD is not yet understood.

Keywords: autism spectrum disorder, gut microbiome, repetitive behavior, microbiome composition, alpha diversity

INTRODUCTION

Autism spectrum disorder (ASD) refers to early-onset neurodevelopmental disorders with core deficits in social interactions and restricted repetitive behavior and interest (RRBI) (Lord et al., 2018). Increasing evidence supports the notion that the gut-brain axis plays a non-negligible regulatory role in autism, while intestinal microbes are critical bidirectional communication components between the central nervous system (CNS) and our gut (Qin et al., 2010; Cryan and O'Mahony, 2011; Dinan and Cryan, 2013). Our brain can modify gastrointestinal dynamics and local blood flow, increasing or decreasing the secretion of gastrointestinal hormones, and thereby affecting the local immune response (Mayer, 2011; Dinan and Cryan, 2017). Simultaneously,

external environmental signals are also mediated by the intestinal microbiome and interact in various ways with the CNS (De Vadder et al., 2014; Sherwin et al., 2018).

Recent studies have shown that the intestinal flora may directly affect our brain function by producing neuroendocrine metabolites such as short chain fatty acids (SCFAs) and tryptophan, or cause interference to other pathways that affect human physiological functions and behavioral performance, including stressful behavior, social interaction, eating, and addiction (Cryan and Dinan, 2012; Cussotto et al., 2018). Research has revealed that one of the gut microbes, *Lactobacillus rhamnosus,* diminishes anxiety-related behavior in rodent models depending on vagus signal transmission (Bravo et al., 2011). Social behavior deficits in germ-free (GF) mice are also considered critical evidence supporting the assertion that changes in the intestinal microbiome can affect brain function as well as behavioral changes in the individual (Desbonnet et al., 2014; Buffington et al., 2016).

Restricted repetitive behavior and interest (RRBI) is considered a key feature of ASDs and may be related to compositional changes of the intestinal flora (Wolff et al., 2014; McKinnon et al., 2019; Osadchiy et al., 2019), but few studies have addressed this domain (Ho et al., 2020). In this cross-sectional study, we hypothesized that the ASD gut microbiome would be reflected by similar community groups and the severity of their repeated, stereotypic behaviors would vary between clusters. Previous studies on intestinal flora alpha diversity in children with ASD have not yet reached a consensus on this (Liu et al., 2019). Thus, we hypothesized that alpha diversity may be related to one or more RRBI sub-domains.

MATERIALS AND METHODS

Materials

Study Population

The research team recruited 62 subjects – (non-twin, from simple families, all skilled in Mandarin) – from southern China. All subjects were diagnosed with ASD according to the DSM-5 criteria by two physicians with extensive clinical experience, and their scores were further determined to be higher than the ASD cut-off by the Autism Diagnostic Interview-Revised (ADI-R) and Autism Diagnostic Observation Schedule (ADOS) assessment. Subjects age ranged from 3 to 10 years, with a male to female ratio of 3:1. The exclusion criteria for this study were genetic diseases with known definite chromosomal disorders, Rett syndrome, 22q13 deficiency syndrome, other degenerative symptoms, other serious neurological diseases (such as seizures, tuberous sclerosis) or severe mental illness, as well as children with significant congenital malformations or parents with serious illnesses. The study was approved by the Institutional Review Committee of the Third Affiliated Hospital of Sun Yat-sen University.

Microbiome Analysis

Parents used a clean disposable container or a non-contaminated urine-clean diaper to collect approximately 10 g of stool sample. Approximately 200 mg was placed in a sampling tube designed for fecal specimen collection (patent number: US 8202693, approved by Illumina for ensuring that the microbiota in human feces is stably stored for more than 1 week at room temperature). Parents returned the fecal specimens through a biological sample transport channel within 1 week and samples were stored at −80°C until analysis.

The 16S ribosomal RNA amplification sequencing of the V3–V4 gene region was performed on the Illumina Miseq X Ten high-throughput sequencing platform to identify and quantify bacterial taxa. Using Quantitative Insights Into Microbial Ecology (QIIME) software (Caporaso et al., 2010), bioinformatics analysis for the 16S ribosomal RNA amplification sequencing data was performed including using the closed-reference algorithm for operational taxonomic unit (OTU) classification unit screening, taxonomic assignment as well as alpha and beta diversity analysis.

Clustering analysis was applied to the relative genus abundance of the 62 subjects using Partitioning Around Medoids (PAM) algorithm. The cluster scoring method was used to assess the optimal number of clusters (**Figure 1**).

Genera Analysis and Co-occurrence Networks

The Wilcoxon signed-rank test was used to identify significant differences in the relative abundance of bacterial genera among clusters. The seeds of each cluster indicating the most significant representative genera were selected to form the co-occurrence networks using Spearman correlations (**Figure 2**) to elucidate the bacterial community dynamics.

Autism Diagnostic Interview-Revised Assessment for Restricted Repetitive Behavior and Interest

The ADI-R is an appraisal-based, standardized, semi-finished, professional-use interview scale (Hus and Lord, 2013; Zander et al., 2017). It was used to differentiate "Autism Spectrum Disorder" in the DSM-5 diagnostic criteria and "Classic Autism" in DSM-4. A higher score indicates more severe symptoms in the field (Hus and Lord, 2013). A total of 14 behavioral items were included in the ADI-R assessment for classification and comparison of repeated stereotypies (Cuccaro et al., 2003; Mooney et al., 2009). This study used the ADI-R C-category scores to obtain the severity of social communication barriers and repetitive stereotypies in the form of parental interviews.

Association of Within-Cluster Restricted Repetitive Behavior and Interest and Alpha Diversity

Alpha diversity is an indicator that describes the diversity of species within each individual (also known as local diversity). We used chao1, observed OTUs, Shannon and Simpson index to measure alpha-diversity for different clusters. Subsequently, Pearson correlation analysis was used to test all four measures of alpha-diversity for associations with repetitive, stereotypic behavior scores in the ADR-I assessment.

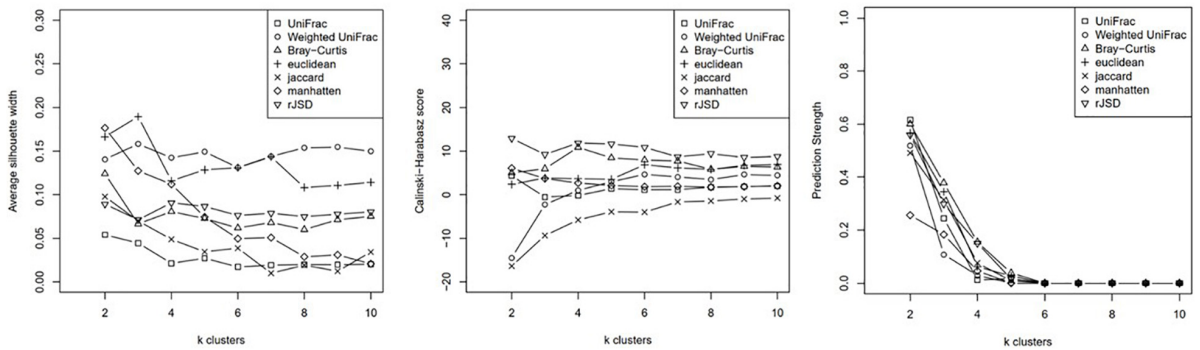

FIGURE 1 | K-means of cluster index.

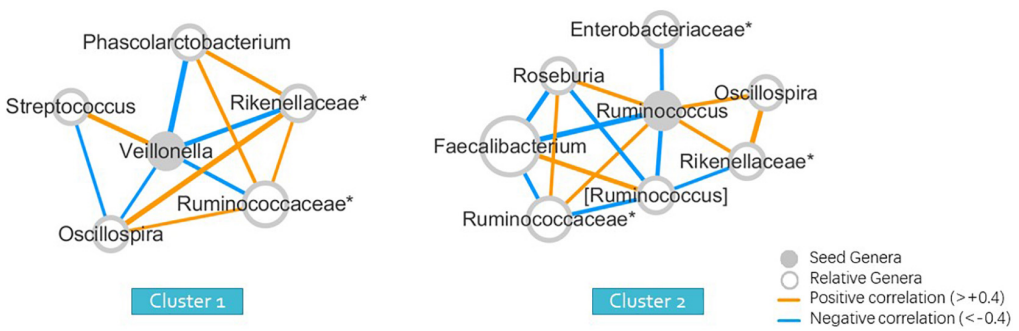

FIGURE 2 | Seed-genera and co-occurrence networks between clusters (wunifrac distance). "*" means the unclassified genera, and specified in the family to which the genera belong.

RESULTS

Autism Spectrum Disorder Microbiota Were Clustered Into Two Groups

Based on the average silhouette width, Calinksi Harabasz score, and prediction strength, the subjects were clustered into two groups using the weighted-UniFrac distance and unweighted-UniFrac distance, which yielded better intergroup discrimination outcomes. Although k clusters of weighted- UniFrac indicated better between-group variance when $k = 3$ (**Figure 1**), the case number for each group was 19, 31, and 11. The power of phenotypic analysis was compromised because of the small sample size. After consulting statisticians, we performed subsequent analysis based on clustering into two groups using weighted- UniFrac (wunifrac) distances.

Genera Analysis of the Two Groups of Seed Genera and the Construction of Co-occurrence Networks

To obtain a more intuitive comparison, we selected a representative seed genera and constructed a co-occurrence network for each cluster (**Figure 2**). The abundance of many genera was different from that of Clusters 1 and 2. The seed of each cluster refers to the one that differed the most between two clusters, with the lowest p-values of the Wilcoxon signed-rank test, with the maximum relative abundance in all samples greater than 0.001 and average relative abundance higher than the other group. The seed genus was *Veillonella* for Cluster 1, and *Ruminococcus* for Cluster 2, with p-values of 0.026 and 0.001 between two clusters, determined using the Wilcoxon signed-rank test, indicating statistically significant results (**Supplementary Material 1**). The members in the co-occurrence network were determined according to their Spearman correlations with the seed genera.

Comparison of Characteristics Between Clusters

Demographic Characteristics

Our participants were recruited from a Han population in southern China. We used the weighted UniFrac distance (hereinafter referred to as wunifrac) to divide clusters for later comparisons. There was no significant difference between the two clusters upon baseline comparison of gender, age, breastfeeding, food allergies, frequency of probiotic or antibiotic intake, and preference for food (meat or vegetarian diets). See **Supplementary Table 1**.

Autism Repetitive Behavior Performance Difference Between Clusters

In this study, we tested whether core phenotypes of autism differed between clusters by analyzing three independent

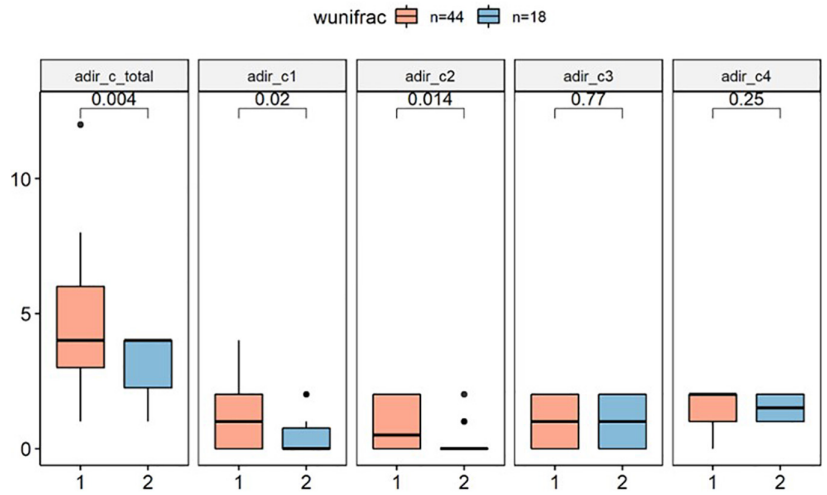

FIGURE 3 | ADI-R C score difference between clusters (wunifrac distance). ADI-R, Autism Diagnostic Interview-Revised. ADI-R C score: Restricted, Repetitive, and Stereotyped Patterns of Behavior, adir_cl: encompassing preoccupation or circumscribed pattern of interest. adir_c2: apparently compulsive adherence to nonfunctional routines or rituals. adir_c3: stereotyped and repetitive motor mannerism. adir_c4: Preoccupation with parts of objects or non-functional elements of material.

domains of the ADI-R. In the RRBI (C score), our primary analysis indicated that Cluster 1 has significantly higher score than Cluster 2 ($p < 0.01$), implying that children in Cluster 1 had more severe repetitive stereotypic behaviors than the other group (**Figure 3**).

Subsequent secondary analysis, separately testing whether the RRBI sub-scale score entries of the repeated stereotypes sub-scale were different between clusters found that C1 scores (encompassing preoccupation or circumscribed patterns of interest) and C2 scores (apparently compulsive adherence to non-functional routines or rituals) were different between groups. However, there was no difference between clusters in the domain of social interaction (A score) and communication (B score) ($p > 0.1$; **Supplementary Material 2**).

Alpha Diversity Between Clusters

The measurement of alpha diversity OS (observed OTUs) showed a difference ($p = 0.04$) between clusters, and Chao1 indicated a trend toward significance ($p = 0.082$), suggesting that Cluster 1 had less diversity and Cluster 2 had higher diversity (**Figure 4**). No between-cluster differences were found using Shannon and Simpson indices.

Alpha Diversity Related to Repetitive Behavior

We tested the association of alpha diversity measured using Shannon and Simpson indices with RRBI (C, C1, and C2 score), which did not show any significant trend in the previous analysis. A negative correlation with alpha diversity (measured by Shannon and Simpson indices) was found in the C2 score (Shannon: $p = 0.021$ and Simpson: $p = 0.029$; **Supplementary Material 3**).

DISCUSSION

We used 16S rRNA high-throughput sequencing technology to obtain the abundance of gut microbial genes with large inter-individual variations and examined the gut microbiota composition correlated with ASD phenotypic features quantitatively for the Chinese population living in southeast-China. Our data suggested that two major subgroups, which were characterized either by the increased abundance of *Veillonella* or *Ruminococcus*, might be correlated with RRBI symptom severity in children with ASD. Cluster 1, with a relatively high abundance of *Veillonella* and a low abundance of *Ruminococcus*, showed more severe RRBI symptoms. However, Cluster 2, with a high abundance of *Ruminococcus* and a low abundance of *Veillonella*, presented milder symptoms of repetitive behaviors.

To our knowledge, this is the first study to show that the composition of the intestinal microbiome is associated with repetitive, stereotyped behaviors in children with ASD. Participants in each group were defined based on the composition of their gut microbiome. Although the use of clustering to analyze the microbiome remains a controversial topic (Knights et al., 2014), this study provides a considerably important translational starting point to reflect the underlying mechanism of autism symptom severity and to explore potential treatment methods.

The genus, *Ruminococcus*, is recognized as the core gut microbiome and is abundant in the human intestinal system. Compared to typically developed children, the abundance of *Ruminococcus torques* is significantly elevated in stool samples from children with autism (Williams et al., 2012; Wang et al., 2013). However, other researchers have reported a decrease in *Ruminococcus* abundance in autism stool samples (Finegold et al., 2010). *Ruminococcus* plays an essential role in boosting intestinal movement and food digestion by degrading mucus.

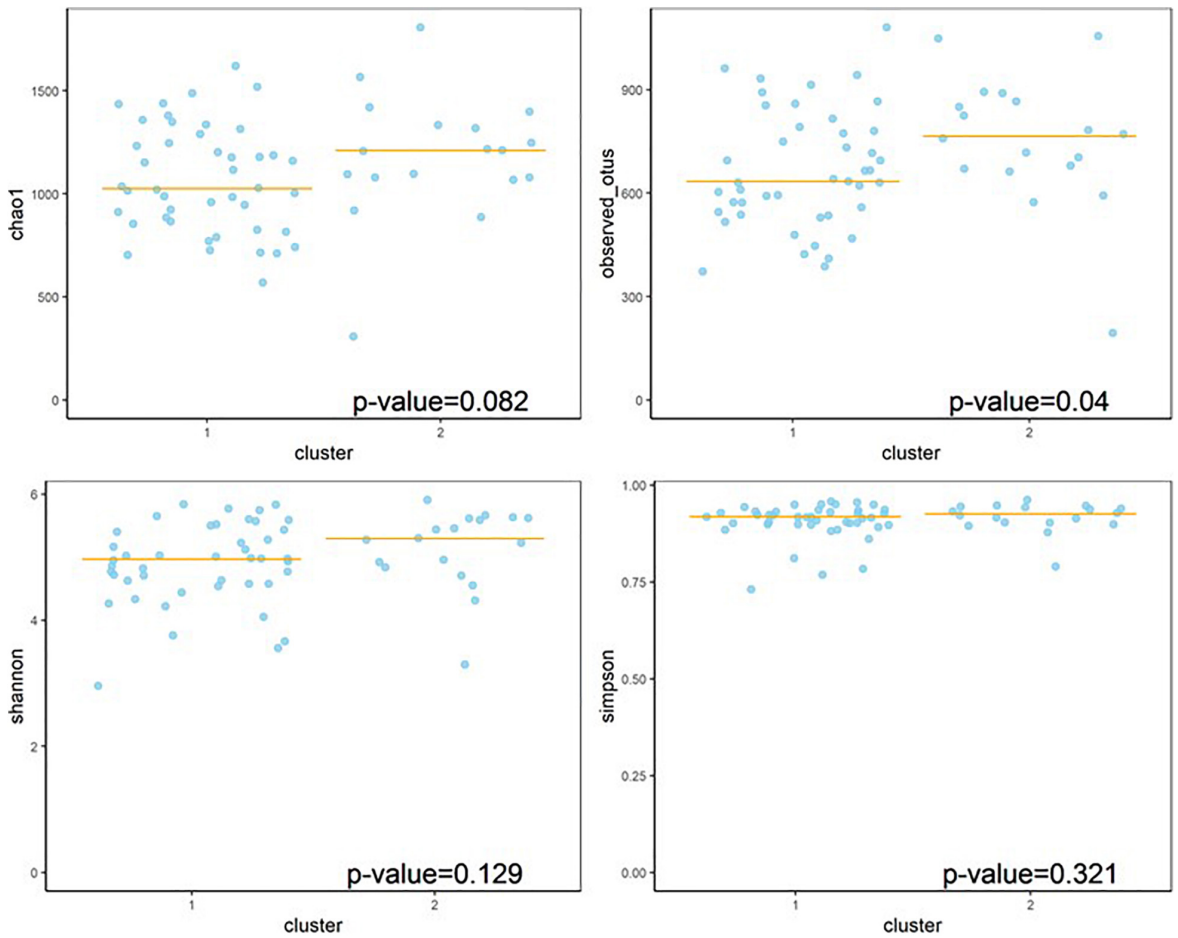

FIGURE 4 | Alpha diversity between clusters (wunifrac distance).

It has been proven that mucin in the large bowel can facilitate the growth of *Ruminococcus torques*, which is also associated with gastrointestinal (GI) disturbance in patients with inflammatory bowel disease (IBD) (Wang et al., 2013). Groups with higher *Ruminococcus* abundance showed less severe repetitive, stereotypical behaviors in our study. The role of *Ruminococcus* spp. in affecting RRBI symptoms and GI symptoms is not clear. *Veillonella* is known to metabolize carbohydrates in the human digestive system and its abundance is decreased in children with ASD in older age groups (Strati et al., 2017). Our study found that toddlers with ASD who carry a higher abundance of *Veillonella* exhibited more severe repetitive, stereotypic behaviors. Thus, further studies are needed to explore the underlying mechanism using metagenome sequencing to describe species in the genera *Ruminococcus* and *Veillonella* quantitatively.

Alpha diversity is an indicator of the richness of species and the diversity of the gut microbiome in a single ecosystem and it reflects local diversity. Lower α-diversity commonly represents a less mature gut microbiome and is often related to unhealthy conditions (Abrahamsson et al., 2014; Kostic et al., 2015). We observed that Cluster 1 had lower alpha diversity and more severe RRBI symptoms (measured by the observed_OTUs method). In addition, one sub-domain of RRBI, apparently compulsively adhering to non-functional routines or rituals, had a negative correlation with alpha diversity in children with autism (measured by the Shannon and Simpson indices), which is in line with the previously obtained outcomes. Hence, the alteration of alpha-diversity in relation to autism or other developmental delays is still not clear. Some studies have shown that alpha-diversity decreases in patients with ASD (Kang et al., 2013, 2017, 2018), while others show no significant changes (Gondalia et al., 2012; Kushak et al., 2017; Strati et al., 2017), or an increase (Finegold et al., 2010; De Angelis et al., 2013). Further research is needed to target clinical heterogeneity, and a larger population would provide further evidence of the relationship between alpha-diversity and ASD phenotypes.

This is a preliminary study to explore the relationship between composition and alpha-diversity in the gut microbiome and repetitive behavior in ASD. Because of the nature of the unsupervised clustering method, we need to explain the outcomes cautiously and be aware of generalization.

In summary, we demonstrated that the difference in intestinal microbiome composition and altered alpha diversity

can be associated with repetitive, stereotypic behavior in autism. The role of *Ruminococcus* and *Veillonella* in ASD is not yet understood.

DATA AVAILABILITY STATEMENT

The data presented in the study are included in the article/**Supplementary Material**, further inquiries can be directed to the corresponding authors.

ETHICS STATEMENT

The studies involving human participants were reviewed and approved by the Ethics Committee of Third Hospital of Sun Yat-sen University. Written informed consent to participate in this study was provided by the participants' legal guardian/next of kin.

AUTHOR CONTRIBUTIONS

BC contributed to sample preparation, data collection, and took the lead in writing the manuscript. NY contributed to the interpretation of the results. BP and XH contributed to data analysis. XZ contributed to the leading of all research steps and interpretation of the results. All authors provided critical feedback and helped shape the research, analysis, and manuscript.

FUNDING

This work was supported by the National Natural Science Foundation of China (81873801 and 11671409), the Science and Technology Program of Guangzhou, China (201903010040), the Science and Technology Program of Guangzhou, China, and the Key Area Research and Development Program (202007030011).

ACKNOWLEDGMENTS

We would like to acknowledge the contributions of Rebecca C. Knickmeyer and Kai Xia from the University of North Carolina Chapel Hill for their scientific discussions during the preparation and data analysis of this manuscript. We are thankful for the support from all patients and families, your participation helps us understand more about autism.

SUPPLEMENTARY MATERIAL

The Supplementary Material for this article can be found online at: https://www.frontiersin.org/articles/10.3389/fnins.2021.760779/full#supplementary-material

REFERENCES

Abrahamsson, T. R., Jakobsson, H. E., Andersson, A. F., Bjorksten, B., Engstrand, L., and Jenmalm, M. C. (2014). Low gut microbiota diversity in early infancy precedes asthma at school age. *Clin. Exp. Allergy* 44, 842–850. doi: 10.1111/cea.12253

Bravo, J. A., Forsythe, P., Chew, M. V., Escaravage, E., Savignac, H. M., Dinan, T. G., et al. (2011). Ingestion of Lactobacillus strain regulates emotional behavior and central GABA receptor expression in a mouse via the vagus nerve. *Proc. Natl. Acad. Sci. U.S.A.* 108, 16050–16055. doi: 10.1073/pnas.1102999108

Buffington, S. A., Di Prisco, G. V., Auchtung, T. A., Ajami, N. J., Petrosino, J. F., and Costa-Mattioli, M. (2016). Microbial reconstitution reverses maternal diet-induced social and synaptic deficits in offspring. *Cell* 165, 1762–1775. doi: 10.1016/j.cell.2016.06.001

Caporaso, J. G., Kuczynski, J., Stombaugh, J., Bittinger, K., Bushman, F. D., Costello, E. K., et al. (2010). QIIME allows analysis of high-throughput community sequencing data. *Nat. Methods*. 7, 335–336. doi: 10.1038/nmeth.f.303

Cryan, J. F., and Dinan, T. G. (2012). Mind-altering microorganisms: the impact of the gut microbiota on brain and behaviour. *Nat. Rev. Neurosci.* 13, 701–712. doi: 10.1038/nrn3346

Cryan, J. F., and O'Mahony, S. M. (2011). The microbiome-gut-brain axis: from bowel to behavior. *Neurogastroenterol. Motil.* 23, 187–192. doi: 10.1111/j.1365-2982.2010.01664.x

Cuccaro, M. L., Shao, Y., Grubber, J., Slifer, M., Wolpert, C. M., Donnelly, S. L., et al. (2003). Factor analysis of restricted and repetitive behaviors in autism using the Autism Diagnostic Interview-R. *Child Psychiatry Hum. Dev.* 34, 3–17. doi: 10.1023/a:1025321707947

Cussotto, S., Sandhu, K. V., Dinan, T. G., and Cryan, J. F. (2018). The neuroendocrinology of the microbiota-gut-brain axis: a behavioural perspective. *Front. Neuroendocrin.* 51:80–101. doi: 10.1016/j.yfrne.2018.04.002

De Angelis, M., Piccolo, M., Vannini, L., Siragusa, S., De Giacomo, A., Serrazzanetti, D. I., et al. (2013). Fecal microbiota and metabolome of children with autism and pervasive developmental disorder not otherwise specified. *PLoS One* 8:e76993. doi: 10.1371/journal.pone.0076993

De Vadder, F., Kovatcheva-Datchary, P., Goncalves, D., Vinera, J., Zitoun, C., Duchampt, A., et al. (2014). Microbiota-generated metabolites promote metabolic benefits via gut-brain neural circuits. *Cell* 156, 84–96. doi: 10.1016/j.cell.2013.12.016

Desbonnet, L., Clarke, G., Shanahan, F., Dinan, T. G., and Cryan, J. F. (2014). Microbiota is essential for social development in the mouse. *Mol. Psychiatr.* 19, 146–148. doi: 10.1038/mp.2013.65

Dinan, T. G., and Cryan, J. F. (2013). Melancholic microbes: a link between gut microbiota and depression? *Neurogastroenterol. Motil.* 25, 713–719. doi: 10.1111/nmo.12198

Dinan, T. G., and Cryan, J. F. (2017). Brain-gut-microbiota axis and mental health. *Psychosom. Med.* 79, 920–926. doi: 10.1097/PSY.0000000000000519

Finegold, S. M., Dowd, S. E., Gontcharova, V., Liu, C., Henley, K. E., Wolcott, R. D., et al. (2010). Pyrosequencing study of fecal microflora of autistic and control children. *Anaerobe* 16, 444–453. doi: 10.1016/j.anaerobe.2010.06.008

Gondalia, S. V., Palombo, E. A., Knowles, S. R., Cox, S. B., Meyer, D., and Austin, D. W. (2012). Molecular characterisation of gastrointestinal microbiota of children with autism (With and Without Gastrointestinal Dysfunction) and their neurotypical siblings. *Autism Res.* 5, 419–427. doi: 10.1002/aur.1253

Ho, L. K. H., Tong, V. J. W., Syn, N., Nagarajan, N., Tham, E. H., Tay, S. K., et al. (2020). Gut microbiota changes in children with autism spectrum disorder: a systematic review. *Gut Pathog.* 12:6. doi: 10.1186/s13099-020-0346-1

Hus, V., and Lord, C. (2013). Effects of child characteristics on the autism diagnostic interview-revised: implications for use of scores as a measure of ASD severity. *J. Autism Dev. Disord.* 43, 371–381. doi: 10.1007/s10803-012-1576-y

Kang, D., Adams, J. B., Gregory, A. C., Borody, T., Chittick, L., Fasano, A., et al. (2017). Microbiota Transfer Therapy alters gut ecosystem and improves gastrointestinal and autism symptoms: an open-label study. *Microbiome* 5:10. doi: 10.1186/s40168-016-0225-7

Kang, D., Ilhan, Z. E., Isern, N. G., Hoyt, D. W., Howsmon, D. P., Shaffer, M., et al. (2018). Differences in fecal microbial metabolites and microbiota of children with autism spectrum disorders. *Anaerobe* 49, 121–131. doi: 10.1016/j.anaerobe.2017.12.007

Kang, D., Park, J. G., Ilhan, Z. E., Wallstrom, G., LaBaer, J., Adams, J. B., et al. (2013). Reduced incidence of prevotella and other fermenters in intestinal microflora of autistic children. *PLoS One* 8:e68322. doi: 10.1371/journal.pone.0068322

Knights, D., Ward, T. L., McKinlay, C. E., Miller, H., Gonzalez, A., McDonald, D., et al. (2014). Rethinking "Enterotypes". *Cell Host. Microbe* 16, 433–437. doi: 10.1016/j.chom.2014.09.013

Kostic, A. D., Gevers, D., Siljander, H., Vatanen, T., Hyotylainen, T., Hamalainen, A. M., et al. (2015). The dynamics of the human infant gut microbiome in development and in progression toward type 1 diabetes. *Cell Host Microbe* 17, 260–273. doi: 10.1016/j.chom.2015.01.001

Kushak, R. I., Winter, H. S., Buie, T. M., Cox, S. B., Phillips, C. D., and Ward, N. L. (2017). Analysis of the duodenal microbiome in autistic individuals: association with carbohydrate digestion. *J. Pediatr. Gastr. Nutr.* 64, E110–E116. doi: 10.1097/MPG.0000000000001458

Liu, F., Li, J., Wu, F., Zheng, H., Peng, Q., and Zhou, H. (2019). Altered composition and function of intestinal microbiota in autism spectrum disorders: a systematic review. *Transl. Psychiat.* 9:42. doi: 10.1038/s41398-019-0389-6

Lord, C., Elsabbagh, M., Baird, G., and Veenstra-Vanderweele, J. (2018). Autism spectrum disorder. *Lancet* 392, 508–520. doi: 10.1016/S0140-6736(18)31129-2

Mayer, E. A. (2011). Gut feelings: the emerging biology of gut-brain communication. *Nat. Rev. Neurosci.* 12, 453–466. doi: 10.1038/nrn3071

McKinnon, C. J., Eggebrecht, A. T., Todorov, A., Wolff, J. J., Elison, J. T., Adams, C. M., et al. (2019). Restricted and repetitive behavior and brain functional connectivity in infants at risk for developing autism spectrum disorder. *Biol. Psychiatry Cogn. Neurosci. Neuroimaging* 4, 50–61. doi: 10.1016/j.bpsc.2018.09.008

Mooney, E. L., Gray, K. M., Tonge, B. J., Sweeney, D. J., and Taffe, J. R. (2009). Factor analytic study of repetitive behaviours in young children with pervasive developmental disorders. *J. Autism Dev. Disord.* 39, 765–774. doi: 10.1007/s10803-008-0680-5

Osadchiy, V., Martin, C. R., and Mayer, E. A. (2019). The Gut–Brain axis and the microbiome: mechanisms and clinical implications. *Clin. Gastroenterol. Hepatol.* 17, 322–332. doi: 10.1016/j.cgh.2018.10.002

Qin, J., Li, R., Raes, J., Arumugam, M., Burgdorf, K. S., Manichanh, C., et al. (2010). A human gut microbial gene catalogue established by metagenomic sequencing. *Nature* 464, 59–65. doi: 10.1038/nature08821

Sherwin, E., Dinan, T. G., and Cryan, J. F. (2018). Recent developments in understanding the role of the gut microbiota in brain health and disease. *Ann. N. Y. Acad. Sci.* 1420, 5–25. doi: 10.1111/nyas.13416

Strati, F., Cavalieri, D., Albanese, D., De Felice, C., Donati, C., Hayek, J., et al. (2017). New evidences on the altered gut microbiota in autism spectrum disorders. *Microbiome* 5:24. doi: 10.1186/s40168-017-0242-1

Wang, L., Christophersen, C. T., Sorich, M. J., Gerber, J. P., Angley, M. T., and Conlon, M. A. (2013). Increased abundance of Sutterella spp. and Ruminococcus torques in feces of children with autism spectrum disorder. *Mol. Autism*. 4:42. doi: 10.1186/2040-2392-4-42

Williams, B. L., Hornig, M., Parekh, T., and Lipkin, W. I. (2012). Application of novel PCR-based methods for detection, quantitation, and phylogenetic characterization of Sutterella species in intestinal biopsy samples from children with autism and gastrointestinal disturbances. *Mbio* 3, e261–e211. doi: 10.1128/mBio.00261-11

Wolff, J. J., Botteron, K. N., Dager, S. R., Elison, J. T., Estes, A. M., Gu, H., et al. (2014). Longitudinal patterns of repetitive behavior in toddlers with autism. *J. Child Psychol. Psychiatry* 55, 945–953. doi: 10.1111/jcpp.12207

Zander, E., Willfors, C., Berggren, S., Coco, C., Holm, A., Jifält, I., et al. (2017). The interrater reliability of the autism diagnostic interview-revised (ADI-R) in clinical settings. *Psychopathology* 50, 219–227. doi: 10.1159/000474949

Conflict of Interest: The authors declare that the research was conducted in the absence of any commercial or financial relationships that could be construed as a potential conflict of interest.

Publisher's Note: All claims expressed in this article are solely those of the authors and do not necessarily represent those of their affiliated organizations, or those of the publisher, the editors and the reviewers. Any product that may be evaluated in this article, or claim that may be made by its manufacturer, is not guaranteed or endorsed by the publisher.

frontiers in Neuroscience

ORIGINAL RESEARCH
published: 02 December 2021
doi: 10.3389/fnins.2021.761473

Phenotypes in Children With *SYNGAP1* Encephalopathy in China

*Huiting Zhang[1], Liu Yang[2], Jing Duan[3], Qi Zeng[3], Li Chen[3], Yu Fang[1], Junjie Hu[4], Dezhi Cao[3] and Jianxiang Liao[3]**

[1] Shenzhen Children's Hospital, China Medical University, Shenzhen, China, [2] Guangdong Women and Children Hospital, Guangzhou, China, [3] Department of Neurology, Shenzhen Children's Hospital, Shenzhen, China, [4] Shenzhen Children's Hospital, Shantou University, Shenzhen, China

Objective: We aimed to explore the associated clinical phenotype and the natural history of patients with *SYNGAP1* gene variations during early childhood and to identify their genotype–phenotype correlations.

Methods: This study used a cohort of 13 patients with epilepsy and developmental disorder due to *SYNGAP1* mutations, namely, 7 patients from Shenzhen Children's Hospital between September 2014 and January 2020 and 6 patients from previously published studies. Their clinical data were studied.

Results: A total of 13 children with *SYNGAP1* gene variants (eight boys and five girls) were identified. The age of disease onset was in infancy. Mutations were located between exons 8 and 15; most were frameshift or truncated mutations. Four mutation sites (c.924G > A, c.1532-2_1532del, c.1747_1755dup, and c.1735_1738del) had not been reported before. All patients had global developmental delay within the first year of life, and intellectual impairment became gradually apparent. Some of them developed behavioral problems. The developmental delay occurred before the onset of seizures. All seven patients in our cohort presented with epilepsy; myoclonic seizures, absence seizures, and epileptic spasms were the most common seizure types. Abnormal electroencephalograms were identified from five patients before the onset of their seizures. All patients suffered from drug-resistance seizures. However, comorbidities such as behavioral problems were less frequently observed.

Conclusion: The most common age of disease onset in *SYNGAP1* gene mutations is in infancy, while neurodevelopmental delay and epilepsy are the major phenotypes. They have a higher percentage of drug-resistant epilepsy and epileptic spasms than those in previous reports. We should give attention to the patients with abnormal EEGs without seizures and think about the suitable time of the anti-seizure medications for them. We have not found the genotype–phenotype correlation.

Trial registration: Chinese Clinical Trial Registry, Registration number: ChiCTR2100049289 (https://www.chictr.org.cn/listbycreater.aspx).

Keywords: *SYNGAP1* gene, intellectual disability, China, epilepsy, neurodevelopmental disorder

OPEN ACCESS

Edited by:
Li Yang,
Peking University Sixth Hospital, China

Reviewed by:
Hirokazu Oguni,
TMG Asaka Medical Center, Japan
Tudor Constantin Badea,
Transilvania University of Braşov, Romania

****Correspondence:***
Jianxiang Liao
liaojianxiang@vip.sina.com

Specialty section:
This article was submitted to Neurodevelopment, a section of the journal Frontiers in Neuroscience

Received: *19 August 2021*
Accepted: *22 October 2021*
Published: *02 December 2021*

Citation:
Zhang H, Yang L, Duan J, Zeng Q, Chen L, Fang Y, Hu J, Cao D and Liao J (2021) Phenotypes in Children With SYNGAP1 Encephalopathy in China. Front. Neurosci. 15:761473. doi: 10.3389/fnins.2021.761473

Abbreviations: ACMG, American College of Medical Genetics and Genomics; ASMs, anti-seizure medications; ASD, autism spectrum disorder; CT, computed tomography; DEE, developmental and epileptic encephalopathy; EEG, electroencephalogram; GTPase, guanosine triphosphatase; ID, intellectual disability; KDT, ketogenic diet therapy; MRI, magnetic resonance imaging; MRD5, mental retardation type 5; NDD, neurodevelopmental disorders; SD, standard deviation; SynGAP, synaptic guanosine triphosphatase activating protein; *SYNGAP1*, synaptic Ras GTPase activating protein 1; WES, whole-exome sequencing.

BACKGROUND

Previous studies have shown that the brain-specific synaptic guanosine triphosphatase (GTPase) activating protein (SynGAP) is important for synaptic plasticity. The synaptic Ras GTPase activating protein 1 (*SYNGAP1*) gene (MIM:603384) is located on chromosome 6p21.3. The protein encoded is SynGAP, including Ras and Rap GTPases. The protein is enriched in the postsynaptic membranes and plays an essential role in the plasticity of synapses that excite them (Gamache et al., 2020). The mutation of the *SYNGAP1* gene can lead to an imbalance of excitement and inhibition in the central nervous system, which affects the formation of synapses during learning and memorizing (Nakajima et al., 2019; Araki et al., 2020). SynGAP sequence contained six various predicted functional domains: pleckstrin homology (PH) domain (27-253AA), C2 domain (263-362AA), RasGAP domain (392-729AA), SH3 domain (785-815AA), coiled-coil (CC) domain (1189-1262AA), and other C-terminal domains of unknown function (Hamdan et al., 2009; Berryer et al., 2013; Gamache et al., 2020). The SynGAP protein has multiple biological functions and interacts with numerous proteins (Meili et al., 2021). The loss of function of the *SYNGAP1* gene has been linked to a variety of neurodevelopmental disorders (NDD), including autism spectrum disorder (ASD), intellectual disability (ID), and epilepsy. Encephalopathy caused by the variation of the *SYNGAP1* gene has also been referred to as mental retardation type 5 (MRD5) (Weldon et al., 2018; Agarwal et al., 2019). *SYNGAP1* variants accounted for 0.75% of all NDD (Deciphering Developmental Disorders Study, 2015). MRD5 has a reported incidence of one to four people in 10,000. It is involved in about 0.5–1.0% of all ID patients (Mignot et al., 2016). MRD5 is believed to be the leading cause of ID.

SYNGAP1 encephalopathy is a rare disease with approximately 200 reported cases worldwide (Agarwal et al., 2019). Most of these patients are from Europe and only six patients have previously been described in detail from China; hence, the clinical and genetic characteristics regarding Chinese patients with mutation of the *SYNGAP1* gene were scarce. In this study, we additionally identified seven patients with *SYNGAP1* gene mutations. We reviewed the phenotypes and molecular structures of these patients in details together with those previously reported in China and analyzed the genotype-phenotype correlation. We reported four novel mutations of the *SYNGAP1* gene.

MATERIALS AND METHODS

Patients

We retrospectively analyzed the clinical data of seven patients who had been diagnosed with developmental disorder comorbid epilepsy from September 2014 to January 2020 at Shenzhen Children's Hospital. This study was approved by the Institutional Review Board of Shenzhen Children's Hospital. Written informed consents were obtained from the patients' parents or legal guardians for the participation of this study and publication of data.

Inclusion and Exclusion Criteria

Children under 18 years of age were recruited in this study. The results of their genetic testing suggested deleterious *SYNGAP1* variants, and the variants were classified as "likely pathogenic" or "pathogenic" according to the American College of Medical Genetics and Genomics (ACMG) guideline. Patients with epilepsy caused by intracranial infection, congenital metabolic disease, head trauma, structural abnormality of the brain, and birth asphyxia were excluded. Patients with other genetic mutations or chromosomal abnormalities were also excluded.

Gene Sequencing and Validation Analysis

Genetic tests were carried out on all recruited children. *SYNGAP1* gene mutations were identified in seven children using trio-based whole-exome sequencing (WES). The test was verified for their probands. The pathogenicity of the variants was assessed according to the ACMG guidelines (Richards et al., 2015).

Literature Review of Previously Published Reports

We used the search terms "China," "*SYNGAP1*," and "mutation" in the China Knowledge Network (in Chinese), Wanfang Data (in Chinese), and PubMed. We also compared the mutation sites of the present study with the database.

RESULTS

Demographic Information

Seven patients (five males and two females) were recruited in this study. Six patients were of Han ethnicity and one patient was of Tujia ethnicity (Patient 2). The children were aged 31 to 75 months (median, 57 months) when reported. All patients reported no related family history related to developmental disorder and epilepsy, and the birth history was unremarkable. In addition, we collected data from another six patients from previously published literature.

Clinical Symptoms

All patients showed varying degrees of growth and developmental retardation and intellectual disability within the first year of life (**Tables 1**, **2**). The ability to speak was severely impaired. One patient remained verbally disabled until the last follow-up at 31 months. The mean age of the first spoken word for the remaining six patients was 34 months (median age was 37 months, range between 18 and 55 months). Motor developments, including head control, sitting, standing, and walking, were delayed but better than language development. Two patients had sleep problems, manifested as the difficulties of falling asleep and waking up at night. One presented with aggressive behavior (**Table 1**). Severe, moderate, and mild developmental delay was noted in one, five, and one patient, respectively. In total, two patients older than 3 years old were diagnosed with ASD, both of whom had moderate developmental delay. Feeble verbal and non-verbal communication skills and impaired social interactions were observed in patients with ASD.

TABLE 1 | Clinical information of seven patients in our cohort.

ID	1	2	3	4	5	6	7
Gender	Female	Male	Male	Male	Male	Female	Male
Age (months)	75	69	60	59	60	46	31
Developmental delay	Moderate (32 months)	Severe (54 months)	Moderate (38 months)	Moderate (40 months)	Mild (32 months)	Moderate (29 months)	Moderate (20 months)
Age of walking (months)	17	24	18	28	19	18	20
Age of standing (months)	15	18	/	18	/	11	18
First word spoken (months)	44	18	55	30	18	44	Verbal disability
Developmental regression	−	−	−	−	−	−	+
ASD	+	−	+	−	−	−	−
Sleeping problem	−	−	+	−	−	−	+
Seizures	+	+	+	+	+	+	+
Neuroimaging	+	−	−	−	+	−	−
Metabolic screening	−	−	−	−	−	−	−

All the patients with *SYNGAP1* gene mutations had seizures and these patients were prescribed anti-seizure medications (ASMs) (**Table 3**). The age of onset of the seizure ranged from 0 to 4 years, while the mean age at diagnosis was 26.8 months (median age 30 months). Types of seizures during the course of disease consisted of myoclonic seizures, myoclonic absence, or absence seizures, and epileptic spasms. Four children had myoclonic seizures, two of which had falling seizures. Three children had eyelid myoclonia, and two of them were together with absence. Three patients had epileptic spasms. The triggers of seizures have been identified in five patients. Eating-induced seizures were observed in 42.8% (three of seven) of patients, and no light-evoked seizures were observed in our cohort. None of the patients had status epilepticus. Developmental regression occurred in two individuals after the onset of seizures. We also found no significant features in the physical or neurological examinations except for one patient who developed acquired microcephaly (Patient 1). In addition, the summary of the reported data of the six children is shown in **Table 2**. All 13 patients suffering from mild to severe developmental delay and seizures were observed in 11 of the 13 patients.

Gene

Seven different pathogenic mutation sites were detected in this study, and seven patients were confirmed as *de novo* mutations. Three sites [c.2059C > T (Vlaskamp et al., 2019), c.2764C > T (Parker et al., 2015), and c.1167_1168del (Yang et al., 2014)] had been previously reported. The other four loci had not been reported. A total of 13 mutation sites have been identified in Chinese children, including 6 mutations that had been observed in previously reported cases (Lu et al., 2019; Gao et al., 2020; Tian et al., 2020). The mutation sites of the 13 patients were located in exons 1, 5–8, 10–13, and 15 (**Supplementary Figure 1**). The mutation sites of the 13 children on the domains of SynGAP are shown in **Figure 1**. Among the mutations of the seven patients recruited in this study, three had frameshifted mutations, one patient had splice mutation, and three patients had non-sense mutations. These variations caused truncated proteins in six patients and aberrant splicing proteins in one patient (**Table 4**). We found that the mutations distributed PH to RasGAP domain of SynGAP. Of 13 variations, 7 were located on the RasGAP domain, 2 were on the PH domain, and 4 others were on the DUF domains.

TABLE 2 | Clinical information of six patients reported previously.

ID	8	9	10	11	12	13
Gender	Male	Male	Female	Female	Female	Male
Age (months)	96	69	9	34	46	48
Developmental delay	Moderate (96 months)	Mild (42 months)	Mild (9 months)	+	Profound	+
ASD	+	−	/	/	/	+
Seizures	+	+	+	+	−	−
Neuroimaging	−	−	−	+	+	−
Metabolic screening	−	−	−	/	−	−

Electroencephalogram Findings, Imaging Results, and Metabolic Screening

Screening tests of metabolic diseases in all seven children were unremarkable. Patients 1 and 6 showed mild demyelination and widened extracerebral interspace in the left temporal polar, respectively, in the brain magnetic resonance imaging (MRI). No obvious abnormality was found in the brain MRI or computed tomography (CT) from the remaining five patients. Notably, abnormal electroencephalograms (EEGs) were identified in five patients before seizure was diagnosed. The EEG was unremarkable in one patient. Another patient (Patient 5) had not obtained EEG before the onset of the seizures. All of our patients underwent video EEG at least once for 12 h. Six patients had a diffuse slow background rhythm, and no predominant background was found in one patient. Six patients had generalized spikes and waves, single or repetitive. All patients had multi-focal spikes and waves on EEG. Three in seven children had hypsarrhythmia. Clinically, they had epileptic spasms, and two of them had developmental regression. Clinical seizures were captured by video EEG in all children. Eyelid myoclonia with absence in three patients was reported, epileptic spasms were

TABLE 3 | Epilepsy characteristics of seven patients.

ID	1	2	3	4	5	6	7
Age of seizure onset	37 months	30 months	30 months	10 months	26 months	25 months	30 months
Seizure type	Myoclonic seizures, absence, falling seizures	Eyelid myoclonia, myoclonic seizures with eyelid myoclonic	Myoclonic seizures, West syndrome	Eyelid myoclonia with atypical absences	Eyelid myoclonia, falling seizures	Absence with eyelid myoclonia, eyelid myoclonia	Myoclonic seizures
Precipitating factors	Weariness	–	Eating (suspected)	–	Eating	Eating	Crying
Status epilepticus	–	–	–	–	–	–	–
Seizure frequency	6–7/day	10 + /day	20 + /day	7–8/day	7–8/day	6–7/day	10–15/day
Alterations of seizure type	–	+	+	+	–	–	+
ASMs	LEV-TPM-VPA	LEV-VPA-ZNS	LEV-VPA-CZP-ACTH-prednisone	VPA-LEV-NZP	VPA-LEV-LCM	OXC-VPA (OXC discontinued) -LEV-NZP-CLB-LTG-KDT	VPA-NZP-LEV
Seizure free	+	+	+	–	–	–	–
Seizures at last follow-up	Seizure-free for 24 months	Seizure-free for 14 months	Seizure-free for 18 months	Seizure-free for 10 months	Eyelid myoclonia	Absence with eyelid myoclonia	Myoclonus
EEG before seizure onset	Abnormal	Abnormal	Normal	Abnormal	/	Abnormal	Abnormal
EEG, generalized spike and waves	+	+	+	–	+	+	+
EEG, multi-focal spike and waves	+	+	+	+	+	+	+
EEG, hypsarrhythmia.	–	+	+	–	–	–	+
Video-EEG Captured seizures	Myoclonic seizures with absence.	Myoclonic seizures, eyelid myoclonia, epileptic spasms.	Epileptic spasms.	Eyelid myoclonia.	Epileptic spasms, myoclonic seizures.	Atypical absence, eyelid myoclonia with absence, absence atonic seizures, focal seizures	Epileptic spasms.

VPA, valproate; ZNS, zonisamide; LEV, levetiracetam; NZP, nitrazepam; CZP, clonazepam; CLB, clobazam; OXC, oxcarbazepine; LTG, lamotrigine; TPM, topiramate; ACTH, adrenocorticotropic hormone; KDT, ketogenic diet therapy; LCM, 1acosamide.

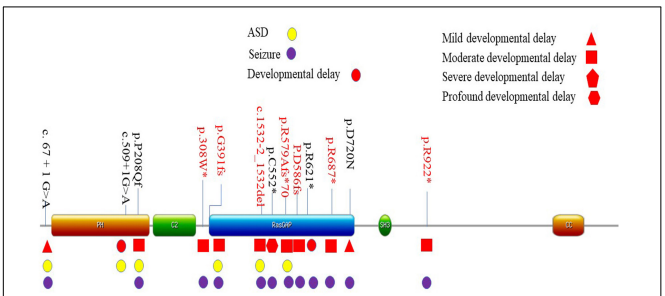

FIGURE 1 | Location of mutation sites of 13 patients in China. Localization of the *SYNGAP1* mutations identified in Amino acid positions are based on the longest SynGAP isoform (NM_006772.3). The main phenotype was listed in corresponding domains. *These variations caused truncated proteins.

observed in three, myoclonic seizures in two, atypical absence in one, myoclonic seizures with absence in one, absence with atonic seizures in one, and focal seizures in one. Because our patients were young, only one patient finished the test of hyperventilation and photic stimulation, and the result was negative.

Treatment Outcome of Seizures

All patients were receiving ASM treatments and rehabilitation training. Three became seizure-free for more than 1 year after 6 months of anti-seizure therapy. Patient 1 was seizure-free for 2 years with a medication regimen of sodium valproate combined with topiramate and levetiracetam. Patient 2 was seizure-free for 14 months with a medication regimen of sodium valproate combined with levetiracetam and zonisamide. Patient 3 experienced recurrence after 18 months of seizure-free with a medication regimen of ACTH, oral prednisolone, levetiracetam, sodium valproate, and clonazepam. When the oral prednisolone was discontinued for 3 months, recurrent seizures presented as eyelid blinking when nervous, which was considered eating-induced. When prednisone was administered, he did not have episodes of seizure for more than a month until the last follow-up. Patient 4 had been seizure-free for 10 months on medication containing sodium valproate, levetiracetam, and nitrazepam. The remaining three patients still suffered from seizures of varying frequency and severity despite being given continuous treatment with multiple anti-seizure medications. Patient 5 took the valproate first, and the frequency was cut down to half. However, 5 days later, he suffered more frequent seizures. When the levetiracetam was subscribed, the same reaction process occurred. He was intolerant of the nitrazepam, topiramate, and perampanel. Then, the lacosamide was added to his medication regime. It worked to reduce the frequency, but he still suffered seizures every day. For patient 6, the oxcarbazepine was first given and the seizures became more frequent. Then, she took sodium valproate. Instead, the seizures were reduced. Then, levetiracetam and nitrazepam were added. The drugs worked at first, but then her seizures became drug-resistant. Then, she tried clobazam and lamotrigine, and ketogenic diet therapy (KDT).

TABLE 4 | List of 13 patients with *SYNGAP1* gene molecular information in China.

ID	cDNA	Mutation type	Changes in protein	ACMG	Pathogenicity	Inheritance
1	c.1735_1738del	Frameshift	p.R579Afs*70	PVS1 + PS2 + PM2	Pathogenic	*De novo*
2	c.924G > A	Non-sense	p.W308*	PVS1 + PS2 + PM2	Pathogenic	*De novo*
3	c.1167_1168del	Frameshift	p.G391fs*27	PVS1 + PS2 + PM2	Pathogenic	*De novo*
4	c.2059C > T	Non-sense	p.R687*	PVS1 + PM6 + PM2 + PP4	Pathogenic	*De novo*
5	c.1747_1755dup	Frameshift	p.D586fs	PVS1 + PM6PM2	Pathogenic	*De novo*
6	c.2764C > T	Non-sense	p.R922*	PVS1 + PS1 + PS2 + PM4	Pathogenic	*De novo*
7	c.1532-2_1532del	Splice site	/	PVS1 + PM2 + PM6	Pathogenic	*De novo*
8	c.623delC (Tian et al., 2020)	Frameshift	p.P208Qfs*15	PVS1 + PM2 + PM6	Pathogenic	*De novo*
9	c.67 + 1G > A (Tian et al., 2020)	Splice site	/	PVS1 + PM2 + PM6	Pathogenic	*De novo*
10	c.2158 G > A (Tian et al., 2020)	Missense	p.D720N	PM2 + PM6 + PP3 + PP4	Likely pathogenic	*De novo*
11	c.1861C > T (Gao et al., 2020)	Non-sense	p.R621*	PVS1 + PS2 + PM2 + PP4	Pathogenic	*De novo*
12	c.1656C > A (Lu et al., 2019)	Non-sense	p.C552*	PVS1 + PM2 + PM6	Pathogenic	*De novo*
13	c.509 + 1G > A (Pei et al., 2018)	Splice site	/	PVS1 + PM2 + PM6	Pathogenic	*De novo*

**These variations caused truncated proteins.*

The seizure frequency was halved after 1 month of KDT. Patient 7 took sodium valproate firstly with the seizure frequency reduced. Then, the levetiracetam and nitrazepam were added, and his seizure was reduced gradually. Although the KDT was effective in epilepsy and could benefit mental development, the efficacy of KDT for patients with *SYNGAP1* gene mutation was not previously reported.

DISCUSSION

SYNGAP1 encephalopathy is a genetically determined brain disease and a significant cause of NDD and developmental and epileptic encephalopathy (DEE) in children (Vlaskamp et al., 2019). It is an attractive candidate for in-depth research across multiple model systems. *SYNGAP1* gene has become a high-risk gene for neuropsychiatric disorders in the differential diagnosis of NDD (Kilinc et al., 2018). In this study, we described phenotypes in patients with *SYNGAP1* gene mutations, which were characterized by intellectual disability, epilepsy, ASD, and behavioral problems. Epileptic spasms were captured in three of the seven patients probably because our patients underwent video-EEG examinations during infancy.

The global developmental delay was the first manifestation in patients with *SYNGAP1* gene mutations associated encephalopathies of this study. Intellectual or developmental disabilities (IDDs) appeared within the first year of life and deteriorated with age. In addition, the language impairment was more severe than the motor delay, which is similar to what has been reported in two previously reported cohorts (Parker et al., 2015; Mignot et al., 2016). Moreover, little improvements were observed in all patients after specific training, particularly for those with language impairment. However, the information about the long-term follow-up about their adult living ability was still lacking.

The most prominent clinical feature among seizure types in our patient cohort was myoclonic seizures, which was consistent with previously published literature (Parker et al., 2015; Mignot et al., 2016). The main EEG features in our patients were generalized bursts of spikes, poly spikes, spikes, and slow waves, sometimes with an occipital predominance. While Vlaskamp et al. first reported spasms in 1 of 57 children, we found that 42.8% (three of seven) of our patients suffered epileptic spams. In this study, fewer children were induced by eating (von Stulpnagel et al., 2019), and the number of children with aggressive behavioral problems combined with ASD was also lower than that reported in the literature (Weldon et al., 2018).

Taking into account the six patients reported, all the patients experienced a developmental delay. Moreover, according to the limited information, we could learn that mostly moderate developmental delay was observed among patients; 84.6% (11 out of 13) of children experienced seizures, similar to the previous study (Parker et al., 2015; Mignot et al., 2016).

It was consistent with the literature (Vlaskamp et al., 2019). Most of the mutations identified in the present study were *de novo* heterozygous mutations that caused losses of function of SynGAP due to conformational defects of frameshifted, splice-site, and truncated mutations. Only one study had so far reported mutations in exon 1 (Tian et al., 2020), which caused the loss of promoters for the transcription. However, the mutation frequency of the *SYNGAP1* gene in the Chinese population was unknown due to the lack of a large multicenter prospective cohort study. Thus, the exact function in the pathogenesis of the disease remains uncertain. Previous studies reported that mutations in *SYNGAP1* gene caused NDD by inducing haploinsufficiency (Berryer et al., 2013). Animal models suggested that homozygous SynGAP-/- mice were not able to survive after 48 h (Berryer et al., 2013). Based on the results from an animal experiment, different mutation subtypes have different effects on neuronal activity (Araki et al., 2020), while how different gene mutations, such as mutation forms of mutation loci, influence phenotypes and prognosis remained unknown (Agarwal et al., 2019). However, we could not distinguish the difference in the clinical features among different domains.

At the last follow-up, three children had recurrent seizures and poor responses to the anti-seizure medications. Four children

never achieved seizure-free effect. All the patients were taking three or more anti-seizure medications. All patients suffered from drug-resistance epilepsy, which was higher than what has been reported in a large cohort of 57 patients with *SYNGAP1*-DEE (Vlaskamp et al., 2019). It has been reported that epilepsy induced by *SYNGAP1* gene mutations responded better to topiramate and cannabidiol (Kuchenbuch et al., 2020), and we found that valproate seemed of benefit to our patients. There was no related efficacy of the ketogenic diet in children with *SYNGAP1* mutation reported in the literature. We need more experience about the effect of KDT on seizures and development improvement in *SYNGAP1* gene-related patients.

This study has several limitations. This study is an observational retrospective study of a relatively small cohort of patients, and hence, the actual frequency of the *SYNGAP1* gene mutation in children is unknown. Abnormal EEG patterns were observed in five patients before the onset of seizures. Whether the prompt treatment for a patient with an abnormal EEG can prevent development plateauing or regression, even to improve growth and cognitive development, requires further investigation. Additionally, the limited age range and follow-up time window of the patients could not provide the long-term prognosis. Ample multicenter research with long-term follow-up is still needed to see how mutation forms of mutation loci relate to phenotypes and prognosis.

CONCLUSION

Developmental delay and epilepsy are the main clinical manifestations in patients with *SYNGAP1* gene mutations. *SYNGAP1* gene variants are mainly *de novo*. Almost all patients showed varying degrees of intellectual deficiency and developmental delay before the onset of epilepsy. The primary seizure type in *SYNGAP1*-related epilepsy was myoclonic seizures. Abnormal EEGs were observed in most patients, and we predicted that the earlier administration of ASMs might be beneficial to the patients due to the fact that epilepsy was common among these patients and some experience developmental regression after the onset of seizures. We had not found the genotype–phenotype correlation, and the severity of disease correlated with the level of the protein truncation.

DATA AVAILABILITY STATEMENT

The original contributions presented in the study are included in the article/**Supplementary Material**, further inquiries can be directed to the corresponding author.

ETHICS STATEMENT

The studies involving human participants were reviewed and approved by the Shenzhen Children's Hospital. Written informed consent to participate in this study was provided by the participants' legal guardian/next of kin.

AUTHOR CONTRIBUTIONS

HZ, LY, and JD designed the study. JL obtained funding. JH, YF, QZ, and HZ acquired the data. HZ, LC, DC, and JL analyzed clinical records and interpreted the data. HZ and JL drafted and revised the manuscript. All authors revised this draft, read, and approved the final manuscript.

FUNDING

This work was supported by the Sanming Project of Medicine in Shenzhen (Grant Number: SZSM201812005) and Shenzhen Key Medical Discipline Construction Fund (Grant Number: SZXK033).

ACKNOWLEDGMENTS

We would like to thank all the participants and their families. Furthermore, we also thank the research teams in the institutions collaborating on this project.

SUPPLEMENTARY MATERIAL

The Supplementary Material for this article can be found online at: https://www.frontiersin.org/articles/10.3389/fnins.2021.761473/full#supplementary-material

REFERENCES

Agarwal, M., Johnston, M. V., and Stafstrom, C. E. (2019). SYNGAP1 mutations: clinical, genetic, and pathophysiological features. *Int. J. Dev. Neurosci.* 78, 65–76. doi: 10.1016/j.ijdevneu.2019.08.003

Araki, Y., Hong, I., Gamache, T. R., Ju, S., Collado-Torres, L., Shin, J. H., et al. (2020). SynGAP isoforms differentially regulate synaptic plasticity and dendritic development. *eLife* 9:e56273. doi: 10.7554/eLife.56273

Berryer, M. H., Hamdan, F. F., Klitten, L. L., Moller, R. S., Carmant, L., Schwartzentruber, J., et al. (2013). Mutations in SYNGAP1 cause intellectual disability, autism, and a specific form of epilepsy by inducing haploinsufficiency. *Hum. Mutat.* 34, 385–394. doi: 10.1002/humu.22248

Deciphering Developmental, and Disorders Study. (2015). Large-scale discovery of novel genetic causes of developmental disorders. *Nature* 519, 223–228. doi: 10.1038/nature14135

Gamache, T. R., Araki, Y., and Huganir, R. L. (2020). Twenty years of SynGAP research: from synapses to cognition. *J. Neurosci.* 40, 1596–1605. doi: 10.1523/JNEUROSCI.0420-19.2020

Gao, Z. F., Lv, Y. Q., Zhang, K. H., Gao, M., Ma, J., Wang, D., et al. (2020). A case with autosomal dominant mental retardation type 5 due to de novo SYNGAP1 variant. *Chin. J. Med. Genet.* 37, 661–664.

Hamdan, F. F., Gauthier, J., Spiegelman, D., Noreau, A., Yang, Y., Pellerin, S., et al. (2009). Mutations in SYNGAP1 in autosomal nonsyndromic mental retardation. *N. Engl. J. Med.* 360, 599–605. doi: 10.1056/NEJMoa0805392

Kilinc, M., Creson, T., Rojas, C., Aceti, M., Ellegood, J., Vaissiere, T., et al. (2018). Species-conserved SYNGAP1 phenotypes associated with neurodevelopmental disorders. *Mol. Cell. Neurosci.* 91, 140–150. doi: 10.1016/j.mcn.2018.03.008

Kuchenbuch, M., D'Onofrio, G., Chemaly, N., Barcia, G., Teng, T., and Nabbout, R. (2020). Add-on cannabidiol significantly decreases seizures in 3 patients with SYNGAP1 developmental and epileptic encephalopathy. *Epilepsia Open* 5, 496–500. doi: 10.1002/epi4.12411

Lu, J., Zhang, Y., Han, C., Zhu, J. Y., Wang, J., and Yao, Z. E. (2019). Identification of a novel SYNGAP1 mutation in a child with intellectual disability. *Chin. J. Med. Genet.* 36, 716–719.

Meili, F., Wei, W. J., Sin, W.-C., Meyers, W. M., Dascalu, I., Callaghan, D. B., et al. (2021). Multi-parametric analysis of 57 SYNGAP1 variants reveal impacts on GTPase signaling, localization, and protein stability. *Am. J. Hum. Genet.* 108, 148–162. doi: 10.1016/j.ajhg.2020.11.011

Mignot, C., von Stulpnagel, C., Nava, C., Ville, D., Sanlaville, D., Lesca, G., et al. (2016). Genetic and neurodevelopmental spectrum of SYNGAP1-associated intellectual disability and epilepsy. *J. Med. Genet.* 53, 511–522. doi: 10.1136/jmedgenet-2015-103451

Nakajima, R., Takao, K., Hattori, S., Shoji, H., Komiyama, N. H., Grant, S. G. N., et al. (2019). Comprehensive behavioral analysis of heterozygous Syngap1 knockout mice. *Neuropsychopharmacol. Rep.* 39, 223–237. doi: 10.1002/npr2.12073

Parker, M. J., Fryer, A. E., Shears, D. J., Lachlan, K. L., McKee, S. A., Magee, A. C., et al. (2015). De novo, heterozygous, loss-of-function mutations in SYNGAP1 cause a syndromic form of intellectual disability. *Am. J. Med. Genet. A* 167A, 2231–2237. doi: 10.1002/ajmg.a.37189

Pei, Y., Li, W., Du, L., and Wei, F. (2018). Novel mutation of SYNGAP1 associated with autosomal dominant mental retardation 5 in a Chinese patient. *Fetal. Pediatr. Pathol.* 37, 400–403. doi: 10.1080/15513815.2018.1497113

Richards, S., Aziz, N., Bale, S., Bick, D., Das, S., Gastier-Foster, J., et al. (2015). Standards and guidelines for the interpretation of sequence variants: a joint consensus recommendation of the American College of Medical Genetics and Genomics and the Association for Molecular Pathology. *Genet. Med.* 17, 405–424. doi: 10.1038/gim.2015.30

Tian, Y., Peng, B. W., Li, J. L., Hou, C., Zeng, Y. R., Liao, Y. T., et al. (2020). Clinical analysis of epilepsy with cognitive development disorder caused by SYNGAP1 gene mutation in three cases. *J. Clin. Pediatr.* 38, 571–574.

Vlaskamp, D. R. M., Shaw, B. J., Burgess, R., Mei, D., Montomoli, M., Xie, H., et al. (2019). SYNGAP1 encephalopathy: a distinctive generalized developmental and epileptic encephalopathy. *Neurology* 92, e96–e107. doi: 10.1212/WNL.0000000000006729

von Stulpnagel, C., Hartlieb, T., Borggrafe, I., Coppola, A., Gennaro, E., Eschermann, K., et al. (2019). Chewing induced reflex seizures ("eating epilepsy") and eye closure sensitivity as a common feature in pediatric patients with SYNGAP1 mutations: review of literature and report of 8 cases. *Seizure* 65, 131–137. doi: 10.1016/j.seizure.2018.12.020

Weldon, M., Kilinc, M., Lloyd Holder, J. Jr., and Rumbaugh, G. (2018). The first international conference on SYNGAP1-related brain disorders: a stakeholder meeting of families, researchers, clinicians, and regulators. *J. Neurodev. Disord.* 10:6. doi: 10.1186/s11689-018-9225-9221

Yang, Y., Muzny, D. M., Xia, F., Niu, Z., Person, R., Ding, Y., et al. (2014). Molecular findings among patients referred for clinical whole-exome sequencing. *JAMA* 312, 1870–1879. doi: 10.1001/jama.2014.14601

Conflict of Interest: The authors declare that the research was conducted in the absence of any commercial or financial relationships that could be construed as a potential conflict of interest.

Publisher's Note: All claims expressed in this article are solely those of the authors and do not necessarily represent those of their affiliated organizations, or those of the publisher, the editors and the reviewers. Any product that may be evaluated in this article, or claim that may be made by its manufacturer, is not guaranteed or endorsed by the publisher.

frontiers in Neuroscience

REVIEW
published: 02 March 2022
doi: 10.3389/fnins.2022.780407

Repetitive Restricted Behaviors in Autism Spectrum Disorder: From Mechanism to Development of Therapeutics

*Junbin Tian, Xuping Gao and Li Yang**

Peking University Sixth Hospital, Peking University Institute of Mental Health, National Clinical Research Center for Mental Disorders (Peking University Sixth Hospital), NHC Key Laboratory of Mental Health (Peking University), Beijing, China

Autism spectrum disorder (ASD) is a complex neurodevelopmental disorder characterized by deficits in social communication, social interaction, and repetitive restricted behaviors (RRBs). It is usually detected in early childhood. RRBs are behavioral patterns characterized by repetition, inflexibility, invariance, inappropriateness, and frequent lack of obvious function or specific purpose. To date, the classification of RRBs is contentious. Understanding the potential mechanisms of RRBs in children with ASD, such as neural connectivity disorders and abnormal immune functions, will contribute to finding new therapeutic targets. Although behavioral intervention remains the most effective and safe strategy for RRBs treatment, some promising drugs and new treatment options (e.g., supplementary and cell therapy) have shown positive effects on RRBs in recent studies. In this review, we summarize the latest advances of RRBs from mechanistic to therapeutic approaches and propose potential future directions in research on RRBs.

Keywords: autism spectrum disorder, repetitive restricted behaviors, mechanism, therapeutics, neural circuit

OPEN ACCESS

Edited by:
Yuri Bozzi,
University of Trento, Italy

Reviewed by:
Shelly Alexandra Buffington,
University of Texas Medical Branch at Galveston, United States
Mark H. Lewis,
University of Florida, United States

***Correspondence:**
Li Yang
yangli_pkuimh@bjmu.edu.cn

Specialty section:
This article was submitted to Neurodevelopment, a section of the journal Frontiers in Neuroscience

Received: *21 September 2021*
Accepted: *09 February 2022*
Published: *02 March 2022*

Citation:
Tian J, Gao X and Yang L (2022) Repetitive Restricted Behaviors in Autism Spectrum Disorder: From Mechanism to Development of Therapeutics. Front. Neurosci. 16:780407. doi: 10.3389/fnins.2022.780407

INTRODUCTION

Autism spectrum disorder (ASD) is a common, heritable, and heterogeneous neurodevelopmental disorder characterized by deficits in social communication, social interaction, and repetitive restricted behaviors (RRBs). Kanner (1943) first described the autistic symptoms. The latest study has shown that the prevalence of ASD among American children aged 8 years was 1/44 or 2.27% (Maenner et al., 2021). RRBs are purposeless behavior patterns that interfere with normal behaviors and were confirmed as the core symptom of ASD in the Diagnostic and Statistical Manual of Mental Disorders, Fifth Edition (DSM-5) released by the American Psychiatric Association (2013).

Compared with social communication impairment, RRBs have gained less attention in ASD studies. RRBs occur in the early developmental stage and may interfere with the acquisition of essential life skills in the future. Furthermore, RRBs severely affect the quality of life and impose additional burdens on the family (Leekam et al., 2011; Wolff et al., 2014). Although behavioral intervention has achieved positive effects on RRBs (Boyd et al., 2012), the evidence of medication for RRBs remains insufficient. In this review, we summarize the latest studies on RRBs in ASD and suggest future directions in research on RRBs.

REPETITIVE RESTRICTED BEHAVIORS

As an independent predictor of the prognosis of ASD (Troyb et al., 2016), the term "RRBs" is used to describe various behaviors and activities characterized by repetition, inflexibility, invariance, inappropriateness and frequent lack of obvious function and specific purpose, and highly restricted, fixated interests distinguished from the peers (Turner, 1999; Langen et al., 2011a). RRBs are thought pathological symptoms when they interfere with social relationships and impede daily activities. RRBs are non-specific symptoms observed in many other psychiatric disorders and developmental disabilities (Moss et al., 2009; Flores et al., 2011; Oakes et al., 2016; Evans, 2017). Moreover, RRBs also occur as common behaviors in typically developmental (TD) children, such as ritual behavior (Leekam et al., 2007; Arnott et al., 2010). In the section of ASD in DSM-5 (American Psychiatric Association, 2013), RRBs are divided into four subtypes: (a) Stereotyped or repetitive motor movements, use of objects, or speech. (b) Insistence on sameness, inflexible adherence to routines, or ritualized patterns of verbal or non-verbal behavior. (c) Highly restricted, fixated interests that are abnormal in intensity or focus. (d) Hyper- or hyporeactivity to sensory input or unusual interests in sensory aspects of the environment. Despite a lack of specific criteria to define different subtypes of RRBs, we can also identify the abnormal manifestation of repetitive behaviors depending on their characteristics and contexts in which they occur. For example, just turning lights and radios on or off is not considered RRBs, yet doing these repetitively without any specific purpose is recognized as abnormal RRBs. Because of the heterogeneity of RRBs, there are great challenges of deep understanding and completely assessing RRBs.

Firstly, there is rarely a consensus on the classification of RRBs by clinicians. In 1999, Turner classified RRBs into two types: "low-order" RRBs characterized by repetitive body movements (dyskinesia, convulsion, motor stereotypy, repeated manipulation of objects, and repetitive self-injury behavior) and "high-level" RRBs characterized by procedural and ritual behavioral patterns (insistence on sameness, resistance to change, repetitive language, and limited interest) (Turner, 1999). More studies divided RRBs into repetitive sensory motor (RSM) behaviors and insistence on Sameness (IS) behaviors (Cuccaro et al., 2003; Georgiades et al., 2010; Bishop et al., 2013). This two-factor model was consistent with the above classification described by Turner. However, the two-factor model has not been adopted in all studies. To date, many factor analysis studies have further examined the subtypes of RRBs by questionnaires designed for RRBs. The factor analysis based on repetitive behavior scale–revised (RBS-R) proposed a six-factor model: stereotyped behavior, self-injurious behavior, compulsive behavior, ritualistic behavior, sameness behavior, and restricted behavior (Bodfish et al., 2000; Esbensen et al., 2009). At present, based on the six-factor model of RBS-R, other researchers have also developed five-factor and three-factor models (Lam and Aman, 2007; Mirenda et al., 2010; He et al., 2019). The five-factor model merged the original subscales of ritualistic behavior and sameness behavior into one (ritualistic/sameness behavior subscale). This model seemed reasonable because both behaviors showed the same invariance and consistency needs and was more stable and reproducible than the original RBS-R (Lam and Aman, 2007). The three-factor model comprised compulsive ritualistic sameness behaviors, self-injurious behaviors, and restricted stereotyped behaviors. Mirenda et al. suggested that five- and six-factor models showed a better statistical fit than the three-factor model. However, the three-factor model also had advantages in genetic quantitative trait locus (QTL) analyses (Mirenda et al., 2010). He et al. (2019) considered the five-factor model preferable because the five-factor model had good psychometric characteristics and was more concise than the six-factor model. In addition, Leekam et al. (2007) obtained the four-factor model via repetitive behavior questionnaire-2 (RBQ-2). In a word, the classification criteria of RRBs are controversial. The variability of classification of RRBs may impact the consistency of results in different studies. That is to say, different measurement tools may divide a certain type of RRBs into different subcategories. For example, the item, arrange toys or other things in rows or patterns, was loaded into the subscale of preoccupation with restricted patterns of interest in RBQ-2, but the same-meaning item was allocated to the compulsive behavior subscale in RBS-R. This inconsistency may lead to the wrong conclusion regarding the more specific RRBs classification. Thus, it is necessary to compare various scales to confirm unified classification criteria and develop recognized assessment tools. These ensure results are comparable in different studies and further help to reveal more differences of RRBs in different populations, such as more severe self-injurious behavior in girls with ASD that cannot be found in studies using the two-factor model (Antezana et al., 2019).

Secondly, typically developing children also manifest some ritualistic, repetitive behaviors during early development (Evans et al., 1997; Leekam et al., 2007; Arnott et al., 2010). Then how can we differentiate RRBs between children with ASD and TD children? Usually, the RRBs in children with ASD are more excessive and diverse than those in TD children and result in severe impairments (Bodfish et al., 2000; Richler et al., 2007; Mandy et al., 2011; Harrop et al., 2014). Furthermore, following up repetitive behaviors across the developmental course is essential to determine whether it is aberrant. In TD children, repetitive behaviors are more common in toddlers than preschoolers (Kim and Lord, 2010). In early infancy, the stereotyped motor is considered a developmental manifestation of intrinsic central motor programs (Thelen, 1981). Repetitive behaviors may weaken with age in TD children (Larkin et al., 2017; Uljarevic et al., 2017; Sifre et al., 2021). However, the RRBs in children with ASD remain or aggravate with age (Leekam et al., 2007; Richler et al., 2010; Joseph et al., 2013).

ASSESSMENT OF REPETITIVE RESTRICTED BEHAVIORS

Early specific RRB symptoms predict the severity and outcome of ASD (Troyb et al., 2016; Miller et al., 2021). Moreover, two early studies indicated that preschool children with ASD displaying RRBs tended to have worse school-age language outcomes than

those who did not exhibit RRBs (Charman et al., 2005; Paul et al., 2008). These findings emphasize the importance of early evaluation of all subtypes of RRBs.

There are three main methods to assess RRBs: parent interview, observation, and questionnaire. The autism diagnostic interview-revised (ADI-R), a semi-structured, standardized interview, is an acknowledged diagnostic tool of ASD (Lord et al., 1994). However, the items related to RRBs are scarce and concentrated in the dimension of restricted interest and behavior. Thus, some researchers contended that ADI-R was insufficient to cover all relevant RRBs occurring in children with ASD. The autism diagnostic observation schedule, 2nd edition (ADOS-2) combined with ADI-R, has been regarded as the gold standard for assessing children with ASD (Lord et al., 2012; McCrimmon and Rostad, 2014). Although some items about RRBs are included in the ADOS-2 algorithm, it is worth noting that this assessment may not find children's RRBs in a limited time and single environment, thereby affecting the accuracy of assessment (Hus et al., 2014).

In addition, questionnaire is an excellent supplement to parent interview and observation. We summarize frequently used RRBs questionnaires and their relative strengths and weaknesses in **Panel 1**.

NEUROPSYCHOLOGY OF REPETITIVE RESTRICTED BEHAVIORS

Cognition

In the early stages, executive function (EF) impairment was thought an explanation for RRBs, starting with Turner (1997, 1999). EF first develops in the early stages of development, approximately the end of the first year of life, and develops rapidly at the age of 2–5, which is in line with alterations of RRBs with age (Leekam et al., 2011). Numerous studies have supported a close connection between elevated RRB levels and EF impairments in children with ASD (Lopez et al., 2005) and TD children (Iversen and Lewis, 2021), such as set-shifting (Miller et al., 2015), inhibitory control (Mosconi et al., 2009), cognitive flexibility, and working memory (Van Eylen et al., 2015). An alternative view suggested that impaired EF was another manifestation of RRBs rather than an independent causative force driving RRBs. For example, the impairment of inhibitory control and set shifting seemed to be more related to the "high-order" RRBs, indicating that it might be that we were looking at the same general phenomenon (i.e., behavioral inflexibility or cognitive inflexibility) through different lenses (Mosconi et al., 2009; Van Eylen et al., 2015; Schmitt et al., 2018; Faja and Nelson Darling, 2019). Overall, RRBs can be indexed in many ways, including direct observations of behaviors, standardized rating scales, and neuropsychological tests of, for example, set-shifting or cognitive flexibility.

Reinforcement and Habit

Organisms are motivated to seek reward stimuli (e.g., pleasant experiences or positive outcomes) or achieve specific goals, which increases the probability that specific behavior will be repeated (Wenzel and Cheer, 2018). This process is called reinforcement. Initially, ASD studies of reinforcement focused on social stimuli (Dawson et al., 1998; Klin et al., 2009). However, more attention has been given to the social motivation theory of autism in recent years (Chevallier et al., 2012). Children with ASD show diminished social motivation and a preference for non-social stimuli. This imbalance of motivations between non-social and social stimuli reflects the dysfunction of reward system (Dichter et al., 2012; Kohls et al., 2013), which may be the neurobiological basis of restricted interests (a subtype of RRBs) (Cascio et al., 2014; Clements et al., 2018; Kohls et al., 2018). Imaging studies revealed that the ventromedial prefrontal cortex (vmPFC) – ventral striatum (VS) – amygdala circuitry related to reward system seemed to be dysfunctional in ASD and underlay atypical reward responsiveness in individuals with ASD in part (Kohls et al., 2012; Langen et al., 2014). The activation of striatal regions increased in response to restricted interests in ASD (Clements et al., 2018). Similarly, Kohls et al. (2018) reported the stronger responsiveness of reward system to restricted interests rather than social rewards in children with ASD than TD children. Generally speaking, some types of RRBs may reflect, at least to a degree, reward-based processes (e.g., strong interest, motivation, and pleasure in response to unusual behaviors, objects, and

Panel 1 | Currently used RRB questionnaires.

- Repetitive Behavior Scale-Revised (RBS-R): This scale is the most frequently used to measure the severity of RRBs. The 43 items were compiled into six subscales: stereotyped behavior, self-injurious behavior, restricted behavior, compulsive behavior, ritualistic behavior, and sameness behavior (Bodfish et al., 2000). RBS-R has a good psychometric criterion. Some researchers have also developed five- and three-factor models (Lam and Aman, 2007; Mirenda et al., 2010; He et al., 2019), but their applicability needs to be proven in future studies. Considering comprehensive items and convenient use, RBS-R has a wide range of clinical applications (Lam and Aman, 2007; Mirenda et al., 2010; Bishop et al., 2013; He et al., 2019).
- Aberrant Behavior Checklist (ABC): This is a caregiver rating scale used to assess behavioral problems in ASD (Aman et al., 1985; Kaat et al., 2014). Compared with other tools, ABC includes more comprehensive behavioral problems. Besides RRBs, it also investigates other aspects, such as emotional stability, attention, and hyperactivity. Currently, ABC applies to children and adults and is used for measuring the results of drugs and behavioral interventions in individuals with ASD (Owen et al., 2009; Bearss et al., 2013). Nevertheless, a potential disadvantage is that the stereotypic behavior subscale contains only seven items mainly describing stereotyped motor and limb movements.
- Repetitive Behavior Questionnaire (RBQ): The RBQ is created for the sole purpose of assessing RRBs and includes 33 items (Honey et al., 2012). Twenty-nine items examine four subtypes of RRBs, including repetitive movements, sameness behaviors, repetitive use of language, and circumscribed interests. The four additional items consist of a summary item, which examines children's overall interests or hobbies, and three open questions: the earliest repetitive activity, the most marked or noticeable behaviors, and the problematic repetitive behaviors. Based on RBQ, some researchers have developed RBQ-2 (Leekam et al., 2007) and RBQ-2A (Barrett et al., 2015) suitable for adults and children, respectively. RBQ checks the frequency of specific RRBs. Thus, it is very suitable to study the frequency or prevalence of RRBs. Moreover, three open questions also provide more information. So far, RBQ is not widely used in clinical practice.

activity) (Kohls et al., 2018). However, there is a lack of studies on the relationship between reward system and other subtypes of RRBs. Moreover, a part of individuals with ASD described that they felt pleasure when RRBs occurred, which urged them to do it again (Joyce et al., 2017). On the contrary, facing social communication, children with ASD had to confront the changing environments and unexpected events (Dawson et al., 1998). Thus, it is reasonable to presume that the preference for non-social stimuli reduces unpredictability and brings pleasant experiences to compensate for the anxiety and aversion of social communication in individuals with ASD. However, the contention is speculative and in need of empirical testing beyond a subjective sense of function (e.g., feeling pleasure).

In addition, reward-guided behaviors usually start as goal-directed actions that are controlled by the anticipation of the outcome. However, these behaviors can become stimulus-driven habits under certain conditions, which are not controlled by outcome expectancy (Yin and Knowlton, 2006). After achieving the same results via repetitive behaviors multiple times, we may focus less on the outcomes of actions, and goal-directed actions become automatized and habitual (Simmler and Ozawa, 2019). That is to say, goal-directed actions are controlled by their consequences, habits by antecedent stimuli (Yin and Knowlton, 2006). Alvares et al. (2016) found reduced goal-directed action control in individuals with ASD, which promoted habitual actions in an anxiety-inducing environment (e.g., social encounters). However, Geurts and De Wit (2014) did not find a disruption in the balance between goal-directed and habitual behavioral control in children with ASD. This inconsistency may be due to the age difference in the two studies (Alvares et al., 2016). Moreover, the corticostriatal connectivity is the neurobiological basis of the balance between habitual and goal-directed action control (Yin and Knowlton, 2006; Wit et al., 2012). Augustine et al. showed the reduced functional connectivity between the prefrontal and striatal regions (i.e., regions associated with goal-directed behaviors). However, the functional connectivity between motor/premotor cortex and striatal regions (i.e., regions critical for developing and regulating habitual behaviors) had no difference in children with motor stereotypies (a type of RRBs) compared to TD children (Augustine et al., 2021). A speculative contention was decreased prefrontal – striatal connectivity altered the balance between habitual and goal-directed action control, which resulted in enduring motor stereotypies. To sum up, it is unclear whether RRBs can be considered persistent and habitual actions based on a functional imbalance hypothesis referring to habitual and goal-directed action control. The notion is largely needed to be supported by empirical evidence.

Habituation

Habituation is defined by an increasing reduction in behaviors and neural responses to repetitive stimuli, not caused by adaptation of sensory receptors or motor fatigue (Thompson and Spencer, 1966; Schmid et al., 2014). For example, repetitive affective and facial expression stimuli resulted in the habituation of automatic nervous systems and amygdala responses (Klorman et al., 1977; Klorman and Ryan, 1980; Breiter et al., 1996; Knight et al., 2005; Hare et al., 2008). In addition, habituation, in turn, facilitates children to pay more attention to the unknown from something acquainted, which promotes learning and adaptive responses to environmental changes (Groves and Thompson, 1970; Lloyd et al., 2014). Current studies supported the abnormal habituation in ASD (Guiraud et al., 2011; Swartz et al., 2013). Due to the abnormal habituation to normal input of sensory signals, individuals with ASD exhibited abnormal hyperresponsivity to environmental stimuli. Green et al. (2015) found that youth with ASD and sensory overresponsivity had attenuated neural habituation to stimuli in sensory cortices and the amygdala compared to the control and showed that this hyperresponsivity was due to failure to habituate. Hyperresponsivity to environmental stimuli was related to negative emotional reactions (e.g., anxiety) and highly uncertain perception of the environment (Uljarevic, 2013; Black et al., 2017; Vasa et al., 2018; Pickard et al., 2020). In addition, there is an apparent correlation between anxiety and RRBs. RRBs play a potential role in alleviating anxiety, and anxiety is an intrinsic motivator for repetitive behaviors (Joosten et al., 2009; Leekam et al., 2011; Rodgers et al., 2012; Spiker et al., 2012; Lidstone et al., 2014). Thus, we speculate RRBs may diminish the unpleasant emotional reactions due to the sensory hyperresponsivity and environmental uncertainty by some behaviors related to escape or avoidance in part. In conclusion, it is proposed that RRBs are coping strategies of hyperresponsivity to sensory stimuli caused by abnormal habituation. However, this contention is speculative and also lacks empirical support. It is essential to conduct more studies to explore the relationship between RRBs and habituation.

MECHANISM OF REPETITIVE RESTRICTED BEHAVIORS

Autism spectrum disorder (ASD) is primarily caused by multiple genetic mutations that affect the structure and function of neural circuits. Various abnormities of brain regions and circuits are related to repetitive behaviors. In addition, the latest neurobiological and immunological findings suggest complex and diverse mechanisms of RRBs. Further understanding the mechanisms of RRBs helps to find more potential therapeutic targets.

Cortico-Striatal-Thalamo-Cortical Circuit

Autism spectrum disorder (ASD) has been conceptualized as a brain network connectivity disorder (Just et al., 2004). The aberrant circuits predicted distinct RRBs in children with ASD (Supekar et al., 2021). Many studies focused on the role of the cortico-striatal-thalamo-cortical (CSTC) circuit in RRBs because this circuit is closely related to the execution of goal-oriented behavior. Interruptions or abnormalities (e.g., neuronal alterations and aberrant projections) in the CSTC circuit caused dysfunctional motor control (Lewis and Kim, 2009; Graybiel and Grafton, 2015). Previous and more comprehensive reviews have summarized neuroimaging (Wilkes and Lewis, 2018; Hiremath et al., 2021) and neurobiological studies (Gandhi and Lee, 2020; Vicente et al., 2020) of the role of CSTC in RRBs. In this section, we will review new findings of RRBs.

Neuroimaging of Cortico-Striatal-Thalamo-Cortical Circuit

Structural magnetic resonance imaging (MRI) studies found some abnormalities of the CSTC circuit with corresponding changes in RRBs. The orbitofrontal cortex (OFC) gray matter volume was positively associated with the severity of RRBs (Hegarty et al., 2020). However, right caudal anterior cingulate U-fiber volume was negatively associated with RRBs (Hau et al., 2019). Interestingly, sex differences in brain structure were associated with RRBs symptoms in autism. The female twin with more severe RRBs had increased thickness of the right intraparietal sulcus and decreased volume of the right orbital gyrus. However, increased volume of the bilateral pallidum was related to more severe RRBs in males (Van't Westeinde et al., 2020). In addition, structural covariance describes the anatomical association in brain regions, which partially recapitulate networks of synchronized brain activity and is connected with the coordinated rates of developmental change in co-varying regions (Alexander-Bloch et al., 2013). Aberrant structural covariance in subcortical regions, such as thalami and basal ganglia, occurred in children with ASD and predicted the severity of RRBs, which suggested that abnormities of coordinating development of subcortical regions played an essential role in RRBs (Duan et al., 2020). Similarly, Mei et al. (2020) also reported that the structural covariation in brain areas associated with the CSTC circuit was significantly correlated with RRBs in individuals with ASD. A latest preclinical neuroimaging study on RRBs showed that reduced volume in key cortical and basal ganglia regions, including the motor cortex, striatum, globus pallidus, and subthalamic nucleus, was associated with repetitive behaviors in C58/J mice (Wilkes et al., 2020).

There were some new reports of functional connectivity changes of the CSTC circuit in recent years. For example, the over-connectivity pattern primarily in networks involving the fronto-temporal nodes related to RRBs occurred in individuals with ASD (Conti et al., 2017). Ma et al. (2021) showed the increased cortico-striatal intrinsic functional connectivities (iFC) with age in ASD and significant correlations between ADOS-RRB scores and iFC of the dorsal attention network-posterior cingulate cortex/precuneus. Furthermore, Akkermans et al. (2019) showed that increased functional connectivity between the left nucleus accumbens (NAcc) and a cluster in the right premotor cortex/middle frontal gyrus was correlated to more severe RRBs in children with ASD.

Langen et al. suggested the cortico-striatal circuit could be functionally divided into three "macro-circuits." Each circuit was comprised of discrete, essentially non-overlapping subcortical structures, such as the striatum, globus pallidus, and thalamus, and received multiple inputs from functionally related and interconnected cortexes (Langen et al., 2011b). The CSTC circuit mainly included the sensorimotor circuit (comprising the motor and oculomotor loops), the associative circuit (dorsolateral prefrontal loop), and the limbic circuit (lateral orbitofrontal and anterior cingulate loops) (Groenewegen et al., 2003; Langen et al., 2011a). The abnormities of any circuit could give rise to different RRBs types. Some studies focused on these discrete loops. For example, Abbott et al. reported that the individuals with ASD and high RRBs showed depressed frontoparietal/limbic and motor/limbic circuit ratios. In other words, RRBs seemed to be linked to the imbalance of cortico-striatal connectivity, which showed increased connectivity of limbic circuits, but reduced connectivity of frontoparietal and motor circuits (Abbott et al., 2018). Moreover, complex motor stereotypies (CMS) were rhythmic, repetitive, fixed, and purposeless movements (Oakley et al., 2015). Augustine et al. (2021) found reduced functional connectivity between the prefrontal cortex and striatal regions in children with CMS. However, functional connectivity between motor/premotor cortex and striatal regions was no different from the control group. In a word, these findings offered evidence of the role of discrete loops in RRBs.

Neurobiology of Cortico-Striatal-Thalamo-Cortical Circuit

How this circuit regulates repetitive behaviors, here we describe the underlying neurobiological mechanisms of RRBs. Based on the neurobiological studies, the CSTC circuit is composed mainly of the direct pathway (cerebral cortex-striatum-internal segment of the globus pallidus/substantia nigra-thalamus-cerebral cortex) and indirect pathway (cerebral cortex-striatum-external segment of the globus pallidus-subthalamic nucleus-internal segment of the globus pallidus/substantia nigra-thalamus-cerebral cortex) (**Figure 1**) (Kim et al., 2016). There are two major classes of medium spiny neurons (MSNs) in the striatum [i.e., D1R-expressing direct pathway MSNs (dMSNs) and D2R-expressing indirect-pathway MSNs (iMSNs)], and MSNs respectively project to different brain areas (**Figure 1**). The behavioral result of activation of the direct pathway is motor activation/movements. However, activating the indirect pathway will reduce motor activity and movement (Calabresi et al., 2014). There was abundant evidence of dysfunction of direct and indirect pathways in ASD. Either of dysfunctions gave rise to the imbalance of both pathways (Kim et al., 2016; Gandhi and Lee, 2020), which might underlie RRBs (Lewis and Kim, 2009; Burguière et al., 2015; Monteiro and Feng, 2016).

Recently, some studies reported abnormal activation of the direct pathway in RRBs. In conditional knockout mice, the overactivation of dMSNs caused excessive self-grooming (a pathological repetitive behavior in mice), which suggested the role of direct-pathway deficiency in RRBs (Shonesy et al., 2018). Similarly, optogenetic activation of dMSNs also resulted in sustained and chronic repetitive behaviors (Bouchekioua et al., 2018). Engeln et al. (2021) found chemogenetic inhibition of dMSN can reduce repetitive rotations. In addition, the increased RRBs related to aberrant dMSNs have been found in Neuroligin 1 and Neuroligin-3 mutant mice (Rothwell et al., 2014; Espinosa et al., 2015).

Other studies revealed the indirect pathway role in RRBs. Shank3 deletion preferentially caused synaptic defects in iMSNs in Shank3B-KO mice, which provided direct evidence that a primary dysfunction of indirect pathway brought about the RRBs in ASD mice (Wang et al., 2017). In addition, Brandenburg et al. (2020) reported the increased dopamine type 2 gene expression in the dorsal striatum in postmortem brain tissue from an individual with ASD, which implied the alteration of

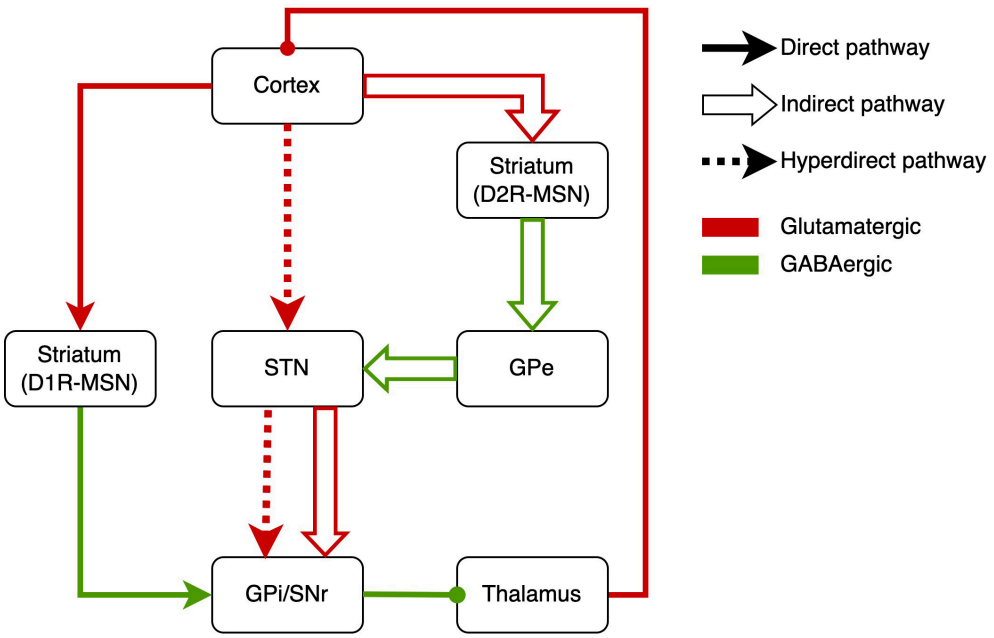

FIGURE 1 | Schematic drawings of the direct pathway, indirect pathway, and hyperdirect pathway. GPe, external segment of the globus pallidus; GPi, internal segment of the globus pallidus; SNr, substantia nigra pars reticulata; STN, subthalamic nucleus; MSN, medium spiny neuron.

indirect pathway in ASD. When it comes to the indirect pathway, STN, a vital part of the indirect pathway, has to be mentioned (Tanimura et al., 2011; Wilkes et al., 2020). In C58/J mice, reduced volume in STNs was associated with repetitive behaviors (Wilkes et al., 2020). The pharmacological studies on the indirect pathway also implied the indirect-pathway role in RRBs. For example, sub-chronic drug treatment targeting the indirect pathway reduced repetitive behavior in C58 mice and improved the STN dysfunction (Muehlmann et al., 2020). Similarly, adenosine A2A receptor agonist treatment attenuated increased grooming behaviors in BTBR mice (Amodeo et al., 2018). Selectively enhancing the indirect striatal pathway activation also corrected the RRBs in Shank3B-KO mice (Wang et al., 2017). Moreover, exposure to environmental enrichment retarded the development of stereotypy and recovered the decreased STN activation related to RRBs in high-stereotypy mice (Tanimura et al., 2010). Subsequently, the same team reported that this effect was based on the increased neuronal activation and dendritic spine densities in STN (Bechard et al., 2016). Besides, high-frequency stimulation at STN significantly alleviated RRBs in rodents (Aliane et al., 2012; Chang et al., 2016) and primates (Baup et al., 2008). However, there was a lack of neuroimaging studies that revealed the relation between RRBs and STN in humans. To sum up, the activations of direct and indirect pathways determine behavioral responses, and the imbalance of activations will give rise to RRBs.

The hyperdirect pathway, an integral component of the CSTC circuit, may be involved in the occurrence of RRBs (**Figure 1**). The STN is considered to receive fast monosynaptic projections from motor areas of the cortex via the hyperdirect pathway (Nambu et al., 2002). This pathway has been verified in humans (Brunenberg et al., 2012; Kelley et al., 2018) and animal models (Haynes and Haber, 2013; Averbeck et al., 2014). Activation of hyperdirect pathway will inhibit ongoing motor movements (Bahuguna et al., 2015). Increasing studies on the role of the hyperdirect pathway in inhibitory control have been reported in humans and animals (Eagle et al., 2008; Rae et al., 2015; Pasquereau and Turner, 2017; Jahfari et al., 2019). Cai et al. (2019) showed that the hyperdirect pathway predicted the inhibitory control in children. As mentioned earlier, inhibitory control may be another manifestation of RRBs. Thus, we suggested the hyperdirect pathway is related to RRBs, although there is a lack of direct evidence for the correlation between hyperdirect pathway and RRBs in ASD.

Moreover, the CSTC circuit is modulated by endogenous neuropeptides, including cannabinoids, opioids, and several other neurotransmitters. Shonesy et al. (2018) found that regulating endocannabinoid signaling in the direct pathway influenced the level of RRBs. Endogenous opioids in the frontal cortex (i.e., the starting site of projections in direct and indirect pathways) were negatively correlated to RRBs (Augustine et al., 2020). In addition, some studies have found abnormalities in the CSTC circuit in genetically mutated mice with particular signal transduction deficits, such as Dlg2 deletion mice (Yoo et al., 2020) and xCT −/− mice (Bentea et al., 2020). These studies gave support to the importance of the CSTC circuit in RRBs.

Cerebellum

The cerebellum is related to sensorimotor processing and motor control (Bostan et al., 2010; Mosconi et al., 2015a). Increasing evidence suggests cerebellar connection dysfunction in ASD (Mosconi et al., 2015a,b), and these structural and functional

alterations of the cerebellum are associated with RRBs (Rojas et al., 2006; Cheung et al., 2009; D'Mello et al., 2015; Wolff et al., 2017). The loss of Purkinje cells in the cerebellum may be the biological basis of RRBs (Al Sagheer et al., 2018). In this section, we summarize the new findings based on previous reviews (Wilkes and Lewis, 2018; Gandhi and Lee, 2020; Vicente et al., 2020).

Alteration of cerebellum structure related to RRBs has been reported in ASD. Srivastava et al. (2019) showed that cerebellar vermis volume reduced with high RRBs score and may predict severity of RRBs in Phelan-McDermid syndrome. However, a study of children at high risk of ASD found that high-risk infants have larger cerebellar at 4–6 months of age, and alterations in the volume are positively correlated with repetitive behaviors at 36 months. The study suggests that early cerebellar and subcortical volumes predicted repetitive behaviors in children (Pote et al., 2019). These inconsistent results may be due to the different ages of participants. Previous studies of younger children with ASD found larger total cerebellum (Sparks et al., 2002) and cerebellar white matter volume (Courchesne et al., 2001). In addition, RRBs were related to the volume of the crus II of the cerebellum in C58/J mice (Wilkes et al., 2020). All above data supported the cerebellum volume to be a potential biomarker for predicting RRBs severity.

Functional magnetic resonance imaging (fMRI) studies indicated aberrant connectivity between the cerebellum and cerebral cortex. Lidstone et al. collected resting-state fMRI from 105 children with ASD and found that elevated RRBs were associated with low right posterior cerebellum-left inferior parietal lobule (IPL) connectivity and high right posterior cerebellar-right IPL connectivity (Lidstone et al., 2021). Kelly demonstrated disrupted functional connectivity between the cerebellum and the medial prefrontal cortex (mPFC) in multiple mouse models of ASD-linked genetic mutations and individuals with ASD. Modulating the circuit from the right cerebellum crus1 area to the mPFC can lead to repetitive behaviors in Tsc1 mutant mice (Kelly et al., 2020).

Recently, the connection between the basal ganglia and cerebellum has increased attention. Two-way communication between the basal ganglia and cerebellum has also been proved in primates (Bostan et al., 2010). In addition, Chen et al. found a disynaptic pathway between striatum and cerebellum in mice. This short-latency pathway allowed rapid communication between the cerebellum and the basal ganglia. Thus, cerebellum can regulate the corticostriatal plasticity. Under pathological conditions, abnormal activity from the cerebellum was transmitted to the basal ganglia, which led to dysfunctional behaviors (Chen et al., 2014). Other studies also provided evidence of a powerful, short-latency pathway that connected the cerebellar dentate nucleus with the dorsolateral striatum (Bareš et al., 2015). The above reports were based on animal models. This connection also appears in humans. Milardi et al. found a direct route linking the dentate nucleus to the internal globus pallidus and the STN in healthy people (Milardi et al., 2016). Moreover, the basal ganglia and cerebellum were involved in different learning systems (i.e., reward-based learning and developing specific conditioned responses). Dasgupta et al. suggested their complementary roles in behavioral learning and the substantial bidirectional communication between these two brain structures. The combination of learning systems based on the basal ganglia and cerebellum allows for more stable and faster learning of goal-directed behavior than individual systems (Dasgupta et al., 2014). The imbalance between the two systems may lead to aberrant motor and non-motor functions (Subramanian et al., 2017). Based on these studies, the interaction between the cerebellum and basal ganglia may play an important role in RRBs. However, there is a lack of direct evidence to clarify the correlation between this connectivity and RRBs.

The cerebellar Purkinje cell (PC) dysfunction in the cerebellum may be the biological basis of RRBs (Mejias et al., 2019; Winkler et al., 2020). For example, the Shank3 mutant mouse exhibited significantly stereotyped behavior with fewer PC in cerebellar sub-regions (Matas et al., 2021). PC activation improved RRBs in PC-TSC1 mutant mice (Kelly et al., 2020). In addition, increased oxidative stress resulted in cerebellum dysfunction, which is associated with RRBs. Nadeem et al. (2019a,b) found that the deficiency of an adaptive antioxidant response in the cerebellum was related to increased repetitive behaviors in BTBR mice, and sulforaphane can restore this deficiency to improve the RRBs.

Abnormal Immune Functions

Abnormal immune functions are related to ASD symptoms (Moradi et al., 2021). The immune dysfunction in ASD directly affects various neurodevelopmental and neurological processes, resulting in behavioral abnormality (Mead and Ashwood, 2015). In primate models of maternal immune activation (MIA), rhesus monkey offspring exposed to MIA *in utero* exhibited an increased frequency of motor stereotypies (Bauman et al., 2014; Rose et al., 2017). It has been demonstrated that the increased level of maternal autoantibody was associated with more severe RRBs. For example, exposure to endogenous maternal anti-Caspr2 antibody *in utero* led to robust RRBs in male mice (Bagnall-Moreau et al., 2020). Similarly, constant exposure to the autism-specific maternal autoantibodies throughout gestation result in apparent RRBs in C57BL/6J mice (Jones et al., 2020). In addition, offspring mice received a single intraventricular injection of IgG from two mothers of children with ASD on embryonic day 14 displayed RRBs (Camacho et al., 2014). Martin et al. (2008) found treatment with IgG from mothers of children with ASD induced offspring to exhibit whole-body stereotypies in rhesus monkeys. However, Bauman et al. (2013) did not find any alterations of repetitive behaviors in rhesus monkeys injected with human IgG isolated from mothers of children with ASD six times during early and mid-gestation. The inconsistency of offspring behaviors was probably due to the route and number of injections administered, different animal models (Watson and Platt, 2012), the pregnancy time of the injection, the alteration of testing circumstances (Hutt and Hutt, 1965; Runco et al., 1986), and most importantly, the source of IgG used (Salloum-Asfar et al., 2019). Further studies are needed to determine the influence of these factors. However, there was no doubt that maternal antibodies played a role in RRBs. In addition, BTBR mice exhibited increased oxidative stress and insufficient enzymatic

antioxidant responses associated with autistic repetitive behaviors (Nadeem et al., 2019a). In recent years, more clinical studies have found that higher levels of proinflammatory factors, such as IL-1β (Ashwood et al., 2011b) and IL-10 (Meyer et al., 2008), were related to more severe RRBs (Ashwood et al., 2011a; Careaga et al., 2017; Rose et al., 2017). Regulating immune pathways in BTBR mice reduced RRBs with decreased levels of proinflammatory cytokines (Zhang et al., 2019). In summary, proinflammatory factors may be the mediator between immune dysfunction and RRBs. Many pharmacological studies of RRBs were based on immune abnormalities in ASD (Ahmad et al., 2019). For example, Mirza and Sharma (2019b) found that pioglitazone reduced oxidative stress and nerve inflammation in related brain regions and improved propionic acid-induced neurobehavioral and biochemical impairments in rats. Li et al. (2020) found that aberrant eating behaviors and high food-specific IgG antibody concentrations were related to more severe RRBs in children with ASD. In addition, the ketogenic diet could improve the high levels of repetitive behavior in male C57Bl/6 mice affected by MIA (Ruskin et al., 2017). At present, most studies were based on animal models with ASD, and a few measured the indicators of proinflammatory factors (Bryn et al., 2017). Moreover, more scholars focused on the relationship between immune dysfunction and abnormal gut microflora in individuals with ASD (Moradi et al., 2021). Based on the above findings, related immune pathways may become one of the therapeutic targets of RRBs.

Other Potential Neural Mechanism

Most studies of the mechanism of RRBs were conducted in animal models with related genetic mutations. Researchers observed the typical core symptoms of ASD in various mutated mice (Satterstrom et al., 2020). Neurotransmitters, such as glutamate and γ-aminobutyric acid (GABA), regulated the balance of excitation and inhibition (E/I) in the brain (Cai et al., 2017). The increased excitatory signals and decreased inhibitory interneurons would induce RRBs in ASD animals (Rinaldi et al., 2007; Gogolla et al., 2009). Moreover, modulating the level of transmitters could change RRBs (Rhine et al., 2019). Abnormal neurotransmitter systems of brain areas related to RRBs would give rise to RRBs (Peca et al., 2011; Bentea et al., 2020), such as glutamate receptor-interacting proteins 1/2 (Grip1/2) (Mejias et al., 2019), metabotropic glutamate receptor 5 (mGluR5) (Silverman et al., 2010; Luo et al., 2018), and $GABA_A$ receptor (Yoshimura et al., 2017). Yang et al. (2021) reported that acute administration of GABA-A or/and GABA-B receptor agonists could palliate repetitive behaviors in ASD mice.

Serotonin (5-hydroxytryptamine, 5-HT) plays a complex role in regulating neural circuits during prenatal and postnatal development (Whitaker-Azmitia, 2001; Veenstra-VanderWeele et al., 2012; Wirth et al., 2017). The alteration of the 5-HT neurotransmitter system in the brain has been reported in animal models and individuals with ASD (Muller et al., 2016). The studies of treatment with selective serotonin reuptake inhibitors (SSRIs) produced inconsistent results on RRBs (Costa et al., 2018; Reddihough et al., 2019; Herscu et al., 2020). Diverse 5-HT receptors have different effects on RRBs. For example, the blockades of 5-HT_{2A} receptor (Amodeo et al., 2017) and 5-HT_6 receptor (Amodeo et al., 2021) reduced RRBs. Decreased activation of 5-HT_{1A} also achieved the same effect (Chugani et al., 2016). However, activating the 5-HT_7 receptor reversed repetitive behaviors in Fragile X syndrome (Costa et al., 2018). The current studies on serotonin were based on animal models, and more complete studies in humans will confirm the relationship between 5-HT and RRBs.

Increasing studies related to RRBs focused on other neural signalings, such as dopaminergic signaling (Lee et al., 2018b; Venkatachalam et al., 2021), cannabinoid signaling (Marco et al., 2011; Fyke et al., 2021; Nezgovorova et al., 2021), mammalian target of rapamycin (mTOR) signaling (Burket et al., 2014; Chugani et al., 2016; Wu et al., 2017), adenosine signaling (Ansari et al., 2017; Lewis et al., 2019), and histamine signaling (Eissa et al., 2018; Eissa et al., 2020b; Venkatachalam et al., 2021). These signal molecules may play a role in regulating synaptic transmission in brain regions related to RRBs, and multiple signaling pathways might be involved in the pathological process simultaneously (Eissa et al., 2019; Eissa et al., 2020a; Muehlmann et al., 2020; Eissa et al., 2021; Venkatachalam et al., 2021).

TREATMENT AND INTERVENTION OF REPETITIVE RESTRICTED BEHAVIORS

In recent years, the number of studies on RRB treatment and intervention has increased. There is no recognized drug intervention for RRBs at present, and behavioral intervention remains the most effective and safe strategy for RRBs treatment. This section reviews the recent advance in drug intervention, supplementary therapy, and other potential therapies.

Drug Treatment

Although no evidence-based effective medicine for RRBs in ASD has been proposed, some drugs based on new psychopharmacological mechanisms or molecular targets have shown potential benefits in early studies. Given the substantial individual differences in clinical response and side effects observed in current studies, more studies are needed to verify these findings.

Antipsychotic Drug

Risperidone and aripiprazole, the atypical antipsychotic drugs acting on the D2 dopamine receptor, have been approved to reduce irritability, agitation, aggression, and self-harm in ASD by the Food and Drug Administration (FDA) (McCracken et al., 2002; Owen et al., 2009). Although risperidone has been reported to reduce RRBs in salt-induced kinase 1 (SIK1)-mutant mice via attenuating neural excitability and excitatory synaptic transmission (Badawi et al., 2021), a meta-analysis published in 2020 showed that antipsychotics were not beneficial to RRBs in clinical trials (Yu et al., 2020). Subsequently, another meta-analysis including more RCTs pointed out a slight improvement in RRBs after administration of antipsychotics (Zhou et al., 2021). This finding has no practical value because clinicians must weigh these moderate benefits of antipsychotics against the considerable

side effects (Correll et al., 2006). Compared with other clinical pharmacological trials of ASD, the studies of antipsychotics have a smaller sample size and more significant heterogeneity in estimated treatment effect.

Oxytocin

A great number of studies reported the critical role of oxytocin in human social interaction (Insel et al., 1999; Yatawara et al., 2016). Intranasal administration of the neuropeptide oxytocin (IN-OT) has been regarded as a potential therapy for the core symptoms of ASD. However, its effect in RRB has received less attention. An early study revealed oxytocin infusion reduced RRBs in adults with autism and Asperger syndrome (Hollander et al., 2003). This invasive method is not ideal and replaced by IN-OT for researchers and clinicians (Guastella et al., 2013). After 4 weeks of daily oxytocin administration (24 IU/day), RRBs were significantly reduced in 40 adult men with high-functioning autism (Bernaerts et al., 2020). Interestingly, a preliminary trial showed that 6 weeks of IN-OT had a significant effect on social communication rather than RRBs in 18 men with ASD (Watanabe et al., 2015). However, the same research team found that oxytocin reduced ADOS-RRB score in a larger sample (n = 106), which applied the same study design (Yamasue et al., 2020). This difference may be caused by sampling error and less placebo effect on RRBs related to less expectation for effects. In the same year, another randomized controlled trial (RCT) study also verified the benefits of oxytocin to RRBs (Alaerts et al., 2020). Regarding the underlying neural mechanism of the IN-OT effect, Alaerts et al. (2020) suggested that IN-OT might cause long-term alterations in the internal functional connectivity of the amygdala to the OFC, which was related to RRBs improvement. In addition, Watanabe et al. (2015) reported that the improvement of the core social symptoms in ASD was accompanied by oxytocin-induced enhancement of task-independent resting-state functional connectivity between the anterior cingulate cortex (ACC) and dorsomedial prefrontal cortex. As an increasing number of trials have evaluated the clinical response of multiple doses of IN-OT in ASD, Peled-Avron et al. (2020) conducted a meta-analysis that showed that IN-OT was well tolerated and supported that oxytocin could improve RRBs in ASD, although the effect size was small. However, some studies with small sample sizes have not found the benefits of oxytocin to RRBs (Anagnostou et al., 2012; Dadds et al., 2014; Guastella et al., 2015; Kosaka et al., 2016), it is necessary to conduct multi-center RCT studies with a larger sample and focus on the improvement of RRBs.

Bumetanide

Bumetanide is an effective diuretic. As mentioned above, GABAergic signals play a vital role in regulating RRBs (Cellot and Cherubini, 2014). Convincing evidence has shown that defects in inhibitory GABAergic signals led to ASD, and the level of GABAergic inhibition depended on the concentration of intracellular chloride [(Cl-)i] (Schulte et al., 2018). NKCC1 (Na-K-Cl cotransporter 1) is the primary transporter responsible for regulating (Cl-)i, and its activity controls the level of chloride in neurons, which further affects the post-synaptic effect of GABAergic transmission (Schulte et al., 2018). Bumetanide, a selective NKCC1antagonist (Ben-Ari, 2017; Kharod et al., 2019), could restore GABAergic inhibition and weaken behavioral and electrophysiological characteristics in various diseases (e.g., ASD and Fragile X syndrome) by regulating the concentration of neuronal chloride (Payne et al., 2003; He et al., 2014; Kaila et al., 2014; Tyzio et al., 2014; Juarez-Martinez et al., 2021). However, there is a lack of reports on the effects of bumetanide on RRBs in animal models. Increasing studies exhibited a positive effect of bumetanide in children with ASD or Fragile X syndrome (Lemonnier et al., 2013; Du et al., 2015; Zhang et al., 2020; Dai et al., 2021). After a pilot study reported the benefits of bumetanide to RRBs (Lemonnier and Ben-Ari, 2010), Lemonnier et al. conducted two RCT studies to test bumetanide in 60 and 88 patients. Both trials showed a significant reduction in scores of RRBs (Lemonnier et al., 2012; Lemonnier et al., 2017). Similarly, another Phase-2 Superiority Trial also revealed significant effects on RRBs in children aged 7–15, despite no superior effects on the primary outcome of social communication and social interaction (Sprengers et al., 2021). Crutel et al. (2021) described a design of two Phase III studies to evaluate the efficacy/safety of bumetanide oral liquid in ASD, which will provide strong evidence to support the benefits of bumetanide to RRBs. In addition, bumetanide could improve emotional face perception and increase the time spent in spontaneous eye gaze in ASD, with alterations of the activation level in corresponding brain regions (Hadjikhani et al., 2015; Hadjikhani et al., 2018). Current studies were mainly conducted in children and adolescents under 18, and this potential effect in adults should be further verified.

Other Drugs

Based on the possible neurobiological mechanism of RRBs, some emerging treatment methods, such as pioglitazone (Capano et al., 2018), pioglitazone (Chugani et al., 2016), intranasal administration of vasopressin (Parker et al., 2019), and IGF-1 injection (Kolevzon et al., 2014), could significantly improve RRBs in individuals with ASD. Some anti-inflammatory drugs targeting abnormal immune functions in ASD showed the benefits to RRBs, such as memantine plus risperidone (Ghaleiha et al., 2013), org 2766 (a synthetic analog of the adrenocorticotrophic hormone) (Buitelaar et al., 1990; Buitelaar et al., 1992), and celecoxib plus risperidone (Asadabadi et al., 2013). In 2020, a meta-analysis of pharmacological interventions for RRBs in ASD included 64 different trials conducted before November 2019. Except for the drugs mentioned above, divalproex sodium, leucovorin, and guanfacine as monotherapies have a more significant positive effect on RRBs of ASD (Zhou et al., 2021). Most findings of the above drugs were based on studies with a small sample and required to clarify their effects further. No pharmacological drug has shown significant clinical benefits and a solid evidence base of effectiveness.

Preclinical Pharmacological Studies

More drug studies are in preclinical stage, and a variety of ASD animal models have become the essential tools for preclinical studies (Lewis et al., 2007), which provides the theoretical basis for following clinical trials. Increasing drug trials in animal

models are based on the hypotheses of potential mechanisms in ASD, especially abnormal neurotransmitter/neuromodulator systems. In *SHANK3* mutant mice, acute administration of tandospirone, a 5-HT_{1A} receptor agonist, reduced self-grooming behavior (Dunn et al., 2020). In addition, N-methyl-D-aspartate (NMDA) receptor plays an important role in the balance of E/I and postnatal low-dose MK-801, an NMDA receptor blocker, improved ASD-related behaviors in valproic acid (VPA)-treated rats (Kim et al., 2017; Mohammadi et al., 2020). Another potential function mechanism of the NMDA receptor antagonist was to ameliorate immune dysfunction. For example, dextromethorphan rescued the impaired behavioral patterns in VPA-induced autistic rats and decreased the levels of various oxidative stress and inflammatory markers (Singla et al., 2021).

Another area that receives much attention is the drugs targeting abnormal immune function. 5-aminoisoquinolinone (5-AIQ) has the effects of neuroprotection and down-regulated inflammatory responses (Alhosaini et al., 2021). In BTBR mice, the 5-AIQ treatment significantly prevented self-grooming and marble burying behaviors and ameliorated neuroimmune dysfunctions (Ahmad et al., 2020). Similarly, the benefits to RRBs were reported in the study of the administration of catechin hydrate and pioglitazone in VPA-induced rats (Mirza and Sharma, 2019a; Mehta et al., 2021) and sulforaphane in BTBR mice (Nadeem et al., 2019b). They corrected immune dysfunction and oxidant-antioxidant imbalance in periphery and brain in mice. Beyond that, Zhang et al. (2019) showed that folic acid reduced RRBs in BTBR mice via mitigation of oxidative stress, inflammation, and ferroptosis. Another nutritional supplement of gestational B-vitamin alleviated mitochondrial damage in the hippocampus and PM2.5-induced autism-like behaviors in mice offspring (Wang et al., 2019).

Since a large proportion of people with neurodevelopmental disorders such as ASD are disturbed in their daily sleep/wake cycles (Robinson-Shelton and Malow, 2016). In response to this phenomenon, researchers tried melatonin treatment in CNTNAP2 KO mice and found that it improved excessive grooming in mice (Wang et al., 2020). Furthermore, MTHFR polymorphism was associated with an increased risk of ASD, and the offspring of Mthfr +/− mice (Pu et al., 2013), whether wild-type or heterozygous, exhibited autism-like behaviors. It is surprising that after 14 days of choline supplementation, the characteristics of RRBs were offset (Agam et al., 2020). In addition, other supplementary treatments showed promising effects in ASD animals. For example, abnormally high levels of homocysteine (Hcy) were considered to have a relation with ASD (Kałużna-Czaplińska et al., 2013). Administration of betaine, a methyl group donor in Hcy metabolism, significantly ameliorates RRBs in VPA-induced autistic mice (Huang et al., 2019). Furthermore, exposure to VPA might alter zinc metabolism resulting in a transient deficiency of zinc. Cezar et al. (2018) showed that zinc supplements reduced the transient zinc deficiency and prevented VPA-induced RRBs in rats. Autistic children with similar genetic or metabolic alterations would benefit from similar supplementary treatment if these results are replicated. Other drug studies showed initial outcomes of RRBs in animal models (Bhandari and Kuhad, 2015; Luhach et al., 2021). For example, treatment with medical cannabis alleviated RRBs by over 70% in Shank3 mice (Poleg et al., 2021). Administration of beta-carotene (Avraham et al., 2019; Avraham et al., 2021) and curcumin (Zhong et al., 2020) reduced RRBs in BTBR mice. However, the limitations are that these drugs have multi-target effects and their specific mechanisms are unclear, hindering their use in clinical trials. Moreover, some drugs approved to treat other diseases revealed a new therapeutic effect on RRBs (Román et al., 2021; Ryu et al., 2021; Wu et al., 2021). Chinese herbal medicine also positively influenced RRBs in BTBR mice (Park et al., 2021).

Behavioral Intervention

Behavioral intervention is still the most effective and safest intervention for RRBs. The behavioral intervention for RRBs has been comprehensively reviewed elsewhere (Odom et al., 2010; Boyd et al., 2012; Harrop, 2015; Kodak and Bergmann, 2020). This section only reviews the latest reports about the comprehensive treatment model (CTM) (Odom et al., 2010).

At present, the most widely used CTMs include the Denver Model, Structured Teaching (TEACCH), and Early Intensive Behavior Intervention (EIBI). Behavioral parent training (BPT) is considered the first choice of treatment for young children with disruptive behaviors (Kaminski and Claussen, 2017), and parent-child interaction therapy (PCIT) is one of the most supported evidence-based BPTs. After implementing PCIT, 16 individuals showed a significant improvement in RRBs compared to the control group (Parladé et al., 2020). Besides, self-management intervention and pivotal response treatment (PRT) were implemented in three young children with ASD, and results showed improvements in children's higher-order RRBs and interactions with parents (Lin and Koegel, 2018). However, one limitation should also be considered: CTM is a multitarget intervention, and most studies assessed RRBs as one of the secondary results; therefore, limited high-quality research has reported on its efficacy on RRBs.

Supplementary Therapy

Abnormal eating habits in children with ASD play a potential role in exacerbating ASD symptoms (Peretti et al., 2019). In recent years, increasing studies focused on the potential value of nutritional supplements in ASD, but limited evidence supported their effectiveness on RRBs.

Vitamin D

Studies have reported decreased vitamin D levels in the blood of patients with ASD (Wang T. et al., 2016). Vitamin D3 seemed to have therapeutic potential in ASD (Jia et al., 2015). After 3-month vitamin D3 supplementation, RRBs improved in 37 children with ASD, particularly in younger children (Feng et al., 2017). Another study involving 83 children with ASD also found an improvement in RRBs after 3-month treatment (Saad et al., 2016). In contrast, Kerley et al. (2017) conducted an RCT study including 38 children with ASD, which found that vitamin D3 did not affect RRBs after 5-month supplementation.

Folic Acid and Omega-3 Fatty Acid

The abnormal metabolism of folic acid is related to ASD (Castro et al., 2016), and folic acid deficiency have been found in the brains of individuals with ASD (Karin et al., 2017). Supplementing high doses of folic acid in maternal mice can significantly reduce RRBs of offspring (Di et al., 2021). A recent RCT study evaluated the effect of high-dose leucovorin supplementation in ASD. Forty-eight children with ASD and language barriers were randomly given leucovorin or placebo, and RRBs were significantly improved in the leucovorin group (Frye et al., 2018).

Omega-3 fatty acid is associated with mood disorders. Some preliminary studies suggested that Omega-3 fatty acid could effectively treat various mental disorders, such as ASD (Yehuda et al., 2005). Yui conducted a 12-week, 240 mg/day DHA + 240 mg/day arachidonic acid (ARA) intervention on 13 individuals with ASD, and significant improvements in RRBs were observed (Yui et al., 2012). However, the latest meta-analysis, including six studies, suggested no significant effect of omega-3 fatty acids (Zhou et al., 2021).

Other Supplements

Gastrointestinal problems and unique gut flora in individuals with ASD are related to the development and severity of ASD symptoms (Hughes et al., 2018). Changing gut flora is considered a promising treatment for related behavioral disorders. Seventeen children with ASD (3–16 years old) were supplemented with *Lactobacillus Plantarum* WCSF1. After a 12-week intervention, the behavioral score was significantly improved (Parracho et al., 2010). Additionally, some dietary patterns have shown advantages of RRBs in animal models (Castro et al., 2017; Lee et al., 2018a). Gluten-free diets (Ghalichi et al., 2016), casein-free diets (Lucarelli et al., 1995), and ketogenic diets (El-Rashidy et al., 2017) have been verified to have positive effects on ASD symptoms. However, another study reported no significant differences in RRBs (Harris and Card, 2012; Navarro et al., 2015). So, there are still uncertainties about the effects of dietary approaches. Further investigations are needed to confirm these dietary interventions' specific efficacy and safety for RRBs with a larger sample.

Other Treatment

Except for the above three intervention methods, many other emerging non-drug treatments targeting RRBs have been reported. Cell therapy indications have been expanded from hematological malignancies to other diseases. Cell therapy has shown preliminary safety and effectiveness in children with ASD. Moreover, transcranial magnetic stimulation (TMS) is used in various mental diseases with specific effects. Researchers began to explore its effects on ASD symptoms in recent years.

Cell Therapy

The studies of epigenetics, neuroimmunology, and neurobiology in ASD indicated that cell therapy was an effective approach for treating the core symptoms of ASD (Vaccarino et al., 2011; Siniscalco et al., 2012b; Liu et al., 2019; Zhang et al., 2021). Two outstanding features of stem cells are the intense immunosuppressive activity that allows them to be used in autologous or heterologous transplantation (Siniscalco et al., 2012a) and paracrine actions (Baraniak and McDevitt, 2010; Siniscalco, 2012). Stem cells usually synthesize and release a variety of cytokines, chemokines, and growth factors (Beyth et al., 2005; Siniscalco et al., 2012b), which can reduce the proinflammatory state observed in children with ASD (Gupta et al., 2010) and activate endogenous repair mechanism to recover the damaged function of related cells and tissues (Siniscalco et al., 2012b).

Stem cell therapy has shown benefits to RRBs in various ASD models. Intraventricular administration of mesenchymal stem cells (MSCs) significantly improved core ASD-like symptoms in BTBR mice, including social interaction and RRBs (Segal-Gavish et al., 2016). In addition, intranasal administration of human exosomes derived from mesenchymal stem cells (MSC-exos) was effective on all core ASD behaviors in two different mice (BTBR and *SHANK3* KO) (Perets et al., 2018, 2020). Transplantation of mesenchymal stem cells has been proven safe in many clinical trials (Gupta et al., 2010), and whether mesenchymal stem cells apply to individuals with ASD and clinically improve the ASD-like symptoms deserves to be further explored. Regarding clinical trials on cell therapy, Lv et al. conducted a single-center phase I/II trial to assess the safety and efficacy of combined transplantation of human cord blood mononuclear cells (CBMNCs) and umbilical cord-derived mesenchymal stem cells (UCMSCs) in 37 children with ASD (3–12 years of age). Individual transplantation of CBMNCs was demonstrated to remarkably decrease repetitive behaviors compared to the control group. In addition, combined transplantation of CBMNCs and UCMSCs showed better therapeutic effects (Lv et al., 2013). Similarly, Nguyen Thanh et al. (2021) found that transplantation of mononuclear cells of bone marrow combined with educational intervention showed that RRBs and hyperactivity were significantly reduced in children with ASD. These stem cell trials were proved excellent safety, with no safety issues noted during injection and the whole follow-up period (Lv et al., 2013; Nguyen Thanh et al., 2021). Significantly, the benefits of cell therapy to RRBs are necessary to be clarified because most clinical studies in ASD focused on social deficits rather than RRBs or regarded the alterations of RRBs as a secondary result (Bradstreet et al., 2014; Chez et al., 2018; Villarreal-Martínez et al., 2021).

There is still a long way before cell therapy becomes an approved treatment for RRBs in ASD. More in-depth and detailed studies on stem cell biology are necessary to understand the mechanism in RRBs. In addition, the exact dose, time, and site of stem cell infusion, as well as the fatal side effects and long-term safety, need to be further determined. For example, some researchers are concerned about intravenous administration because animal models have shown that it was difficult for transplanted cells to pass through organs (e.g., spleen and kidney) via intravenous administration (Steiner et al., 2012). Moreover, there is a correlation between the dose of transplanted stem cells and the subsequent clinical improvement (Rocha et al., 2002), which emphasized the importance of choosing the exact dose. What should not be ignored is ethical issues in stem cell studies. Such as the acquisition of stem cells, the safety of stem cell

collection and administration, the tumorigenicity of stem cells, and other ethical risks similar to other clinical studies (Siniscalco, 2012). The life expectancy of children with ASD is close to normal, and potential risks of children's medication are difficult to define. Therefore, interventional stem cell therapy is morally untenable unless more studies prove that the apparent benefits outweigh the risks (Yeo-Teh and Tang, 2021).

Transcranial Magnetic Stimulation

Transcranial Magnetic Stimulation is a non-invasive brain stimulation used to treat depression and other mental illnesses via changing the excitability of neural circuits and reorganizing the functions of cortex. Previous pilot studies reported positive effects of repeated TMS (rTMS) in individuals with ASD (Sokhadze et al., 2009; Casanova et al., 2012; Wang Y. et al., 2016). Irritability, hyperactivity, and RRBs were decreased in 27 participants with ASD after 18-rounds rTMS on the dorsolateral prefrontal cortex, and the latest study also drew a similar conclusion (Sokhadze et al., 2014; Abujadi et al., 2018). In addition, adults with autism and major depressive disorder reported improvements in repetitive behaviors after 25-session rTMS (Gwynette et al., 2020). A consensus statement of rTMS for ASD showed that rTMS was a potential treatment for ASD and suggested that existing studies have significant limitations, and more definitive studies needed to be conducted to clarify the safety and efficacy of rTMS in ASD (Cole et al., 2019).

PERSPECTIVE AND FUTURE DIRECTIONS

Compared with studies targeting the social communication deficits in ASD, current evidence of RRBs is limited. As the core symptoms of ASD, the accurate assessment of RRBs is crucial. Individuals with ASD show remarkable differences in types and severity of RRBs, depending on different ages, genders, and functional statuses. Because of the high heterogeneity of RRBs, identifying additional subtypes of RRBs may be useful. In addition, researchers developed assessment tools based on male individuals with ASD and did not consider adequately specific RRBs of the female sample, so it is urgent to develop evaluation tools suitable for different clinical populations with excellent sensitivity and applicability. Salloum-Asfar et al. (2019) suggested that miRNA was a promising biomarker for ASD diagnosis and core symptom assessment. For example, the level of specific miRNA in saliva was positively correlated with the score of repetitive restricted behavior (Hicks et al., 2020). Whether miRNA can be used as a biomarker to assess the severity of RRBs needs further exploring.

Moreover, with the development of new technologies and methods, more specific mechanisms of RRBs will be discovered. RRBs are mostly considered as a secondary outcome in current studies. Thus, it is necessary to explore the relationship between neural circuitry and subtypes of RRBs via more specific assessment tools (e.g., RBS-R). Moreover, Van't Westeinde et al. (2020) found that RRB-related structural alterations of striatal networks are more common in men, while abnormity of frontoparietal networks was more observed in females, which implied some differences in neural networks between male and female were omitted in the studies without enough female sample. Future studies of RRBs will include a larger female sample to reveal possible gender differences in neural circuitry related to RRBs. The related studies of the relationship between hyperdirect pathway and RRBs are scarce. The increasingly recognized importance of the hyperdirect pathway suggest it may play an essential role in RRBs. In addition, the connectivity between the basal ganglia and cerebellum is related to behavior control, but how aberrant connectivity affects RRBs is unclear in ASD. Therefore, there is a strong need to investigate structural and functional connectivity related to RRBs. To date, multiple RRBs-exhibiting ASD animal models have been developed. Focusing on common pathophysiological changes (e.g., abnormal immune function) in different animal models may provide some crucial insights. Furthermore, future studies on the potential neurobiology of reinforcement and habituation will also contribute to a better understanding of RRBs. It is worth noting that some conclusions are based on rodent models, and translation of these findings to RRBs in humans with ASD is difficult. So, the studies in primates may provide more evidence.

Lastly, how to intervene in the core symptoms of ASD is still the most important and meaningful issue for individuals with ASD. So far, behavioral intervention is still an essential part of treatment for RRBs. There are still three significant obstacles in psychopharmacology studies: (a) thus far, most trials have not found significant differences in primary endpoint suggesting insufficient effectiveness; (b) there are vast heterogeneities of clinical effects and side effects in different people; (c) the overlapping symptoms (e.g., anxiety and hyperactivity) and uncertain mechanism of RRBs make it challenging to find a drug aimed at specific targets. Even so, some medications, such as oxytocin and budesonide, seemed to show benefits to RRBs. The RCT studies with a larger sample are necessary to verify their efficacy and safety. Due to the limited number of studies, the specific efficacy and safety of supplementary therapy on RRBs remain unclear. As a promising treatment, cell therapy faces many scientific and ethical issues. In-depth and detailed studies of stem cell biology are required to help understand the mechanism of stem cells. The exact dose, time and site of stem cell infusion, the fatal side effects, and long-term safety should be determined in clinical trials.

AUTHOR CONTRIBUTIONS

JT drafted the manuscript. XG revised the manuscript. LY edited the language and the final version of the manuscript. All authors contributed to the article and approved the submitted version.

FUNDING

This work was supported by grants from the Beijing Municipal Science and Technology Commission (Z181100001518005) and National Natural Science Foundation of China (Grant Number: 81873803).

REFERENCES

Abbott, A. E., Linke, A. C., Nair, A., Jahedi, A., Alba, L. A., Keown, C. L., et al. (2018). Repetitive behaviors in autism are linked to imbalance of corticostriatal connectivity: a functional connectivity MRI study. *Soc Cogn. Affect. Neurosci.* 13, 32–42. doi: 10.1093/scan/nsx129

Abujadi, C., Croarkin, P. E., Bellini, B., Brentani, H., and Marcolin, M. (2018). Intermittent theta-burst transcranial magnetic stimulation for autism spectrum disorder: An open-label pilot study. *Revista Brasileira de Psiquiatria* 40, 309–311. doi: 10.1590/1516-4446-2017-2279

Agam, G., Taylor, Z., Vainer, E., and Golan, H. M. (2020). The influence of choline treatment on behavioral and neurochemical autistic-like phenotype in Mthfr-deficient mice. *Transl. Psychiatry* 10:1. doi: 10.1038/s41398-020-01002-1

Ahmad, S. F., Ansari, M. A., Nadeem, A., Bakheet, S. A., Alqahtani, F., Alhoshani, A. R., et al. (2020). 5-aminoisoquinolinone attenuates social behavior deficits and immune abnormalities in the BTBR T+ Itpr3(t)(f)/J mouse model for autism. *Pharmacol. Biochem. Behav.* 189:9. doi: 10.1016/j.pbb.2020.172859

Ahmad, S. F., Nadeem, A., Ansari, M. A., Bakheet, S. A., Alasmari, F., Alasmari, A. F., et al. (2019). The potent immunomodulatory compound VGX-1027 regulates inflammatory mediators in CD4+ T cells, which are concomitant with the prevention of neuroimmune dysregulation in BTBR T+ Itpr3tf/J mice. *Life Sci.* 237, 930. doi: 10.1016/j.lfs.2019.116930

Akkermans, S. E. A., Rheinheimer, N., Bruchhage, M. M. K., Durston, S., Brandeis, D., Banaschewski, T., et al. (2019). Frontostriatal functional connectivity correlates with repetitive behaviour across autism spectrum disorder and obsessive-compulsive disorder. *Psychol. Med.* 49, 2247–2255. doi: 10.1017/S0033291718003136

Al Sagheer, T., Haida, O., Balbous, A., Francheteau, M., Matas, E., Fernagut, P. O., et al. (2018). Motor Impairments correlate with social deficits and restricted neuronal loss in an environmental model of autism. *Int. J. Neuropsychopharmacol.* 21, 871–882. doi: 10.1093/ijnp/pyy043

Alaerts, K., Bernaerts, S., Prinsen, J., Dillen, C., Steyaert, J., and Wenderoth, N. (2020). Oxytocin induces long-lasting adaptations within amygdala circuitry in autism: a treatment-mechanism study with randomized placebo-controlled design. *Neuropsychopharmacology* 45, 1141–1149. doi: 10.1038/s41386-020-0653-8

Alexander-Bloch, A., Giedd, J. N., and Bullmore, E. (2013). Imaging structural co-variance between human brain regions. *Nature Rev. Neurosci.* 14, 322–336. doi: 10.1038/nrn3465

Alhosaini, K., Ansari, M. A., Nadeem, A., Bakheet, S. A., Attia, S. M., Alhazzani, K., et al. (2021). 5-Aminoisoquinolinone, a PARP-1 Inhibitor, Ameliorates Immune Abnormalities through Upregulation of Anti-Inflammatory and Downregulation of Inflammatory Parameters in T Cells of BTBR Mouse Model of Autism. *Brain Sci.* 11:16. doi: 10.3390/brainsci11020249

Aliane, V., Pérez, S., Deniau, J. M., and Kemel, M. L. (2012). Raclopride or high-frequency stimulation of the subthalamic nucleus stops cocaine-induced motor stereotypy and restores related alterations in prefrontal basal ganglia circuits. *Eur. J. Neurosci.* 36, 3235–3245. doi: 10.1111/j.1460-9568.2012.08245.x

Alvares, G. A., Balleine, B. W., Whittle, L., and Guastella, A. J. (2016). Reduced goal-directed action control in autism spectrum disorder. *Autism Res.* 9, 1285–1293. doi: 10.1002/aur.1613

Aman, M. G., Singh, N. N., Stewart, A. W., and Field, C. J. (1985). The aberrant behavior checklist: a behavior rating scale for the assessment of treatment effects. *Am. J. Ment. Defic.* 89, 485–491.

American Psychiatric Association (2013). *Diagnostic and Statistical Manual of Mental Disorders (DSM-5§)*. Virginia: American Psychiatric Publishing.

Amodeo, D. A., Cuevas, L., Dunn, J. T., Sweeney, J. A., and Ragozzino, M. E. (2018). The adenosine A2A receptor agonist, CGS 21680, attenuates a probabilistic reversal learning deficit and elevated grooming behavior in BTBR mice. *Autism Res.* 11, 223–233. doi: 10.1002/aur.1901

Amodeo, D. A., Oliver, B., Pahua, A., Hitchcock, K., Bykowski, A., Tice, D., et al. (2021). Serotonin 6 receptor blockade reduces repetitive behavior in the BTBR mouse model of autism spectrum disorder. *Pharmacol. Biochem. Behav.* 200:173076. doi: 10.1016/j.pbb.2020.173076

Amodeo, D. A., Rivera, E., Cook, E. H. Jr., Sweeney, J. A., and Ragozzino, M. E. (2017). 5HT(2A) receptor blockade in dorsomedial striatum reduces repetitive behaviors in BTBR mice. *Genes Brain Behav.* 16, 342–351. doi: 10.1111/gbb.12343

Anagnostou, E., Soorya, L., Chaplin, W., Bartz, J., Halpern, D., Wasserman, S., et al. (2012). Intranasal oxytocin versus placebo in the treatment of adults with autism spectrum disorders: a randomized controlled trial. *Mol. Autism* 3:16. doi: 10.1186/2040-2392-3-16

Ansari, M. A., Attia, S. M., Nadeem, A., Bakheet, S. A., Raish, M., Khan, T. H., et al. (2017). Activation of adenosine A2A receptor signaling regulates the expression of cytokines associated with immunologic dysfunction in BTBR T(+) Itpr3(tf)/J mice. *Mol. Cell Neurosci.* 82, 76–87. doi: 10.1016/j.mcn.2017.04.012

Antezana, L., Factor, R. S., Condy, E. E., Strege, M. V., Scarpa, A., and Richey, J. A. (2019). Gender differences in restricted and repetitive behaviors and interests in youth with autism. *Autism Res.* 12, 274–283. doi: 10.1002/aur.2049

Arnott, B., McConachie, H., Meins, E., Fernyhough, C., Couteur, A. L., Turner, M., et al. (2010). The frequency of restricted and repetitive behaviors in a community sample of 15-month-old infants. *J. Dev. Behav. Pediatr.* 31, 223–229. doi: 10.1097/DBP.0b013e3181d5a2ad

Asadabadi, M., Mohammadi, M.-R., Ghanizadeh, A., Modabbernia, A., Ashrafi, M., Hassanzadeh, E., et al. (2013). Celecoxib as adjunctive treatment to risperidone in children with autistic disorder: a randomized, double-blind, placebo-controlled trial. *Psychopharmacology* 225, 51–59. doi: 10.1007/s00213-012-2796-8

Ashwood, P., Krakowiak, P., Hertz-Picciotto, I., Hansen, R., Pessah, I., and de Water, J. V. (2011a). Elevated plasma cytokines in autism spectrum disorders provide evidence of immune dysfunction and are associated with impaired behavioral outcome. *Brain Behav. Immun.* 25, 40–45. doi: 10.1016/j.bbi.2010.08.003

Ashwood, P., Krakowiak, P., Hertz-Picciotto, I., Hansen, R., Pessah, I. N., and Van de Water, J. (2011b). Altered T cell responses in children with autism. *Brain Behav. Immun.* 25, 840–849. doi: 10.1016/j.bbi.2010.09.002

Augustine, F., Nebel, M. B., Mostofsky, S. H., Mahone, E. M., and Singer, H. S. (2021). Aberrant prefrontal cortical-striatal functional connectivity in children with primary complex motor stereotypies. *Cortex* 142, 272–282. doi: 10.1016/j.cortex.2021.05.022

Augustine, F., Rajendran, S., and Singer, H. S. (2020). Cortical endogenous opioids and their role in facilitating repetitive behaviors in deer mice. *Behav. Brain Res.* 379, 112317. doi: 10.1016/j.bbr.2019.112317

Averbeck, B. B., Lehman, J., Jacobson, M., and Haber, S. N. (2014). Estimates of projection overlap and zones of convergence within frontal-striatal circuits. *J. Neurosci.* 34, 9497–9505. doi: 10.1523/jneurosci.5806-12.2014

Avraham, Y., Berry, E. M., Donskoy, M., Abu Ahmad, W., Vorobiev, L., Albeck, A., et al. (2019). Beta-carotene as a novel therapy for the treatment of "Autistic like behavior" in animal models of Autism. *Behav. Brain Res.* 364, 469–479. doi: 10.1016/j.bbr.2017.09.041

Avraham, Y., Mankuta, D., Lipsker, L., Vorobiev, L., Patael, S., Hassid, G., et al. (2021). Beta-Carotene derivatives as novel therapy for the prevention and treatment of autistic symptoms. *Bioorg. Chem.* 115:105224. doi: 10.1016/j.bioorg.2021.105224

Badawi, M., Mori, T., Kurihara, T., Yoshizawa, T., Nohara, K., Kouyama-Suzuki, E., et al. (2021). Risperidone mitigates enhanced excitatory neuronal function and repetitive behavior caused by an ASD-Associated Mutation of SIK1. *Front. Mol. Neurosci.* 14:706494. doi: 10.3389/fnmol.2021.706494

Bagnall-Moreau, C., Huerta, P. T., Comoletti, D., La-Bella, A., Berlin, R., Zhao, C., et al. (2020). In utero exposure to endogenous maternal polyclonal anti-Caspr2 antibody leads to behavioral abnormalities resembling autism spectrum disorder in male mice. *Sci. Rep.* 10:14446. doi: 10.1038/s41598-020-71201-9

Bahuguna, J., Aertsen, A., and Kumar, A. (2015). Existence and control of Go/No-Go decision transition threshold in the striatum. *PLoS Comput. Biol.* 11:e1004233. doi: 10.1371/journal.pcbi.1004233

Baraniak, P. R., and McDevitt, T. C. (2010). Stem cell paracrine actions and tissue regeneration. *Regen. Med.* 5, 121–143. doi: 10.2217/rme.09.74

Bareš, M., Apps, R., Kikinis, Z., Timmann, D., Oz, G., Ashe, J. J., et al. (2015). Proceedings of the workshop on cerebellum, basal ganglia and cortical connections unmasked in health and disorder held in brno, czech republic. *Cerebellum* 14, 142–150. doi: 10.1007/s12311-014-0595-y

Barrett, S. L., Uljarević, M., Baker, E. K., Richdale, A. L., Jones, C. R. G., and Leekam, S. R. (2015). The adult repetitive behaviours questionnaire-2 (RBQ-2A): a self-report measure of restricted and repetitive behaviours. *J. Autism Dev. Disord.* 45, 3680–3692. doi: 10.1007/s10803-015-2514-6

Bauman, M. D., Iosif, A. M., Ashwood, P., Braunschweig, D., Lee, A., Schumann, C. M., et al. (2013). Maternal antibodies from mothers of children with autism alter brain growth and social behavior development in the rhesus monkey. *Transl. Psychiatry* 3:e278. doi: 10.1038/tp.2013.47

Bauman, M. D., Iosif, A. M., Smith, S. E., Bregere, C., Amaral, D. G., and Patterson, P. H. (2014). Activation of the maternal immune system during pregnancy alters behavioral development of rhesus monkey offspring. *Biol. Psychiatry* 75, 332–341. doi: 10.1016/j.biopsych.2013.06.025

Baup, N., Grabli, D., Karachi, C., Mounayar, S., François, C., Yelnik, J., et al. (2008). High-frequency stimulation of the anterior subthalamic nucleus reduces stereotyped behaviors in primates. *J. Neurosci.* 28, 8785–8788. doi: 10.1523/JNEUROSCI.2384-08.2008

Bearss, K., Johnson, C., Handen, B., Smith, T., and Scahill, L. (2013). A pilot study of parent training in young children with autism spectrum disorders and disruptive behavior. *J. Autism Dev. Disord.* 43, 829–840. doi: 10.1007/s10803-012-1624-7

Bechard, A. R., Cacodcar, N., King, M. A., and Lewis, M. H. (2016). How does environmental enrichment reduce repetitive motor behaviors? Neuronal activation and dendritic morphology in the indirect basal ganglia pathway of a mouse model. *Behav. Brain Res.* 299, 122–131. doi: 10.1016/j.bbr.2015.11.029

Ben-Ari, Y. (2017). NKCC1 chloride importer antagonists attenuate many neurological and psychiatric disorders. *Trends Neurosci.* 40, 536–554. doi: 10.1016/j.tins.2017.07.001

Bentea, E., Villers, A., Moore, C., Funk, A. J., O'Donovan, S. M., Verbruggen, L., et al. (2020). Corticostriatal dysfunction and social interaction deficits in mice lacking the cystine/glutamate antiporter. *Mol. Psychiatry* 2020:7513. doi: 10.1038/s41380-020-0751-3

Bernaerts, S., Boets, B., Bosmans, G., Steyaert, J., and Alaerts, K. (2020). Behavioral effects of multiple-dose oxytocin treatment in autism: a randomized, placebo-controlled trial with long-term follow-up. *Mol. Autism* 11:6. doi: 10.1186/s13229-020-0313-1

Beyth, S., Borovsky, Z., Mevorach, D., Liebergall, M., Gazit, Z., Aslan, H., et al. (2005). Human mesenchymal stem cells alter antigen-presenting cell maturation and induce T-cell unresponsiveness. *Blood* 105, 2214–2219. doi: 10.1182/blood-2004-07-2921

Bhandari, R., and Kuhad, A. (2015). Neuropsychopharmacotherapeutic efficacy of curcumin in experimental paradigm of autism spectrum disorders. *Life Sci.* 141, 156–169. doi: 10.1016/j.lfs.2015.09.012

Bishop, S. L., Hus, V., Duncan, A., Huerta, M., Gotham, K., Pickles, A., et al. (2013). Subcategories of restricted and repetitive behaviors in children with autism spectrum disorders. *J. Autism Dev. Disord.* 43, 1287–1297. doi: 10.1007/s10803-012-1671-0

Black, K. R., Stevenson, R. A., Segers, M., Ncube, B. L., Sun, S. Z., Philipp-Muller, A., et al. (2017). Linking anxiety and insistence on sameness in autistic children: the role of sensory hypersensitivity. *J. Autism Dev. Disord.* 47, 2459–2470. doi: 10.1007/s10803-017-3161-x

Bodfish, J. W., Symons, F. J., Parker, D. E., and Lewis, M. H. (2000). Varieties of repetitive behavior in autism: comparisons to mental retardation. *J. Autism Dev. Disord.* 30, 237–243. doi: 10.1023/a:1005596502855

Bostan, A. C., Dum, R. P., and Strick, P. L. (2010). The basal ganglia communicate with the cerebellum. *Proc. Natl. Acad. Sci. USA* 107, 8452–8456. doi: 10.1073/pnas.1000496107

Bouchekioua, Y., Tsutsui-Kimura, I., Sano, H., Koizumi, M., Tanaka, K. F., Yoshida, K., et al. (2018). Striatonigral direct pathway activation is sufficient to induce repetitive behaviors. *Neurosci. Res.* 132, 53–57. doi: 10.1016/j.neures.2017.09.007

Boyd, B. A., McDonough, S. G., and Bodfish, J. W. (2012). Evidence-based behavioral interventions for repetitive behaviors in autism. *J. Autism Dev. Disord.* 42, 1236–1248. doi: 10.1007/s10803-011-1284-z

Bradstreet, J. J., Sych, N., Antonucci, N., Klunnik, M., Ivankova, O., Matyashchuk, I., et al. (2014). Efficacy of fetal stem cell transplantation in autism spectrum disorders: an open-labeled pilot study. *Cell Trans.* 23, S105–S112. doi: 10.3727/096368914x684916

Brandenburg, C., Soghomonian, J. J., Zhang, K., Sulkaj, I., Randolph, B., Kachadoorian, M., et al. (2020). Increased Dopamine Type 2 Gene expression in the dorsal striatum in individuals with autism spectrum disorder suggests alterations in indirect pathway signaling and circuitry. *Front. Cell. Neurosci.* 14:858. doi: 10.3389/fncel.2020.577858

Breiter, H. C., Etcoff, N. L., Whalen, P. J., Kennedy, W. A., Rauch, S. L., Buckner, R. L., et al. (1996). Response and habituation of the human amygdala during visual processing of facial expression. *Neuron* 17, 875–887. doi: 10.1016/s0896-6273(00)80219-6

Brunenberg, E. J., Moeskops, P., Backes, W. H., Pollo, C., Cammoun, L., Vilanova, A., et al. (2012). Structural and resting state functional connectivity of the subthalamic nucleus: identification of motor STN parts and the hyperdirect pathway. *PLoS One* 7:e39061. doi: 10.1371/journal.pone.0039061

Bryn, V., Aass, H. C., Skjeldal, O. H., Isaksen, J., Saugstad, O. D., and Ormstad, H. (2017). Cytokine profile in autism spectrum disorders in children. *J. Mol. Neurosci.* 61, 1–7. doi: 10.1007/s12031-016-0847-z

Buitelaar, J. K., van Engeland, H., de Kogel, K. H., de Vries, H., van Hooff, J. A. R. A. M., and van Ree, J. M. (1992). The use of adrenocorticotrophic hormone (4–9) analog ORG 2766 in autistic children: Effects on the organization of behavior. *Biol. Psychiatry* 31, 1119–1129. doi: 10.1016/0006-3223(92)90156-T

Buitelaar, J. K., van Engeland, H., van Ree, J. M., and de Wied, D. (1990). Behavioral effects of Org 2766, a synthetic analog of the adrenocorticotrophic hormone (4–9), in 14 outpatient autistic children. *J. Autism Dev. Disord.* 20, 467–478. doi: 10.1007/BF02216053

Burguière, E., Monteiro, P., Mallet, L., Feng, G., and Graybiel, A. M. (2015). Striatal circuits, habits, and implications for obsessive-compulsive disorder. *Curr. Opin. Neurobiol.* 30, 59–65. doi: 10.1016/j.conb.2014.08.008

Burket, J. A., Benson, A. D., Tang, A. H., and Deutsch, S. I. (2014). Rapamycin improves sociability in the BTBR T+Itpr3tf/J mouse model of autism spectrum disorders. *Brain Res. Bull.* 100, 70–75. doi: 10.1016/j.brainresbull.2013.11.005

Cai, W., Duberg, K., Padmanabhan, A., Rehert, R., Bradley, T., Carrion, V., et al. (2019). Hyperdirect insula-basal-ganglia pathway and adult-like maturity of global brain responses predict inhibitory control in children. *Nat. Commun.* 10:4798. doi: 10.1038/s41467-019-12756-8

Cai, Y., Wang, L., Xiao, R., Li, X., He, X., Gao, J., et al. (2017). Autism-like behavior in the BTBR mouse model of autism is improved by propofol. *Neuropharmacology* 118, 175–187. doi: 10.1016/j.neuropharm.2017.03.021

Calabresi, P., Picconi, B., Tozzi, A., Ghiglieri, V., and Di Filippo, M. (2014). Direct and indirect pathways of basal ganglia: a critical reappraisal. *Nature Neurosci.* 17, 1022–1030. doi: 10.1038/nn.3743

Camacho, J., Jones, K., Miller, E., Ariza, J., Noctor, S., de Water, J. V., et al. (2014). Embryonic intraventricular exposure to autism-specific maternal autoantibodies produces alterations in autistic-like stereotypical behaviors in offspring mice. *Behav. Brain Res.* 266, 46–51. doi: 10.1016/j.bbr.2014.02.045

Capano, L., Dupuis, A., Brian, J., Mankad, D., Genore, L., Hastie Adams, R., et al. (2018). A pilot dose finding study of pioglitazone in autistic children. *Mol. Autism* 9:5. doi: 10.1186/s13229-018-0241-5

Careaga, M., Rogers, S., Hansen, R. L., Amaral, D. G., Van de Water, J., and Ashwood, P. (2017). Immune endophenotypes in children with autism spectrum disorder. *Biol. Psychiatry* 81, 434–441. doi: 10.1016/j.biopsych.2015.08.036

Casanova, M. F., Baruth, J. M., El-Baz, A., Tasman, A., Sears, L., and Sokhadze, E. (2012). Repetitive transcranial magnetic stimulation (rTMS) modulates event-related potential (ERP) indices of attention in autism. *Transl. Neurosci.* 3, 170–180. doi: 10.2478/s13380-012-0022-0

Cascio, C. J., Foss-Feig, J. H., Heacock, J., Schauder, K. B., Loring, W. A., Rogers, B. P., et al. (2014). Affective neural response to restricted interests in autism spectrum disorders. *J Child Psychol. Psychiatry* 55, 162–171. doi: 10.1111/jcpp.12147

Castro, K., Baronio, D., Perry, I. S., Riesgo, R. D. S., and Gottfried, C. (2017). The effect of ketogenic diet in an animal model of autism induced by prenatal exposure to valproic acid. *Nutr. Neurosci.* 20, 343–350. doi: 10.1080/1028415x.2015.1133029

Castro, K., Klein, L. D. S., Baronio, D., Gottfried, C., Riesgo, R., and Perry, I. S. (2016). Folic acid and autism: What do we know? *Nutrit. Neurosci.* 19, 310–317. doi: 10.1179/1476830514Y.0000000142

Cellot, G., and Cherubini, E. (2014). GABAergic signaling as therapeutic target for autism spectrum disorders. *Front. Pediatrics* 2:70. doi: 10.3389/fped.2014.00070

Cezar, L. C., Kirsten, T. B., da Fonseca, C. C. N., de Lima, A. P. N., Bernardi, M. M., and Felicio, L. F. (2018). Zinc as a therapy in a rat model of autism prenatally induced by valproic acid. *Prog. Neuro-Psychopharmacol. Biol. Psychiatry* 84, 173–180. doi: 10.1016/j.pnpbp.2018.02.008

Chang, A. D., Berges, V. A., Chung, S. J., Fridman, G. Y., Baraban, J. M., and Reti, I. M. (2016). High-Frequency stimulation at the subthalamic nucleus suppresses excessive self-grooming in autism-like mouse models. *Neuropsychopharmacology* 41, 1813–1821. doi: 10.1038/npp.2015.350

Charman, T., Taylor, E., Drew, A., Cockerill, H., Brown, J. A., and Baird, G. (2005). Outcome at 7 years of children diagnosed with autism at age 2: predictive validity of assessments conducted at 2 and 3 years of age and pattern of symptom change over time. *J. Child Psychol. Psychiatry* 46, 500–513. doi: 10.1111/j.1469-7610.2004.00377.x

Chen, C. H., Fremont, R., Arteaga-Bracho, E. E., and Khodakhah, K. (2014). Short latency cerebellar modulation of the basal ganglia. *Nat. Neurosci.* 17, 1767–1775. doi: 10.1038/nn.3868

Cheung, C., Chua, S. E., Cheung, V., Khong, P. L., Tai, K. S., Wong, T. K., et al. (2009). White matter fractional anisotrophy differences and correlates of diagnostic symptoms in autism. *J. Child Psychol. Psychiatry* 50, 1102–1112. doi: 10.1111/j.1469-7610.2009.02086.x

Chevallier, C., Kohls, G., Troiani, V., Brodkin, E. S., and Schultz, R. T. (2012). The social motivation theory of autism. *Trends Cogn. Sci.* 16, 231–239. doi: 10.1016/j.tics.2012.02.007

Chez, M., Lepage, C., Parise, C., Dang-Chu, A., Hankins, A., and Carroll, M. (2018). Safety and observations from a placebo-controlled, crossover study to assess use of autologous umbilical cord blood stem cells to improve symptoms in children with autism. *Stem Cells Transl. Med.* 7, 333–341. doi: 10.1002/sctm.17-0042

Chugani, D. C., Chugani, H. T., Wiznitzer, M., Parikh, S., Evans, P. A., Hansen, R. L., et al. (2016). Efficacy of low-dose buspirone for restricted and repetitive behavior in young children with autism spectrum disorder: a randomized trial. *J. Pediatrics* 170, 45–53. doi: 10.1016/j.jpeds.2015.11.033

Clements, C. C., Zoltowski, A. R., Yankowitz, L. D., Yerys, B. E., Schultz, R. T., and Herrington, J. D. (2018). Evaluation of the social motivation hypothesis of autism: a systematic review and meta-analysis. *JAMA Psychiatry* 75, 797–808. doi: 10.1001/jamapsychiatry.2018.1100

Cole, E. J., Enticott, P. G., Oberman, L. M., Gwynette, M. F., Casanova, M. F., Jackson, S. L. J., et al. (2019). The Potential of repetitive transcranial magnetic stimulation for autism spectrum disorder: a consensus statement. *Biol. Psychiatry* 85, e21–e22. doi: 10.1016/j.biopsych.2018.06.003

Conti, E., Mitra, J., Calderoni, S., Pannek, K., Shen, K. K., Pagnozzi, A., et al. (2017). Network over-connectivity differentiates autism spectrum disorder from other developmental disorders in toddlers: A diffusion MRI study. *Hum. Brain Mapp.* 38, 2333–2344. doi: 10.1002/hbm.23520

Correll, C. U., Penzner, J. B., Parikh, U. H., Mughal, T., Javed, T., Carbon, M., et al. (2006). Recognizing and monitoring adverse events of second-generation antipsychotics in children and adolescents. *Child Adolesc. Psychiatr. Clin. N Am.* 15, 177–206. doi: 10.1016/j.chc.2005.08.007

Costa, L., Sardone, L. M., Bonaccorso, C. M., D'Antoni, S., Spatuzza, M., Gulisano, W., et al. (2018). Activation of Serotonin 5-HT(7) receptors modulates hippocampal synaptic plasticity by stimulation of adenylate cyclases and rescues learning and behavior in a mouse model of fragile X Syndrome. *Front. Mol. Neurosci.* 11:353. doi: 10.3389/fnmol.2018.00353

Courchesne, E., Karns, C. M., Davis, H. R., Ziccardi, R., Carper, R. A., Tigue, Z. D., et al. (2001). Unusual brain growth patterns in early life in patients with autistic disorder: an MRI study. *Neurology* 57, 245–254. doi: 10.1212/wnl.57.2.245

Crutel, V., Lambert, E., Penelaud, P.-F., Albarrán Severo, C., Fuentes, J., Rosier, A., et al. (2021). Bumetanide oral liquid formulation for the treatment of children and adolescents with autism spectrum disorder: design of two phase III Studies (SIGN Trials). *J. Autism Dev. Disord.* 51, 2959–2972. doi: 10.1007/s10803-020-04709-8

Cuccaro, M. L., Shao, Y., Grubber, J., Slifer, M., Wolpert, C. M., Donnelly, S. L., et al. (2003). Factor analysis of restricted and repetitive behaviors in autism using the autism diagnostic interview-R. *Child Psychiatry Human Dev.* 34, 3–17. doi: 10.1023/A:1025321707947

Dadds, M. R., MacDonald, E., Cauchi, A., Williams, K., Levy, F., and Brennan, J. (2014). Nasal oxytocin for social deficits in childhood autism: A randomized controlled trial. *J. Autism Dev. Disord.* 44, 521–531. doi: 10.1007/s10803-013-1899-3

Dai, Y., Zhang, L., Yu, J., Zhou, X., He, H., Ji, Y., et al. (2021). Improved symptoms following bumetanide treatment in children aged 3-6 years with autism spectrum disorder: a randomized, double-blind, placebo-controlled trial. *Sci. Bull.* 66, 1591–1598. doi: 10.1016/j.scib.2021.01.008

Dasgupta, S., Wörgötter, F., and Manoonpong, P. (2014). Neuromodulatory adaptive combination of correlation-based learning in cerebellum and reward-based learning in basal ganglia for goal-directed behavior control. *Front. Neural Circuit.* 8:126. doi: 10.3389/fncir.2014.00126

Dawson, G., Meltzoff, A. N., Osterling, J., Rinaldi, J., and Brown, E. (1998). Children with autism fail to orient to naturally occurring social stimuli. *J. Autism Dev. Disord.* 28, 479–485. doi: 10.1023/a:1026043926488

Di, Y., Li, Z., Li, J., Cheng, Q., Zheng, Q., Zhai, C., et al. (2021). Maternal folic acid supplementation prevents autistic behaviors in a rat model induced by prenatal exposure to valproic acid. *Food Funct.* 12, 4544–4555. doi: 10.1039/d0fo02926b

Dichter, G. S., Damiano, C. A., and Allen, J. A. (2012). Reward circuitry dysfunction in psychiatric and neurodevelopmental disorders and genetic syndromes: animal models and clinical findings. *J. Neurodev. Disord.* 4:19. doi: 10.1186/1866-1955-4-19

D'Mello, A. M., Crocetti, D., Mostofsky, S. H., and Stoodley, C. J. (2015). Cerebellar gray matter and lobular volumes correlate with core autism symptoms. *Neuroimage Clin.* 7, 631–639. doi: 10.1016/j.nicl.2015.02.007

Du, L., Shan, L., Wang, B., Li, H., Xu, Z., Staal, W. G., et al. (2015). A Pilot Study on the combination of applied behavior analysis and bumetanide treatment for children with autism. *J. Child Adoles. Psychopharmacol.* 25, 585–588. doi: 10.1089/cap.2015.0045

Duan, X., Wang, R., Xiao, J., Li, Y., Huang, X., Guo, X., et al. (2020). Subcortical structural covariance in young children with autism spectrum disorder. *Prog. Neuro-Psychopharmacol. Biol. Psychiatry* 99:109874. doi: 10.1016/j.pnpbp.2020.109874

Dunn, J. T., Mroczek, J., Patel, H. R., and Ragozzino, M. E. (2020). Tandospirone, a partial 5-HT1A receptor agonist, administered systemically or into anterior cingulate attenuates repetitive behaviors in Shank3B mice. *Int. J. Neuropsychopharmacol.* 23, 533–542. doi: 10.1093/ijnp/pyaa047

Eagle, D. M., Baunez, C., Hutcheson, D. M., Lehmann, O., Shah, A. P., and Robbins, T. W. (2008). Stop-signal reaction-time task performance: role of prefrontal cortex and subthalamic nucleus. *Cereb. Cortex* 18, 178–188. doi: 10.1093/cercor/bhm044

Eissa, N., Azimullah, S., Jayaprakash, P., Jayaraj, R. L., Reiner, D., Ojha, S. K., et al. (2019). The dual-active histamine H3 receptor antagonist and acetylcholine esterase inhibitor E100 ameliorates stereotyped repetitive behavior and neuroinflammmation in sodium valproate induced autism in mice. *Chemico-Biol. Interact.* 312:8775. doi: 10.1016/j.cbi.2019.108775

Eissa, N., Jayaprakash, P., Azimullah, S., Ojha, S. K., Al-Houqani, M., Jalal, F. Y., et al. (2018). The histamine H3R antagonist DL77 attenuates autistic behaviors in a prenatal valproic acid-induced mouse model of autism. *Sci. Rep.* 8:13077. doi: 10.1038/s41598-018-31385-7

Eissa, N., Jayaprakash, P., Stark, H., Lazewska, D., Kiec-Kononowicz, K., and Sadek, B. (2020a). Simultaneous blockade of histamine h-3 receptors and inhibition of acetylcholine esterase alleviate autistic-like behaviors in BTBR T+ tf/J Mouse Model of Autism. *Biomolecules* 10:20. doi: 10.3390/biom10091251

Eissa, N., Sadeq, A., Sasse, A., and Sadek, B. (2020b). Role of neuroinflammation in autism spectrum disorder and the emergence of brain histaminergic system. Lessons Also for BPSD? *Front. Pharmacol.* 11:886. doi: 10.3389/fphar.2020.00886

Eissa, N., Venkatachalam, K., Jayaprakash, P., Falkenstein, M., Dubiel, M., Frank, A., et al. (2021). The multi-targeting ligand St-2223 with histamine H3 receptor and dopamine D2/D3 receptor antagonist properties mitigates autism-like repetitive behaviors and brain oxidative stress in mice. *Int. J. Mol. Sci.* 22, 1–21. doi: 10.3390/ijms22041947

El-Rashidy, O., El-Baz, F., El-Gendy, Y., Khalaf, R., Reda, D., and Saad, K. (2017). Ketogenic diet versus gluten free casein free diet in autistic children: a case-control study. *Metab. Brain Dis.* 32, 1935–1941. doi: 10.1007/s11011-017-0088-z

Engeln, M., Song, Y., Chandra, R., La, A., Fox, M. E., Evans, B., et al. (2021). Individual differences in stereotypy and neuron subtype translatome with TrkB deletion. *Mol. Psychiatry* 26, 1846–1859. doi: 10.1038/s41380-020-0746-0

Esbensen, A. J., Seltzer, M. M., Lam, K. S. L., and Bodfish, J. W. (2009). Age-related differences in restricted repetitive behaviors in autism spectrum disorders. *J. Autism Dev. Disord.* 39, 57–66. doi: 10.1007/s10803-008-0599-x

Espinosa, F., Xuan, Z., Liu, S., and Powell, C. M. (2015). Neuroligin 1 modulates striatal glutamatergic neurotransmission in a pathway and NMDAR subunit-specific manner. *Front. Synaptic. Neurosci.* 7:11. doi: 10.3389/fnsyn.2015.00011

Evans, D. W. (2017). Development of two dimensional measures of restricted and repetitive behavior in parents and children. *J. Am. Acad. Child Adoles. Psychiatry* 56:1. doi: 10.1016/j.jaac.2016.10.014

Evans, D. W., Leckman, J. F., Carter, A., Reznick, J. S., Henshaw, D., King, R. A., et al. (1997). Ritual, habit, and perfectionism: the prevalence and development of compulsive-like behavior in normal young children. *Child Dev.* 68, 58–68. doi: 10.1111/j.1467-8624.1997.tb01925.x

Faja, S., and Nelson Darling, L. (2019). Variation in restricted and repetitive behaviors and interests relates to inhibitory control and shifting in children with autism spectrum disorder. *Autism* 23, 1262–1272. doi: 10.1177/1362361318804192

Feng, J., Shan, L., Du, L., Wang, B., Li, H., Wang, W., et al. (2017). Clinical improvement following vitamin D3 supplementation in Autism Spectrum Disorder. *Nutrit. Neurosci.* 20, 284–290. doi: 10.1080/1028415X.2015.1123847

Flores, C. G., Valcante, G., Guter, S., Zaytoun, A., Wray, E., Bell, L., et al. (2011). Repetitive behavior profiles: Consistency across autism spectrum disorder cohorts and divergence from Prader-Willi syndrome. *J. Neurodev. Disord.* 3, 316–324. doi: 10.1007/s11689-011-9094-3

Frye, R. E., Slattery, J., Delhey, L., Furgerson, B., Strickland, T., Tippett, M., et al. (2018). Folinic acid improves verbal communication in children with autism and language impairment: a randomized double-blind placebo-controlled trial. *Mol. Psychiatry* 23, 247–256. doi: 10.1038/mp.2016.168

Fyke, W., Alarcon, J. M., Velinov, M., and Chadman, K. K. (2021). Pharmacological inhibition of the primary endocannabinoid producing enzyme, DGL-α, induces autism spectrum disorder-like and co-morbid phenotypes in adult C57BL/J mice. *Autism Res.* 14, 1375–1389. doi: 10.1002/aur.2520

Gandhi, T., and Lee, C. C. (2020). Neural mechanisms underlying repetitive behaviors in rodent models of autism spectrum disorders. *Front. Cell. Neurosci.* 14:710. doi: 10.3389/fncel.2020.592710

Georgiades, S., Papageorgiou, V., and Anagnostou, E. (2010). Brief report: Repetitive behaviours in greek individuals with autism spectrum disorder. *J. Autism Dev. Disord.* 40, 903–906. doi: 10.1007/s10803-009-0927-9

Geurts, H. M., and De Wit, S. (2014). Goal-directed action control in children with autism spectrum disorders. *Autism* 18, 409–418. doi: 10.1177/1362361313477919

Ghaleiha, A., Asadabadi, M., Mohammadi, M.-R., Shahei, M., Tabrizi, M., Hajiaghaee, R., et al. (2013). Memantine as adjunctive treatment to risperidone in children with autistic disorder: a randomized, double-blind, placebo-controlled trial. *Int. J. Neuropsychopharmacol.* 16, 783–789. doi: 10.1017/S1461145712000880

Ghalichi, F., Ghaemmaghami, J., Malek, A., and Ostadrahimi, A. (2016). Effect of gluten free diet on gastrointestinal and behavioral indices for children with autism spectrum disorders: a randomized clinical trial. *World J. Pediatr.* 12, 436–442. doi: 10.1007/s12519-016-0040-z

Gogolla, N., Leblanc, J. J., Quast, K. B., Südhof, T. C., Fagiolini, M., and Hensch, T. K. (2009). Common circuit defect of excitatory-inhibitory balance in mouse models of autism. *J. Neurodev. Disord.* 1, 172–181. doi: 10.1007/s11689-009-9023-x

Graybiel, A. M., and Grafton, S. T. (2015). The striatum: where skills and habits meet. *Cold Spring Harb. Persp. Biol.* 7:a021691. doi: 10.1101/cshperspect.a021691

Green, S. A., Hernandez, L., Tottenham, N., Krasileva, K., Bookheimer, S. Y., and Dapretto, M. (2015). Neurobiology of sensory overresponsivity in youth with autism spectrum disorders. *JAMA Psychiatry* 72, 778–786. doi: 10.1001/jamapsychiatry.2015.0737

Groenewegen, H. J., Van Den Heuvel, O. A., Cath, D. C., Voorn, P., and Veltman, D. J. (2003). Does an imbalance between the dorsal and ventral striatopallidal systems play a role in Tourette's syndrome? A neuronal circuit approach. *Brain Dev.* 25, S3–S14. doi: 10.1016/S0387-7604(03)90001-5

Groves, P. M., and Thompson, R. F. (1970). Habituation: A dual-process theory. *Psychol. Rev.* 77, 419–450. doi: 10.1037/h0029810

Guastella, A. J., Gray, K. M., Rinehart, N. J., Alvares, G. A., Tonge, B. J., Hickie, I. B., et al. (2015). The effects of a course of intranasal oxytocin on social behaviors in youth diagnosed with autism spectrum disorders: a randomized controlled trial. *J. Child Psychol. Psychiatry* 56, 444–452. doi: 10.1111/jcpp.12305

Guastella, A. J., Hickie, I. B., McGuinness, M. M., Otis, M., Woods, E. A., Disinger, H. M., et al. (2013). Recommendations for the standardisation of oxytocin nasal administration and guidelines for its reporting in human research. *Psychoneuroendocrinology* 38, 612–625. doi: 10.1016/j.psyneuen.2012.11.019

Guiraud, J. A., Kushnerenko, E., Tomalski, P., Davies, K., Ribeiro, H., and Johnson, M. H. (2011). Differential habituation to repeated sounds in infants at high risk for autism. *NeuroReport* 22, 845–849. doi: 10.1097/WNR.0b013e32834c0bec

Gupta, S., Samra, D., and Agrawal, S. (2010). Adaptive and innate immune responses in autism: rationale for therapeutic use of intravenous immunoglobulin. *J. Clin. Immunol.* 30, S90–S96. doi: 10.1007/s10875-010-9402-9

Gwynette, M. F., Lowe, D. W., Henneberry, E. A., Sahlem, G. L., Wiley, M. G., Alsarraf, H., et al. (2020). Treatment of adults with autism and major depressive disorder using transcranial magnetic stimulation: an open label pilot study. *Autism Res.* 13, 346–351. doi: 10.1002/aur.2266

Hadjikhani, N., Åsberg Johnels, J., Lassalle, A., Zürcher, N. R., Hippolyte, L., Gillberg, C., et al. (2018). Bumetanide for autism: more eye contact, less amygdala activation. *Sci. Rep.* 8:3602. doi: 10.1038/s41598-018-21958-x

Hadjikhani, N., Zürcher, N. R., Rogier, O., Ruest, T., Hippolyte, L., Ben-Ari, Y., et al. (2015). Improving emotional face perception in autism with diuretic bumetanide: a proof-of-concept behavioral and functional brain imaging pilot study. *Autism* 19, 149–157. doi: 10.1177/1362361313514141

Hare, T. A., Tottenham, N., Galvan, A., Voss, H. U., Glover, G. H., and Casey, B. J. (2008). Biological substrates of emotional reactivity and regulation in adolescence during an emotional go-nogo task. *Biol. Psychiatry* 63, 927–934. doi: 10.1016/j.biopsych.2008.03.015

Harris, C., and Card, B. (2012). A pilot study to evaluate nutritional influences on gastrointestinal symptoms and behavior patterns in children with Autism Spectrum Disorder. *Compl. Ther. Med.* 20, 437–440. doi: 10.1016/j.ctim.2012.08.004

Harrop, C. (2015). Evidence-based, parent-mediated interventions for young children with autism spectrum disorder: The case of restricted and repetitive behaviors. *Autism* 19, 662–672. doi: 10.1177/1362361314545685

Harrop, C., McConachie, H., Emsley, R., Leadbitter, K., and Green, J. (2014). Restricted and repetitive behaviors in autism spectrum disorders and typical development: cross-sectional and longitudinal comparisons. *J. Autism Dev. Disord.* 44, 1207–1219. doi: 10.1007/s10803-013-1986-5

Hau, J., Aljawad, S., Baggett, N., Fishman, I., Carper, R. A., and Müller, R.-A. (2019). The cingulum and cingulate U-fibers in children and adolescents with autism spectrum disorders. *Human Brain Mapp.* 40, 3153–3164. doi: 10.1002/hbm.24586

Haynes, W. I., and Haber, S. N. (2013). The organization of prefrontal-subthalamic inputs in primates provides an anatomical substrate for both functional specificity and integration: implications for Basal Ganglia models and deep brain stimulation. *J. Neurosci.* 33, 4804–4814. doi: 10.1523/jneurosci.4674-12.2013

He, H., Ye, N., Yi, L., and Yang, C. (2019). Validating the repetitive behavior scale-revised for children in china aged 3 to 8 with autism spectrum disorder. *J. Autism Dev. Disord.* 49, 4941–4956. doi: 10.1007/s10803-019-04210-x

He, Q., Nomura, T., Xu, J., and Contractor, A. (2014). The developmental switch in GABA polarity is delayed in fragile X mice. *J. Neurosci.* 34, 446–450. doi: 10.1523/jneurosci.4447-13.2014

Hegarty, J. P., Lazzeroni, L. C., Raman, M. M., Hallmayer, J. F., Cleveland, S. C., Wolke, O. N., et al. (2020). Genetic and environmental influences on corticostriatal circuits in twins with autism. *J. Psychiatry Neurosci.* 45, 188–197. doi: 10.1503/jpn.190030

Herscu, P., Handen, B. L., Arnold, L. E., Snape, M. F., Bregman, J. D., Ginsberg, L., et al. (2020). The SOFIA study: negative multi-center study of low dose fluoxetine on repetitive behaviors in children and adolescents with autistic disorder. *J. Autism Dev. Disord.* 50, 3233–3244. doi: 10.1007/s10803-019-04120-y

Hicks, S. D., Carpenter, R. L., Wagner, K. E., Pauley, R., Barros, M., Tierney-Aves, C., et al. (2020). Saliva MicroRNA differentiates children with autism from peers with typical and atypical development. *J. Am. Acad. Child Adoles. Psychiatry* 59, 296–308. doi: 10.1016/j.jaac.2019.03.017

Hiremath, C. S., Sagar, K. J. V., Yamini, B. K., Girimaji, A. S., Kumar, R., Sravanti, S. L., et al. (2021). Emerging behavioral and neuroimaging biomarkers for early and accurate characterization of autism spectrum disorders: a systematic review. *Transl. Psychiatry* 11:42. doi: 10.1038/s41398-020-01178-6

Hollander, E., Novotny, S., Hanratty, M., Yaffe, R., DeCaria, C. M., Aronowitz, B. R., et al. (2003). Oxytocin infusion reduces repetitive behaviors in adults with autistic and Asperger's disorders. *Neuropsychopharmacology* 28, 193–198. doi: 10.1038/sj.npp.1300021

Honey, E., McConachie, H., Turner, M., and Rodgers, J. (2012). Validation of the repetitive behaviour questionnaire for use with children with autism spectrum disorder. *Res. Autism Spectrum Disord.* 6, 355–364. doi: 10.1016/j.rasd.2011.06.009

Huang, F., Chen, X., Jiang, X., Niu, J., Cui, C., Chen, Z., et al. (2019). Betaine ameliorates prenatal valproic-acid-induced autism-like behavioral abnormalities in mice by promoting homocysteine metabolism. *Psychiatry Clin. Neurosci.* 73, 317–322. doi: 10.1111/pcn.12833

Hughes, H. K., Rose, D., and Ashwood, P. (2018). The gut microbiota and dysbiosis in autism spectrum disorders. *Curr. Neurol. Neurosci. Rep.* 18:6. doi: 10.1007/s11910-018-0887-6

Hus, V., Gotham, K., and Lord, C. (2014). Standardizing ADOS domain scores: Separating severity of social affect and restricted and repetitive behaviors. *J. Autism Dev. Disord.* 44, 2400–2412. doi: 10.1007/s10803-012-1719-1

Hutt, C., and Hutt, S. J. (1965). Effects of environmental complexity on stereotyped behaviours of children. *Animal Behav.* 13, 1–4. doi: 10.1016/0003-3472(65)90064-3

Insel, T. R., O'Brien, D. J., and Leckman, J. F. (1999). Oxytocin, vasopressin, and autism: is there a connection? *Biol. Psychiatry* 45, 145–157. doi: 10.1016/s0006-3223(98)00142-5

Iversen, R. K., and Lewis, C. (2021). Executive function skills are linked to restricted and repetitive behaviors: three correlational meta analyses. *Autism Res.* 2021:2468. doi: 10.1002/aur.2468

Jahfari, S., Ridderinkhof, K. R., Collins, A. G. E., Knapen, T., Waldorp, L. J., and Frank, M. J. (2019). Cross-Task contributions of frontobasal ganglia circuitry in response inhibition and conflict-induced slowing. *Cereb. Cortex* 29, 1969–1983. doi: 10.1093/cercor/bhy076

Jia, F., Wang, B., Shan, L., Xu, Z., Staal, W. G., and Du, L. (2015). Core symptoms of autism improved after vitamin D supplementation. *Pediatrics* 135, e196–e198. doi: 10.1542/peds.2014-2121

Jones, K. L., Pride, M. C., Edmiston, E., Yang, M., Silverman, J. L., Crawley, J. N., et al. (2020). Autism-specific maternal autoantibodies produce behavioral abnormalities in an endogenous antigen-driven mouse model of autism. *Mol. Psychiatry* 25, 2994–3009. doi: 10.1038/s41380-018-0126-1

Joosten, A. V., Bundy, A. C., and Einfeld, S. L. (2009). Intrinsic and extrinsic motivation for stereotypic and repetitive behavior. *J. Autism Dev. Disord.* 39, 521–531. doi: 10.1007/s10803-008-0654-7

Joseph, L., Thurm, A., Farmer, C., and Shumway, S. (2013). Repetitive behavior and restricted interests in young children with autism: comparisons with controls and stability over 2 years. *Autism Res.* 6, 584–595. doi: 10.1002/aur.1316

Joyce, C., Honey, E., Leekam, S. R., Barrett, S. L., and Rodgers, J. (2017). Anxiety, intolerance of uncertainty and restricted and repetitive behaviour: insights directly from young people with ASD. *J. Autism Dev. Disord.* 47, 3789–3802. doi: 10.1007/s10803-017-3027-2

Juarez-Martinez, E. L., Sprengers, J. J., Cristian, G., Oranje, B., van Andel, D. M., Avramiea, A. E., et al. (2021). Prediction of behavioral improvement through resting-state electroencephalography and clinical severity in a randomized controlled trial testing bumetanide in autism spectrum disorder. *Biol. Psychiatry Cogn. Neurosci. Neuroimag.* 2021:9. doi: 10.1016/j.bpsc.2021.08.009

Just, M. A., Cherkassky, V. L., Keller, T. A., and Minshew, N. J. (2004). Cortical activation and synchronization during sentence comprehension in high-functioning autism: Evidence of underconnectivity. *Brain* 127, 1811–1821. doi: 10.1093/brain/awh199

Kaat, A. J., Lecavalier, L., and Aman, M. G. (2014). Validity of the aberrant behavior checklist in children with autism spectrum disorder. *J. Autism Dev. Disord.* 44, 1103–1116. doi: 10.1007/s10803-013-1970-0

Kaila, K., Price, T. J., Payne, J. A., Puskarjov, M., and Voipio, J. (2014). Cation-chloride cotransporters in neuronal development, plasticity and disease. *Nat. Rev. Neurosci.* 15, 637–654. doi: 10.1038/nrn3819

Kałużna-Czaplińska, J., Żurawicz, E., Michalska, M., and Rynkowski, J. (2013). A focus on homocysteine in autism. *Acta Biochim. Pol.* 60, 137–142.

Kaminski, J. W., and Claussen, A. H. (2017). Evidence base update for psychosocial treatments for disruptive behaviors in children. *J. Clin. Child Adolesc. Psychol.* 46, 477–499. doi: 10.1080/15374416.2017.1310044

Kanner, L. (1943). Autistic disturbances of affective contact. *Nervous. Child* 2, 217–250.

Karin, I., Borggraefe, I., Catarino, C. B., Kuhm, C., Hoertnagel, K., Biskup, S., et al. (2017). Folinic acid therapy in cerebral folate deficiency: marked improvement in an adult patient. *J. Neurol.* 264, 578–582. doi: 10.1007/s00415-016-8387-6

Kelley, R., Flouty, O., Emmons, E. B., Kim, Y., Kingyon, J., Wessel, J. R., et al. (2018). A human prefrontal-subthalamic circuit for cognitive control. *Brain* 141, 205–216. doi: 10.1093/brain/awx300

Kelly, E., Meng, F., Fujita, H., Morgado, F., Kazemi, Y., Rice, L. C., et al. (2020). Regulation of autism-relevant behaviors by cerebellar-prefrontal cortical circuits. *Nat. Neurosci.* 23, 1102–1110. doi: 10.1038/s41593-020-0665-z

Kerley, C. P., Power, C., Gallagher, L., and Coghlan, D. (2017). Lack of effect of vitamin D(3) supplementation in autism: a 20-week, placebo-controlled RCT. *Arch. Dis. Child* 102, 1030–1036. doi: 10.1136/archdischild-2017-312783

Kharod, S. C., Kang, S. K., and Kadam, S. D. (2019). Off-Label use of bumetanide for brain disorders: an overview. *Front. Neurosci.* 13:310. doi: 10.3389/fnins.2019.00310

Kim, H., Lim, C. S., and Kaang, B. K. (2016). Neuronal mechanisms and circuits underlying repetitive behaviors in mouse models of autism spectrum disorder. *Behav. Brain Funct.* 12:87. doi: 10.1186/s12993-016-0087-y

Kim, J. W., Seung, H., Kim, K. C., Gonzales, E. L. T., Oh, H. A., Yang, S. M., et al. (2017). Agmatine rescues autistic behaviors in the valproic acid-induced animal model of autism. *Neuropharmacology* 113, 71–81. doi: 10.1016/j.neuropharm.2016.09.014

Kim, S. H., and Lord, C. (2010). Restricted and repetitive behaviors in toddlers and preschoolers with autism spectrum disorders based on the Autism Diagnostic Observation Schedule (ADOS). *Autism Res.* 3, 162–173. doi: 10.1002/aur.142

Klin, A., Lin, D. J., Gorrindo, P., Ramsay, G., and Jones, W. (2009). Two-year-olds with autism orient to non-social contingencies rather than biological motion. *Nature* 459, 257–261. doi: 10.1038/nature07868

Klorman, R., and Ryan, R. M. (1980). Heart rate, contingent negative variation, and evoked potentials during anticipation of affective stimulation. *Psychophysiology* 17, 513–523. doi: 10.1111/j.1469-8986.1980.tb02290.x

Klorman, R., Weissberg, R. P., and Wiesenfeld, A. R. (1977). Individual differences in fear and autonomic reactions to affective stimulation. *Psychophysiology* 14, 45–51. doi: 10.1111/j.1469-8986.1977.tb01154.x

Knight, D. C., Nguyen, H. T., and Bandettini, P. A. (2005). The role of the human amygdala in the production of conditioned fear responses. *Neuroimage* 26, 1193–1200. doi: 10.1016/j.neuroimage.2005.03.020

Kodak, T., and Bergmann, S. (2020). Autism spectrum disorder: characteristics, associated behaviors, and early intervention. *Pediatr. Clin. North Am.* 67, 525–535. doi: 10.1016/j.pcl.2020.02.007

Kohls, G., Antezana, L., Mosner, M. G., Schultz, R. T., and Yerys, B. E. (2018). Altered reward system reactivity for personalized circumscribed interests in autism. *Mol. Autism* 9:9. doi: 10.1186/s13229-018-0195-7

Kohls, G., Chevallier, C., Troiani, V., and Schultz, R. T. (2012). Social 'wanting' dysfunction in autism: neurobiological underpinnings and treatment implications. *J. Neurodev. Disord.* 4:10. doi: 10.1186/1866-1955-4-10

Kohls, G., Schulte-Rüther, M., Nehrkorn, B., Müller, K., Fink, G. R., Kamp-Becker, I., et al. (2013). Reward system dysfunction in autism spectrum disorders. *Soc. Cogn. Affect. Neurosci.* 8, 565–572. doi: 10.1093/scan/nss033

Kolevzon, A., Bush, L., Wang, A. T., Halpern, D., Frank, Y., Grodberg, D., et al. (2014). A pilot controlled trial of insulin-like growth factor-1 in children with Phelan-McDermid syndrome. *Mol. Autism* 5:54. doi: 10.1186/2040-2392-5-54

Kosaka, H., Okamoto, Y., Munesue, T., Yamasue, H., Inohara, K., Fujioka, T., et al. (2016). Oxytocin efficacy is modulated by dosage and oxytocin receptor genotype in young adults with high-functioning autism: a 24-week randomized clinical trial. *Transl. Psychiatry* 6, e872. doi: 10.1038/tp.2016.152

Lam, K. S., and Aman, M. G. (2007). The Repetitive Behavior Scale-Revised: independent validation in individuals with autism spectrum disorders. *J. Autism Dev. Disord.* 37, 855–866. doi: 10.1007/s10803-006-0213-z

Langen, M., Bos, D., Noordermeer, S. D. S., Nederveen, H., Van Engeland, H., and Durston, S. (2014). Changes in the development of striatum are involved in repetitive behavior in autism. *Biol. Psychiatry* 76, 405–411. doi: 10.1016/j.biopsych.2013.08.013

Langen, M., Durston, S., Kas, M. J. H., van Engeland, H., and Staal, W. G. (2011a). The neurobiology of repetitive behavior and men. *Neurosci. Biobehav. Rev.* 35, 356–365. doi: 10.1016/j.neubiorev.2010.02.005

Langen, M., Kas, M. J., Staal, W. G., van Engeland, H., and Durston, S. (2011b). The neurobiology of repetitive behavior: of mice. *Neurosci. Biobehav. Rev.* 35, 345–355. doi: 10.1016/j.neubiorev.2010.02.004

Larkin, F., Meins, E., Centifanti, L. C. M., Fernyhough, C., and Leekam, S. R. (2017). How does restricted and repetitive behavior relate to language and cognition in typical development? *Dev. Psychopathol.* 29, 863–874. doi: 10.1017/s0954579416000535

Lee, Y., Corley, M. J., Pang, A., Arakaki, G., Abbott, L., Nishimoto, M., et al. (2018a). A modified ketogenic gluten-free diet with MCT improves behavior in children with autism spectrum disorder. *Physiol. Behav.* 188, 205–211. doi: 10.1016/j.physbeh.2018.02.006

Lee, Y., Kim, H., Kim, J. E., Park, J. Y., Choi, J., Lee, J. E., et al. (2018b). Excessive D1 dopamine receptor activation in the dorsal striatum promotes autistic-like behaviors. *Mol. Neurobiol.* 55, 5658–5671. doi: 10.1007/s12035-017-0770-5

Leekam, S. R., Prior, M. R., and Uljarevic, M. (2011). Restricted and repetitive behaviors in autism spectrum disorders: A review of research in the last decade. *Psychol. Bull.* 137, 562–593. doi: 10.1037/a0023341

Leekam, S., Tandos, J., McConachie, H., Meins, E., Parkinson, K., Wright, C., et al. (2007). Repetitive behaviours in typically developing 2-year-olds. *J. Child Psychol. Psychiatry* 48, 1131–1138. doi: 10.1111/j.1469-7610.2007.01778.x

Lemonnier, E., and Ben-Ari, Y. (2010). The diuretic bumetanide decreases autistic behaviour in five infants treated during 3 months with no side effects. *Acta Paediatr. Int. J. Paediatrics* 99, 1885–1888. doi: 10.1111/j.1651-2227.2010.01933.x

Lemonnier, E., Degrez, C., Phelep, M., Tyzio, R., Josse, F., Grandgeorge, M., et al. (2012). A randomised controlled trial of bumetanide in the treatment of autism in children. *Transl. Psychiatry* 2:e202. doi: 10.1038/tp.2012.124

Lemonnier, E., Robin, G., Degrez, C., Tyzio, R., Grandgeorge, M., and Ben-Ari, Y. (2013). Treating Fragile X syndrome with the diuretic bumetanide: a case report. *Acta Paediatr.* 102, e288–e290. doi: 10.1111/apa.12235

Lemonnier, E., Villeneuve, N., Sonie, S., Serret, S., Rosier, A., Roue, M., et al. (2017). Effects of bumetanide on neurobehavioral function in children and adolescents with autism spectrum disorders. *Transl. Psychiatry* 7:e1056. doi: 10.1038/tp.2017.10

Lewis, M. H., Rajpal, H., and Muehlmann, A. M. (2019). Reduction of repetitive behavior by co-administration of adenosine receptor agonists in C58 mice. *Pharmacol. Biochem. Behav.* 181, 110–116. doi: 10.1016/j.pbb.2019.04.006

Lewis, M. H., Tanimura, Y., Lee, L. W., and Bodfish, J. W. (2007). Animal models of restricted repetitive behavior in autism. *Behav. Brain Res.* 176, 66–74. doi: 10.1016/j.bbr.2006.08.023

Lewis, M., and Kim, S. J. (2009). The pathophysiology of restricted repetitive behavior. *J. Neurodev. Disord.* 1, 114–132. doi: 10.1007/s11689-009-9019-6

Li, C., Liu, Y., Fang, H., Chen, Y., Weng, J., Zhai, M., et al. (2020). Study on aberrant eating behaviors, food intolerance, and stereotyped behaviors in autism spectrum disorder. *Front. Psychiatry* 11:1152. doi: 10.3389/fpsyt.2020.493695

Lidstone, D. E., Rochowiak, R., Mostofsky, S. H., and Nebel, M. B. (2021). A Data Driven approach reveals that anomalous motor system connectivity is associated with the severity of core autism symptoms. *Autism Res.* 2021:2476. doi: 10.1002/aur.2476

Lidstone, J., Uljarevic, M., Sullivan, J., Rodgers, J., McConachie, H., Freeston, M., et al. (2014). Relations among restricted and repetitive behaviors, anxiety and sensory features in children with autism spectrum disorders. *Res. Autism Spect. Disord.* 8, 82–92. doi: 10.1016/j.rasd.2013.10.001

Lin, C. E., and Koegel, R. (2018). Treatment for higher-order restricted repetitive behaviors (H-RRB) in children with autism spectrum disorder. *J. Autism Dev. Disord.* 48, 3831–3845. doi: 10.1007/s10803-018-3637-3

Liu, Q., Chen, M. X., Sun, L., Wallis, C. U., Zhou, J. S., Ao, L. J., et al. (2019). Rational use of mesenchymal stem cells in the treatment of autism spectrum disorders. *World J. Stem Cells* 11, 55–72. doi: 10.4252/wjsc.v11.i2.55

Lloyd, D., Medina, D., Hawk, L., Fosco, W., and Richards, J. (2014). Habituation of reinforcer effectiveness. *Front. Integr. Neurosci.* 7:107.

Lopez, B. R., Lincoln, A. J., Ozonoff, S., and Lai, Z. (2005). Examining the relationship between executive functions and restricted, repetitive symptoms of Autistic Disorder. *J. Autism Dev. Disord.* 35, 445–460. doi: 10.1007/s10803-005-5035-x

Lord, C., Rutter, M., and Le Couteur, A. (1994). Autism Diagnostic Interview-Revised: a revised version of a diagnostic interview for caregivers of individuals with possible pervasive developmental disorders. *J. Autism Dev. Disord.* 24, 659–685. doi: 10.1007/BF02172145

Lord, C., Rutter, M., DiLavore, P., Risi, S., Gotham, K., and Bishop, S. (2012). *Autism Diagnostic Observation Schedule ADOS-2. Manual (Part I): Modules*. Torrance, CA: Western Psychological Services. 1–4.

Lucarelli, S., Frediani, T., Zingoni, A. M., Ferruzzi, F., Giardini, O., Quintieri, F., et al. (1995). Food allergy and infantile autism. *Panminerva. Med.* 37, 137–141.

Luhach, K., Kulkarni, G. T., Singh, V. P., and Sharma, B. (2021). Attenuation of neurobehavioural abnormalities by papaverine in prenatal valproic acid rat model of ASD. *Eur. J. Pharmacol.* 890:12. doi: 10.1016/j.ejphar.2020.173663

Luo, W., Zhang, C., Jiang, Y. H., and Brouwer, C. R. (2018). Systematic reconstruction of autism biology from massive genetic mutation profiles. *Sci. Adv.* 4:e1701799. doi: 10.1126/sciadv.1701799

Lv, Y. T., Zhang, Y., Liu, M., Qiuwaxi, J. N., Ashwood, P., Cho, S. C., et al. (2013). Transplantation of human cord blood mononuclear cells and umbilical cord-derived mesenchymal stem cells in autism. *J. Transl. Med.* 11:196. doi: 10.1186/1479-5876-11-196

Ma, Z. H., Lu, B., Li, X., Mei, T., Guo, Y. Q., Yang, L., et al. (2021). Atypicalities in the developmental trajectory of cortico-striatal functional connectivity in autism spectrum disorder. *Autism* 2021:904. doi: 10.1177/13623613211041904

Maenner, M. J., Shaw, K. A., Bakian, A. V., Bilder, D. A., Durkin, M. S., Esler, A., et al. (2021). Prevalence and characteristics of autism spectrum disorder among children aged 8 years – autism and developmental disabilities monitoring network, 11 sites, United States, 2018. *MMWR Surveill. Summ.* 70, 1–16. doi: 10.15585/mmwr.ss7011a1

Mandy, W., Charman, T., Gilmour, J., and Skuse, D. (2011). Toward specifying pervasive developmental disorder-not otherwise specified. *Autism Res.* 4, 121–131. doi: 10.1002/aur.178

Marco, E. M., Rapino, C., Caprioli, A., Borsini, F., Maccarrone, M., and Laviola, G. (2011). Social encounter with a novel partner in adolescent rats: activation of the central endocannabinoid system. *Behav. Brain Res.* 220, 140–145. doi: 10.1016/j.bbr.2011.01.044

Martin, L. A., Ashwood, P., Braunschweig, D., Cabanlit, M., Van de Water, J., and Amaral, D. G. (2008). Stereotypies and hyperactivity in rhesus monkeys exposed to IgG from mothers of children with autism. *Brain Behav. Immun.* 22, 806–816. doi: 10.1016/j.bbi.2007.12.007

Matas, E., Maisterrena, A., Thabault, M., Balado, E., Francheteau, M., Balbous, A., et al. (2021). Major motor and gait deficits with sexual dimorphism in a Shank3 mutant mouse model. *Mol. Autism* 12:2. doi: 10.1186/s13229-020-00412-8

McCracken, J. T., McGough, J., Shah, B., Cronin, P., Hong, D., Aman, M. G., et al. (2002). Risperidone in children with autism and serious behavioral problems. *N Engl. J. Med.* 347, 314–321. doi: 10.1056/NEJMoa013171

McCrimmon, A., and Rostad, K. (2014). *Test review: Autism diagnostic observation schedule, (ADOS-2) manual (Part II): Toddler module*. Los Angeles, CA: SAGE Publications Sage CA.

Mead, J., and Ashwood, P. (2015). Evidence supporting an altered immune response in ASD. *Immunol. Lett.* 163, 49–55. doi: 10.1016/j.imlet.2014.11.006

Mehta, R., Bhandari, R., and Kuhad, A. (2021). Effects of catechin on a rodent model of autism spectrum disorder: implications for the role of nitric oxide in neuroinflammatory pathway. *Psychopharmacology* 238, 3249–3271. doi: 10.1007/s00213-021-05941-5

Mei, T., Llera, A., Floris, D. L., Forde, N. J., Tillmann, J., Durston, S., et al. (2020). Gray matter covariations and core symptoms of autism: the EU-AIMS Longitudinal European Autism Project. *Mol. Autism* 11:86. doi: 10.1186/s13229-020-00389-4

Mejias, R., Chiu, S. L., Han, M., Rose, R., Gil-Infante, A., Zhao, Y., et al. (2019). Purkinje cell-specific Grip1/2 knockout mice show increased repetitive self-grooming and enhanced mGluR5 signaling in cerebellum. *Neurobiol. Dis.* 132:602. doi: 10.1016/j.nbd.2019.104602

Meyer, U., Murray, P. J., Urwyler, A., Yee, B. K., Schedlowski, M., and Feldon, J. (2008). Adult behavioral and pharmacological dysfunctions following disruption of the fetal brain balance between pro-inflammatory and IL-10-mediated anti-inflammatory signaling. *Mol. Psychiatry* 13, 208–221. doi: 10.1038/sj.mp.4002042

Milardi, D., Arrigo, A., Anastasi, G., Cacciola, A., Marino, S., Mormina, E., et al. (2016). Extensive direct subcortical cerebellum-basal ganglia connections in human brain as revealed by constrained spherical deconvolution tractography. *Front. Neuroanat.* 10:29. doi: 10.3389/fnana.2016.00029

Miller, H. L., Ragozzino, M. E., Cook, E. H., Sweeney, J. A., and Mosconi, M. W. (2015). Cognitive set shifting deficits and their relationship to repetitive behaviors in autism spectrum disorder. *J. Autism Dev. Disord.* 45, 805–815. doi: 10.1007/s10803-014-2244-1

Miller, M., Sun, S., Iosif, A. M., Young, G. S., Belding, A., Tubbs, A., et al. (2021). Repetitive behavior with objects in infants developing autism predicts diagnosis and later social behavior as early as 9 months. *J. Abnorm. Psychol.* 130, 665–675. doi: 10.1037/abn0000692

Mirenda, P., Smith, I. M., Vaillancourt, T., Georgiades, S., Duku, E., Szatmari, P., et al. (2010). Validating the Repetitive Behavior Scale-revised in young children with autism spectrum disorder. *J. Autism Dev. Disord.* 40, 1521–1530. doi: 10.1007/s10803-010-1012-0

Mirza, R., and Sharma, B. (2019a). Beneficial effects of pioglitazone, a selective peroxisome proliferator-activated receptor-γ agonist in prenatal valproic acid-induced behavioral and biochemical autistic like features in Wistar rats. *Int. J. Dev. Neurosci.* 76, 6–16. doi: 10.1016/j.ijdevneu.2019.05.006

Mirza, R., and Sharma, B. (2019b). A selective peroxisome proliferator-activated receptor-γ agonist benefited propionic acid induced autism-like behavioral phenotypes in rats by attenuation of neuroinflammation and oxidative stress. *Chemico-Biol. Interact.* 311:8758. doi: 10.1016/j.cbi.2019.108758

Mohammadi, S., Asadi-Shekaari, M., Basiri, M., Parvan, M., Shabani, M., and Nozari, M. (2020). Improvement of autistic-like behaviors in adult rats prenatally exposed to valproic acid through early suppression of NMDA receptor function. *Psychopharmacology* 237, 199–208. doi: 10.1007/s00213-019-05357-2

Monteiro, P., and Feng, G. (2016). Learning From Animal Models of Obsessive-Compulsive Disorder. *Bio.l Psychiatry* 79, 7–16. doi: 10.1016/j.biopsych.2015.04.020

Moradi, K., Ashraf-Ganjouei, A., Tavolinejad, H., Bagheri, S., and Akhondzadeh, S. (2021). The interplay between gut microbiota and autism spectrum disorders: A focus on immunological pathways. *Prog. Neuro-Psychopharmacol. Biol. Psychiatry* 106:91. doi: 10.1016/j.pnpbp.2020.110091

Mosconi, M. W., Kay, M., D'Cruz, A. M., Seidenfeld, A., Guter, S., Stanford, L. D., et al. (2009). Impaired inhibitory control is associated with higher-order repetitive behaviors in autism spectrum disorders. *Psychol. Med.* 39, 1559–1566. doi: 10.1017/S0033291708004984

Mosconi, M. W., Mohanty, S., Greene, R. K., Cook, E. H., Vaillancourt, D. E., and Sweeney, J. A. (2015a). Feedforward and feedback motor control abnormalities implicate cerebellar dysfunctions in autism spectrum disorder. *J. Neurosci.* 35, 2015–2025. doi: 10.1523/jneurosci.2731-14.2015

Mosconi, M. W., Wang, Z., Schmitt, L. M., Tsai, P., and Sweeney, J. A. (2015b). The role of cerebellar circuitry alterations in the pathophysiology of autism spectrum disorders. *Front. Neurosci.* 9:296. doi: 10.3389/fnins.2015.00296

Moss, J., Oliver, C., Arron, K., Burbidge, C., and Berg, K. (2009). The prevalence and phenomenology of repetitive behavior in genetic syndromes. *J. Autism Dev. Disord.* 39, 572–588. doi: 10.1007/s10803-008-0655-6

Muehlmann, A. M., Maletz, S., King, M. A., and Lewis, M. H. (2020). Pharmacological targeting of striatal indirect pathway neurons improves subthalamic nucleus dysfunction and reduces repetitive behaviors in C58 mice. *Behav. Brain Res.* 391:112708. doi: 10.1016/j.bbr.2020.112708

Muller, C. L., Anacker, A. M. J., and Veenstra-VanderWeele, J. (2016). The serotonin system in autism spectrum disorder: From biomarker to animal models. *Neuroscience* 321, 24–41. doi: 10.1016/j.neuroscience.2015.11.010

Nadeem, A., Ahmad, S. F., Al-Harbi, N. O., Attia, S. M., Alshammari, M. A., Alzahrani, K. S., et al. (2019a). Increased oxidative stress in the cerebellum and peripheral immune cells leads to exaggerated autism-like repetitive behavior due to deficiency of antioxidant response in BTBR T?+?tf/J mice. *Prog. Neuropsychopharmacol. Biol. Psychiatry* 89, 245–253. doi: 10.1016/j.pnpbp.2018.09.012

Nadeem, A., Ahmad, S. F., Al-Harbi, N. O., Attia, S. M., Bakheet, S. A., Ibrahim, K. E., et al. (2019b). Nrf2 activator, sulforaphane ameliorates autism-like symptoms through suppression of Th17 related signaling and rectification of oxidant-antioxidant imbalance in periphery and brain of BTBR T+tf/J mice. *Behav. Brain Res.* 364, 213–224. doi: 10.1016/j.bbr.2019.02.031

Nambu, A., Tokuno, H., and Takada, M. (2002). Functional significance of the cortico-subthalamo-pallidal 'hyperdirect' pathway. *Neurosci. Res.* 43, 111–117. doi: 10.1016/s0168-0102(02)00027-5

Navarro, F., Pearson, D. A., Fatheree, N., Mansour, R., Hashmi, S. S., and Rhoads, J. M. (2015). Are 'leaky gut' and behavior associated with gluten and dairy containing diet in children with autism spectrum disorders? *Nutr. Neurosci.* 18, 177–185. doi: 10.1179/1476830514y.0000000110

Nezgovorova, V., Ferretti, C. J., Taylor, B. P., Shanahan, E., Uzunova, G., Hong, K., et al. (2021). Potential of cannabinoids as treatments for autism spectrum disorders. *J. Psychiatric Res.* 137, 194–201. doi: 10.1016/j.jpsychires.2021.02.048

Nguyen Thanh, L., Nguyen, H. P., Ngo, M. D., Bui, V. A., Dam, P. T. M., Bui, H. T. P., et al. (2021). Outcomes of bone marrow mononuclear cell transplantation combined with interventional education for autism spectrum disorder. *Stem Cells Transl. Med.* 10, 14–26. doi: 10.1002/sctm.20-0102

Oakes, A., Thurman, A. J., McDuffie, A., Bullard, L. M., Hagerman, R. J., and Abbeduto, L. (2016). Characterising repetitive behaviours in young boys with fragile X syndrome. *J. Intellect. Disabil. Res.* 60, 54–67. doi: 10.1111/jir.12234

Oakley, C., Mahone, E. M., Morris-Berry, C., Kline, T., and Singer, H. S. (2015). Primary complex motor stereotypies in older children and adolescents: clinical features and longitudinal follow-up. *Pediatric. Neurol.* 52, 398–403. doi: 10.1016/j.pediatrneurol.2014.11.002

Odom, S. L., Boyd, B. A., Hall, L. J., and Hume, K. (2010). Evaluation of comprehensive treatment models for individuals with autism spectrum disorders. *J. Autism Dev. Disord.* 40, 425–436. doi: 10.1007/s10803-009-0825-1

Owen, R., Sikich, L., Marcus, R. N., Corey-Lisle, P., Manos, G., McQuade, R. D., et al. (2009). Aripiprazole in the treatment of irritability in children and adolescents with autistic disorder. *Pediatrics* 124, 1533–1540. doi: 10.1542/peds.2008-3782

Park, H. Y., Go, J., Ryu, Y. K., Choi, D. H., Noh, J. R., An, J. P., et al. (2021). Humulus japonicus rescues autistic-like behaviours in the BTBR T(+) Itpr3(tf)/J mouse model of autism. *Mol. Med. Rep.* 23:87. doi: 10.3892/mmr.2021.12087

Parker, K. J., Oztan, O., Libove, R. A., Mohsin, N., Karhson, D. S., Sumiyoshi, R. D., et al. (2019). A randomized placebo-controlled pilot trial shows that intranasal vasopressin improves social deficits in children with autism. *Sci. Transl. Med.* 11:7356. doi: 10.1126/scitranslmed.aau7356

Parladé, M. V., Weinstein, A., Garcia, D., Rowley, A. M., Ginn, N. C., and Jent, J. F. (2020). Parent-Child Interaction Therapy for children with autism spectrum disorder and a matched case-control sample. *Autism* 24, 160–176. doi: 10.1177/1362361319855851

Parracho, H. M. R. T., Gibson, G. R., Knott, F., Bosscher, D., Kleerebezem, M., and McCartney, A. L. (2010). A double-blind, placebo-controlled, crossover-designed probiotic feeding study in children diagnosed with autistic spectrum disorders. *Int. J. Probiot.* 5, 69–74.

Pasquereau, B., and Turner, R. S. (2017). A selective role for ventromedial subthalamic nucleus in inhibitory control. *Elife* 6:627. doi: 10.7554/eLife.31627

Paul, R., Chawarska, K., Cicchetti, D., and Volkmar, F. (2008). Language outcomes of toddlers with autism spectrum disorders: a two year follow-up. *Autism Res.* 1, 97–107. doi: 10.1002/aur.12

Payne, J. A., Rivera, C., Voipio, J., and Kaila, K. (2003). Cation-chloride co-transporters in neuronal communication, development and trauma. *Trends Neurosci.* 26, 199–206. doi: 10.1016/s0166-2236(03)00068-7

Peca, J., Feliciano, C., Ting, J. T., Wang, W., Wells, M. F., Venkatraman, T. N., et al. (2011). Shank3 mutant mice display autistic-like behaviours and striatal dysfunction. *Nature* 472, 437–442. doi: 10.1038/nature09965

Peled-Avron, L., Abu-Akel, A., and Shamay-Tsoory, S. (2020). Exogenous effects of oxytocin in five psychiatric disorders: a systematic review, meta-analyses and a personalized approach through the lens of the social salience hypothesis. *Neurosci. Biobehav. Rev.* 114, 70–95. doi: 10.1016/j.neubiorev.2020.04.023

Perets, N., Hertz, S., London, M., and Offen, D. (2018). Intranasal administration of exosomes derived from mesenchymal stem cells ameliorates autistic-like behaviors of BTBR mice. *Mol. Autism* 9:6. doi: 10.1186/s13229-018-0240-6

Perets, N., Oron, O., Herman, S., Elliott, E., and Offen, D. (2020). Exosomes derived from mesenchymal stem cells improved core symptoms of genetically modified mouse model of autism Shank3B. *Mol. Autism* 11:366. doi: 10.1186/s13229-020-00366-x

Peretti, S., Mariano, M., Mazzocchetti, C., Mazza, M., Pino, M. C., Verrotti, et al. (2019). Diet: the keystone of autism spectrum disorder? *Nutr. Neurosci.* 22, 825–839. doi: 10.1080/1028415X.2018.1464819

Pickard, H., Hirsch, C., Simonoff, E., and Happé, F. (2020). Exploring the cognitive, emotional and sensory correlates of social anxiety in autistic and neurotypical adolescents. *J. Child Psychol. Psychiatry* 61, 1317–1327. doi: 10.1111/jcpp.13214

Poleg, S., Kourieh, E., Ruban, A., Shapira, G., Shomron, N., Barak, B., et al. (2021). Behavioral aspects and neurobiological properties underlying medical cannabis treatment in Shank3 mouse model of autism spectrum disorder. *Transl. Psychiatry* 11:524. doi: 10.1038/s41398-021-01612-3

Pote, I., Wang, S., Sethna, V., Blasi, A., Daly, E., Kuklisova-Murgasova, M., et al. (2019). Familial risk of autism alters subcortical and cerebellar brain anatomy in infants and predicts the emergence of repetitive behaviors in early childhood. *Autism Res.* 12, 614–627. doi: 10.1002/aur.2083

Pu, D. H., Shen, Y. P., and Wu, J. (2013). Association between MTHFR Gene polymorphisms and the risk of autism spectrum disorders: a meta-analysis. *Autism Res.* 6, 384–392. doi: 10.1002/aur.1300

Rae, C. L., Hughes, L. E., Anderson, M. C., and Rowe, J. B. (2015). The prefrontal cortex achieves inhibitory control by facilitating subcortical motor pathway connectivity. *J. Neurosci.* 35, 786–794. doi: 10.1523/jneurosci.3093-13.2015

Reddihough, D. S., Marraffa, C., Mouti, A., O'Sullivan, M., Lee, K. J., Orsini, F., et al. (2019). Effect of fluoxetine on obsessive-compulsive behaviors in children and adolescents with autism spectrum disorders: a randomized clinical trial. *Jama* 322, 1561–1569. doi: 10.1001/jama.2019.14685

Rhine, M. A., Parrott, J. M., Schultz, M. N., Kazdoba, T. M., and Crawley, J. N. (2019). Hypothesis-driven investigations of diverse pharmacological targets in two mouse models of autism. *Autism Res.* 12, 401–421. doi: 10.1002/aur.2066

Richler, J., Bishop, S. L., Kleinke, J. R., and Lord, C. (2007). Restricted and repetitive behaviors in young children with autism spectrum disorders. *J. Autism Dev. Disord.* 37, 73–85. doi: 10.1007/s10803-006-0332-6

Richler, J., Huerta, M., Bishop, S. L., and Lord, C. (2010). Developmental trajectories of restricted and repetitive behaviors and interests in children with autism spectrum disorders. *Dev. Psychopathol.* 22, 55–69. doi: 10.1017/S0954579409990265

Rinaldi, T., Kulangara, K., Antoniello, K., and Markram, H. (2007). Elevated NMDA receptor levels and enhanced postsynaptic long-term potentiation induced by prenatal exposure to valproic acid. *Proc. Natl. Acad. Sci. USA* 104, 13501–13506. doi: 10.1073/pnas.0704391104

Robinson-Shelton, A., and Malow, B. A. (2016). Sleep Disturbances in Neurodevelopmental Disorders. *Curr. Psychiatry Rep.* 18:6. doi: 10.1007/s11920-015-0638-1

Rocha, V., Labopin, M., Gluckman, E., Powles, R., Arcese, W., Bacigalupo, A., et al. (2002). Relevance of bone marrow cell dose on allogeneic transplantation outcomes for patients with acute myeloid leukemia in first complete remission: results of a European survey. *J. Clin. Oncol.* 20, 4324–4330. doi: 10.1200/jco.2002.11.058

Rodgers, J., Glod, M., Connolly, B., and McConachie, H. (2012). The relationship between anxiety and repetitive behaviours in autism spectrum disorder. *J. Autism Dev. Disord.* 42, 2404–2409. doi: 10.1007/s10803-012-1531-y

Rojas, D. C., Peterson, E., Winterrowd, E., Reite, M. L., Rogers, S. J., and Tregellas, J. R. (2006). Regional gray matter volumetric changes in autism associated with social and repetitive behavior symptoms. *BMC Psychiatry* 6:56. doi: 10.1186/1471-244X-6-56

Román, V., Adham, N., Foley, A. G., Hanratty, L., Farkas, B., Lendvai, B., et al. (2021). Cariprazine alleviates core behavioral deficits in the prenatal valproic acid exposure model of autism spectrum disorder. *Psychopharmacology* 238, 2381–2392. doi: 10.1007/s00213-021-05851-6

Rose, D. R., Careaga, M., Van de Water, J., McAllister, K., Bauman, M. D., and Ashwood, P. (2017). Long-term altered immune responses following fetal priming in a non-human primate model of maternal immune activation. *Brain Behav. Immun.* 63, 60–70. doi: 10.1016/j.bbi.2016.11.020

Rothwell, P. E., Fuccillo, M. V., Maxeiner, S., Hayton, S. J., Gokce, O., Lim, B. K., et al. (2014). Autism-associated neuroligin-3 mutations commonly impair striatal circuits to boost repetitive behaviors. *Cell* 158, 198–212. doi: 10.1016/j.cell.2014.04.045

Runco, M. A., Charlop, M. H., and Schreibman, L. (1986). The occurrence of autistic children's self-stimulation as a function of familiar versus unfamiliar stimulus conditions. *J. Autism Dev. Disord.* 16, 31–44. doi: 10.1007/BF01531576

Ruskin, D. N., Murphy, M. I., Slade, S. L., and Masino, S. A. (2017). Ketogenic diet improves behaviors in a maternal immune activation model of autism spectrum disorder. *Plos One* 12:14. doi: 10.1371/journal.pone.0171643

Ryu, Y. K., Park, H. Y., Go, J., Choi, D. H., Choi, Y. K., Rhee, M., et al. (2021). Sodium phenylbutyrate reduces repetitive self-grooming behavior and rescues social and cognitive deficits in mouse models of autism. *Psychopharmacology* 238, 1833–1845. doi: 10.1007/s00213-021-05812-z

Saad, K., Abdel-rahman, A. A., Elserogy, Y. M., Al-Atram, A. A., Cannell, J. J., Bjørklund, G., et al. (2016). Vitamin D status in autism spectrum disorders and the efficacy of vitamin D supplementation in autistic children. *Nutrit. Neurosci.* 19, 346–351. doi: 10.1179/1476830515Y.0000000019

Salloum-Asfar, S., Satheesh, N. J., and Abdulla, S. A. (2019). Circulating miRNAs, Small but Promising Biomarkers for Autism Spectrum Disorder. *Front. Mol. Neurosci.* 12:253. doi: 10.3389/fnmol.2019.00253

Satterstrom, F. K., Kosmicki, J. A., Wang, J., Breen, M. S., De Rubeis, S., An, J. Y., et al. (2020). Large-scale exome sequencing study implicates both developmental and functional changes in the neurobiology of autism. *Cell* 180, 568–584. doi: 10.1016/j.cell.2019.12.036

Schmid, S., Wilson, D. A., and Rankin, C. H. (2014). Habituation mechanisms and their importance for cognitive function. *Front. Integr. Neurosci.* 8:97. doi: 10.3389/fnint.2014.00097

Schmitt, L. M., White, S. P., Cook, E. H., Sweeney, J. A., and Mosconi, M. W. (2018). Cognitive mechanisms of inhibitory control deficits in autism spectrum disorder. *J. child Psychol. Psychiatry Allied Discipl.* 59, 586–595. doi: 10.1111/jcpp.12837

Schulte, J. T., Wierenga, C. J., and Bruining, H. (2018). Chloride transporters and GABA polarity in developmental, neurological and psychiatric conditions. *Neurosci. Biobehav. Rev.* 90, 260–271. doi: 10.1016/j.neubiorev.2018.05.001

Segal-Gavish, H., Karvat, G., Barak, N., Barzilay, R., Ganz, J., Edry, L., et al. (2016). Mesenchymal Stem Cell Transplantation Promotes Neurogenesis and Ameliorates Autism Related Behaviors in BTBR Mice. *Autism Res.* 9, 17–32. doi: 10.1002/aur.1530

Shonesy, B. C., Parrish, W. P., Haddad, H. K., Stephenson, J. R., Báldi, R., Bluett, R. J., et al. (2018). Role of Striatal Direct Pathway 2-Arachidonoylglycerol Signaling in Sociability and Repetitive Behavior. *Biol. Psychiatry* 84, 304–315. doi: 10.1016/j.biopsych.2017.11.036

Sifre, R., Berry, D., Wolff, J. J., and Elison, J. T. (2021). Longitudinal change in restricted and repetitive behaviors from 8-36?months. *J. Neurodev. Disord.* 13:7. doi: 10.1186/s11689-020-09335-0

Silverman, J. L., Tolu, S. S., Barkan, C. L., and Crawley, J. N. (2010). Repetitive self-grooming behavior in the BTBR mouse model of autism is blocked by the mGluR5 antagonist MPEP. *Neuropsychopharmacology* 35, 976–989. doi: 10.1038/npp.2009.201

Simmler, L. D., and Ozawa, T. (2019). Neural circuits in goal-directed and habitual behavior: Implications for circuit dysfunction in obsessive-compulsive disorder. *Neurochem. Int.* 129:104464. doi: 10.1016/j.neuint.2019.104464

Singla, R., Mishra, A., Joshi, R., Kumar, R., Sarma, P., Sharma, A. R., et al. (2021). Inhibition of the ERK1/2 Phosphorylation by Dextromethorphan Protects against Core Autistic Symptoms in VPA Induced Autistic Rats: In Silico and in Vivo Drug Repurposition Study. *ACS Chem. Neurosci.* 12, 1749–1767. doi: 10.1021/acschemneuro.0c00672

Siniscalco, D. (2012). Stem cell research: an opportunity for autism spectrum disorders treatment. *Autism Open Access* 2:3.

Siniscalco, D., Bradstreet, J. J., and Antonucci, N. (2012a). Cell therapies for autism spectrum disorders. *Ann. Transl. Med.* 7:110.

Siniscalco, D., Sapone, A., Cirillo, A., Giordano, C., Maione, S., and Antonucci, N. (2012b). Autism spectrum disorders: is mesenchymal stem cell personalized therapy the future? *J Biomed. Biotechnol.* 2012:480289. doi: 10.1155/2012/480289

Sokhadze, E. M., El-Baz, A. S., Sears, L. L., Opris, I., and Casanova, M. F. (2014). rTMS neuromodulation improves electrocortical functional measures of information processing and behavioral responses in autism. *Front. Syst. Neurosci.* 8:134. doi: 10.3389/fnsys.2014.00134

Sokhadze, E. M., El-Baz, A., Baruth, J., Mathai, G., Sears, L., and Casanova, M. F. (2009). Effects of low frequency repetitive transcranial magnetic stimulation (rTMS) on gamma frequency oscillations and event-related potentials during processing of illusory figures in autism. *J. Autism Dev. Disord.* 39, 619–634. doi: 10.1007/s10803-008-0662-7

Sparks, B. F., Friedman, S. D., Shaw, D. W., Aylward, E. H., Echelard, D., Artru, A. A., et al. (2002). Brain structural abnormalities in young children with autism spectrum disorder. *Neurology* 59, 184–192. doi: 10.1212/wnl.59.2.184

Spiker, M. A., Lin, C. E., Van Dyke, M., and Wood, J. J. (2012). Restricted interests and anxiety in children with autism. *Autism* 16, 306–320. doi: 10.1177/1362361311401763

Sprengers, J. J., van Andel, D. M., Zuithoff, N. P. A., Keijzer-Veen, M. G., Schulp, A. J. A., Scheepers, F. E., et al. (2021). Bumetanide for Core Symptoms of Autism Spectrum Disorder (BAMBI): A Single Center, Double-Blinded, Participant-Randomized, Placebo-Controlled, Phase-2 Superiority Trial. *J. Am. Acad. Child Adoles. Psychiatry* 60, 865–876. doi: 10.1016/j.jaac.2020.07.888

Srivastava, S., Scherrer, B., Prohl, A. K., Filip-Dhima, R., Kapur, K., Kolevzon, A., et al. (2019). Volumetric Analysis of the Basal Ganglia and Cerebellar Structures in Patients with Phelan-McDermid Syndrome. *Pediatr. Neurol.* 90, 37–43. doi: 10.1016/j.pediatrneurol.2018.09.008

Steiner, B., Roch, M., Holtkamp, N., and Kurtz, A. (2012). Systemically administered human bone marrow-derived mesenchymal stem home into peripheral organs but do not induce neuroprotective effects in the MCAo-mouse model for cerebral ischemia. *Neurosci. Lett.* 513, 25–30. doi: 10.1016/j.neulet.2012.01.078

Subramanian, K., Brandenburg, C., Orsati, F., Soghomonian, J. J., Hussman, J. P., and Blatt, G. J. (2017). Basal ganglia and autism – a translational perspective. *Autism Res.* 10, 1751–1775. doi: 10.1002/aur.1837

Supekar, K., Ryali, S., Mistry, P., and Menon, V. (2021). Aberrant dynamics of cognitive control and motor circuits predict distinct restricted and repetitive behaviors in children with autism. *Nat. Commun.* 12:3537. doi: 10.1038/s41467-021-23822-5

Swartz, J. R., Wiggins, J. L., Carrasco, M., Lord, C., and Monk, C. S. (2013). Amygdala habituation and prefrontal functional connectivity in youth with autism spectrum disorders. *J. Am. Acad. Child Adoles. Psychiatry* 52, 84–93. doi: 10.1016/j.jaac.2012.10.012

Tanimura, Y., King, M. A., Williams, D. K., and Lewis, M. H. (2011). Development of repetitive behavior in a mouse model: roles of indirect and striosomal basal ganglia pathways. *Int. J. Dev. Neurosci.* 29, 461–467. doi: 10.1016/j.ijdevneu.2011.02.004

Tanimura, Y., Vaziri, S., and Lewis, M. H. (2010). Indirect basal ganglia pathway mediation of repetitive behavior: Attenuation by adenosine receptor agonists. *Behav. Brain Res.* 210, 116–122. doi: 10.1016/j.bbr.2010.02.030

Thelen, E. (1981). Rhythmical behavior in infancy: An ethological perspective. *Dev. Psychol.* 17, 237–257. doi: 10.1037/0012-1649.17.3.237

Thompson, R. F., and Spencer, W. A. (1966). Habituation: a model phenomenon for the study of neuronal substrates of behavior. *Psychol. Rev.* 73, 16–43. doi: 10.1037/h0022681

Troyb, E., Knoch, K., Herlihy, L., Stevens, M. C., Chen, C. M., Barton, M., et al. (2016). Restricted and Repetitive Behaviors as Predictors of Outcome in Autism Spectrum Disorders. *J. Autism Dev. Disord.* 46, 1282–1296. doi: 10.1007/s10803-015-2668-2

Turner, M. (1997). Towards an executive dysfunction account of repetitive behaviour in autism.in *Autism as an executive disorder*. J. Russell (Ed.), 57–100. Oxford: Oxford University Press.

Turner, M. (1999). Annotation: Repetitive behaviour in autism: A review of psychological research. *J. Child Psychol. Psychiatry* 40, 839–849. doi: 10.1017/s0021963099004278

Tyzio, R., Nardou, R., Ferrari, D. C., Tsintsadze, T., Shahrokhi, A., Eftekhari, S., et al. (2014). Oxytocin-mediated GABA inhibition during delivery attenuates autism pathogenesis in rodent offspring. *Science* 343, 675–679. doi: 10.1126/science.1247190

Uljarevic, M. (2013). *Repetitive behaviours, anxiety and sensory problems in children with autism and correlates of anxiety in their parents*. Cardiff: Cardiff University.

Uljarevic, M., Carrington, S. J., Fernyhough, C., Arnott, B., Meins, E., McConachie, H., et al. (2017). Development of Restricted and Repetitive Behaviors From 15 to 77 Months: Stability of Two Distinct Subtypes? *Dev. Psychol.* 53, 1859–1868. doi: 10.1037/dev0000324

Vaccarino, F. M., Urban, A. E., Stevens, H. E., Szekely, A., Abyzov, A., Grigorenko, E. L., et al. (2011). Annual Research Review: The promise of stem cell research for neuropsychiatric disorders. *J. Child Psychol. Psychiatry* 52, 504–516. doi: 10.1111/j.1469-7610.2010.02348.x

Van Eylen, L., Boets, B., Steyaert, J., Wagemans, J., and Noens, I. (2015). Executive functioning in autism spectrum disorders: influence of task and sample characteristics and relation to symptom severity. *Eur. Child Adolesc. Psychiatry* 24, 1399–1417. doi: 10.1007/s00787-015-0689-1

Van't Westeinde, A., Cauvet, E., Toro, R., Kuja-Halkola, R., Neufeld, J., Mevel, K., et al. (2020). Sex differences in brain structure: a twin study on restricted and repetitive behaviors in twin pairs with and without autism. *Mol. Autism* 11:1. doi: 10.1186/s13229-019-0309-x

Vasa, R. A., Kreiser, N. L., Keefer, A., Singh, V., and Mostofsky, S. H. (2018). Relationships between autism spectrum disorder and intolerance of uncertainty. *Autism Res.* 11, 636–644. doi: 10.1002/aur.1916

Veenstra-VanderWeele, J., Muller, C. L., Iwamoto, H., Sauer, J. E., Owens, W. A., Shah, C. R., et al. (2012). Autism gene variant causes hyperserotonemia, serotonin receptor hypersensitivity, social impairment and repetitive behavior. *Proc. Nat. Acad. Sci. USA* 109, 5469–5474. doi: 10.1073/pnas.1112345109

Venkatachalam, K., Eissa, N., Al Awad, M., Jayaprakash, P., Zhong, S. C., Stolting, F., et al. (2021). The histamine H3R and dopamine D2R/D3R antagonist ST-713 ameliorates autism-like behavioral features in BTBR T plus tf/J mice by multiple actions. *Biomed. Pharmacother.* 138:13. doi: 10.1016/j.biopha.2021.111517

Vicente, A. M., Martins, G. J., and Costa, R. M. (2020). Cortico-basal ganglia circuits underlying dysfunctional control of motor behaviors in neuropsychiatric disorders. *Curr. Opin. Genet. Dev.* 65, 151–159. doi: 10.1016/j.gde.2020.05.042

Villarreal-Martínez, L., González-Martínez, G., Sáenz-Flores, M., Bautista-Gómez, A. J., González-Martínez, A., Ortiz-Castillo, M., et al. (2021). Stem Cell Therapy in the Treatment of Patients With Autism Spectrum Disorder: a Systematic Review and Meta-analysis. *Stem Cell Rev. Rep.* 2021:257. doi: 10.1007/s12015-021-10257-0

Wang, H. B., Tahara, Y., Luk, S. H. C., Kim, Y. S., Hitchcock, O. N., MacDowell Kaswan, Z. A., et al. (2020). Melatonin treatment of repetitive behavioral deficits in the Cntnap2 mouse model of autism spectrum disorder. *Neurobiol. Dis.* 145:64. doi: 10.1016/j.nbd.2020.105064

Wang, T., Shan, L., Du, L., Feng, J., Xu, Z., Staal, W. G., et al. (2016). Serum concentration of 25-hydroxyvitamin D in autism spectrum disorder: a systematic review and meta-analysis. *Eur. Child Adolesc. Psychiatry* 25, 341–350. doi: 10.1007/s00787-015-0786-1

Wang, T., Zhang, T., Sun, L., Li, W., Zhang, C., Yu, L., et al. (2019). Gestational B-vitamin supplementation alleviates PM2.5-induced autism-like behavior and hippocampal neurodevelopmental impairment in mice offspring. *Ecotoxicol. Environ. Safety* 185:9686. doi: 10.1016/j.ecoenv.2019.109686

Wang, W., Li, C., Chen, Q., Van Der Goes, M. S., Hawrot, J., Yao, A. Y., et al. (2017). Striatopallidal dysfunction underlies repetitive behavior in Shank3-deficient model of autism. *J. Clin. Investig.* 127, 1978–1990. doi: 10.1172/JCI87997

Wang, Y., Hensley, M. K., Tasman, A., Sears, L., Casanova, M. F., and Sokhadze, E. M. (2016). Heart Rate Variability and Skin Conductance During Repetitive TMS Course in Children with Autism. *Appl. Psychophysiol. Biofeedback* 41, 47–60. doi: 10.1007/s10484-015-9311-z

Watanabe, T., Kuroda, M., Kuwabara, H., Aoki, Y., Iwashiro, N., Tatsunobu, N., et al. (2015). Clinical and neural effects of six-week administration of oxytocin on core symptoms of autism. *Brain* 138, 3400–3412. doi: 10.1093/brain/awv249

Watson, K. K., and Platt, M. L. (2012). Of mice and monkeys: using non-human primate models to bridge mouse- and human-based investigations of autism spectrum disorders. *J. Neurodev. Disord.* 4:21. doi: 10.1186/1866-1955-4-21

Wenzel, J. M., and Cheer, J. F. (2018). Endocannabinoid Regulation of Reward and Reinforcement through Interaction with Dopamine and Endogenous Opioid Signaling. *Neuropsychopharmacology* 43, 103–115. doi: 10.1038/npp.2017.126

Whitaker-Azmitia, P. M. (2001). Serotonin and brain development: role in human developmental diseases. *Brain Res. Bull.* 56, 479–485. doi: 10.1016/s0361-9230(01)00615-3

Wilkes, B. J., and Lewis, M. H. (2018). The neural circuitry of restricted repetitive behavior: Magnetic resonance imaging in neurodevelopmental disorders and animal models. *Neurosci. Biobehav. Rev.* 92, 152–171. doi: 10.1016/j.neubiorev.2018.05.022

Wilkes, B. J., Bass, C., Korah, H., Febo, M., and Lewis, M. H. (2020). Volumetric magnetic resonance and diffusion tensor imaging of C58/J mice: neural correlates of repetitive behavior. *Brain Imag. Behav.* 14, 2084–2096. doi: 10.1007/s11682-019-00158-9

Winkler, M., Biswas, S., Berger, S. M., Küchler, M., Preisendörfer, L., Choo, M., et al. (2020). Pianp deficiency links GABA(B) receptor signaling and hippocampal and cerebellar neuronal cell composition to autism-like behavior. *Mol. Psychiatry* 25, 2979–2993. doi: 10.1038/s41380-019-0519-9

Wirth, A., Holst, K., and Ponimaskin, E. (2017). How serotonin receptors regulate morphogenic signalling in neurons. *Prog. Neurobiol.* 151, 35–56. doi: 10.1016/j.pneurobio.2016.03.007

Wit, S. D., Watson, P., Harsay, H. A., Cohen, M. X., Van, D., and Ridderinkhof, K. R. (2012). Corticostriatal Connectivity Underlies Individual Differences in the Balance between Habitual and Goal-Directed Action Control. *J. Neurosci.* 32, 35. doi: 10.1523/JNEUROSCI.1088-12.2012

Wolff, J. J., Botteron, K. N., Dager, S. R., Elison, J. T., Estes, A. M., Gu, H., et al. (2014). Longitudinal patterns of repetitive behavior in toddlers with autism. *J. Child Psychol. PsychiatryAllied Discip.* 55, 945–953. doi: 10.1111/jcpp.12207

Wolff, J. J., Swanson, M. R., Elison, J. T., Gerig, G., Pruett, J. R., Styner, M. A., et al. (2017). Neural circuitry at age 6 months associated with later repetitive behavior and sensory responsiveness in autism. *Mol. Autism* 8:126. doi: 10.1186/s13229-017-0126-z

Wu, J., Dai, Y. C., Lan, X. Y., Zhang, H. F., Bai, S. Z., Hu, Y., et al. (2021). Postnatal AVP treatments prevent social deficit in adolescence of valproic acid-induced rat autism model. *Peptides* 137, 170493. doi: 10.1016/j.peptides.2021.170493

Wu, J., de Theije, C. G. M., da Silva, S. L., Abbring, S., van der Horst, H., Broersen, L. M., et al. (2017). Dietary interventions that reduce mTOR activity rescue autistic-like behavioral deficits in mice. *Brain Behav. Immun.* 59, 273–287. doi: 10.1016/j.bbi.2016.09.016

Yamasue, H., Okada, T., Munesue, T., Kuroda, M., Fujioka, T., Uno, Y., et al. (2020). Effect of intranasal oxytocin on the core social symptoms of autism spectrum disorder: a randomized clinical trial. *Mol. Psychiatry* 25, 1849–1858. doi: 10.1038/s41380-018-0097-2

Yang, J. Q., Yang, C. H., and Yin, B. Q. (2021). Combined the GABA-A and GABA-B receptor agonists attenuates autistic behaviors in a prenatal valproic acid-induced mouse model of autism. *Behav. Brain Res.* 403:94. doi: 10.1016/j.bbr.2020.113094

Yatawara, C. J., Einfeld, S. L., Hickie, I. B., Davenport, T. A., and Guastella, A. J. (2016). The effect of oxytocin nasal spray on social interaction deficits observed in young children with autism: a randomized clinical crossover trial. *Mol, Psychiatry* 21, 1225–1231. doi: 10.1038/mp.2015.162

Yehuda, S., Rabinovitz, S., and Mostofsky, D. I. (2005). Essential fatty acids and the brain: from infancy to aging. *Neurobiol. Aging* 26, 98–102. doi: 10.1016/j.neurobiolaging.2005.09.013

Yeo-Teh, N. S. L., and Tang, B. L. (2021). Moral obligations in conducting stem cell-based therapy trials for autism spectrum disorder. *J. Med. Ethics* 2021:106. doi: 10.1136/medethics-2020-107106

Yin, H. H., and Knowlton, B. J. (2006). The role of the basal ganglia in habit formation. *Nat. Rev. Neurosci.* 7, 464–476. doi: 10.1038/nrn1919

Yoo, T., Kim, S. G., Yang, S. H., Kim, H., Kim, E., and Kim, S. Y. (2020). A DLG2 deficiency in mice leads to reduced sociability and increased repetitive behavior accompanied by aberrant synaptic transmission in the dorsal striatum. *Mol. Autism* 11:3247. doi: 10.1186/s13229-020-00324-7

Yoshimura, R. F., Tran, M. B., Hogenkamp, D. J., Ayala, N. L., Johnstone, T., Dunnigan, A. J., et al. (2017). Allosteric modulation of nicotinic and GABAA receptor subtypes differentially modify autism-like behaviors in the BTBR mouse model. *Neuropharmacology* 126, 38–47. doi: 10.1016/j.neuropharm.2017.08.029

Yu, Y., Chaulagain, A., Pedersen, S. A., Lydersen, S., Leventhal, B. L., Szatmari, P., et al. (2020). Pharmacotherapy of restricted/repetitive behavior in autism spectrum disorder:a systematic review and meta-analysis. *BMC Psychiatry* 20:2477. doi: 10.1186/s12888-020-2477-9

Yui, K., Koshiba, M., Nakamura, S., and Kobayashi, Y. (2012). Effects of large doses of arachidonic acid added to docosahexaenoic acid on social impairment in individuals with autism spectrum disorders: a double-blind, placebo-controlled, randomized trial. *J. Clin. Psychopharmacol.* 32, 200–206. doi: 10.1097/JCP.0b013e3182485791

Zhang, L. L., Huang, C. C., Dai, Y., Luo, Q., Ji, Y. T., Wang, K., et al. (2020). Symptom improvement in children with autism spectrum disorder following bumetanide administration is associated with decreased GABA/glutamate ratios (vol 10, 63, 2020). *Transl. Psychiatry* 10:747. doi: 10.1038/s41398-020-0747-4

Zhang, Q., Wu, H., Zou, M., Li, L., Li, Q., Sun, C., et al. (2019). Folic acid improves abnormal behavior via mitigation of oxidative stress, inflammation, and ferroptosis in the BTBR T+ tf/J mouse model of autism. *J. Nutrit. Biochem.* 71, 98–109. doi: 10.1016/j.jnutbio.2019.05.002

Zhang, X., Li, Z., Liu, Y., and Gai, Z. (2021). Great Expectations: Induced pluripotent stem cell technologies in neurodevelopmental impairments. *Int. J. Med. Sci.* 18, 459–473. doi: 10.7150/ijms.51842

Zhong, H., Xiao, R., Ruan, R., Liu, H., Li, X., Cai, Y., et al. (2020). Neonatal curcumin treatment restores hippocampal neurogenesis and improves autism-related behaviors in a mouse model of autism. *Psychopharmacology* 237, 3539–3552. doi: 10.1007/s00213-020-05634-5

Zhou, M. S., Nasir, M., Farhat, L. C., Kook, M., Artukoglu, B. B., and Bloch, M. H. (2021). Meta-analysis: pharmacologic treatment of restricted and repetitive behaviors in autism spectrum disorders. *J. Am. Acad. Child Adoles. Psychiatry* 60, 35–45. doi: 10.1016/j.jaac.2020.03.007

Conflict of Interest: The authors declare that the research was conducted in the absence of any commercial or financial relationships that could be construed as a potential conflict of interest.

Advantages of publishing in Frontiers

OPEN ACCESS
Articles are free to read for greatest visibility and readership

FAST PUBLICATION
Around 90 days from submission to decision

HIGH QUALITY PEER-REVIEW
Rigorous, collaborative, and constructive peer-review

TRANSPARENT PEER-REVIEW
Editors and reviewers acknowledged by name on published articles

Frontiers
Avenue du Tribunal-Fédéral 34
1005 Lausanne | Switzerland

Visit us: www.frontiersin.org
Contact us: frontiersin.org/about/contact

REPRODUCIBILITY OF RESEARCH
Support open data and methods to enhance research reproducibility

DIGITAL PUBLISHING
Articles designed for optimal readership across devices

FOLLOW US
@frontiersin

IMPACT METRICS
Advanced article metrics track visibility across digital media

EXTENSIVE PROMOTION
Marketing and promotion of impactful research

LOOP RESEARCH NETWORK
Our network increases your article's readership